UNLV

UNIVERSITY LIBRARIES

1-1-2008

Parametric study of self -consolidating concrete

Hamidou Diawara
University of Nevada, Las Vegas

PARAMETRIC STUDY OF SELF-CONSOLIDATING CONCRETE

by

Hamidou Diawara

Bachelor of Science
National School of Engineering, Mali
1987

Master of Science
Southern Illinois University at Carbondale
1998

A dissertation submitted in partial fulfillment
of the requirements for the

Doctorate of Philosophy Degree in Civil and Environmental Engineering
Department of Civil and Environmental Engineering
Howard R. Hughes College of Engineering

Graduate College
University of Nevada, Las Vegas
December 2008

UMI Number: 3352169

INFORMATION TO USERS

The quality of this reproduction is dependent upon the quality of the copy submitted. Broken or indistinct print, colored or poor quality illustrations and photographs, print bleed-through, substandard margins, and improper alignment can adversely affect reproduction.

In the unlikely event that the author did not send a complete manuscript and there are missing pages, these will be noted. Also, if unauthorized copyright material had to be removed, a note will indicate the deletion.

UMI®

UNLV
UNIVERSITY OF NEVADA LAS VEGAS

Dissertation Approval
The Graduate College
University of Nevada, Las Vegas

December 15 , 20 08

The Dissertation prepared by

Hamidou Diawara

Entitled

Parametric Study of Self-Consolidating Concrete

is approved in partial fulfillment of the requirements for the degree of

Doctorate of Philosophy in Civil and Environmental Engineering

Examination Committee Chair

Dean of the Graduate College

Examination Committee Member

Examination Committee Member

Examination Committee Member

Graduate College Faculty Representative

Examination Committee Member

ABSTRACT

Parametric Study of Self-Consolidating Concrete

by

Hamidou Diawara

Dr. Nader Ghafoori, Examination Committee Chair
Professor and Chairman of Civil and Environmental Engineering Department
University of Nevada, Las Vegas

The research investigation presented herein was intended to study the influence of

parameters, such as aggregate size, admixture source, hauling time, and temperature on

the fresh and hardened properties of three distinct groups of self-consolidating concretes

(SCC). Within each group, the selected SCCs were made with a constant water-to-

cementitious materials ratio, a uniform cementitious materials (cement and fly ash)

content, and a constant coarse-to-fine aggregate ratio that provided the optimum

aggregate gradation. Three coarse aggregate sizes (ASTM C 33 #8, #7, and #67)

obtained from two different quarries were investigated. Four sources of polycarboxylate-

based high range water-reducing admixtures (HRWRA) and viscosity modifying

admixtures (VMA) were used. All raw materials were evaluated for their physico-

chemical characteristics.

The investigation presented herein was divided into two major phases. The first

phase aimed at: (1) comparing the optimum dosage requirements of four different sources of polycarboxylate-based HRWRA and VMA in attaining the target slump flow of 508 mm (20 inches), 635 mm (25 inches), and 711 mm (28 inches), T_{50} of 2 seconds or more, and a visual stability index (VSI) of 0 (Highly stable concrete) or 1 (Stable concrete), (2) evaluating the flow rate/plastic viscosity, static and dynamic stabilities, passing ability, and filling ability of the selected self-consolidating concretes, and (3) examining the properties of the trial self-consolidating concretes as related to air content, bleeding, time of setting, adiabatic temperature, demolded unit weight, compressive strength and modulus of elasticity.

In the second phase, the influence of hauling time, temperature, and combined hauling time and temperature on the fresh properties of the selected self-consolidating concretes was evaluated. Seven different temperatures (43, 36, 28, 21, 14, 7, and -0.5 °C (109, 96, 83, 70, 57, 44, and 31 °F)) and nine different hauling times (10, 20, 30, 40, 50, 60, 70, 80, and 90 minutes) were used to determine the loss in unconfined workability, dynamic stability, and flow ability rate of the designed matrices. The adverse effect of the above-mentioned variables was remediated by way of overdosing and retempering techniques which resulted in achieving the desired fresh characteristics of the designed self-consolidating concretes for different hauling times and temperatures.

TABLE OF CONTENTS

LIST OF TABLES

LIST OF FIGURES

This dissertation is dedicated to my father. He fought a loosing battle
against heart disease. His courage and unrelenting optimism
will always remain an inspiration in my life.

ACKNOWLEDGMENTS

I would like to express my profound gratitude to my academic advisor, Dr. Nader Ghafoori, for his scholastic advice and technical guidance throughout this investigation His devotion, patience, and focus on excellence allowed me to reach this important milestone in my life. I also wish to extend my acknowledge to my examination committee members, Dr. Samaan Ladkany, Dr. Moses Karakouzian, Dr. Aly Said, Dr. Spencer M. Steinberg, and Dr. Samir Moujaes for their guidance and suggestions.

I wish to thank Mr. Alan Sampson, the research shop technician, for providing unlimited assistance and technical supports during the experimental program. I thank Mrs. Mary E. Barfield and Mr. Patrick Morehead for being my teammates during this memorable journey.

Lastly, but not least, my thanks are extended to my wife Astan Guindo, my daughters Fatoumata and Alima, my sons Kandé dit Hamet Jr. and Oumar, my parents Mr. and Mrs. Kandé dit Hamet Sr. and Aminata Camara, and all my family and friends for their love and patience throughout my education.

CHAPTER 1

INTRODUCTION

The objective of this chapter is to present an overview of self-consolidating concrete (SCC), its components, and physico-chemical properties of different ingredients used in its production. The specifications and suggested guidelines for the raw materials used in self-consolidating concrete are also covered.

1.1   General background on self-consolidating concrete

Self-consolidating concrete (SCC) is a highly flowable non-segregating matrix that can spread into place, fill the formwork, and encapsulate the reinforcement without mechanical consolidation[1].

Self-consolidating concrete was first developed in Japan in the late 1980's, by Okamura and his coworkers, to reduce the labor required to properly place concrete[2]. Their initial motivation stemmed from durability considerations. Under or over consolidation of concrete was common in Japan, due to lack of skilled workers, compromising the durability of concrete structures. Insufficient consolidation led to excessive occurrence of entrapped air and other flaws, especially adjacent to rebars and other confined areas, whereas excessive vibration resulted in considerable segregation, external and internal bleeding and destruction of the air void system. Shortly after Japan, the use of self-consolidating concretes spread rapidly in Europe. The use of SCC has

been promoted in the United States by various public and private entities only in the most recent years.

The main idea behind modern self-consolidating concrete is to produce a matrix with low yield value and adequate viscosity that can easily be spread without any densification effort. This type of concrete is typically proportioned with a relatively high content of cementitious materials and sufficient chemical admixtures, leading to a relatively high initial material cost. Increases in cost can be tolerated in high-value added applications, especially when cost savings can be realized from using self-consolidating concrete; given the reduced effort in concrete placement, the reduction in construction time and labor cost and greater flexibility in placement operation (particularly in highly-congested reinforced areas), scheduling, and procuring the required resource[2,3,4]. Self-consolidating concrete provides better consolidation around reinforcement, reduces noise due to the elimination of vibration, improves surface appearance, enhances working conditions and safety, and reduces in-place cost when compared to vibratory-placed concrete.

A review of the related literatures revealed a number of investigations detailing the mixture constituents and proportions in SCC construction applications. While considerable variations have been shown, several factors common to the majority of the trial SCC matrices are still apparent. Self-consolidating concrete is characterized by a slump flow of 508 to 850 mm (20 to 33 inches)[5]. Binding materials contents such as cementitious and pozzolanic materials are high, typically 350 - 650 kg/m^3 (590 - 1095 lb/yd^3), but use of Portland cement exclusively is reported to result in inadequate cohesion or segregation resistance. In that respect, the utilization of fly ash, silica fume,

and ground granulated blast furnace slag as pozzolanic additives were found beneficial in multiple ways that impact properties, such as: workability, bleeding and segregations, air content, heat of hydration, setting time, finishability, pumpability, plastic shrinkage cracking, strength and stiffness, permeability, and durability[4,6].

The fluidity is provided by High Range Water-Reducing Admixture (HRWRA), most based either on polycarboxylate, naphthalene, or melamine formaldehyde, modified to provide extended retention of fluidity and set times and to control all important viscosity of the matrix. By far, polycarboxylate-based high range water reducing admixtures are the most widely used for developing and proportioning SCC. Strong segregation resistance can be achieved at the water-to-cementitious materials ratio of 0.3 – 0.4 (or higher) if an appropriate quantity of Viscosity Modifying Admixture (VMA) is added in addition to the HRWRA[7]. The use of a VMA is not always necessary, but VMA can be advantageous when using lower powder contents and gapgraded or demanding aggregates[8]. Factors that influence the fluidity of self-consolidating concrete are: (1) fine and coarse aggregates grading and ratio, and aggregates shape and surface texture, (2) fine aggregate-to-paste ratio, (3) fine aggregate volume-to-total-aggregate volume ratio, (4) cementitious materials type and factor, (5) water-to-cementitious materials ratio, (6) admixture type and dosage, (8) environmental condition (i.e., temperature and relative humidity), and (9) delivery method and transportation duration[1,3,6,8].

Self-consolidating concrete is a highly engineered material in which the selection and proportioning of its constituent require careful attention. To achieve specified fresh and hardened properties required for a specified application, the proportion of fine and coarse aggregates, cement and supplementary cementitious materials, water, and

admixtures should be well balanced. The review of related literature revealed three basic types of self-consolidating concrete which are [1,9]:

(a) High powder type SCC: This type of SCC is characterized by the large amount of powder (material less than 0.006 inch (0.15 mm)) which is usually in the range of 550 to 650 kg/m^3 (925 to 1095 lb/yd^3). The fluidity is provided by the addition of superplasticizer.

(b) Low powder type SCC: This type of SCC, also referred as viscosity type, is characterized by the powder content of 350 to 450 kg/m^3 (590 to 760 lb/yd^3). The segregation resistance is mainly controlled by the incorporation of a viscosity modifying admixture, while the fluidity is achieved with a superplasticizer.

(c) Moderate powder type SCC: This type of SCC is a combination of the first two types. The powder content is between 450 and 550 kg/m^3 (760 to 925 lb/yd^3). A good balance between the HRWRA and VMA is used to achieve the required rheological properties.

1.2   Constituent's materials and their physico-chemical properties

1.2.1   Aggregates

The importance of using the right type and quality of aggregate cannot be overemphasized since the coarse and fine aggregates generally occupy 60 to 75% of the concrete volume (70 to 85% by weight)[10]. It has been customary to consider aggregates as inert and inexpensive material. This belief is abandoned nowadays, because the aggregate physical, thermal, and chemical properties have a great influence on the concrete fresh and hardened properties. Aggregates must meet certain standard for optimum engineering use: they must be clean; hard; string; durable; and free of absorbed chemicals, coatings of clay, and other fine materials in amounts that could affect

hydration and bond of the cement paste[10]. In the case of self-consolidating concrete, a great attention is given to the aggregates types, grading, and coarse-to-fine aggregate ratio due to their critical role in mixture performance. Other characteristics such as shape, texture, bulk density, specific gravity, porosity, bond and strength also influence the overall performance of SCC mixtures. The mineralogical and petrographical compositions of aggregate greatly impact its bulk density[11]. The important minerals found in aggregate are: silica minerals (quartz, opal, chalcedony, etc.), carbonate minerals, sulfate mineral, iron sulfide minerals, ferromagnesian minerals, zeolites, iron oxide minerals, clay minerals, etc. The presence of some unstable forms of silica can adversely affect the performance of the concrete[11].

1.2.2   Portland cement

Joseph Aspin, an English mason, is known as the inventor of Portland cement in 1824[10]. Naturally occurring calcium carbonate materials such as limestone, chalk, marl, and seashells are the common industrial sources of calcium, but clay and dolomite ($CaCO_3 \cdot MgCO_3$) are present as principal impurities. Clays and shales, rather than quartzs or sandstone, are the preferred sources of additional silica for making calcium silicates because quartzitic silica does not react easily[12]. Table 1.1 presents the sources of other raw materials used in the manufacture of Portland cement. The Calcium oxide and the silica are essential, whereas alumina and iron oxides are mainly used to decrease the temperature of manufacturing.

ASTM C 150[13] defines Portland cement as hydraulic cement produced by pulverizing clinkers consisting essentially of hydraulic calcium silicates, usually containing one or more of the forms of calcium sulfate as an interground addition.

Table 1.1: Source of raw materials used in producing Portland cement[10].

Lime, CaO	Iron, Fe_2O_3	Silica, SiO_2	Alumina, Al_2O_3	Gypsum, $CaSO_4 \cdot 2H_2O$	Magnesia, MgO
Alkali waste	Blast furnace	Calcium silicate	Aluminum-ore refuse	Anhydrite	Cement rock
Aragonite	Clay	Cement rock	Bauxite	Calcium sulfate	Limestone
Calcite	Iron ore	Clay	Cement rock	Gypsum	Slag
Cement-kiln dust	Mill scale	Fly ash	Clay		
Cement rock	Ore washings	Fuller's earth	Copper slag		
Chalk	Pyrite cinders	Limestone	Fly ash		
Clay	Shale	Loess	Fuller's earth		
Fuller's earth		Marl	Granodiorite		
Limestone		Ore washings	Limestone		
Marble		Quartzite	Loess		
Marl		Rice-hull ash	Ore washings		
Seashells		Sand	Shale		
Shale		Sandstone	Slag		
Slag		Shale	Staurolite		
		Slag			
		Traprock			

Clinkers are 5 to 25 mm (0.2 to 1 inch) diameter nodules of a sintered material which is produced when a raw mixture of predetermined composition is heated to high temperature. Hydraulic cements are defined as cements that not only hardened by reacting with water but also form a water-resistant product. Because of the high number of publications available on Portland cement, this review is brief.

1.2.2.1 Manufacturing process of Portland cement

Cement manufacturing involves heating, calcining and sintering. In the calcining phase, limestone is converted into lime, releasing carbon dioxide ($CaCO_3 \rightarrow CaO + CO_2$) and clay is converted into silicon dioxide, alumina and iron (Clay $\rightarrow SiO_2 + Al_2O_3 + Fe_2O_3 + H_2O$). Sintering is the process, in which fine particles of a material become chemically bonded at a temperature that is sufficient for atomic diffusion. Chemically, the produced calcium oxide in the first stage reacts with silicon dioxide and alumina – and iron-bearing compounds to form C_3S and C_2S plus lesser quantities of C_3A, C_4AF, and several other compounds[14].

Two processes of manufacture, namely: wet and dry, are employed, the latter being more common in North America. The dry process is more energy efficient than the wet process because the water used for slurring must subsequently be evaporated before the clinkering operation. In the dry process the materials are crushed, dried, and then ground in ball mills to a powder which is burnt in its dry condition. In the wet process the materials are first crushed and then ground to form slurry in wash mills. After passing through the wash mills and the slurry silos, the slurry passes to slurry tanks. Samples of the slurry are tested and any correction in the chemical composition is made by changing the proportions of the calcareous and argillaceous constituents. The ground raw material is fed into the upper end of a kiln. Cement kilns may be as large as 5.7 m (18.7 ft) in diameter and about 200 m (650 f) in length, and with an output of as much as 76 tonnes per hour[16]. The raw mix passes through the kiln at a rate controlled by the slope and rotational speed of the kiln. Burning fuel (powered coal, oil, or gas) is forced into the lower end of the kiln where temperatures of 1430 °C to 1650 °C (2600 °F to 3000 °F)

change the raw materials chemically into cement clinker. The clinker is cooled and then pulverized. During this operation a small amount, 3 to 5 percent, of retarder (gypsum being the material generally used) is added to regulate the setting time of the cement. The clinker is ground so fine that nearly all of it passes through a No. 200 mesh (75 microns (0.003 inch)) sieve with 40,000 openings per square inch. This extremely fine gray powder is called Portland cement. The temperature of the cement as it comes out the grinding mill can be as high as 70 °C (158 °F)[10,12,14].

1.2.2.2   Chemistry of Portland cement

The chemistry of Portland cement is very complex. This section is intended to give an overview of the main chemical compounds. The chemical analysis of Portland cement gives its composition in form of oxides. The acidic components of the raw mixture react with the calcium oxide during the burning operation of Portland cement clinker to form principal compounds that make up to 90% of cement by weight. Table 1.2 provides the name and the chemical formula of each of these oxides, Table 1.3 presents the primary compounds, their chemical formula and abbreviation, and Table 1.4 shows the main phases of Portland cement and their characterizations.

When cement is mixed with water, a chemical action begins between the various compounds and water. In the initial stage, the small quantity of retarder (gypsum) quickly goes into solution, and is thus able to exert its influence on the other chemical reactions which are starting. These reactions resulted in the formation of various compounds which cause setting and hardening. The four most important being[10,12]:

- *Tricalcium silicate (C_3S):* The reaction of this compound commences within a few hours and generates considerable amount of heat. The resulting hydrate from the reaction

8

Table 1.2: Chemical compositions of Portland cement in form of oxide[15]

Name	Chemical Formula	Abbreviation
Lime	CaO	C
Silica	SiO_2	S
Iron	Fe_2O_3	F
Alumina	Al_2O_3	A
Trioxide of sulfur	SO_3	S
Magnesia	MgO	M
Sodium oxide	Na_2O	-
Potassium oxide	K_2O	-
Equivalent Alkalis	$0.342\%Na_2O + 0.658\%K_2O$	-

Table 1.3: Primary chemical compounds of Portland cement[10]

Name	Chemical Formula	Abbreviation
Tricalcium silicate	$3CaO . SiO_2$	C_3S
Dicalcium silicate	$2CaO . SiO_2$	C_2S
Tricalcium aluminate	$3CaO . Al_2O_3$	C_3A
Tetracalcium aluminoferrite	$4CaO . Al_2O_3 . Fe_2O_3$	C_4AF

Table 1.4: Main phases of Portland cement and their characteristics[14]

Parameter	C_3S	C_2S	C_3A	C_4AF
Reactivity	high	low	very high	low
Impurities	Al_2O_3, Fe_2O_3, MgO	Al_2O_3, Fe_2O_3, Na2O, K_2O, SO_3	Fe_2O_3, Na_2O, K_2O, MgO	MgO, SiO_3, TiO_2
Technical name	alite	belite	aluminate phase	ferrite phase
Heat of hydration (j/g)	500	250	1340	420
Contribution to strength	high at early age	high at late age	high at very early age	very low

has a significant influence on the strength of concrete at early age, mainly in the first 14 days. The approximate hydration reactions can be written as follow:

$$2C_3S \quad + \quad 6H \quad \rightarrow \quad C_3S_2H_3 \quad + \quad 3Ca(OH)_2 \qquad (1.1)$$

[100]   [24]   [75]   [49]
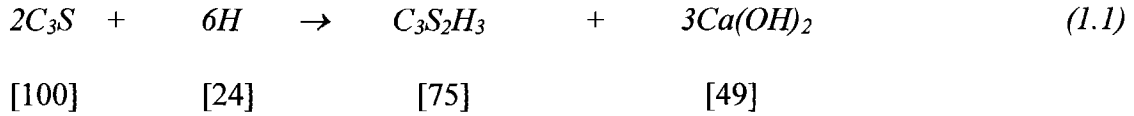
- *Dicalcium silicate (C_2S):* The hydrate of this compound is formed slowly with a low rate of heat evolution. It is mainly responsible for the progressive increase in strength which occurs from 14 to 28 days, and onwards. Cements containing a high C_2S content have a relatively high chemical resistance, a low drying shrinkage, and hence, are the most durable of the Portland cement. The approximate hydration reactions can be written as follow:

$$2C_2S \quad + \quad 4H \quad \rightarrow \quad C_3S_2H_3 \quad + \quad Ca(OH)_2 \qquad (1.2)$$

[100]   [21]   [99]   [22]
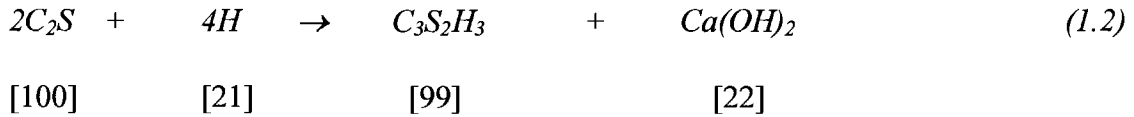
It can be seen from equations (1.1) and (1.2) that the hydration of C_3S and C_2S generates two forms of hydrates, namely: Portlandite (CH) and the Calcium Silicate Hydrate, CSH-phase (previously referred to as tobermorite). The numbers in the square brackets are the corresponding masses, and on this basis both silicates require approximately the same amount of water for hydration, but C_3S produces more than twice as much $3Ca(OH)_2$ as is formed by the hydration of C_2S.

- *Tricalcium aluminate (C_3A):* The amount of C_3A in most Portland cement is comparatively small. The C_3A compound hydrates very rapidly and produces a considerable amount of heat. It is responsible for the initial stiffening, but contributes least to ultimate strength. It is very vulnerable to sulfate environment and has the

10

tendency to cause cracking due to volume change. The approximate reaction can be written as follow:

$$C_3A \quad + \quad 6H \quad \rightarrow \quad C_3AH_6 \qquad\qquad (1.3)$$

$$[100] \qquad\quad [40] \qquad\quad [140]$$
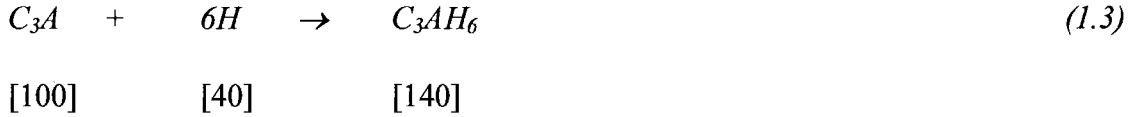
The masses shown in the brackets indicate that a higher proportion of water is required than for the hydration of silicates. The hydration of C_3A is highly influenced by the presence of gypsum. Without gypsum the initial hydration reaction is very quick. C_3A is first converted into unstable phases, further into stable calcium aluminate hydrate phase (C_3AH_6).

$$2C_3A + 21H \Rightarrow C_4AH_{13} \ (unstable) + C_2AH_8 \ (unstable) \qquad\qquad (1.4)$$

$$C_4AH_{13} + C_2AH_8 \Rightarrow 2C_3AH_6 \ (stable) + 9H \qquad\qquad (1.5)$$
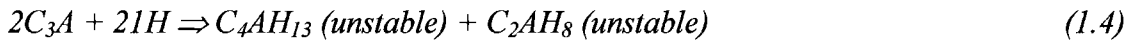
The addition of gypsum makes concrete placeable. In the presence of its dissolved components Ca^{2+} and SiO_4^{2-}, C_3A is converted into ettringite, which is a calcium aluminate trisulfate.

$$C_3A + 3Ca^{2+} + 3SO_4^{2-} + 32H \Rightarrow C_3A \cdot 3Cs \cdot H_{32} \ (ettringite) \qquad\qquad (1.6)$$
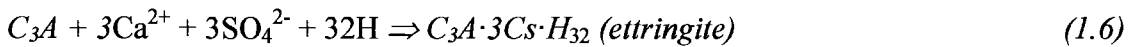
Ettringite has a fibrous morphology consisting of long hexagonal needles. The length of needles strongly depends on the environmental conditions. As it is detailed in the next section (1.2.2.3 - Portland cement hydration), the hydrated phase of ettringite is formed around the C_3A containing grains and protects them from further rapid hydration during the dormant period. During the deceleration period, ettringite becomes unstable due to an insufficient sulfate ion supply. It is converted into calcium aluminate monosulfate[11,14].

$$C_3A \cdot 3Cs \cdot H_{32} + 2C_3A + 4H \Rightarrow 3C_3A \cdot 3Cs \cdot H_{12} \ (monosulfate) \qquad\qquad (1.7)$$
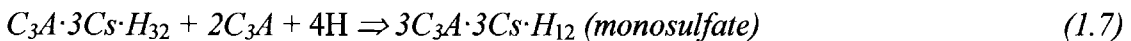
- *Tetracalcium aluminoferrite (C_4AF):* This compound is of little importance since it has no marked importance on the strength and other hardened properties. It provides the cement its grey color[11,12]. The calcium aluminoferrite reacts slowly due to precipitation of hydrated iron oxide.

$$2Ca_2AlFeO_5 + CaSO_4 + 16H_2O \rightarrow Ca_4(AlO_3)_2(SO_4).12H_2O + Ca(OH)_2 + 2Fe(OH)_3$$

From the above equations it can be seen that the aluminate phases and their hydration products play an important role in the early hydration processes. The relative reactivity of the different mineral phases with water can be classify as $C_3A > C_3S > C_2S \cong C_4AF$[16]. In order to obtain a desired type of cement or cement with desired properties, type and proportion of the raw materials, and manufacturing process (i.e., mode of burning, speed of cooling, and fineness) should be altered. The ASTM C 150[13], Standard Specifications for Portland cement, identifies eight types of Portland cement as follows:

(1) Type I: Normal; (2) Type IA: Normal, air-entrained; (3) Type II: Moderate sulfate resistance; (4) Type IIA: Moderate sulfate resistance, air-entrained; (5) Type III: High early strength; (6) Type IIIA: High early strength, air-entrained; (7) Type IV: Low heat of hydration; and (8) Type V: High sulfate resistance

1.2.2.3   Portland cement hydration

Immediately after the first contact of cement with water, various reactions occur through several types of bonding interaction leading to a final dense and stable matrix. Typical representation of cement hydration stages is illustrated in Figure 1.1, which can be obtained by using a conduction calorimeter. As shown in Figure 1.1, it can be seen that the occurrence of hydration with time involves five stages which are:

12
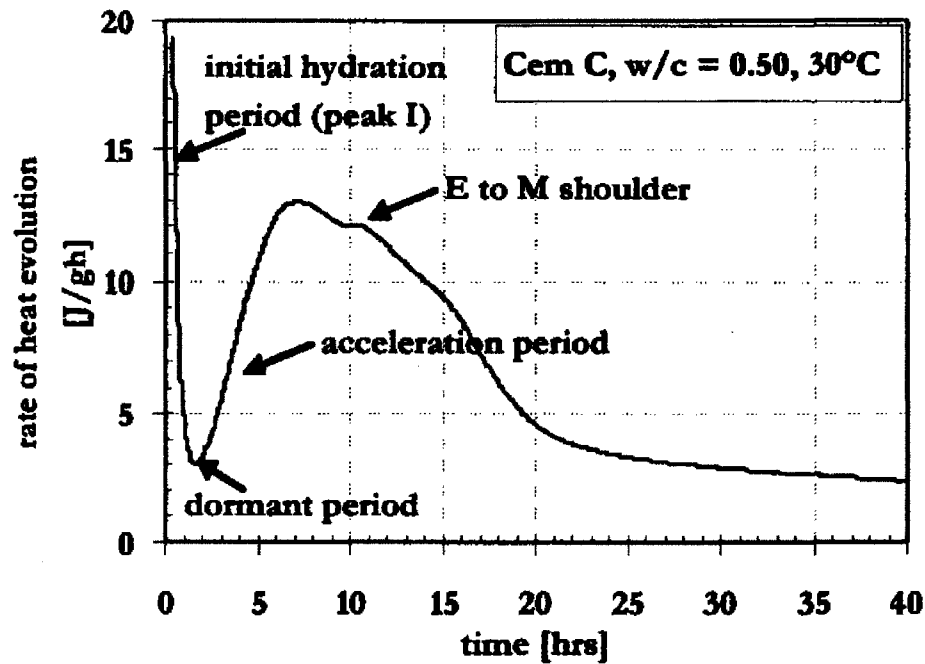
Figure 1.1: The four stages of Portland cement hydration[14]

- *Initial hydration:* During the initial hydration water wets the cement particles and solubilizes the cement phases. The easily soluble components like alkalis, calcium sulfate phases and free lime are dissolved by the surrounding water[14]. A rapid heat evolution, representing probably the heat of solutions of aluminates and silica, lasting a few minutes (0 to 15), occurs. Na^+, K^+, Ca^{2+}, SO_4^{2-}, and OH^- ions are enriched in the pore water. Meanwhile, Ca^{2+} and $H_2SiO_4^{2-}$ are hydrolyzed from the most reactive cement particles C_3A and C_3S, and C_3A is converted into ettringite (calcium aluminate trisulfate). Besides ettringite, a small amount of calcium silicate hydrate (CSH) gel is formed around the C_3S containing cement grains. The initial heat flux drastically decreases when the solubility of aluminate is depressed in the presence of sulfate in the solution and the cement grains are coated with a protective layer of hydration products[11,12,14,16].

- *Induction period or dormant period*: The induction period usually lasts 15 minutes to 4 hours, during which the concrete should be transported and placed. This hydration stage is characterized by a very low heat flow. In the early part of the dormant period, reactions of the aluminate and gypsum phases play predominant role in the setting of the paste. If the solubilization of gypsum (to produce sulfate ion) is too low, flash set may occur (flash set is distinguished from false set in that it evolves considerable heat and the rigidity of the mix cannot be dispelled by further mixing without adding water). False set is caused by the presence of the hemihydrate or anhydrite. If the solubilization of gypsum is too high (because of the presence of hemihydrate form of gypsum, sodium, and potassium sulfates), then extensive growth of gypsum crystals occurs, resulting in false set. The pore water during the induction period consists of alkali hydroxides[11,12,14,17].

- *Acceleration and setting period:* Near the end of the dormant period, the rate of cement hydration increases sharply because of the disruption of the protective hydrates layer, the nucleation, the growth of calcium silicate hydrates (CHS-phase) and calcium hydroxide (portlandite), and the recrystallization of ettringite leading to setting and hardening[14]. The concrete is no longer placeable. C_2S starts to hydrate. C_3A and to a lesser extent C_4AF continue to hydrate. The paste of a properly retarded cement will retain much of its plasticity before the commencement of this heat cycle and will stiffen and show the initial set (beginning of solidification) before reaching the apex, which corresponds to the final set (complete solidification and beginning of hardening). During the acceleration period the calcium and sulfate ion concentration in the pore water decrease due to the ettringite formation. The acceleration period lasts 4 to 8 hours for

most Portland cement[11,12,14,17].

- *Deceleration and hardening period:* The hardening of the cement paste or concrete occurs during the deceleration period and can lasts 8 to 24 hours. During this stage the pore volume decreases with increasing time and decreasing water-to-cementitious materials ratio. At the end of the deceleration period, the cement hydrated product mainly consists of calcium silicate hydrate (CSH) and portlandite (CH). As shown in Figure 1.1, sometimes a shoulder (conversion of ettringite (E) to monosulfate (M)) is visible at the deceleration period[11,12,14,16].

- *Curing period (1 to several weeks):* The last stage of concrete hydration is curing, which consists in maintaining satisfactory moisture content and temperature in concrete for a period of time immediately following placing and finishing so that the desired properties may develop. During curing, concrete properties improve rapidly at early age but continue more slowly thereafter for an indefinite period [11,14].

1.2.3 Chemical admixtures

ACI 116R[18] defines an admixture as a material other than water, aggregates, hydraulic cements, and fiber reinforcement, used as an ingredient of a cementitious mixture to modify its freshly mixed, setting, or hardening properties and that is added to the batch before or during its mixing.

ACI committee 212-3R[19] lists 19 important purposes for which admixtures are used. The most important contributions are: to increase the plasticity of concrete without increasing the water content, to reduce bleeding and segregation, to retard or accelerate the rate of heat evolution, to increase the durability of concrete to specific exposure condition, to improve pumpability, and to produce colored concrete or colored mortar.

15

The importance of admixture use in concrete was proven since the ancient time. Materials used as admixtures included milk and lard by Romans; eggs during the middle ages in Europe; polished glutinous rice paste, lacquer, tung oil, blackstrap molasses, and extracts from elm soaked in water and boiled bananas by the Chinese; and in Mesoamerica and Peru, cactus juice and latex from rubber plants. The Mayans also used bark extracts and other substances, such as set-retarder, to keep stucco workable for a long period of time[18,20]. In the last 70 years or more, considerable research and development have been done and many organic and polymer-based admixtures have been developed for use in various applications in construction. The performance of a chemical admixture depends on its type, chemical composition and dosage; specific surface area of the cement; type and proportions of aggregate; sequence of addition of water and admixture; compatibility of admixtures; water-to-cementitious material ratio; and temperature and conditions of curing[17]. An overview of the main chemical admixtures used in the manufacturing of self-consolidating concrete; including their types, functions, chemical compositions, and mechanism of actions; is presented below.

Admixtures are incorporated in concrete in order to alter one or more of its fresh or hardened properties. They vary considerably in chemical composition and some of them can perform more than one function which makes it difficult to classify them according to their function[12]. Admixtures are classified by the ASTM C 494[21] "Standard Specification for Chemical Admixtures for Concrete," by function as follows: (1) Type A, Water-reducing admixtures; (2) Type B, Retarding admixtures; (3) Type C, Accelerating admixtures; (4) Type D, Water-reducing and retarding admixtures; (5) Type E, Water-reducing and accelerating admixtures; (6) Type F, Water-reducing, high-range,

admixtures; and (7) Type G, Water-reducing, high-range and retarding admixtures.

Depending on their mechanism of action, chemical admixture can be broadly divided into two groups. The first group (surface active chemical) begins to act on the cement-water system instantaneously by influencing the surface tension of water and by adsorbing on the surface of cement particles. The second group (set-controlling admixture) breaks up into their ionic constituents and affects the chemical reactions between cement compounds and water from several minutes to several hours after addition[12].

Surface-active chemicals, also called surfactants, cover admixtures that are generally used for air-entrainment or reduction of water in concrete mixtures. They are organic or polymer-based admixtures, which consist essentially of long-chain molecules, one end of which is hydrophilic (water-attracting) and the other hydrophobic (water-repelling). The hydrophilic end contains one or more polar groups, such as $-COO^-, -SO_3^-$, or $-NH_3^+$. Anionic admixtures are used in concrete technology either with a nonpolar chain or with a chain containing some polar groups. The admixture with nonpolar chain serves as air-entraining admixture and the one with polar group as water-reducing admixture. During the cement hydration, the surfactants become adsorbed at the air-water and the cement-water interfaces with an orientation of the molecule that determines whether the predominant effect is the entrainment of air or plasticization of the cement-water system[12].

1.2.3.1   Air-entraining admixtures

1.2.3.1.1   Function

When an air-entraining surfactant is added to the cement-water system, as a result

of the mixing action, it forms and stabilizes air bubbles that become a component of the hardened concrete. The main application of air-entraining admixtures is for concrete mixtures designed to resist against damage from repeated freezing-and-thawing. The air bubbles must have a diameter between 10 and 1000 micrometers (0.0004 to 0.04 inch) and must be present in the proper amount and spacing (spacing factor larger than 0.200 mm (0.008 inch)) to be effective at providing freezing and thawing protection. The term spacing factor represents the maximum distance that the water would have to move before reaching the air void reservoir or safety valve[20]. Entrained air should not be confused with entrapped air.

The concrete air content can be affected by several factors which can be summarized as follows[20]:

- Cement: An increase in the fineness or in the cementitious materials content can decrease the air content. An increase in the Alkali content of the cement increases the air content.

- Fine aggregate: An increase in the amount of fine fraction passing the No. 100 sieve (150 μm (0.0059 inch)) will decrease the amount of entrained air, while an increase in the middle fraction passing the No. 16 sieve (1.18 mm (0.0469 inch)) but retained on the No. 30 sieve (600 μm (0.0236 inch)) and No. 50 sieve (300 μm (0.0118 inch)), will increase the air content.

- Coarse aggregate: Crushed stone concrete may result in lower air than a gravel concrete

- Water: Hard water or industrial detergent-contaminated water may reduce the air content.

18

- Pozzolans and slag: Fly ash, silica fume, natural Pozzolans, and ground granulated blast-furnace slag can affect the dosage rate of air-entraining admixtures.

- Chemical admixtures: chemical admixtures generally affect the dosage rate of air-entraining admixtures.

- Temperature: An increase in concrete temperature will decrease the air content. Increase in temperature from 21 to 38 °C (70 to 100 °F) may reduce air contents by 25%. Reductions of temperature from 21 to 4 °C (70 to 40 °F) may increase air contents by as much as 40%.

- Concrete mixer: The type of mixer, the energy of mixing, the state of the mixer blade (worn or coated with hardened concrete buildup), and the loaded volume (under or overloaded) of a mixer can affect the air content.

The incorporation of air-entraining surfactant in concrete mixture can induce some side effect. The most important are: improvement of workability, and reduction of unit weight and strength. An increase of 1% in air content will decrease the compressive strength by about 5% in concrete mixtures with a compressive strength in the range of 21 to 35 MPa (3000 to 5000 psi). Since air-entraining surfactant renders the cement particles hydrophobic, an over dose of the admixture would cause an excessive delay in cement hydration[12].

1.2.3.1.2 Chemical composition

Surfactants used as air-entraining admixtures generally consist of salts of wood resins, proteinaceous materials and petroleum acids, and some synthetic detergents[12]. They are used in concrete to produce and stabilize tiny air bubbles, which are produced by mixing action. Figure 1.2 presents a typical chemical formula of a nonpolar

hydrocarbon chain with an anionic polar group of an air-entraining surfactant.

Abietic Acid

CH₃   COOH

CH₃

CH₃
CH
CH₃
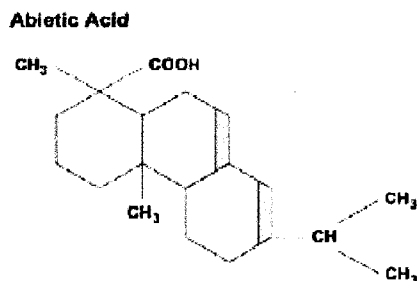
Figure 1.2: Chemical structure of a typical air-entraining surfactant derived from pine

oil or tall oil processing[12]

1.2.3.1.3   Mechanism of action

The mechanism of action of an air-entrainment admixture consists to lower the

surface tension of the water to facilitate bubble formation.   Figure 1.3 presents an

illustration of the mechanism of air entrainment in concrete.   Lea[22] reported a detailed

air-entrainment and stabilization actions as follows[12]: *"At the air-water interface the*

polar groups are oriented towards the water phase lowering the surfacing tension,

promoting bubble formation and counteracting the tendency for the dispersed bubbles to

coalesce.   At the solid-water interface where directive forces exist in the cement surface,

the polar groups become bound to the solid with the nonpolar groups oriented towards

the water, making the cement surface hydrophobic so that air can displace water and

remain attached to the solid particles as bubbles".

20
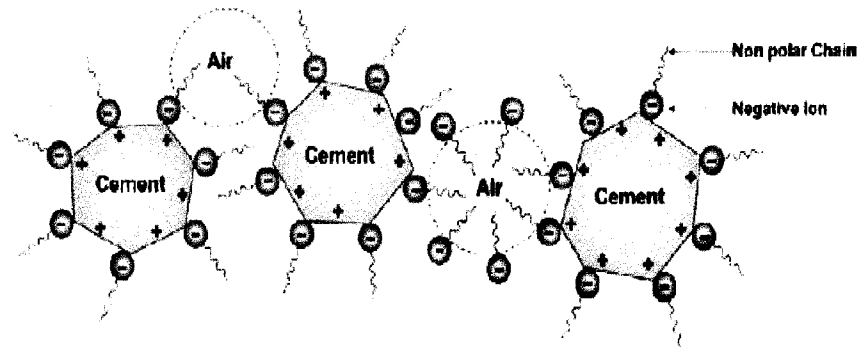
Figure 1.3: Mechanism of air entrainment when an anionic surfactant with a nonpolar hydro-carbon chain is added to the cement paste[12]

1.2.3.2 Water-reducing admixtures or normal plasticizers

1.2.3.2.1 Function

Water-reducing admixtures (WRA) or plasticizing admixture are surface-active chemicals consisting of water-soluble organic materials. Depending on their chemical composition, they can perform more than one function. However, their main role is to disperse cement particles which are strongly agglomerated when cement is in contact with water. The main benefits obtained when WRA are used in concrete are: (1) to increase the workability without changing the mixture composition; (2) to reduce the amount of water needed to achieve a given workability, without significantly affecting the air content and the setting characteristics, in order to improve strength and durability; (3) to decrease both water and cement content, without changing the workability, in order to produce a cost-saving. Typically, the use of a water-reducing admixture decreases the required mixing water content by 5 to 12%. It is important that the manufacture's recommended dosage rates should be strictly followed and trial batches with local

materials should be performed to determine the proper dosage rate for a given concrete mixture.

1.2.3.2.2 Chemical composition

Table 1.5 presents the main ingredients used for making water-reducing admixture. It can be seen that surfactants used as plasticizing admixtures usually are salts, modifications, and derivatives of lignosulfonic acids, hydroxylated carboxylic acids, and polysaccharides, or any combinations of the foregoing three, with or without other subsidiary constituents. Figure 1.4 presents the chemical structure of the most important sulfonated and acrylic polymers used as active ingredients of plasticizing and superplasticizing admixtures.

Table 1.5: Main and secondary ingredients in plasticizing and superplasticizing admixtures[23]

Superplasticizers		Plasticizers	
Main ingredients	Secondary ingredients	Main ingredients	Secondary ingredients
SMF	MLS	LS/MLS	TEA
SNF	Retarders	HC	Inorganic salts
AP	Inoeganic salts	CH	Defoaming agents
Others	TEA	Others	Anti-bacterial products

SMF, sulfonated melamine formaldehyde; SNF, sulfonated naphtalene formaldehyde; AP, acrylic polymers; MLS, modified form; TEA, triethanolamine; LS, lignosulfonic acid; HC, hydroxycarboxylic acids; CH, carbohydrates.
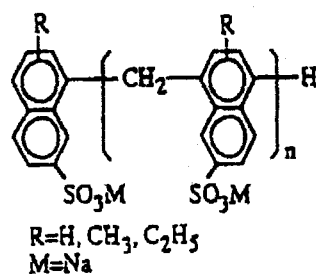
R=H, CH$_3$, C$_2$H$_5$
M=Na

SNF
(Sulfonated naphtalene formaldehyde)

EO: Ethylene oxide

PC
(Polycarboxylate ester)

M=Na

SMF
(Sulfonated melamine formaldehyde)

R=CH$_3$
M=Na

CAE
(Copolymer of carboxylic acrylic acid with acrylic ester)
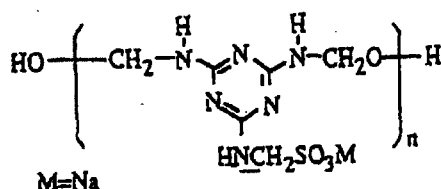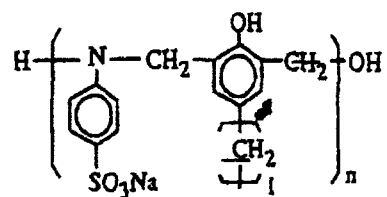
AS
(Amino-sulfonate polymer)

(X) ← Crosslinked point

Me=CH$_3$, M=Na

LS
(Lignosulfonate)
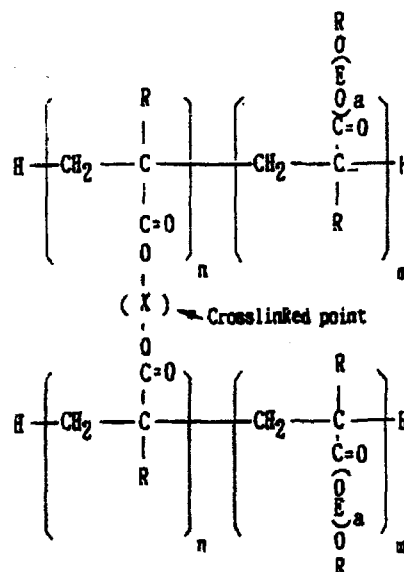
CLAP
(Cross-linked acrylic polymer)

Figure 1.4: Chemical structure of sulfonated and acrylic polymers[23]

23

1.2.3.2.3 Mechanism of action

The fundamental mechanism of action of plasticizers has been established and reported by several studies[1,10,12,23]. It depends mostly on the surface chemistry. When a small quantity of water is added to the cement, without the presence of surfactant a well-dispersed system is not attained because, first, the water possesses high surface tension (hydrogen-bonded molecular structure), and second, the cement particles tend to cluster together or form flocs (attractive force exists between positively and negatively charged edges, corners, and surfaces when crystalline minerals or compounds are finely grounded)[10,12]. The diagram representing the flocculation system is shown in Figure 1.5.
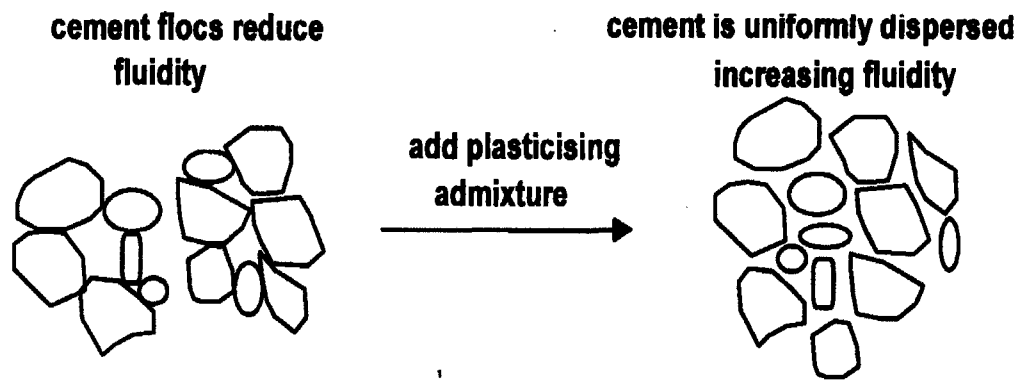
Figure 1.5: Mechanism of flocs of cement break-up[24]

During the flocculation system a faster coagulation of cement grain occurs because C_2S and C_3S have a negative zeta potential while C_3A and C_4AF have a positive zeta potential[25]. Particle charge can be controlled by modifying the suspending liquid characteristics. Modifications include changing pH of liquid or changing the ionic species in solution. Another direct technique is to use surface active agent which directly

adsorbs to the surface of colloid and changes its characteristics. The improvement of fresh concrete's fluidity by the incorporation of a water-reducing admixture is considered to be caused by its dissociation in water to give negative charges on the $-COO^-$, $-SO_3^-$, or OH^- groups. Some of these are adsorbed onto the positive sites of the cement particles; others form an outer negative charge around the grain lowering the inter-particle attraction by the electrostatic repulsion mechanisms. An overview of the main physico-chemical effects involved in cement-plasticizer interactions is presented below.

1.2.3.2.3.1 Adsorption

The plasticizer has to be adsorbed first to the cement particle surface before being able to play dispersing role. In fact, as reported in section 1.2.2.3 during the hydration of Portland cement the soluble compounds of cement particles such as alkalis, calcium sulfate phase and free lime are dissolved by the surrounding water as soon as cement and water come into contact, and the Ca^{2+} and $H_2SiO_4^{2-}$ ions are hydrolyzed from C_3A and C_3S. The sustainability of this theory has been proven by the chemical analysis of cement particles from an electron spectroscopy for chemical analysis (ESCA, a test used to determine the elements on the sample surface by irradiating the sample with soft x-ray), which showed that calcium ions can be dissolved from the surface of the clinker without destroying the skeletal structure of clinker material, leading to a formation of a Silicon (SiO_4^{4-}) or Aluminum ($Al_2O_3^{3-}$) rich surface[14]. The dissolved Ca^{2+} ions produce positive charged surface-adsorbed layer around the cement particles. Consequently, in the presence of plasticizer, the hydrophilic end of the molecule chain (i.e. COO^-, SO_3^-

for organic molecules, and OH^- for polar functional group of organic molecules (e.g.

sugar)) is adsorbed to the cement particles. For the case of polymeric admixtures (e.g.

lignosulfonates) containing hydrophobic, polar and ionic groups, the adsorption results

from a sum of effect and often stabilize the adsorption rate[16]. Figure 1.6 is a typical

representation of an adsorption of organic molecules at the cement-solution interface.
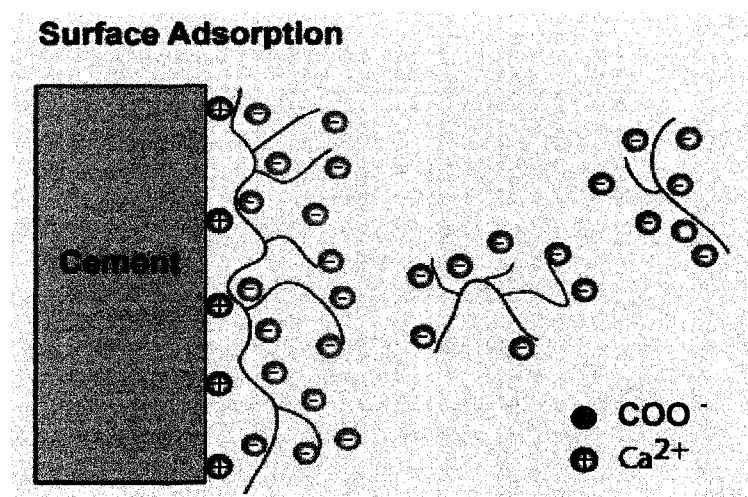
Figure 1.6: Adsorption mechanism of organic molecules at the cement-solution interface[12]

This theory was disputed by some researchers since plasticizers are also

negatively charged and the surface charge of cement particle is low or even negative

because the interstitial cement solution has a pH between 12 and 13. However, even if a

surface has an overall negative charge, it carries also positively charged site, and the

surface complexation (not adsorption), which does not depend on the overall surface

charge, may be the main mechanism binding polycarboxylate to a surface for most of

organic admixtures[26].

The adsorption amount of admixture can be evaluated using ultraviolet-visible (UV/Vis) spectroscopy[27].

Background on UV/Vis spectroscopy:

Electromagnetic radiation such as visible light is commonly treated as a wave phenomenon, characterized by a wavelength or frequency. Wavelength is the linear distance between any maxima or minima, and is designated in meters, centimeters or nanometer (1 nm = 10^{-9} m). The frequency is the number of oscillations of an electromagnetic field that occur per second and is equal to the inverse of the period, which is the time in seconds required for the passage of successive maxima or minima. Visible wavelengths cover a range from approximately 400 to 800 nm[28]. The range of wavelength for different color can be summarized as follow: Violet: 400 – 420 nm, Indigo: 420 – 440 nm, Blue: 440 – 490 nm, Green: 490 – 570 nm, Yellow: 570 – 585 nm, Orange: 585 – 620 nm, and Red: 620 – 780 nm[28]. The longest visible wavelength is red and the shortest is violet.

When samples are exposed to light having energy, or when radiation passes through a layer of solid, liquid, or gas, certain frequencies may be selectively absorbed, a process in which electromagnetic energy is transferred to the atoms, ions, or molecules composing the sample. Absorption promotes theses particles from their normal room temperature state to one or more higher-energy excited states[29]. According to quantum theory, atoms, molecules, or ions have only a limited number of discrete energy levels for absorption of radiation to occur[29]. The energy of the exiting photon must exactly match the energy difference between the normal room temperature state and one of the excited states of the absorbing species. Since these energy differences are unique for each

27

species, a study of the frequencies of absorbed radiation provides a means of characterizing the constituents of a sample of matter. For this purpose, ultraviolet visible (UV/Vis) spectroscopy is commonly used to determine the absorption or transmission of UV/Vis light of a sample. A plot of absorbance as a function of wavelength or frequency is experimentally determined.

The Beer-Lambert law is most often used in a quantitative way to determine concentrations of an absorbing species in solution. It is expressed as: $A = \log \frac{P_o}{P} = \varepsilon \cdot c \cdot L$. Where A is the measured absorbance, (P_o) is the intensity of the incident light at a given wavelength, (P) is the transmitted intensity (see Figure 1.7). L is the pathlength through the sample, and c the concentration of the absorbing species. For each species and wavelength, ε is a constant known as the molar absorptivity or extinction coefficient. This constant is a fundamental molecular property in a given solvent, at a particular temperature and pressure, and has units of $1/M \cdot cm$.
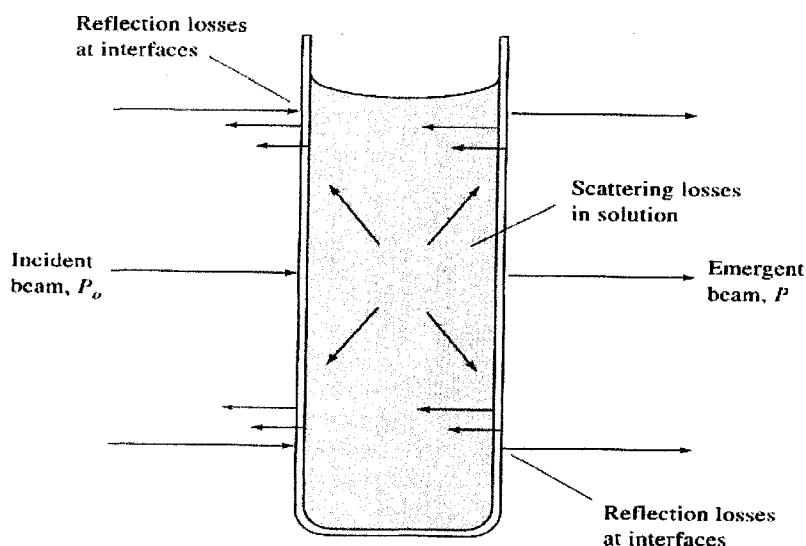
Figure 1.7: Reflection and scattering loss[29]

The Beer-Lambert Law is useful for characterizing many compounds but does not hold as a universal relationship for the concentration and absorption of all substances.

1.2.3.2.3.2   Electrostatic repulsion

The second mechanism of action of plasticizer in a concrete mixture is electrostatic repulsion. Electrostatic forces can be either repulsive between particles of identical charges or attractive between particles of opposite charge. As described above, a negative charge is induced by the adsorption of anionic plasticizer resulting in repulsive forces. In fact, the adsorbed anionic surfactant will send a net negative electrical charge to the particle surface (i.e zeta potential) inducing repulsion between neighboring cement particles and increasing their dispersion, thus requiring less water for a given degree of concrete workability. Figure 1.8 shows a typical electrostatic repulsion mechanism.
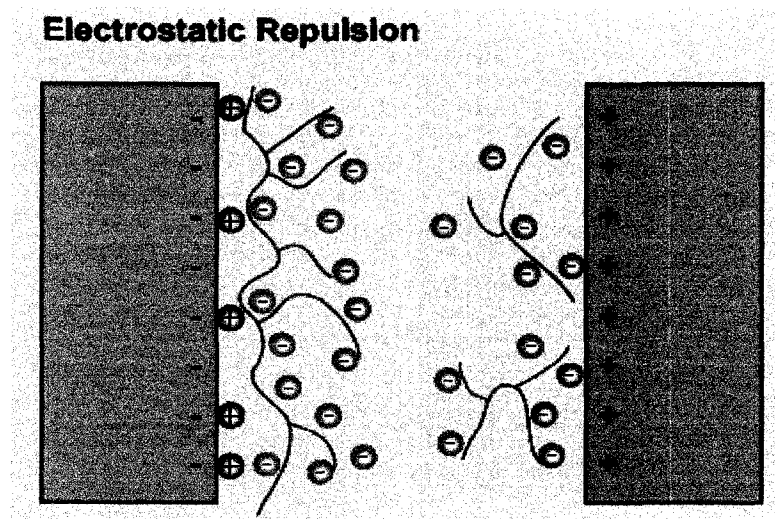
Figure 1.8: Electrostatic repulsion mechanism of organic molecules at the cement solution interface[12]

Figure 1.9 documents a schematic representation of zeta potential. The zeta potential is the overall charge a particle acquires in a specific medium. The surface of a solid particle is usually charged in presence of a fluid flow. Ions of negative and positive charges within the medium are attracted to the particles surface in order to neutralize the surface charge, and thus, create what is commonly referred to as an electric double layer. This liquid layer surrounding the particle is divided into two parts; an inner zone, called the stern layer, where the ions are strongly bound and an outer zone, a diffuse region, where the ions are less firmly attached. Inside the diffuse layer there is a theoretical boundary inside which the ions and particles form a stable entity. When a particle moves (e.g. due to gravity), ions within the boundary move with it, but any ions beyond the boundary do not travel with the particle. This boundary is called the surface of hydrodynamic shear or slipping plane. The potential that exists at this boundary is known as the Zeta potential[30].

The magnitude of the zeta potential gives an indication of the potential stability of the medium. If the particles in a suspension have a large negative or positive zeta potential then they will tend to repel each other and resist the formation of aggregates. In the case of low zeta potential values there is no force to prevent the particles coming together and there is dispersion instability. A dividing line between stable and unstable aqueous dispersion is generally taken at either +30 or -30 mV. Particle with zeta potentials more positive than +30 mV are normally considered stable, and particle with zeta potentials more negative than -30 mV are normally considered stable. The most important factor that affects the zeta potential is the pH. Zeta potential is typically quoted

Electrical double layer

Slipping plane

Particle with negative surface charge

Stern layer | Diffuse layer

-100

mV

Surface potential
Stern potential
Zeta potential

0

Distance from particle surface
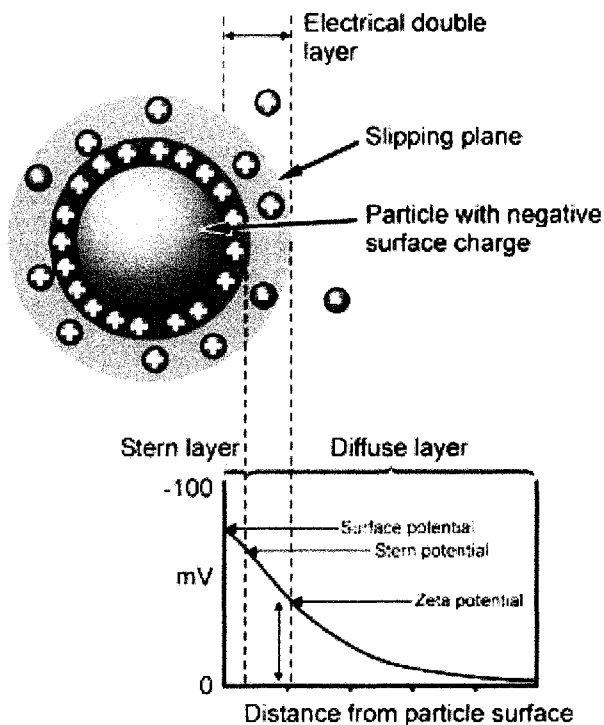
Figure 1.9: Schematic representation of zeta potential[30].

as a function of pH for a particular surface under investigation. The zeta potential versus pH curve will be positive at low pH and lower or negative at high pH. The pH at which the surface is zero is called the point of zero charge and is typically used to quantify or define the electro kinetic properties of the surface[30].

Flatt et al.[31] indicated that the electrostatic repulsion is intimately linked to the function of zeta potential and the polycarboxylic acid polymers (PCA) induce larger final zeta potential (around -23 mV), while polycarboxylic ester polymer polymers (PCE) induce lower potential ranging from -5 to -18 mV. This difference can be attributed to the fact that the PA-polymers are all strong electrolytes, and the PC-polymers are weak or very weak electrolytes. Thus, it is more likely that the dispersion by electrostatic repulsion of PA-polymers can be higher that of PE-polymers.

1.2.3.3   High range water-reducing admixture or superplasticizers

1.2.3.3.1   Function

Superplasticizers or high range water-reducing admixtures (HRWRA) have similar functions of normal plasticizers but are more powerful in their cement dispersing action and fluidity retention. The use of chemical admixture date from 1930s, but it was not until the 1970s that sulphonated melamine formaldehydes (in Germany) and analogous naphthalene derivatives (in Japan) were developed using reactive polymer[32]. In the early 1990s, superplasticizers or high range water-reducing admixtures (HRWRA) consisting of sulphonated salts of melamine or naphthalene formaldehyde condensates or copolymers of carboxylic acrylic acids were developed in order to improve the dispersibility and the slump retention of melamine and naphthalene type admixtures. HRWRA extends the working life of concrete up to 2 hours, depending on mixture type and environmental condition[33]. They are capable of reducing water requirements at a given workability by up to 30 to 45 %. The increase use of polycarboxylate-type admixture has limited the use of the melamine and naphthalene type admixtures in precast concrete and other high slump concrete application.

1.2.3.3.2   Chemical composition

The chemical composition of water-reducing admixture (WRA) and high range water-reducing admixture (HRWRA) are quite different. The main ingredients in superplasticizer are synthetic water-soluble polymers and that of plasticizer are organic products. Table 1.5, shown earlier, presents the main and secondary ingredients used in manufacturing of superplasticizing and plasticizing admixtures. The sulfonated melamine formaldehyde (SMF) and the sulfonated naphthalene formaldehyde (SNF) are

ionic linear organic polymers with sulphonate groups at regular intervals. Polycarboxylate (PC) is a generic name given to compounds that are classified into acrylate-based, methacrylate-based, or maleate-based, depending on the type of the main chain[34]. Figure 1.4 shows the formula of unit molecule of different sulfonated and acrylate-based polymers. The superplasticizer is formed by a repetition of these molecular units. For the case of polycarboxylate, at the backbone chain of the above cited polymers, various functional groups (polar or ionic, carboxyl, hydroxyl groups) are attached as side chains. The variations in type and length of the main and side chain of PC-type superplasticizer can affect its dispersibility.

1.2.3.3.3 Mechanism of action

The fundamental mechanism of action of superplasticizers has also been established and reported by several studies[1,10,12,23]. Most of HRWRA work in a very similar way to normal WRA. When naphthalene or melamine based-admixture is used, the action dispersing the particle is in most part due to the electrostatic repulsive force. Steric hindrance mechanism is the predominant effect for the polycarbonate-based admixtures mainly composed of an acrylic acid-acrylic acid ester copolymer. Uchikata et al.[35] reported that steric repulsive force is a short-range repulsive force caused by the overlapping of the adsorbed polymers. The steric repulsion effect is mainly attributed to the molecular structure of PC admixtures which is composed of a long straight chain of carbon atoms with the side chains branching from it[35]. Steric interaction occurs if the distance between the adsorbed polymers (as shown in Figure 1.10) is smaller than twice the thickness of superplasticizers[14]. Collerpardi et al.[23] found that the polymers molecules of CAE (see Figure 1.4) on the surface of cement might themselves hinder
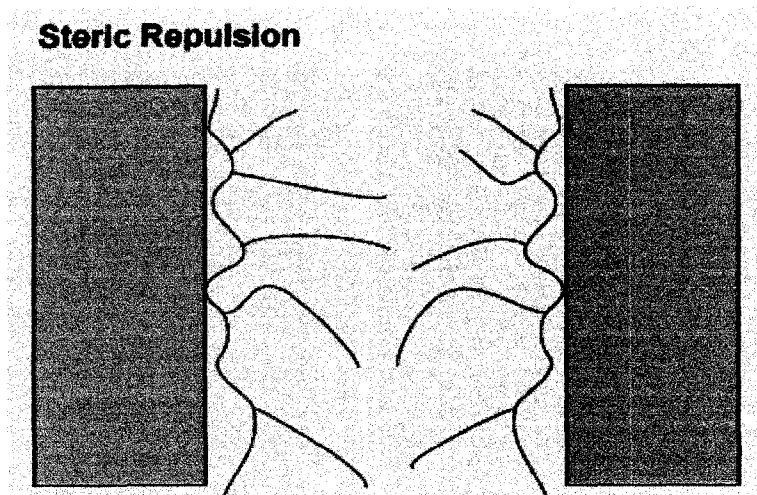
Figure 1.10: Steric hindrance mechanism of synthetic water-soluble polymers at the cement-solution interface[12]

flocculation into large and irregular agglomeration of cement particles. This mechanism would be in agreement with the relatively smaller number of negative anionic groups COO^- in the CAE copolymer in comparison with those present as SO_3^- in the SMF and SNF polymer.

In addition to electrostatic repulsive forces (F_{el}) and steric repulsive forces (F_{st}), it is reported in literature that Van der Waal's forces (F_{vdw}) are also acting between superplasticized-cement particles. They include momentary attraction between molecules, diatomic free elements, and individual atoms. They differ from ionic bonding in that they are not stable, but are caused by momentary polarization of the particle[14].

In summary, it can be reported that a superplasticizing admixture's mechanism of action involves adsorption of the polymer's anionic surfactants into the cement particles; electrostatic repulsive forces between neighboring cement particles; steric repulsive

forces consisting of short-range repulsive forces caused by the overlapping of the adsorbed polymers; and Van der Waal's forces i.e. momentary attraction between molecules, diatomic free elements, and individual atoms.

1.2.3.3.4 Superplasticizer in cement hydration products

The distribution of superplasticizer polymers can be divided into: (1) polymers in the pore water (P_w), dissolved in the pore water; (2) adsorbed polymers (P_{ads}), located on the hydrating cement surface; and (3) incorporated polymers (P_{inc}), incorporated in the hydrate products[15]. The total superplasticizer content (P_{tot}) which is initially added to the concrete is the sum of the above three portions.

$$P_{tot} = P_w + P_{ads} + P_{inc} = P_w + P_{cem} ,$$

Or

$$P_{cem} = P_{tot} - P_w$$

Where: P_{cem} is the superplasticizer adsorbed or incorporated in the cement hydration product.

Andrea[15] reported that since the determination of P_{ads} and P_{inc} is very complicated or impossible, then P_{cem} can be obtained through the total superplasticizer added to the matrix. It is not a direct measure of dispersion or fluidity because it contains P_{ads} and P_{inc}.

1.2.3.3.5 Time of addition of superplasticizer

The time of addition of the superplasticizer or plasticizer can affect the duration of its effectiveness. SMF and SNF polymers are adsorbed more, particularly on the C_3A hydration products, when the immediate addition in mixing water is adopted. This effect seems to be related to the production of large amount of ettringite coating on the surface

of cement particles during the initial cement hydration (see sections 1.2.2.3). An increase in superplasticizer dosage is not a solution, because larger amount of admixture than normally needed may retard the time of set by preventing or delaying the hydration product to flocculate. Also the addition of superplasticizer with mixing water causes strong incorporation of the polymer molecules into the C_3A-gypsum system, and leaves only small amounts of polymers for dispersion of C_3S and C_2S. The acrylic polymer-based superplasticizers are proven to be much less independent of the time and method of addition[23].

1.2.3.3.6 Effect of chemical structure on polycarboxylate polymer

The modification of the chemical structure of polycarboxylate-based polymer admixture is easier than that of the naphthalene-based[34]. As shown in Figure 1.11, the ratio of the acid and ester can be varied by changing modulus n and m. The higher the acid ratio, the higher the carboxylic group content, and easily the polymer can adsorb to cement particles leading to a higher dispersibility. On the other hand, the higher the ester ratio, the higher the side chain content, therefore, the content of carboxylic group relatively decreases and the polymer cannot so easily adsorb to the cement particles, consequently the dispersibility of the polycarboxylate polymer at the same dosage decreases. In the later case, the remaining molecules adsorbed gradually to cement particles as time elapsed, thus increased the fluidity retention[34].

The cement composition, especially the C_3A, SO_3 and alkali contents, which control the rate of ettringite formation, may have an effect on cement-admixture interaction. The cement fineness also increases the surface area, decreasing the adsorption for a given superplasticizer dosage. The relative reactivity of the four main

36
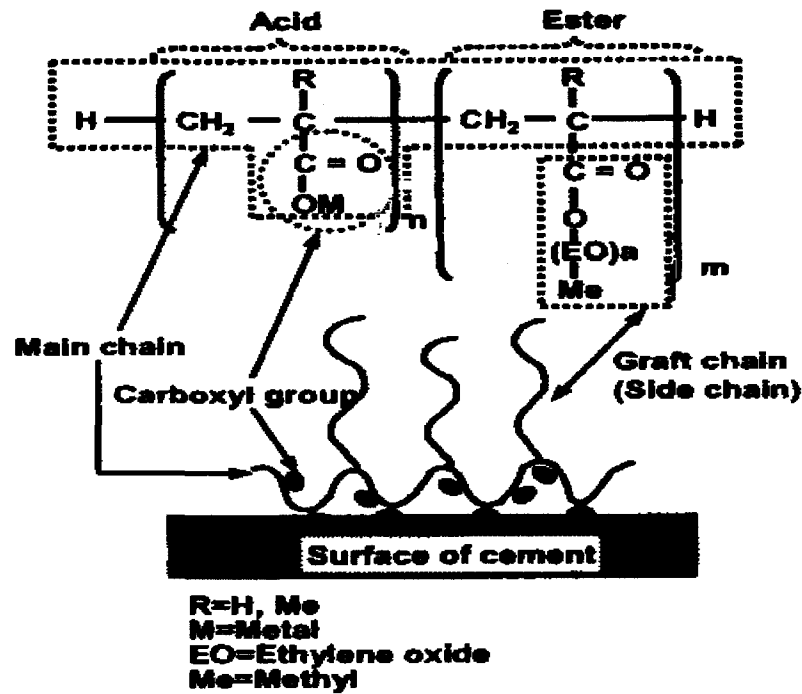
Figure 1.11: Polycarboxylate-cement system: Model of copolymer of acrylic acid and

acrylic ester[34]

mineral phases with water can be classified as $C_3A > C_3S > C_2S \cong C_4AF$. During the

initial cement hydration, because of its high reactivity, the C_3A is converted into

ettringite in the presence of the dissolved components Ca^{2+} and SiO_4^{2-} of gypsum. An

increase in the cement C_3A content will lead to an increase of the surface area of the

hydrate cement product due to the increase in formation of ettringite compounds.

Therefore, the adsorbed volume of polymer per unit area of cement particle decreases

along with its dispersibility[18,34].

Alkali by itself does not affect the performance of a superplasticizer[34], but SO_4^{2-}

affects it greatly because its concentration in the liquid phase is varied by the presence of

alkali. When the concentration of SO_4^{2-} increases, the main chain of the PC-polymer

contracts, decreasing the steric hindrance effect. Both SO_4^{2-} and PC polymer competitively adsorb onto the surface of solid phase. The presence of SO_4^{2-} can detach the already adsorbed PC polymer, decreasing the adsorption volume[34].

1.2.3.4   Viscosity modifying admixture (VMA)

With the increased use of flowable concretes, such as SCC, to facilitate placement in congested and/or restricted areas, unstable dispersion of cement paste and aggregate particles become recurrent. The tendency of heterogeneous materials to separate increases with the reduction of viscosity, due to an increase fluidity of the concrete, or when the concrete is subjected to a high shear rate, such as that encountered during pumping[36]. Viscosity modifying admixtures (VMA) are relatively new admixtures engineered and formulated to enhance concrete performance by modifying the viscosity and controlling the rheological properties of the concrete mixtures. They were first used in Germany in the mid-1970s, later in Japan in the early 1980s, and in the North America in late 1980s.

1.2.3.4.1   Function

The key function of a VMA is to modify the rheological properties of the cement paste, i.e. the yield point and the plastic viscosity. Yield point is the force needed to start the concrete moving. It is related to the workability of the concrete. The plastic viscosity, usually caused by internal friction, describes the resistance of a concrete to flow under external stress and relates to the speed of concrete flow. The incorporation of VMA in a concrete mixture can improve its rheological properties, cohesion and stability, thixotropic properties, stability during transport and placement, pumpability, finishability, and bleeding[9,36].

1.2.3.4.2 Chemical composition

Viscosity modifying admixtures are water-soluble polymers which can be natural, semi-synthetic, and synthetic[37]. Natural polymers include starches, guar gum, locust bean gum, alginates, agar, gum arabic, welan gum, xanthan gum, rhamsan gum, and gellan gum, as well as plant protein. Semi-synthetic polymers include decomposed starch and its derivatives; cellulose-ether derivatives, such as hydroxypropyl methyl cellulose (HPMC), hydroxyethyl cellulose (HEC) and carboxy methyl cellulose (CMC); as well as electrolytes such as sodium alginate and propyleneglycol alginate. Finally, synthetic polymers include polymers based on ethylene, such as polyethylene oxide, polyacrylamide, polyacrylate, and those based on vinyl, such as polyvinyl alcohol. Some VMAs are based on inorganic materials such as colloidal silica which is amorphous with small insoluble, non-diffusible particles, larger than molecules but small enough to remain suspended in water without setting. By ionic interaction of the silica and calcium from the cement a three dimensional gel is formed which increases the viscosity and/or yield point of the paste[9,36].

The viscosity modifying admixtures commonly used in cement-based system are water-soluble polysaccharides, such as cellulose ether derivatives and microbial-source polysaccharides, such as welan gum, that bind some of the mixing water, thus enhancing viscosity. Acrylic-based polymers, such as partial hydrolysis products of a polyacrylamide copolymer and sodium acrylate, are also employed. Welan gum is an anionic, high molecular weight (around 2 millions g/mol) polysaccharide produced by a controlled aerobic fermentation process. Welan gum is a long-chain biopolymer with sugar backbone substituted with sugar chains[9,36].

Viscosity modifying admixtures can be supplied as a powder blend or liquid-based products to make dosing easier and accurate. The dosage depends on the application but typically ranges from 0.1 to 1.5% by weight of cement. Most VMAs have little effect on other concrete properties in either the fresh or hardened state but some, if used in high dosage, can affect setting time and/or the content and stability of entrained air[9].

1.2.3.4.3   Mechanism of action

Khayat[36] reported that the mode of action of VMA in cement-based system can be attributed to adsorption, association, and intertwining.

- Adsorption: First, the long-chain polymer molecules adhere to the periphery of water molecules, thus adsorbing and fixing part of the mix water and thereby expanding, and increasing the viscosity of the mix water and cement-based product.

- Association: The molecules in adjacent polymer chains can develop attractive forces, thus further blocking the motion of water, causing a gel formation and an increase in viscosity.

- Intertwining: At low rates of shear, and especially at high concentrations, the polymer chains can intertwine and entangle, resulting in an increase in the apparent viscosity. Such entanglement can disaggregate, and the polymer chains can align in the direction of the flow at high shear rates, hence resulting in shear thinning.

Viscosity modifying admixtures can be grouped into two main types based on the mechanism by which they function, namely: thickening-type and binding-type[38].

- Thickening-Type VMA: The VMAs in this group function by thickening the concrete, making it very cohesive without significantly affecting the fluidity of the mixture.

- Binding-Type VMA: These VMAs function by binding water within the concrete mixture. This mechanism results in an increase in the viscosity of the mixture, while reducing or eliminating concrete bleeding. This type of VMA is more potent in modifying the viscosity of SCC mixture compared to a thickening-type VMA. They also take on the concrete's thixotropic characteristic, which means that fresh concrete may gel up if left in a mixing vessel, truck, or form without agitation. Simply re-mixing the concrete can restore workability.

1.2.3.5 Admixture compatibility

When using flowable concrete such as self-consolidating concrete, the balance between the yield point and the plastic viscosity is the key in obtaining the appropriate concrete rheology. VMA is used to increase the plastic viscosity but usually causes only a small increase in yield point whereas HRWRAs are used to decrease the yield point. Since HRWRAs are sometimes used in conjunction with a VMA to optimize the yield point[9], their compatibility becomes important. The use of polyalkylaryl sulphonate water-reducing admixture in aqueous solutions containing cellulose VMA was reported to cause an abnormal increase in viscosity[36]. Kawai and Okada[37] also found that the use of hydroxypropyl methyl cellulose (HPMC) in an aqueous solution possessing a pH of 13 and containing a naphthalene-based HRWRA can result in a sharp increase in viscosity when the HPMC and HRWRA contents were respectively greater than 0.8% and 1% by mass of water. This was attributed to the formation of chemical gel resulting from the incompatibility between the two admixtures. Welan gum does not exhibit an incompatibility with either melamine-based or naphthalene-based HRWRAs[36].

1.2.4 Mineral admixtures

The mineral admixtures are usually added to concrete in large amounts. Beside cost reduction and workability improvement of the fresh concrete, they can successfully be employed to improve the resistance of concrete to thermal cracking, alkali-aggregate expansion, and sulfate attack. Some mineral admixtures are pozzolanic, some are cementitious and others are both pozzolanic and cementitious. The mineral admixtures can be divided into two main groups: natural materials and by-product materials. The natural materials all mostly derived from volcanic rocks and mineral (except diatomaceous earths). They are processed for the sole purpose of producing a pozzolan, by crushing, grinding, and separating the sizes. Based on the principal reactive constituent, the natural material can be classified into volcanic glasses, volcanic tuffs, calcined clays or shales, and diatomaceous earths[10]. The by-product material mineral admixtures are not the primary products of the industry producing them. They may or may not require any drying or pulverization before use as mineral admixture. The most important by-product materials, used in production of self-consolidating concrete, are described below:

1.2.4.1 Fly ash

Fly ash is the most widely used supplementary cementitious material in concrete. It is comprised of the non-combustible mineral portion of coal. When coal is consumed in a power plant, it is first ground to the fineness of powder and blown into the boiler where after the consumption of carbon molten particles rich in silica, alumina and calcium are formed. These particles solidify as microscopic, glassy spheres that are collected from the power plant's exhaust[39].

According to the "Standard Specification for Fly Ash and Raw or Calcinated Natural Pozzolan for Use as Mineral Admixture in Portland Cement Concrete," (ASTM C 618[40]) three mains classes of fly ashes exist:

- Class F fly ash is normally produced from burning anthracite or bituminous coal. Class F materials are generally low-calcium (less than 10% CaO) fly ashes with carbon content usually less than 5%, but some may be as high as 10%;

- Class C fly ash is normally produced from burning lignite or subbituminous coal. Class C materials are often high-calcium (10% to 30% CaO) fly ashes with carbon contents less than 2%. In addition to being pozzolanic, class C fly ash is also cementitious. When exposed to water it will hydrate and harden in less than 45 minutes. Some fly ashes meet both Class F and Class C classification; and

- Class N fly ash, is a natural mineral admixture. It consists of raw or calcinated pozzolans such as diatomaceous earths, opaline cherts and shales, tuffs and volcanic ashes or pumicite, and calcinated materials such as clays and shales[10].

Most of the fly ash particles are solid spheres and some are hollow cenospheres[10]. The particles sizes vary from less than 1 μm (0.00004 inch) to more than 100 μm (0.004 inch) with the typical particle size measuring less than 20 μm (0.0008 inch). They are generally finer than cement. The surface area is typically 300 to 500 m^2/kg (176 to 293 yd^2/lb), although some fly ash can have surface areas as low as 200 m^2/kg (117 yd^2/lb) and as high as 700 m^2/kg (410 yd^2/lb). For fly ash without close compaction, the bulk density (mass per unit volume including air between particle) can vary from 540 to 860 kg/m^3 (34 to 54 lb/ft^3), whereas with close packed storage or vibration, it can range from 1120 to 1500 kg/m^3 (70 to 94 lb/ft^3)[10].

Chemically, fly ash is a pozzolan. ASTM C 125[41] defines pozzolan as a siliceous, or siliceous and aluminous material which in itself possesses little or no cementitious value but will, in finely divided form and in the presence of moisture, chemically react with calcium hydroxide at ordinary temperature to form compound possessing cementitious properties. One of the primary benefits of fly ash is its reaction with available lime and alkali in concrete, producing additional cementitious compounds which allow fly ash concrete to continue to gain strength over time. The following equations illustrate the pozzolanic reaction of fly ash with lime to produce additional calcium silica hydrate (C-S-H) binder.

Cement reaction: $C_3S + H \rightarrow C\text{-}S\text{-}H + CaOH$ (1.8)

Pozzolanic reaction: $CaOH + S \rightarrow C\text{-}S\text{-}H$ (1.9)
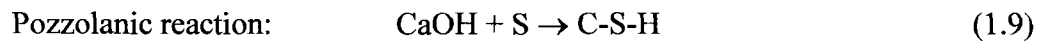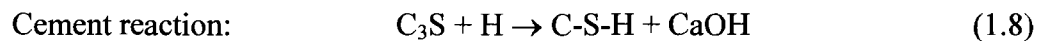
Where S is the silica from ash constituents.

1.2.4.2 Silica fume

Silica fume is a by-product of the manufacture of silicon or various silicon alloys produced in submerged electric arc furnaces (ASTM C 1240)[42]. The production of silicon consists of reducing a white quartzite (99.3% SiO_2) to silicon using high quality charcoal in an electric-arc furnace. A mixture of crushed quartzite, charcoal, and wood chips is continuously fed to the top of the furnaces. The furnaces, by rotating very slowly around the carbon electrodes, create electric arcs deep in the furnace bed and hence the high temperature needed to produce molten silicon. The production of ferro-silicon is similar to silicon production; however iron and lime are added to produce iron ferro-silicon. This does not necessarily lead to a reduction in SiO_2 content as ferro-silicon plants often have low carbon content.

Silica fume's particles are spherical in shape. They average 0.15 micron (6×10^{-6} inch) but vary from 0.01 to 1 micron (0.39×10^{-6} to 39×10^{-6} inch). Its color varies from pale to dark gray and is mostly influenced by the carbon and iron content. Silica fume is available in several forms according to its bulk density. The main three different forms are:

- Undensified form: In undensified form, the raw silica fume direct from the bag house ($160 - 240$ kg/m^3 ($10 - 15$ pcf)) is like a dense smoke. Yet because it is so light it almost floats, and handling becomes a major problem. Undensified silica fume is predominantly used in refractory grout, and mortars.

- Densified form: The densified form is obtained by blowing air through the fume in a silo to agglomerate the undensified silica fume. This forces the particles to move around other particles and adhere to them by surface force. Densification takes a couple of day with the silica fume's appearance changing. The bulk density increases to about $35 - 42$ pcf ($561 - 673$ kg/m^3) where the grain size increases to about 0.02 inch (0.5 mm). The fineness of silica fume is one of the two characteristics that make its super pozzolanic nature. Hence, it is vital that the agglomerations formed by densification breakdown during mixing. Densified silica fume is well-suited for concrete.

- Slurry form: Slurries are generally made from undensified silica fume. A conditioner (pH neutralizer) is added to stop setting and silica fume is mixed with water (approximately 1:1 weight). Other admixtures (e.g. superplasticizer) may be incorporated to the slurry. The main requirement of silica fume slurry is that it should not settle. Its ability to not settle is dependent on the particle size and added dispersants. Slurry has a unit weight of about 1300 kg/m^3 (82 pcf).

- Pelletized form: Water is sprayed onto the undensified silica in a pug to produce pellets. The pellets produced are 10 mm (3/8 of an inch), dustless and do not break down easily during concrete mixing. This form of silica fume is utilized in inter-ground silica fume blended cement.

The chemical composition of silica fume varies depending on the type of plant (silicon or ferro-silicon), the source of materials, and the method of plant operation. The major chemical components of silica fume are: silicon dioxide (SiO_2), ferric oxide (Fe_2O_3), and carbon (C). ASTM C 1240[42] requires the following chemical composition:

- SiO_2 85% minimum

- Moisture content   3% maximum

- Loss on ignition   6% maximum

The most important compound of silica fume is the SiO_2 content. The higher the SiO_2 content, the better silica fume performs when used as a mineral admixture in concrete. The primary benefit of silica fume is its pozzolanic reaction during secondary hydration process where it reacts with calcium hydroxide (hydrated lime) of Portland cement to form more C-S-H gel during the pozzolanic reaction. The hydration of silica fume concrete can be explained through equations 1.8 and 1.9 where S represents the silica from silica fume.

In addition to being much finer than cement (100 times finer), silica fume acts as a filler for the spaces between the cement grains. This higher fineness increases the rate at which silica fume hydrates and thus accelerates strength development. Several other physical properties of silica fume contribute to the enhancement of concrete. These include the increase in density of the composite system, the increase in cohesiveness, and

the decrease of bleeding due to the high surface area of the particle. However, the addition of silica fume increases the water demand, and unless a water reducer is used, more water is needed to achieve a desirable level of fluidity.

1.2.4.3   Ground granulated blast furnace slag (GGBFS)

ASTM C 989[43] defines blast furnace slag as a non-metallic product mainly consisting of calcium silicates and other bases that is developed in a molten condition simultaneously with iron in a blast furnace. Ground Granulated Blast Furnace Slag (GGBFS) is a by-product of the steel industry which is obtained when molten slag is quenched rapidly using water jets. GGBFS is granular with very limited crystal formation. It is classified into three grades, namely, 80, 100, and 120, according to the slag activity index which is the average compressive strength of the slag-reference cement cubes (SP), divided by the average compressive strength of the reference cement cube (P), and multiplied by 100.

The primary chemical composition of slag (about 95%) is in the form of silica, alumina, calcium oxide, and magnesia. The remaining 5% consists of manganese, iron, and sulfur. GGBFS becomes highly cementitious in the presence of water by using its SiO_2 to react with the $Ca(OH)_2$ generated by the hydration of cement in order to produce additional calcium silicate hydrate (C-S-H). This process is similar to the hydration of silica fume and fly ash, as shown by Equations 1.8 and 1.9, where S represents the silica from GGBFS. The additional C-S-H brought to the matrix by the incorporation of GGBFS increases the concrete strength and durability over time.

1.3   Specifications for the raw materials used in self-consolidating concrete

1.3.1   Aggregates

The coarse and fine aggregates meeting the requirements specified in ASTM C 33[44] shall be used. The nominal maximum size of coarse aggregate shall meet the followings:

- Not larger than 1/3 of the depth of slabs or panels

- Not larger than 3/4 of the minimum clear depth cover

- Not larger than 2/3 of the minimum clear distance between reinforcing bars or between bars and forms, whichever is least

- In no instance shall the nominal maximum size of aggregates exceed 20 mm (3/4 inch).

In the absence of a specific gradation target, and if approved by the Engineer, the combined gradation of coarse and fine aggregates may be within the bands of the following Table 1.6. Targets and production tolerances necessary to meet the requirements of the table shall be established by the Engineer. The Contractor shall submit documentation to the Engineer justifying any deviation from the approved gradation.

1.3.2   Portland cement

Portland cement suitable for use in self-consolidating concrete shall conform meet one of the following specifications: ASTM C 150[13], C 595[45], or C 1157[46]. Cement of the same type, brand, and color from the same mill shall be used throughout any given project. Unless otherwise stated, Type II or V Portland cement shall be used.

Table 1.6: Aggregate gradations (Percent passing by dry weight of aggregate)[47]

Sieve size	¾" Operating bands	½" Operating bands
¾ inch	95 - 100	
½ inch	65 - 95	95-100
3/8 inch	58 - 83	65 - 95
No. 4	35 - 65	50 - 80
No. 8	25 – 50	30 - 60
No. 16	15 - 35	20 - 45
No. 30	10-35	12-35
No. 50	5-20	5-20
No. 100	1-12	2-12
No. 200	0 - 2	0 - 2

1.3.3   Mineral fillers and pozzolanic/hydraulic materials

Due to the fresh property requirements of SCC, inert and pozzolanic/hydraulic additions are commonly used to improve and maintain the cohesion and segregation resistance. The addition will also regulate the cement content in order to reduce the heat of hydration and thermal shrinkage. All mineral admixtures or pozzolans meeting ASTM C 618[40] (Fly ash), C 989[43] (Ground blast furnace slag), or C 1240[42] (Silica fume) may be used.

1.3.4   Water type and quality

Water shall be potable or meet the specified test standard in AASHTO M 157[48], or complied with the requirements of ACI 301[49] "Specifications for Structural Concrete for Buildings." Water shall not contain iron or iron oxides.

1.3.5 Admixtures

The self-consolidating concrete admixture system shall consist of either a polycarboxylate-based high range water-reducing admixture or a polycarboxylate-based high range water-reducing admixture combined with a separate viscosity modifying admixture. The same brand and type of admixtures shall be used throughout all parts of the project. Admixtures containing chloride ions shall not be used in prestressed concrete, or in concrete containing aluminum embedment or galvanized reinforcement and/or hardware. Producer shall verify via trial that admixtures are compatible.

1.3.5.1 High range water reducing admixture:

The polycarboxylate-based high range water-reducing admixture (HRWRA) shall be in accordance with AASHTO M194[50], Type F or G, or ASTM C 494[21] Type F or G, or ASTM C 1017[51]. All HRWRA admixtures must be compatible with admixtures that are present in slurry silica fume, if any.

1.3.5.2 Viscosity modifying admixture:

The viscosity modifying admixture (VMA) shall be evaluated according to the test methods and mixture design proportions referenced in AASHTO M 194[50]. Although not required, a VMA is recommended as a way to enhance the resistance to segregation, homogeneity, and flow of SCC.

1.3.5.3 Other admixtures:

Other admixtures including air entraining, accelerating and retarding may be used in the same way as in traditional vibrated concrete but advice should be sought from the admixture manufacturer on the use and the optimum time for addition. They should conform to ASTM C 260[52] or C 494[21]. Any coloring admixtures used shall also conform

to ASTM C 979[53].

1.4   Suggested guidelines for mixture proportioning of self-consolidating concrete

The guidelines presented herein are obtained from various national and international sources[47].

1.4.1   Aggregate ratio

A fine aggregate content of 40 to 60% of the combined coarse and fine aggregates weight shall be used. Particle size of 12 mm (1/2 inch) shall be between 28 to 32% of the total absolute volume of coarse aggregates, and up to 50% shall be more than 10 mm (3/8 inch).

1.4.2   Cement factor

A minimum of 380 kg/m^3 (639 pcy) for a w/cm ratio between 0.44 and 0.37, a minimum of 490 kg/m^3 (825 pcy) for a w/cm ratio between 0.37 and 0.33, or a minimum of 535 kg/m^3 (900 pcy) for a w/cm ratio of below 0.33 shall be used.

1.4.3   Water-to-cementitious materials ratio

Water-to-cementitious materials ratio (w/cm) shall not exceed 0.48.

1.4.4   Pozzolanic/hydraulic additions

With approval of the Engineer, pozzolanic and hydraulic materials may be substituted for a portion of the cement for the limits indicated below:

• Fly ash: a minimum of 20% and a maximum of 40% by weight shall be used.

• Silica fume: a minimum of 6% and a maximum of 8% by weight shall be used.

• Ground granulated blast furnace slag (GGBFS): a maximum of 40% by weight shall be used. A minimum of 10% fly ash shall be used with GGBFS.

• Total Pozzolanic/Hydraulic Additions: the total ternary combinations shall not exceed

40%.

1.4.5 Water-reducing, high range water-reducing, and viscosity modifying admixtures

The recommended dosage range for admixture is usually given by the manufacturer. However, trial mixes should be done to verify plastic and hardened performance with local materials.

1.4.6 Air Entrainment

Units subject to freezing and thawing, deicer, and wet-dry conditions shall be fabricated from air-entrained concrete and shall conform to the following Table 1.7. If approved by the Engineer, for the specified compressive strength greater than 35 MPa (5,000 psi), a reduction in air content by 1 percent may be permitted.

Table 1.7: Required air content of self-consolidating concrete[47]

Nominal maximum size of aggregate, inch (mm)	Total air content, percent by volume	
	Severe Exposure	Moderate Exposure
Less than 3/8 (9)	9.00	7.00
3/8 (9)	7.50	6.00
1/2 (13)	7.00	5.50
3/4 (19)	6.00	5.00

Additionally, particular attention should be given to air void characteristics and stability. In order to be effective at providing freezing and thawing protection, the diameter of the air bubbles must be between 10 and 1000 micrometers (0.0004 to 0.04 inch). They must also be in proper amount and spacing (spacing factor larger than 0.200 mm (0.008 inch)).

1.6   Research objectives

The research study presented herein was intended to compare the influence of four different admixture sources, and to study the impact of construction-related variables on the fresh and hardened properties of three distinct groups of self-consolidating concretes (SCC) using local raw materials. The investigation was divided into two major phases. The first phase studied the influence of four distinct sources of polycarboxylate-based high range water-reducing admixtures and their corresponding viscosity modifying admixtures on the fresh and hardened performance of the three groups of self-consolidating concrete. The second phase investigated the effect of hauling time, temperature, and combined hauling time and temperature on the fresh properties of the selected self-consolidating concretes. The adverse influence of the above-mentioned parameters was remediated by way of overdosing and retempering.

In order to achieve the stated objectives, the findings of the study are divided into seven chapters.

• Chapter 1 is devoted to the background related to ordinary and self-consolidating concretes' constituent materials, their actions and interaction mechanisms, the specifications of raw materials for use in self-consolidating concrete, and the suggested guidelines for the self-consolidating concrete mixture proportioning.

• Chapter 2 presents the experimental program used herein including the preparation and appraisal of raw materials, the mixing sequence and sampling procedure, and the description of the testing equipments and procedures.

• Chapter 3 reports on the findings of three distinct groups of the self-consolidating concretes which were produced with four different admixture sources. The influences of

admixture sources and slump flow values on the fresh and hardened properties of the designed self-consolidating concretes were examined.

- Chapter 4 discusses the influence of hauling time on flow ability, flow rate, and dynamic stability of the selected self-consolidating concretes. The remediation of the matrices affected by the adverse impact of hauling times is also presented.

- Chapter 5 presents the influence of extreme hot and cold temperatures on flow ability, flow rate, and dynamic stability of the selected self-consolidating concretes. Additionally, the remediation methodology used to revert the adverse effect of extreme temperatures on the trial plastic concrete is discussed.

- Chapter 6 examines the influence of the combined hauling time and temperature on the properties of the fresh self-consolidating concretes. The effectiveness of two remediation methods by way of overdosing and retempering to encounter the influence of combined hauling time and temperature on the trial fresh matrices is discussed.

- Chapter 7 summarizes the mains conclusions of the investigation and suggests recommendations for future companion investigations.

1.7   Research significance

The world climate has been unusual and unnatural during the last half of this century due to the global warming. Warmer, colder, drier and wetter climate than the climatic average have been recorded all over the world during the last several years. Undeniably, one of the negative effects of this global warning is its influence in construction industry and, particularly, in concrete designing, mixing, transporting, placing, and curing.

The attractiveness of self-consolidating concrete stems from its multiple benefits

in both cast-in-place and pre-cast applications. Examples of such benefits include: placement without vibration, placement in a highly congested formwork, self-leveling and less screeding, higher quality surface finishing, faster construction scheduling and less labor efforts, and reduction in construction noise and in-place cost.

The results of the present study are useful to the efforts aimed at:

(1) Understanding the role of different admixture sources on fresh properties of self-consolidating concretes, (2) simulating concrete mixing and hauling by the mean of truck mixer during extreme temperatures, (3) evaluating the effectiveness of two remediation methods to combat the adverse impact of hauling time and temperature on plastic self-consolidating concrete, and (4) predicting the losses in fresh properties of self-consolidating concrete induced by hauling time, temperature, and combined temperature and transportation time.

CHAPTER 2

EXPERIMENTAL PROGRAM

Modern concrete technology produces highly engineering materials in which, by the careful selection and proportioning of constituents, their characteristics are designed to fulfill specific needs. The more advanced the concrete becomes; such as self-consolidating concrete, high performance concrete, pumpable concrete; the more sensitive it gets to materials' variations and fluctuations during production and placement. Variations in the moisture content or grading of the aggregates, and fluctuations in the fine content of the aggregate are among the major problems encountered in production sites. The goal of the present chapter is to present the experimental program used throughout this investigation. Preparation and appraisal of the raw materials, description of testing equipments and procedures are also covered.

2.1   Material preparation and appraisal

Self-consolidating concrete is a concrete made mainly with conventional concrete materials such as aggregates, cement, supplementary cementitious materials, admixtures, and water. The descriptions of the raw materials used in this investigation are presented below.

2.1.1   Aggregates

Because coarse and fine aggregates generally occupy 60 to 75% of the concrete volume, the selection of aggregates becomes significant in developing concrete that

meets the required specifications. Coarse aggregate size, shape, and total volume play a critical role in SCC performance. A rounded coarse aggregate imparts greater filling ability for the same water content when compared with a crushed stone of similar size. Additionally, when all others mixture parameters are equal, a concrete mixture containing well-rounded natural gravel can be used at a higher volume than angular crushed aggregate of the same gradation. The fine aggregate gradation is equally important and should be evaluated for suitability in self-consolidating concrete.

For the purpose of this investigation, three distinct sizes of coarse aggregate, provided by two different Southern Nevada quarries, were selected. The aggregates were given designations of R8, R67, and S7 to avoid any commercialization interest. The letters R and S refer to the quarries in which the aggregates were obtained from, and numbers "8", "67", and "7" indicate their size designations based on the requirement of ASTM C 33[44].

- *Quarry R*

The aggregates from the Quarry R were evaluated in the laboratory. The test results revealed that they satisfied the requirements of ASTM C 33[44] fine aggregate, and ASTM C 33[13] #8 or #67 coarse aggregates. The fine aggregate had well-rounded particles that were dense and relatively smooth in nature. The coarse aggregate was crushed stone, angular to irregular shape with a granular surface texture. The physical properties of Quarry R aggregates are shown in Table 2.1, whereas their size distributions are presented in Figures 2.1, 2.2, and 2.3.

- *Quarry S*

Samples of fine and coarse aggregates obtained from Quarry S were also tested

per ASTM C 33[44]. The coarse aggregates satisfied the gradation requirements of ASTM C 33[44] #7 and the fine aggregate remained within the allowable size limit. While the aggregates' shape and texture were similar to those of Quarry R, their color and bulk density indicated a different mineralogical origin. The size gradations of these aggregates are presented in Figures 2.4 and 2.5 and their physical properties are given in Table 2.1.

All aggregates were shipped from the quarries in an open station truck and were stored in 208-liter (55-gallon) steel drums. Each time, approximately 68 kg (150 lbs) of material were air- dried until moisture contents of about 0.15 and 0.20% were obtained for fine and coarse aggregates, respectively. The aggregates were then placed in sealed cans in order to prevent any moisture variation. The moisture content of the aggregates was monitored on a weekly basis.

2.1.2 Portland cement

Portland cements suitable for use in self-consolidating concrete should meet one of the following specifications: ASTM C 150[13], C 595[45], or C 1157[46]. Commercially available Type V Portland cement was used in this study. This type of cement is suitable for uses where special properties, such as a sulfate resistance, are required. The cement, obtained from a single supplier, complied with the ASTM C 150[13] specifications and its physico-chemical characteristics are shown in Tables 2.2. These data are the average information provided by the supplier for five different deliveries (average data of five mill certificates). Upon delivery, the Portland cement was placed in plastic bags and stored in sealed cans in the laboratory room at temperature of 21 ± 2 °C (70 ± 3 °F), prior to use.

Table 2.1: Physical properties of aggregates

Aggregates		Color	Bulk specific gravity (SSD)	Absorption (%)	Dry rodded unit weight (kg/m^3)	Fineness Modulus
Quarry R	Fine aggregate	Yellow dark	2.54	1.50	-	2.85
	Coarse aggregate ASTM C33 #8	Gray	2.58	1.40	1515	N/A
	Coarse aggregate ASTM C 33 #67	Gray	2.60	1.00	1546.00	N/A
Quarry S	Fine aggregate	White	2.78	0.80	-	3.00
	Coarse aggregate ASTM C #7	White	2.79	0.60	1634.00	N/A

1 kg/m^3 = 1.684 lb/yd^3
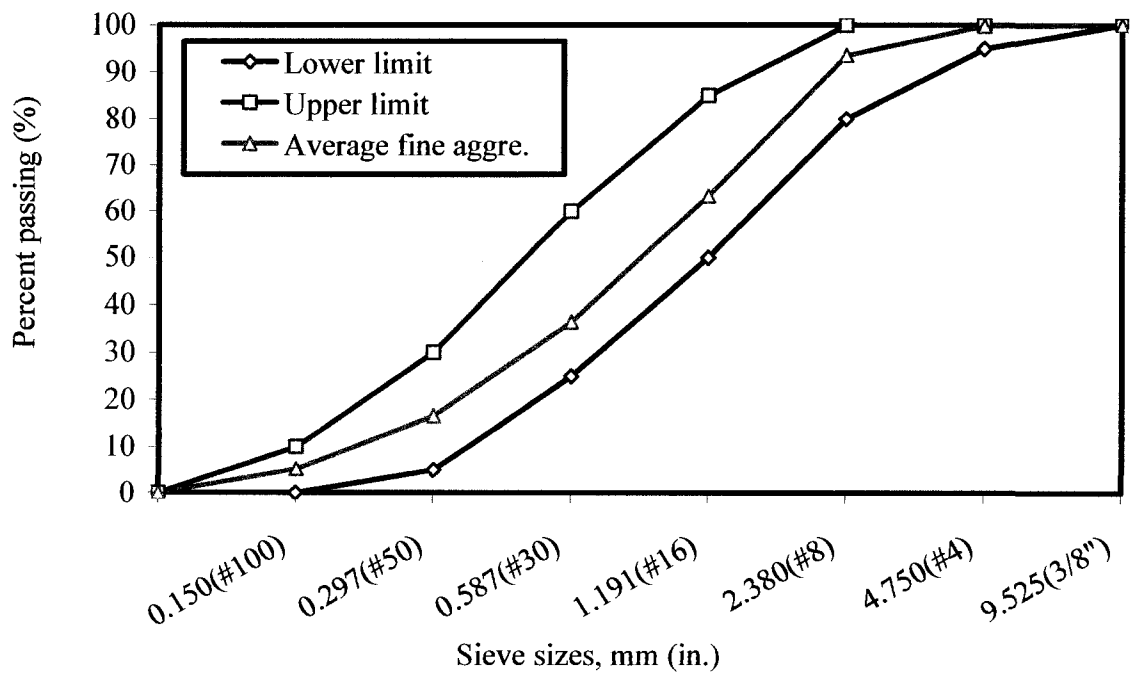
Figure 2.1: Quarry R fine aggregate size distribution
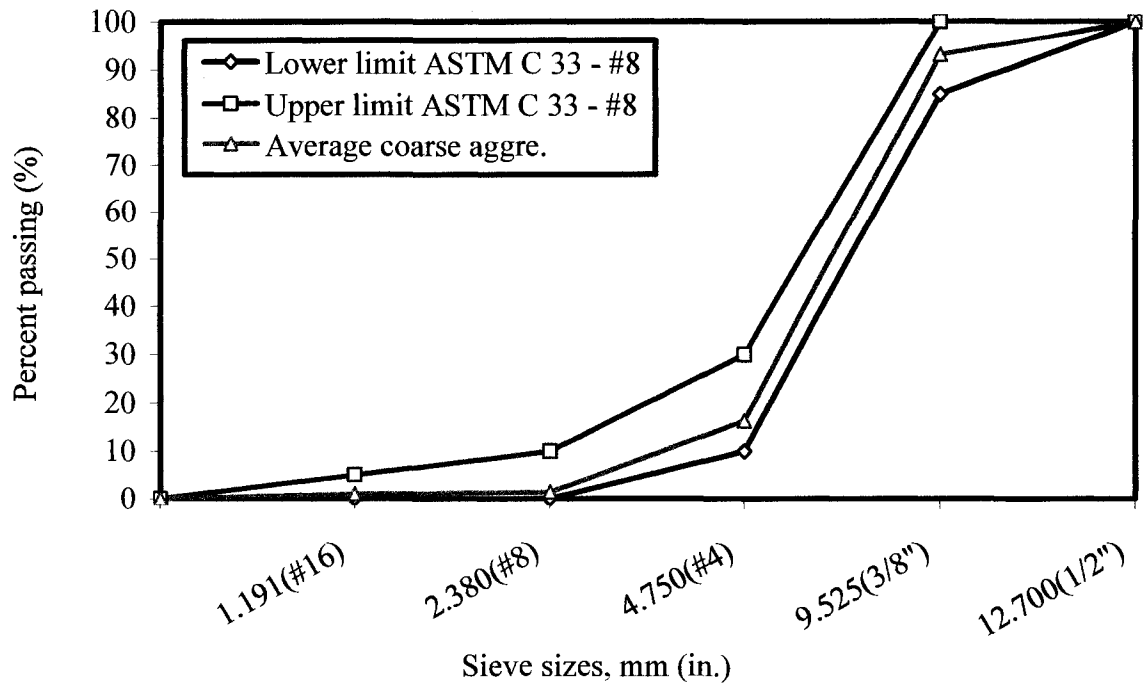
Figure 2.2: Quarry R ASTM C 33 #8 coarse aggregate size distribution
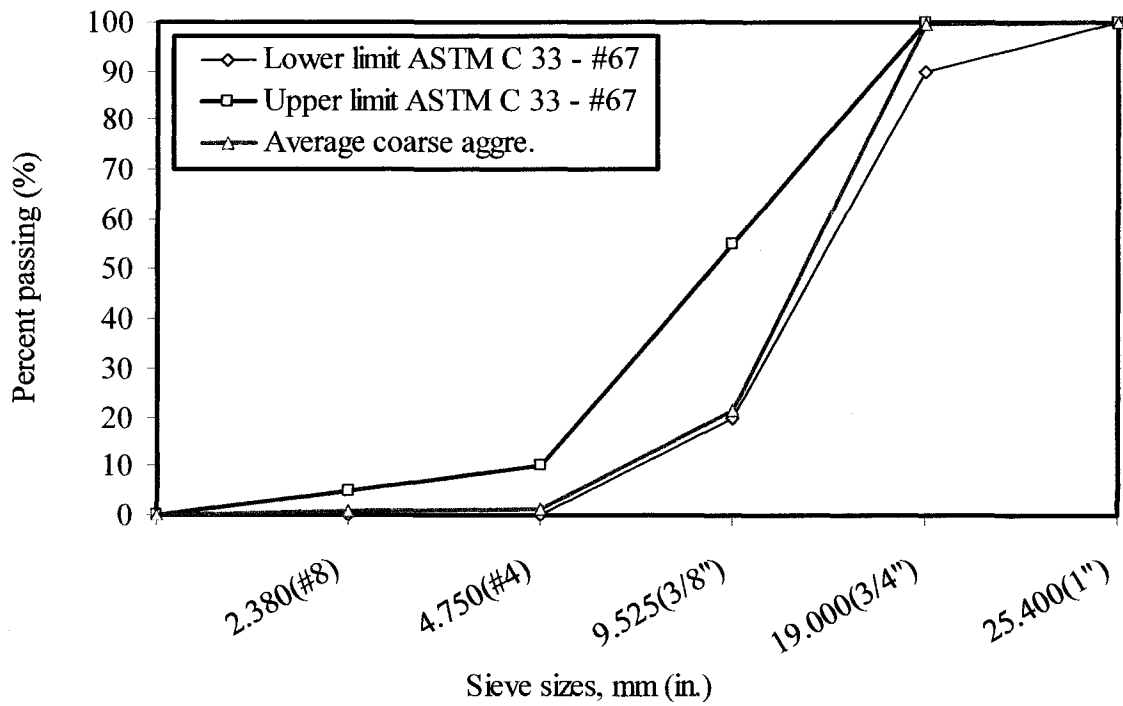
Figure 2.3: Quarry R ASTM C 33 #67 coarse aggregate size distribution
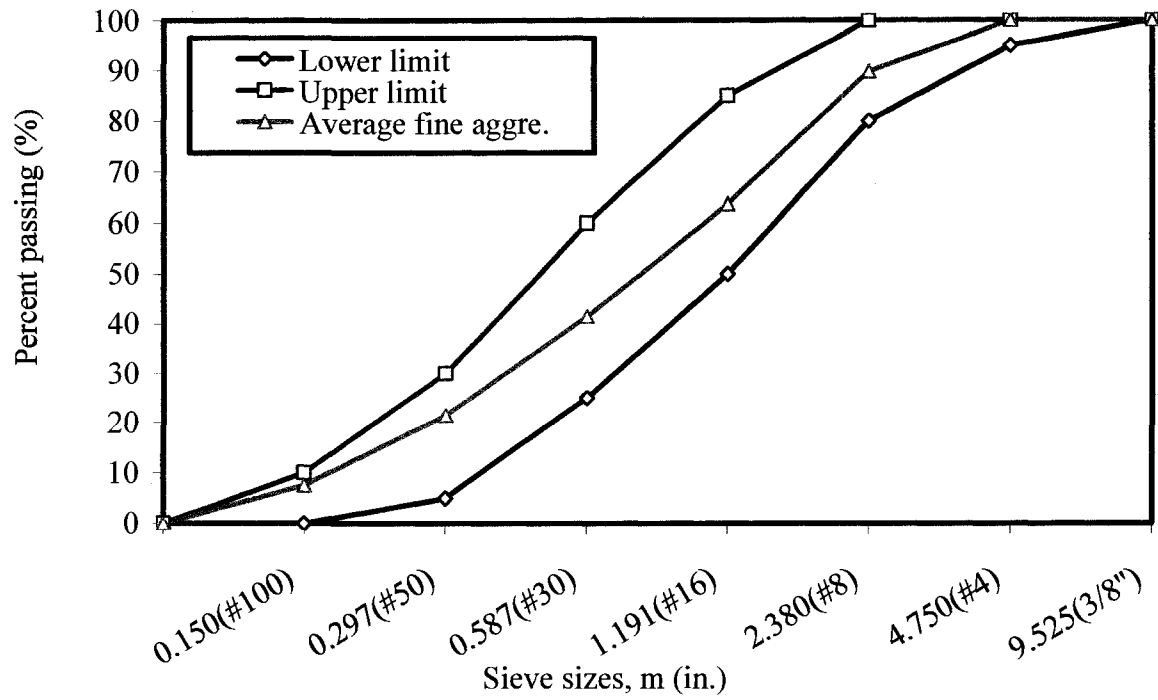
Figure 2.4: Quarry S fine aggregate size distribution
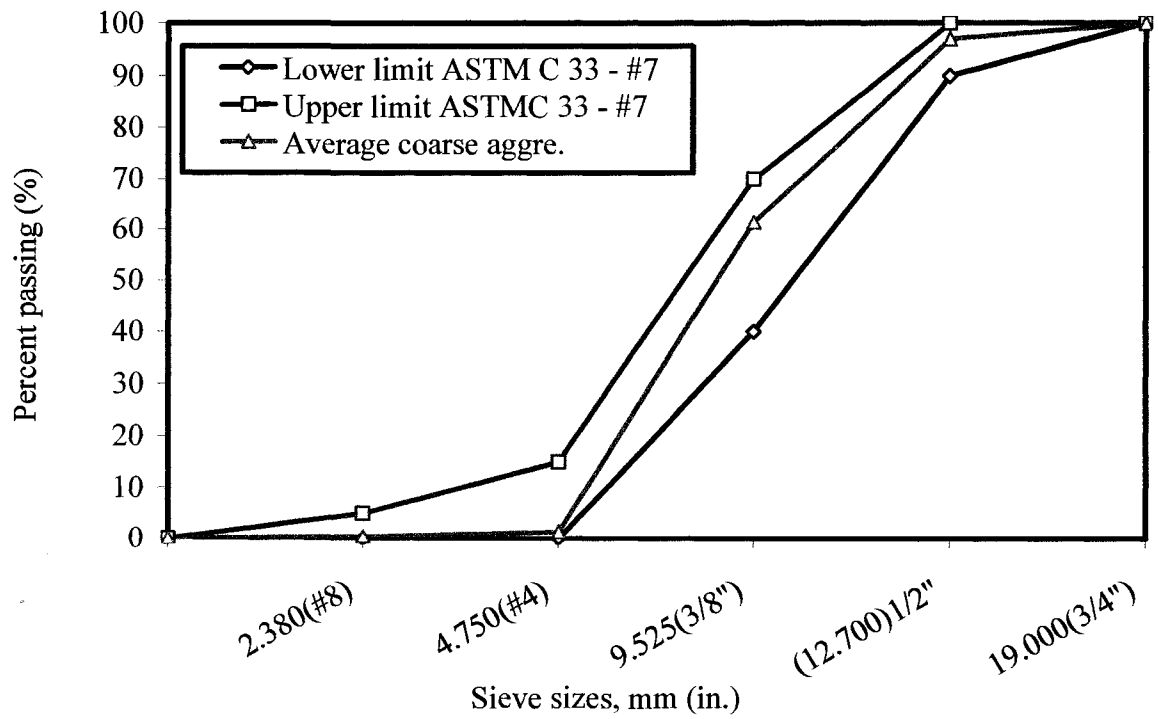
Figure 2.5: Quarry S ASTM C 33 #7 coarse aggregate size distribution

Table 2.2: Chemical and physical properties of Portland cement and fly ash

Chemical Composition	Portland Cement, (%)	Fly Ash, (%)
SiO_2	20.64	58.9
AL_2O_3	3.4	20.5
Fe_2O_3	3.4	5.6
CaO	63.5	7.5
MgO	4.7	
SO_3	2.4	0.4
Na_2O equivalent K_2O	0.46	-
C_2S	9	-
C_3S	66	-
C_3A	4	-
Loss on Ignition	1.20	0.3
Insoluble residue	0.14	-
Moisture content		0
Fineness Blaine, cm^2/g	3810	-
Autoclave expansion, %	0.18	0.02
Time of set, minutes		
Initial	96	-
Final	205	-
False Set, %	94	
Air content, %	6.3	-
Compressive strength, (MPa)		
3-day	27.4	-
7-day	33.9	-
28-day	42.7	-
325 sieve passing, (%)	97.9	23.5
Specific gravity	3.15	2.33

1 MPa = 145 psi, 1 cm^2 = 1.55 in^2, 1 g = 0.002205 lb

2.1.3 Fly ash

The fly ash used in this investigation was provided by the same supplier as the Portland cement. It was delivered in 208 liters (55 gallons) metallic drums and stored away from the humidity in the laboratory. Its physical and chemical properties are presented in Table 2.2. These data represent the average of five mill certificates obtained upon delivery. The fly ash complied with the ASTM C 618[40], class F specifications.

2.1.4 Water

Throughout this investigation, tap water complying with the requirements of ACI 310[49] "Specifications for Structural Concrete for Buildings," was used.

2.1.5 Chemical admixtures

Among a variety of commercially available plasticizers and superplasticizers, polycarboxylate-based (PC) high range water-reducing admixtures (HRWRA) are most widely used for developing and proportioning self-consolidating concrete[1]. While PC-HRWRA is used to impart fluidity on SCC, a viscosity modifying admixture (VMA) is also used to increase concrete's cohesiveness (improve segregation resistance). For the purpose of this study, liquid high range water-reducing and viscosity modifying admixtures were received from four different manufacturers, namely: EUCLID chemical, SIKA, BASF, and GRACE in sealed 19-liter (5.0-gallon) plastic containers. To avoid any commercialization interest, the admixture manufacturers were herein designated as A, B, C, and D without any reference. They were stored in the laboratory at a temperature of 21 $\pm$ 2 °C (70 $\pm$ 3 °F). All admixtures were manufactured and formulated to comply with the specifications of chemical admixtures for concrete, Type F ASTM C 494[21]. Their chemical types and properties are presented in Tables 2.3 and 2.4. These data are obtained

Table 2.3: Chemical compositon of high range water-reducing admixtures (HRWRA)

Designation	Source A	Source B
Chemical type	Polycarboxylate ester	Polycarboxylate acid
Volatiles (%)	-	60.00%
Specific gravity	1.05	1.09
pH	5.0 to 8.0	6.2 to 6.6
Water reduction range	20 to 30%	up to 40%

Table 2.3: Chemical compositon of high range water-reducing admixtures (HRWRA) (cont'd)

Designation	Source C	Source D
Chemical type	Polycarboxylate acid	Polycarboxylate acid
Volatiles (%)	approx. 70%	approx. 60%
Specific gravity	1.02 to 1.10	approx. 1.1
pH	5.0 to 7.0	3.0 to 7.0
Water reduction range	up to 40%	up to 45%

Table 2.4: Chemical compositon of viscosity modifying admixtures (VMA)

Designation	Source A	Source B
Chemical type	Polysaccharides	NS and welan gum
Volatiles (%)	-	56.90%
Specific gravity	1.002	1.207
pH	8.0	7.5 to 10.5

Table 2.4: Chemical compositon of viscosity modifying admixtures (VMA) (cont'd)

Designation	Source C	Source D
Chemical type	Methyl isothiocyanate	NS and melamine polymer
Volatiles (%)	approx. 80%	-
Specific gravity	1.100	1.23
pH	n/a	> 8.0

from Manufacturer Supplied Product Data (PD) and Material Safety Data Sheet (MSDS).

2.2   Mixing sequence

The mixing sequence was primarily based on ASTM C 192[54], "Standard Practice for Making and Curing Concrete Test Specimens in the Laboratory." In the present study the mixture sequences were modified to simulate the investigated parameters. The detailed mixing procedure and sequence is presented in the subsequent section.

2.3   Testing equipments and procedures

Table 2.5 presents the fresh and hardened properties evaluated in the present study. It also documents the testing equipments and the specifications governing their use.

2.3.1   Slump flow, T_{50}, and dynamic segregation resistance tests

The slump flow, T_{50}, and dynamic segregation resistance tests were conducted in accordance with the ASTM C 1611[55], American Society for Testing and Materials, "Standard Test Method for Slump Flow of Self-Consolidating Concrete." The slump flow (SF) test, as a measure of the unconfined workability of self-consolidating concrete, was carried out using a traditional slump cone where the horizontal spread, rather than the vertical slump, of the fresh concrete was measured. The test result is a mean spread value determined from the measurements of two perpendicular concrete spread diameters. The test was also used to determine T_{50} time (flow rate) which is the time in second it took for the fresh concrete's horizontal spread to reach a diameter of 508 mm (20 inches) from the moment the cone is lifted. The visual stability index (VSI) was used to examine the dynamic segregation resistance of fresh self-consolidating concrete by measuring the thickness of cement paste extended beyond the coarse aggregate. The VSI rate of 0 (highly stable matrix) corresponded to no evidence of segregation or bleeding in

65

Table 2.5: Test methods for evaluation of self-consolidating concrete's characteristics

Characteristic	Test method	Specification
Flow ability - Unconfined workability - Confined workability	 Slump flow V-funnel	 ASTM C 1611 ASTM Commitee C 09.47
Flow rate/plastic viscosity	T_{50}	ASTM C 1611
Passing ability 	 J-ring U-box L-box	 ASTM C 1621 ASTM Commitee C 09.47 ASTM Commitee C 09.47
Filling ability 	 V-funnel U-box	 ASTM Commitee C 09.47 ASTM Commitee C 09.47
Dynamic stability	Visual Stability Index (VSI)	ASTM C 1611
Static stability	Column segregation technique	ASTM C 1610
Setting time	Setting time	ASTM C 403
Bleeding	Bleeding	ASTM C 232
Air content	Air content	ASTM C 173
Adiabatic temperature	Adiabatic temperature	ASTM C 1064
Compressive strength	Compressive strength	ASTM C 39
Modulus of elasticity	Modulus of elasticity	ASTM C 469

slump flow, mixer drum/pan, or sampling receptacle; and the VSI rate of 1 (stable matrix) was attributed to the mixture when no evidence of segregation and slight bleeding was observed as a sheen on the slump flow spread. The test apparatus required: (1) a mold and tamping rod, conforming to the requirements of AASHTO T 119[56], (2) a strike-off bar, consisting of a flat straight bar of 3 x 20 x 300 mm (0.125 x 0.75 x 12 inches), (3) a

metallic base plate with a plane area of at least 900 x 900 mm (35 x 35 inches). The center of the plate was scribed with a cross, the lines of which ran parallel to the edges of the plate, and with two centroidal circular marks of 200 and 508 mm (8 and 20 inches) of diameter, (4) a suitable container for filling the slump cone, (5) a measuring tape with a minimum gradation of 12.5 mm (0.5 inch), and (6) a stopwatch with a minimum reading of 0.2 second. Figure 2.6 represents the base plate for slump flow test and Figure 2.7 displays an actual slump flow test.

The following steps were taken to perform the test:

(1)　The slump cone and base plate were cleaned and dampened. The excess water was removed from the testing surface as too much water could influence the VSI rating.

(2)　The base plate was placed on leveled seating and the cone was centered on the base plate at the 200 mm (8 inches) circular mark. The mold was placed with the smaller diameter opening up, (the inverted cone with the smaller diameter opening down was also accepted).

(3)　The cone was filled without any vibration, rodding, or tapping.

(4)　The surplus concrete was stricken off from the top of the cone using the tamping rod or strike off bar, and the filled cone was allowed to stand for not more than 30 seconds. During this time, excess concrete from the base plate was removed.

(5)　The cone was raised vertically for a distance of 225 ± 75 mm (9 ± 3 inches) in 3 ± 1 seconds without any lateral or torsional motion. The test procedure was completed from the start of filling through removal of the mold without interruption and within an elapsed time of 2.5 minutes.
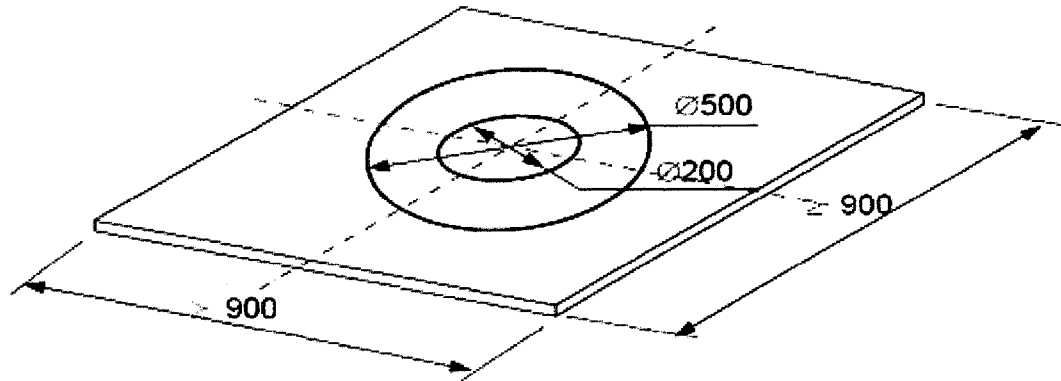
Figure 2.6: Scheme of the base plate for slump flow test
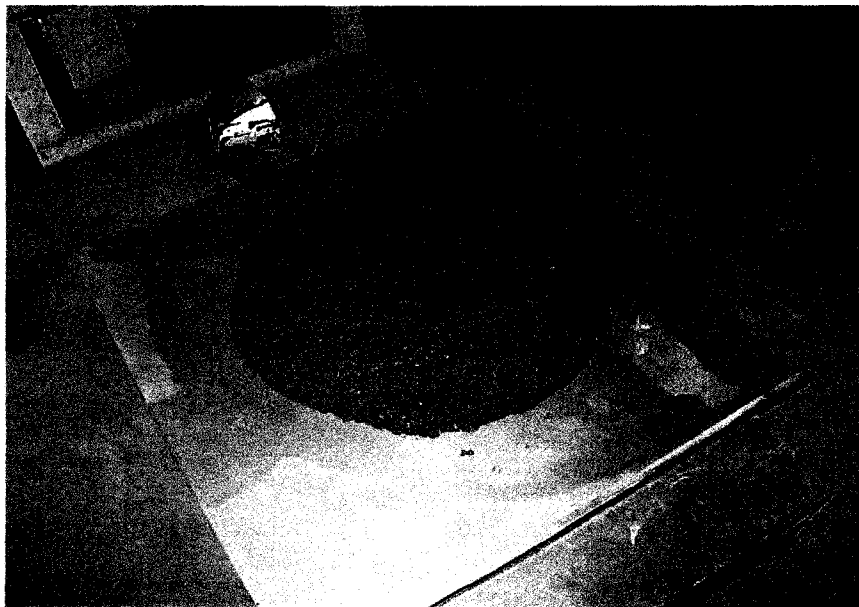
Figure 2.7: Slump flow, T_{50} and Visual stability index (VSI) tests

(6) To measure the T_{50} time, the stopwatch was started immediately after the cone ceased to be in contact with the base plate and the time, to the nearest 0.1 second, was recorded when the concrete reached the 508-mm (20-inch) circular mark.

(7) When the concrete stopped flowing, the maximum diameter of the slump flow and its perpendicular length were measured. Each measurement was to the nearest 12.5 mm (0.5 inch). When the two measurements differed by more than 50 mm (2 inches), the base plate was verified and the test repeated. The average length of the two perpendicular diameters was regarded as the slump flow of self-consolidating concrete.

(8) By visual examination, the concrete spread was checked for segregation. The cement paste could segregate from the coarse aggregate to give a ring of paste extending several millimeters (inches) beyond the coarse aggregate. The visual stability index (VSI) of the freshly-mixed concrete was rated based on the criteria noted in Table 2.6.

2.3.2 V-funnel test

The filling ability of self-consolidating concrete, as a measure of its confined workability, was evaluated using the V-funnel test. The V-funnel test was performed in accordance with the recommendations of the American Society for Testing and Materials (ASTM) Committee C09.47[57] for self-consolidating concrete. The test is not suitable when the maximum size of the aggregate exceeds 20 mm (3/4 inch). The testing apparatus is shown in Figures 2.8 and 2.9. It required: (1) a V-funnel apparatus made to the dimensions ± 1 mm shown in Figure 2.8, fitted with a quick release, watertight gate at its base and supported by a frame to keep the funnel horizontal. The V-funnel was made from metal; the surface was smooth, and not be readily attacked by cement paste or be liable to rusting, (2) a container to hold the test sample, having a volume larger than the

Table 2.6: Visual stability index (VSI) of fresh SCC rating criteria[55]

Rating	Criteria
0 Highly stable	No evidence of segregation or bleeding in slump flow, mixer drum/pan, or sampling receptacle (e.g. wheelbarrow).
1 Stable	No mortar halo or coarse aggregate heaping in the slump flow, but some slight bleeding and/or air popping is evident on the surface of the slump flow, or concrete in the mixer drum/pan or sampling receptacle (e.g. wheelbarrow).
Unstable	Slight mortar halo, 10 mm ($\leq$ 0.5 inch mm) wide, and/or coarse aggregate heaping in the slump flow, and highly noticeable bleeding in the mixer drum/pan or sampling receptacle (e.g. wheelbarrow).
3 Unstable	Clearly segregated by evidence of a large mortar halo, > 10 mm (0.5 inch), and/or large coarse aggregate pile in the slump flow, and a thick layer of paste on the surface of the concrete sample in the mixer drum or sampling receptacle (e.g. wheelbarrow).
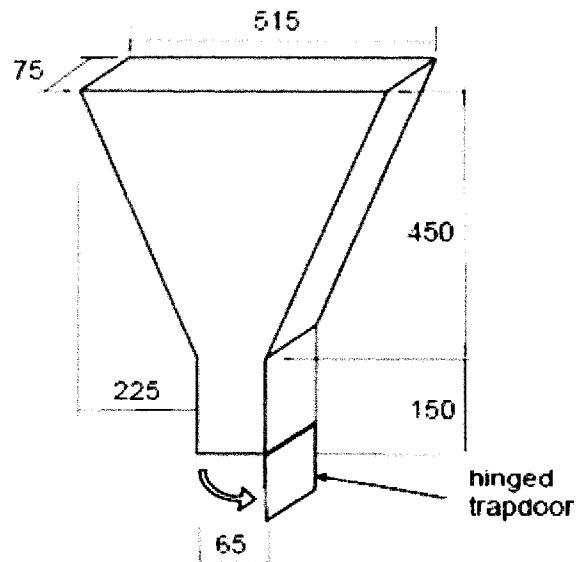
Figure 2.8: V-funnel apparatus
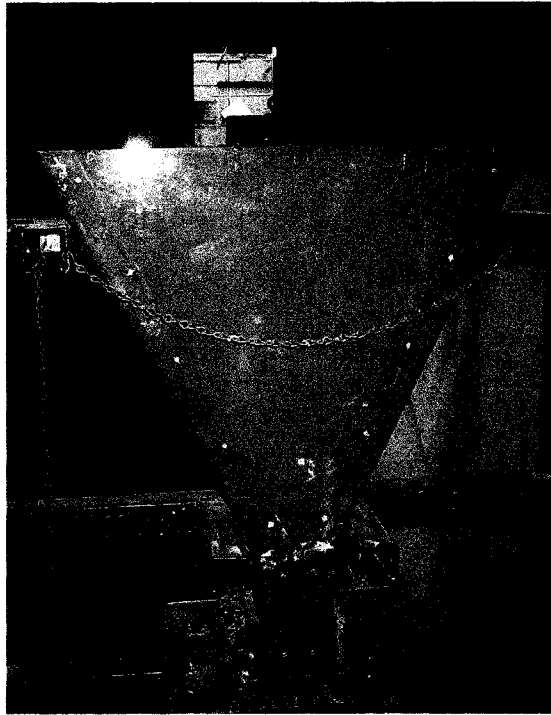
Figure 2.9: V-funnel test

volume of the funnel and not less than 12 liters (0.42 cu. ft.), (3) a stopwatch with a minimum reading of 0.2 second, and (4) a strike-off bar consisting of a flat straight bar of 3 x 20 x 300 mm (0.125 x 0.75 x 12 inches).

Prior to the actual experimentation, the inside surface of the funnel was cleaned and dampened before the bottom gate was clamped. The test began by filling the V-shaped funnel to its upper level with concrete. After the concrete rested for one minute in the V-funnel, the gate was opened and the time taken for the concrete to flow out of the funnel was measured and recorded as the V-funnel flow time (t_v).

2.3.3   U-box test

The U-box test was used to determine the filling ability and passing ability of self-consolidating concrete. The test was performed in accordance with the requirement set

forth by ASTM Committee C09.47[57] for self-consolidating concrete. The testing apparatus required: (1) a U-box made to the dimensions (tolerance $\pm$ 1 mm) shown in Figure 2.10, fitted with a quick release. The U-box was made from metal with a smooth surface resistance against rusting, (2) a suitable container for filling the U-box having a volume larger than its volume, (3) a strike-off bar consisting of a flat straight bar at least of 3 x 20 x 300 mm (0.125 x 0.75 x 12 inches), and (4) a measuring tape with a minimum gradation of 12.5 mm (0.5 inch).

The following testing procedure was used to conduct the U-box test:

(1)   The inside surface of the U-box was cleaned and slightly moistened.

(2)   The gate was secured in its place and fresh concrete was poured into the left hand section of the U-box to its upper level without any agitation or rodding. The strike off bar was used to flush the concrete with the upper part of the funnel.

(3)   After a delay of one minute from filling the box, the gate was lifted and the concrete allowed flowing upwards into the right-hand section.

(4)   The heights H_1 and H_2 of the concrete in both compartments were measured to the nearest 5 mm (0.2 inch) and their difference H_1-H_2, referred as U-box filling height, was used to evaluate the filling ability and passing ability of the self-consolidating concrete.

2.3.4   J-ring test

The J-ring test was used to determine the passing ability of self-consolidating concrete using the J-ring and slump cone. The diameters of the unobstructed and obstructed slump flows were used to assess the degree of passing ability of self-consolidating concrete. The test was conducted in accordance with the ASTM C 1621[58] "Standard Test Method for Passing Ability of Self-Consolidating Concrete by J-ring."
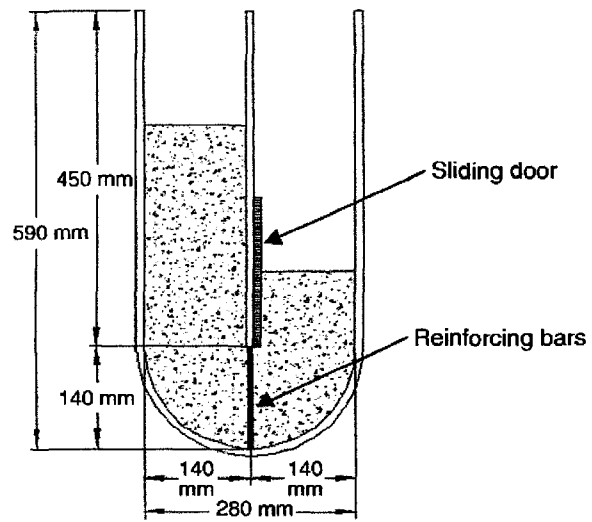
Figure 2.10: U-box apparatus
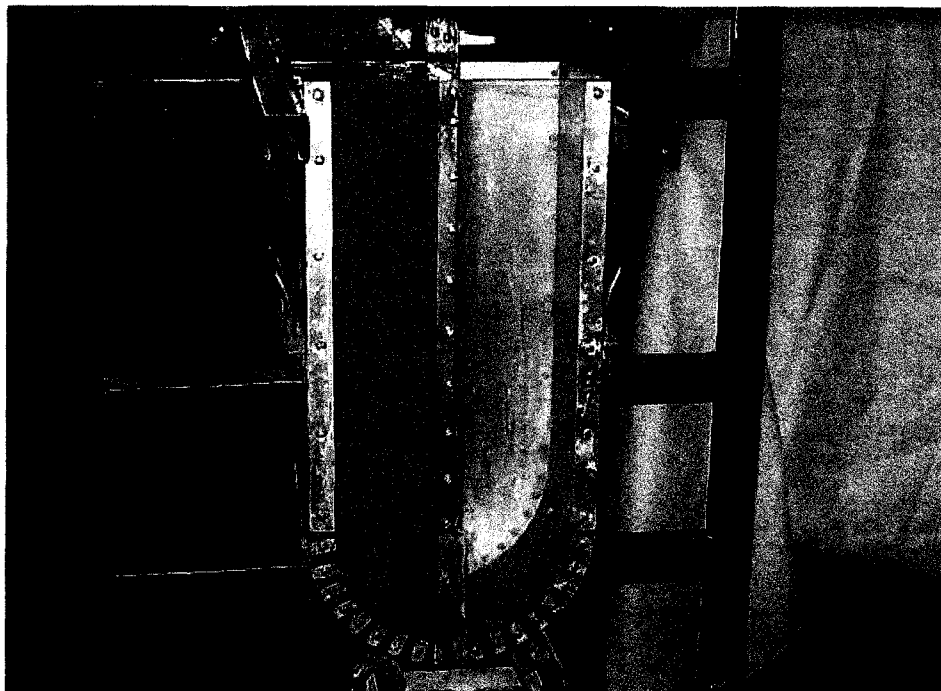
Figure 2.11: U-box test

73

The testing apparatus is shown in Figures 2.12 and 2.13. It consisted of: (1) an open steel ring, drilled vertically with holes to accept threaded sections of reinforcing bars. The bars could be of different diameters and/or spaced at different intervals. The diameter of the ring of the vertical bars was 305 mm (12 inches) with a height of 100 mm (4 inches), (2) a mold and tamping rod per requirement of AASHTO T 119[56], (3) a strike-off bar consisting of a flat straight bar of 3 x 20 x 300 mm (0.125 x 0.75 x 12 inches), (4) a base plate as specified in the slump flow test, (5) a suitable container for filling the slump cone, and (6) a measuring tape with a minimum gradation of 12.5 mm (0.5 inch).

The following J-ring passing ability test procedure was used:

(1)   The J-ring, slump cone, and base plate were cleaned and dampened.

(2)   The base plate was positioned on leveled seating, and the J-ring placed on the base plate. The cone was centered within the J-ring and upward with the smaller diameter opening up.

(3)   The cone was filled with fresh concrete without vibration, rodding, or tapping.

(4)   The surface of the concrete was leveled with the top of the mold using the tamping rod or strike off bar. The surplus of concrete removed from around the base of the cone and base plate surface.

(5)   The mold was raised vertically to a distance of 225 ± 75 mm (9 ± 3 inches) in 3 ± 1 seconds without any lateral or torsional motion. The test was completed from the start of filling through the removal of the mold without interruption and within an elapsed time of 2.5 minutes.

(6)   When the concrete stopped flowing, the lengths of two perpendicular slump flows were measured. Each measurement was the nearest 12.5 mm (0.5 inch). If the two

units: mm (in.)
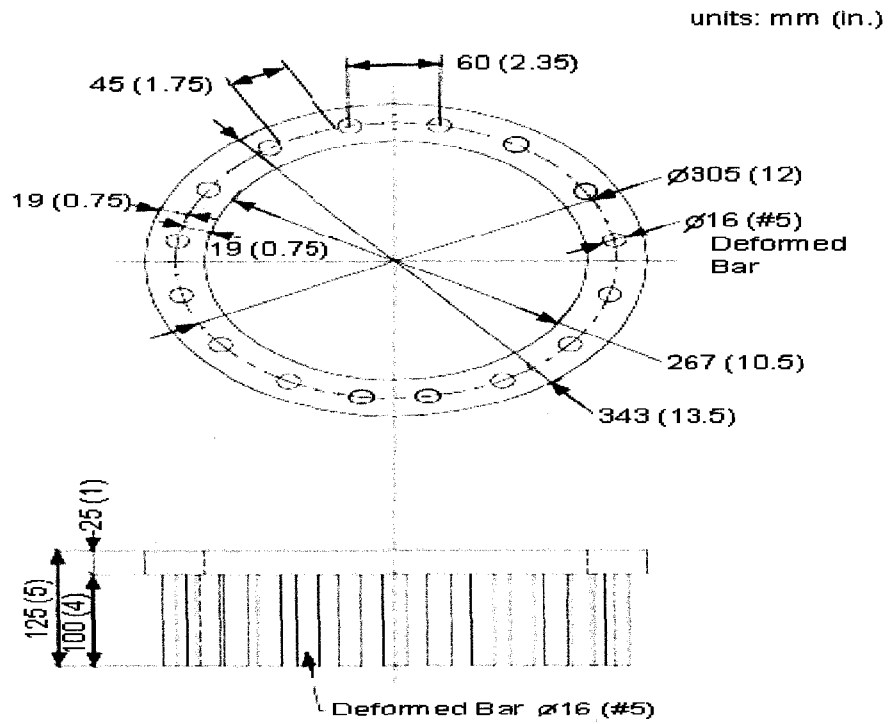
Figure 2.12: J-ring apparatus
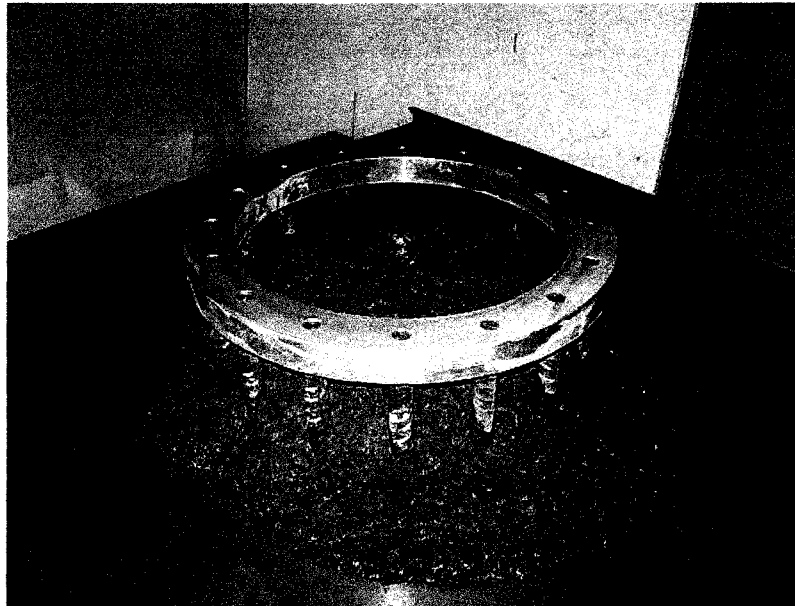
Figure 2.13: J-ring test

75

measurements differed by more than 50 mm (2 inches), the base plate was leveled and test repeated.

(7)   The J-ring flow was calculated as the average of the two measured diameters.

(8)   The J-ring value was calculated as the difference between the J-ring flow and the unobstructed slump flow as tested according to slump flow test of the same representative sample.

(9)   The passing ability of freshly-mixed self-consolidating concrete was rated based on the criteria in Table 2.7.

Table 2.7: Passing ability rating[58]

J-ring value mm (inch)	Passing ability rating	Remarks
0 – 25 (0 – 1)	0	High passing ability
>25 – 50 (> 1 – 2)	1	Moderate passing ability
>50 (> 2)	2	Low passing ability

2.3.5   L-box test

The L-box test was used to determine the passing ability of self-consolidating concrete.   The test was performed in accordance with the recommendations of the American Society for Testing and Materials (ASTM) Committee C09.47[57] on self-consolidating concrete.

The L-box was made to the dimensions (tolerance ± 1 mm) shown in Figures 2.14 and 2.15.   It was a rigid construction with a corrosion-resistant inner.   With the gate closed, the volume of the vertical hopper was 12 liters (0.42 cu. ft.) when filled to the top with fresh concrete.   The assemblies holding the reinforcement bars had 2 smooth bars of
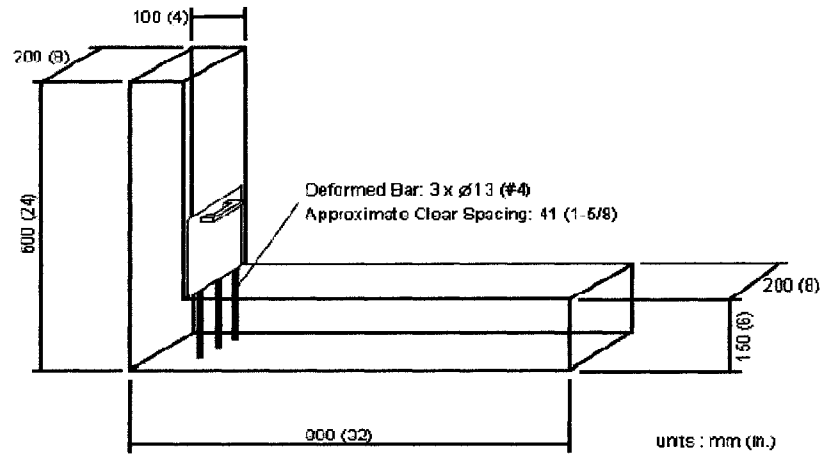
Figure 2.14: L-box apparatus
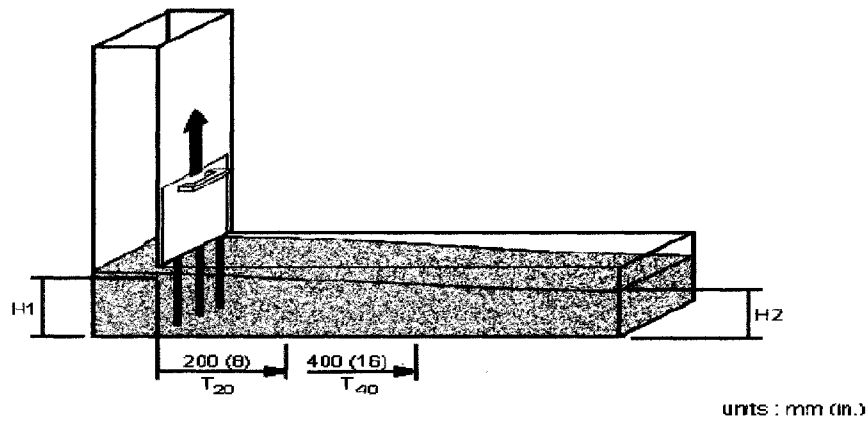
Figure 2.15: L-box apparatus (continued)

Figure 2.16: L-box test

77

12.5 mm (0.5 inch) diameter with a gap of 59 mm (2.3 inches) for the two-bar test, and 3 smooth bars of 12 mm (0.5 inch) diameter with a gap of 41 mm (1.6 inches) for the three-bar test. These assemblies were interchangeable and the bars were placed vertical and equidistant across the width of the box. A steel mold was preferred but 12.5 mm (0.5 inch) coated formwork plywood with the end grain sealed has been found to be suitable. The L-box test required: (1) a L-box made to the dimensions (tolerance $\pm$ 1 mm) shown in Figure 2.14, (2) a tamping rod or a strike off bar conforming the requirement of AASHTO T 119[56], (3) a strike-off bar consisting of a flat straight bar of 3 x 20 x 300 mm (0.125 x 0.75 x 12 inches), (4) a suitable container for filling L-box, (5) a measuring tape with a minimum gradation of 10 mm (0.5 inch), and (6) a stopwatch with a minimum reading of 0.2 second.

To perform the L-box test, the following steps were taken:

(1)   The L-box was cleaned, moistened, and placed on leveled stable seating.

(2)   After the sliding gate was securely closed, the concrete was poured vertically from the container into the filling hopper of the L-box without vibration, rodding, or tapping.

(3)   The surface of the concrete was leveled with the top of the L-box using the tamping rod or strike-off bar.

(4)   The test specimen was allowed to stand for 60 $\pm$ 10 seconds, during which any segregation was recorded.

(5)   The sliding gate was raised allowing the concrete to flow into the horizontal section of the box. The test procedure was completed from the start of filling through the opening of the sliding gate without interruption, and within 5 minutes.

(6)   Optional. The T_{20} and T_{40} times were determined as the time in seconds it took for

the concrete flow to travel 200 mm (8 inches) and 400 mm (16 inches), respectively, as measured from the time the sliding gate was lifted.

(7)   When the concrete movement ceased, the heights of the resulting flow at the sliding gate, H_1, and at the end of the horizontal section, H_2, were measured to the nearest 6 mm (0.25 inch).

(8)   The blocking ratio was calculated as: (H_2/H_1) x 100.

The flow height ratio H_2/H_1 was used to evaluate the passing ability of the self-consolidating concretes. The flow times T_{20} and T_{40} were used to examine the flow ability of the selected self-consolidating concretes.

2.3.6   Column technique

The static segregation resistance (or static stability) of self-consolidating concrete was determined using the column segregation test. The test was conducted in accordance with the ASTM C 1610[59], "Standard Test Method for Static Segregation of Self-Consolidating Concrete Using Column Technique." The testing apparatus is shown in Figures 2.17 through 2.20. The equipment assembly consisted of: (1) a column mold in Poly Vinyl Chloride (PVC) plastic pipe meeting the requirements of ASTM D 1785[60]. The column was 200 mm (8 inches) diameter by 660 mm (26 inches) height and separated into 3 sections. The top section was 160 mm (6.5 inches) deep, whereas the middle and bottom sections were 330 and 160 mm (13 and 6.5 inches) in height, respectively, as shown in Figure 2.17. Each section had its ends flat and plane and marked as "Top", "Middle", or "Bottom" relative to its location in the column. In order to form mortar-tight joints, couplers, brackets, clamps, or other equivalent fastening systems were used to secure the column sections together and to the base plate, (2) a base
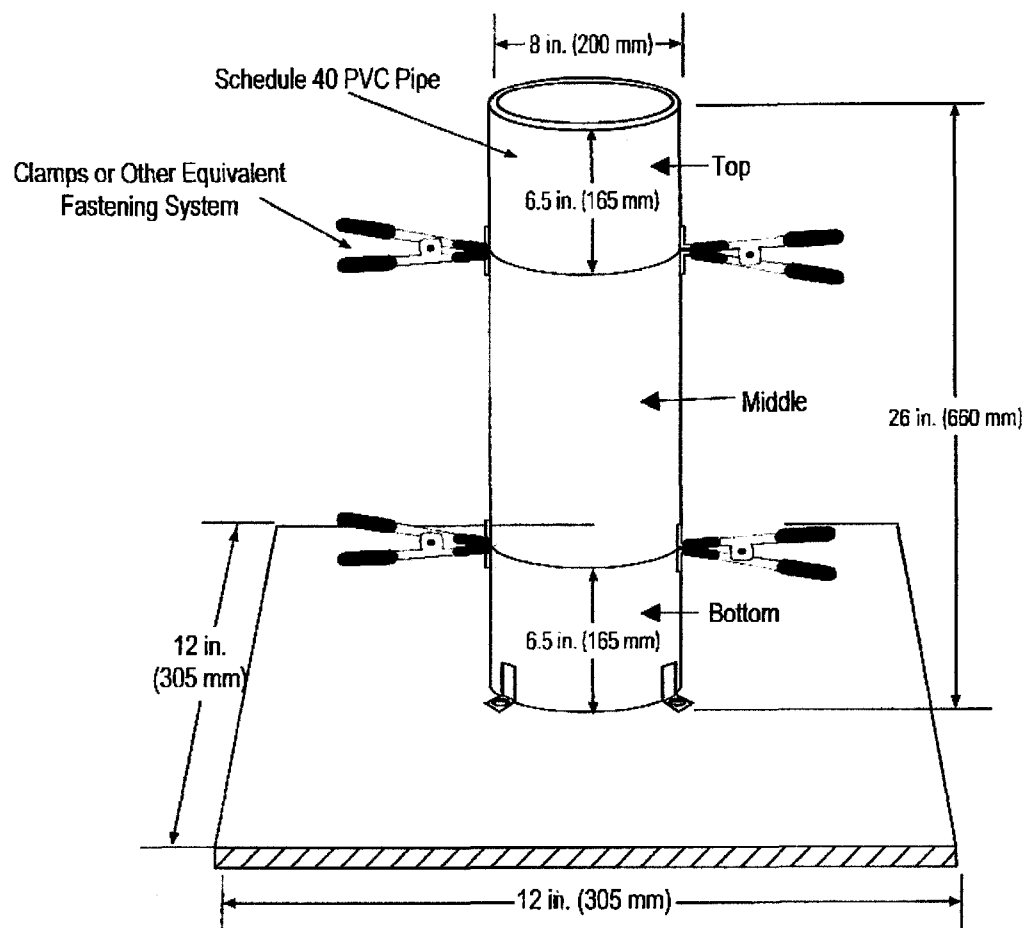
Figure 2.17: Column mold
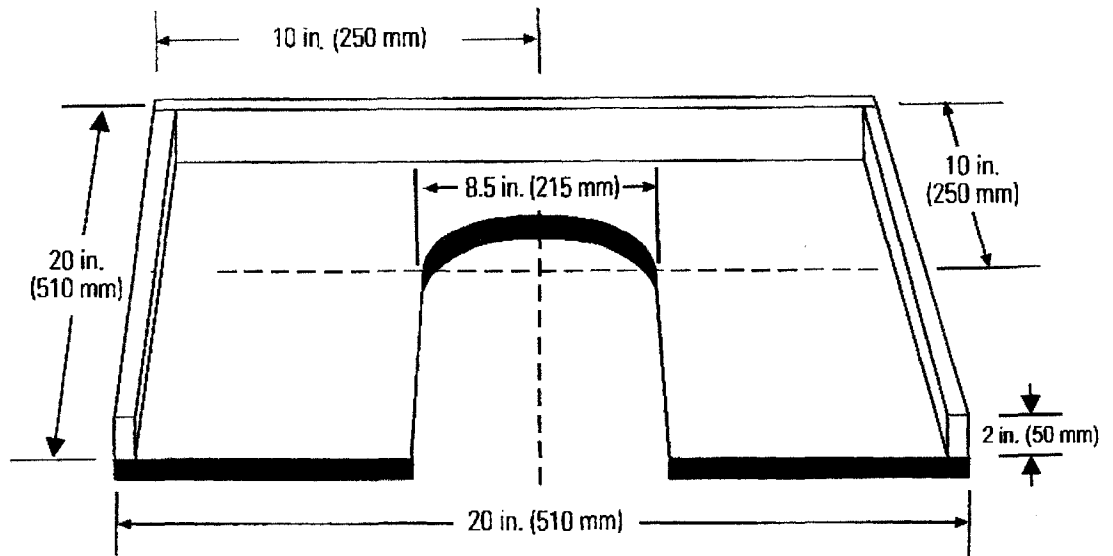
Figure 2.18: Collector plate
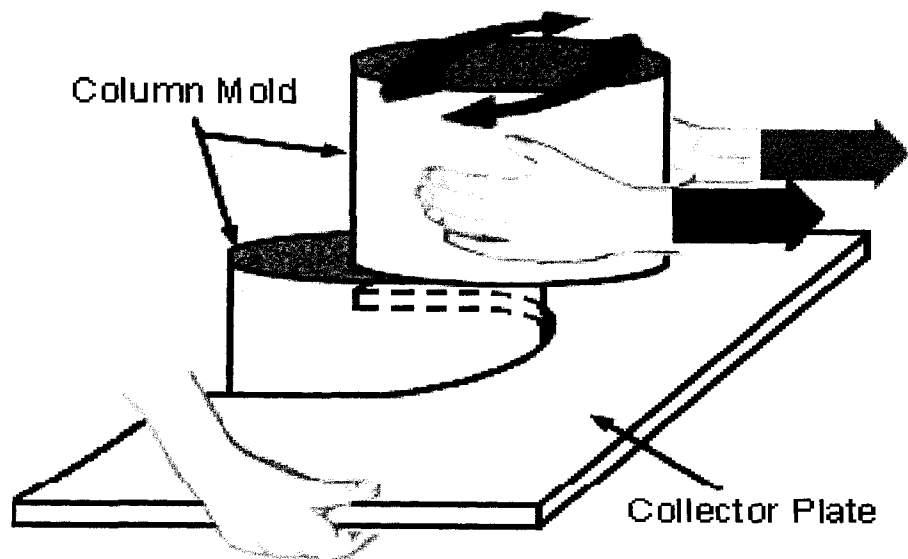
Figure 2.19: Horizontal rotating and twisting action

81
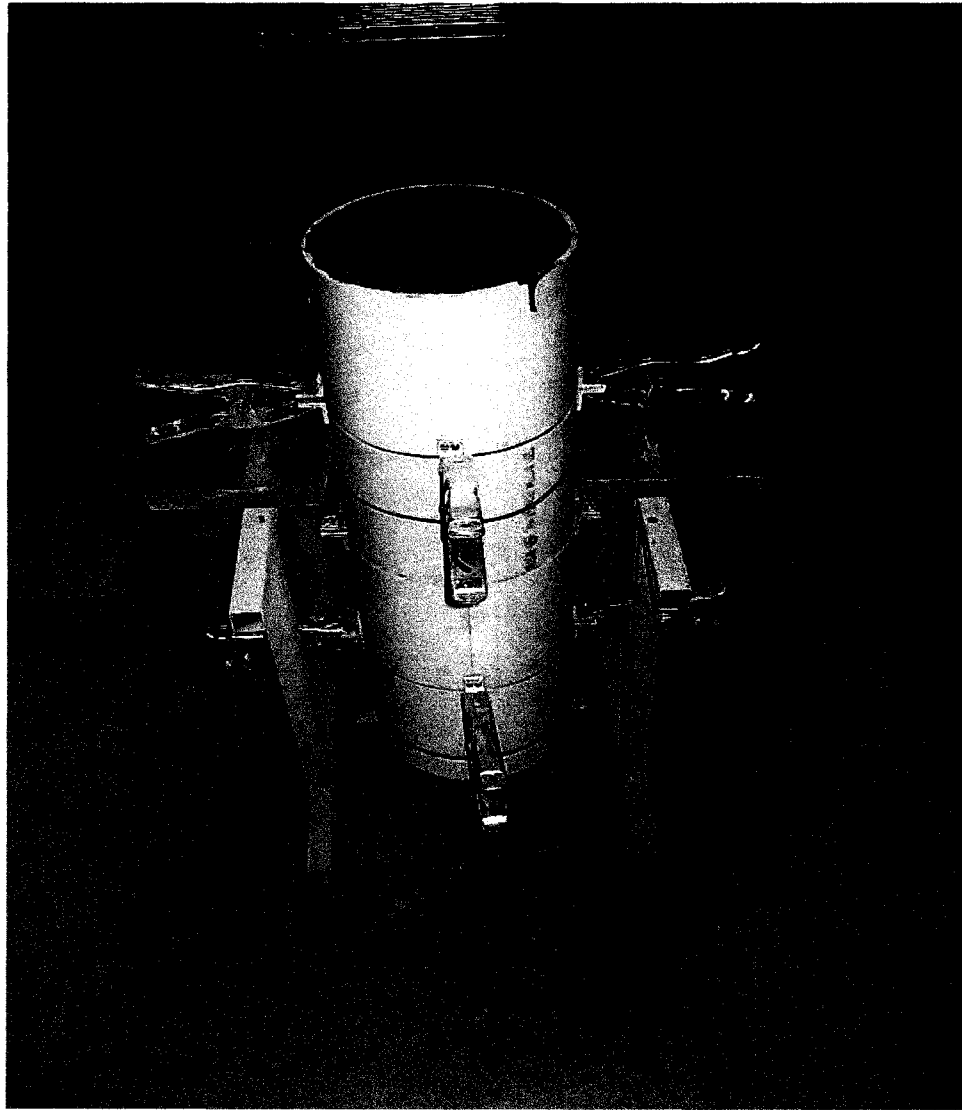
Figure 2.20: Column technique test

plate, smooth, rigid, and nonabsorbent material, with a minimum of 12 inches (305 mm) square, (3) a collector plate, used to obtain concrete from the top section of the column, made of any smooth, rigid, and nonabsorbent rigid material measuring at least 20 inches (510 mm) square, as shown in Figure 2.18, (4) a No. 4 (4.75 mm) sieve of minimum dimensions of 330 x 635 mm (13 x 25 inches) manufactured in accordance with the AASHTO M 92[61], (5) a tamping rod or a strike off bar per requirement of AASHTO T 119[56]. The strike-off bar was flat straight bar of 3 x 20 x 300 mm (0.125 x 0.75 x 12 inches), (6) a suitable container for filling column mold, and (7) a balance accurate to 0.05 kg (0.1 lb).

To perform the column technique test, the following steps were used:

(1) The inside of the column mold and base plate were cleaned and dampened.

(2) The base plate was placed on a leveled seating with the column mold centered and attached on the base plate.

(3) The test sample was remixed in the receptacle using a shovel or scoop so that the concrete was homogeneous and representative of the mixture proportion.

(4) Immediately thereafter, the column mold was filled with concrete completely and above the rim using a shovel, scoop, or plastic pail, within 2 minutes.

(5) After filling the mold, the top surface was stricken off by sliding the strike-off bar across the top rim of the mold with a sawing motion until the concrete surface was leveled with the top of the mold.

(6) The concrete was allowed to stand in the column mold undisturbed for 15 minutes.

(7) Immediately following the standing period, the top section of the mold was securely hold and the fastening system removed. Steps (8) – (16) were completed within 20 min.

(8)   The cut out section of the collector plate around the column was placed just below the joint between the "Top" and "Middle" sections to catch and collect concrete.

(9)   The upper section of the column mold was grasped and using a horizontal rotating motion, the concrete was screed from the top section of the column onto the collector plate and then deposited into a plastic pail (see Figure 2.19).

(10) Steps (7) – (9) were repeated to remove the concrete from the middle section of the column mold and discard.

(11) The concrete sample collected from the upper section was placed onto the No. 4 (4.75 mm sieve).

(12) The concrete was washed on the No. 4 (4.75 mm) sieve so that only the coarse aggregate remained on the sieve, and then the coarse aggregate was placed into a plastic pail.

(13) Steps (11) – (12) were repeated for the concrete retained in the bottom section of the mold.

(14) The obtained coarse aggregate from both the top and bottom sections was brought to the saturated-surface-dry (SSD) condition.

(15) The mass of the coarse aggregate from each of the top and bottom sections of the column mold was measured separately to the nearest 45 g (0.1 lb).

(16) The segregation index, SI, was calculated as follows:

$SI\% = [(CA_B - CA_T) / ((CA_B + CA_T)/2)] \times 100$,   if $CA_B > CA_T$

$SI\% = 0$ if $CA_B \leq CA_T$

Where: CA_T = mass (weight) of coarse aggregate in the top section

CA_B = mass (weight) of coarse aggregate in the bottom section.

2.3.7 Time of setting

The ASTM C 403[62], "Standard Test Method for Time of Setting of Concrete Mixture by Penetration Resistance," was used to evaluate the times of setting of the trial mixtures. Figure 2.21 displays a photo of an actual time of setting test. Tap water at temperature of 70 ± 3 °F (21 ± 2 °C) was used for matrix preparation and the test samples were stored in a laboratory room characterized by 25 ± 5% relative humidity and 70 ± 3 °F (21 ± 2 °C) temperature. A mortar sample was obtained by sieving a representative sample of fresh SCC using a No. 4 sieve (4.75mm (3/16 inch) opening). The mortar was placed in a 152 mm (6 inches) diameter by 152 mm (6 inches) tall plastic cylinder. This container was filled in one single layer without any consolidation. The initial test was made after an elapsed time of 3 to 4 hours from the initial contact between cement and water by recording the penetration resistance of 645 millimeters square (1 square inch) needle. Subsequent readings were taken at approximately 1/2 hour intervals until a penetration of 27.6 MPa (4,000 psi) was reached. The penetration resistance was plotted against elapsed time. The initial and final times of setting were calculated at the penetration resistances of 3.5 MPa (500 psi) and 27.6 MPa (4,000 psi), respectively.

2.3.8 Bleeding

The bleeding of concrete was assessed using ASTM C 232[63] "Standard Test Method for Bleeding of Concrete." Similar mixing water temperature and laboratory conditions to those of the setting time test were used to conduct the bleeding test. The concrete sample was placed into a cylindrical metal container of approximately 0.014 m^3 (0.5 ft^3) capacity, as shown in Figure 2.22, in one single layer with no densification effort. The top surface was troweled, the time recorded, and the mass of the concrete-

85
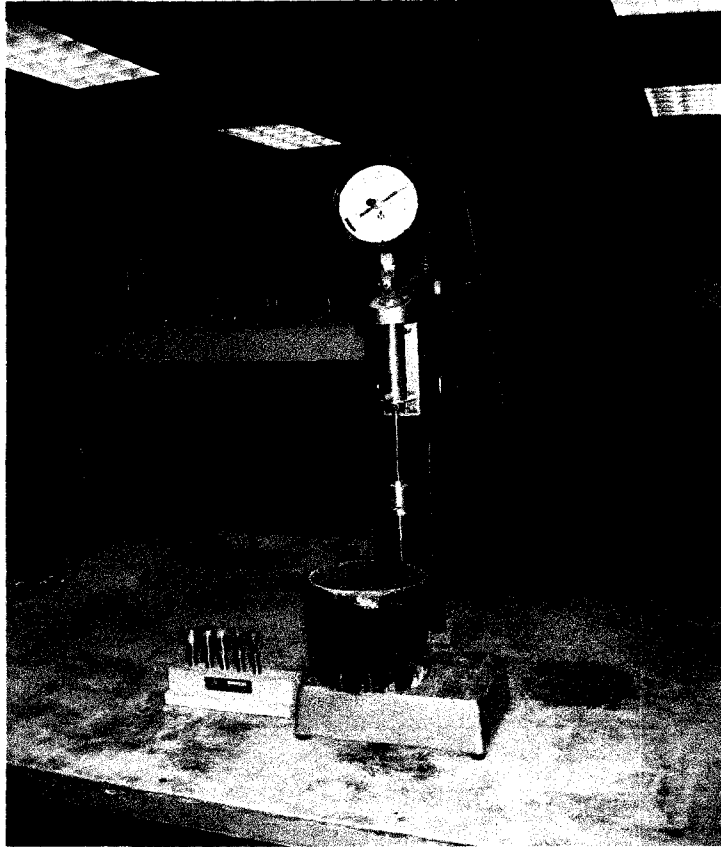
Figure 2.21: Time of setting apparatus and test

Figure 2.22: Cylindrical metal container used for the bleeding test

filled container was determined. The container was then covered with a plastic sheet to prevent evaporation of the bleed water. An ambient temperature of between 18 to 24° C (65 and 75° F) was maintained during the test by adjusting the room temperature. The accumulated water on the surface was drawn off with a pipette and placed into a sealed pre-tarred beaker at 10-minute intervals during the first 40 minutes and at 30-minute intervals thereafter until a complete cessation of bleeding took place.

2.3.9 Air content

Several methods of measuring air content of freshly-mixed concrete exist. ASTM standards include: (1) pressure method (ASTM C 231)[64], (2) gravimetric method (ASTM C 138)[65], and (3) volumetric method (ASTM C 173)[66]. In this investigation, the air content of the non-air entrained self-consolidating concretes was evaluated using ASTM C 173[66] "Standard Test Method for Air Content of Freshly Mixed Concrete by the Volumetric Method." The airmeter consisting of a bowl and a top section was calibrated according to the ASTM C 173[74] specifications. A sample of freshly-mixed concrete was placed into the measuring bowl in one single layer without any consolidation. The top surface was then struck-off with a strike-off bar and the flange of the bowl was wiped clean. The top section was then clamped in place and water was added until it was leveled off in the neck of the airmeter at the zero mark. A watertight cap was used to tighten the unit. The unit was then inverted and agitated for a minimum of 45 seconds in order to displace the volume of air in the concrete specimen. The airmeter was then tilted approximately 45 degrees and vigorously rolled and rocked for nearly 1 minute. Finally, the unit was set upright allowing it to stand while the air rose to the top and the liquid level was stabilized. If the liquid level was obscured by foam, a rubber syringe was used

to add sufficient alcohol in one calibrated cup of 23 ml (0.78 oz) increments until a readable liquid level was reached. The 23 ml (0.78 oz) of alcohol was sufficient to reduce the air reading by 1%. The volume of the consumed alcohol and the reading of the liquid in the neck of the airmeter were recorded. The air content was calculated in percentage by adding the reading to the amount of alcohol used. Figure 2.23 shows the volumetric air content apparatus.
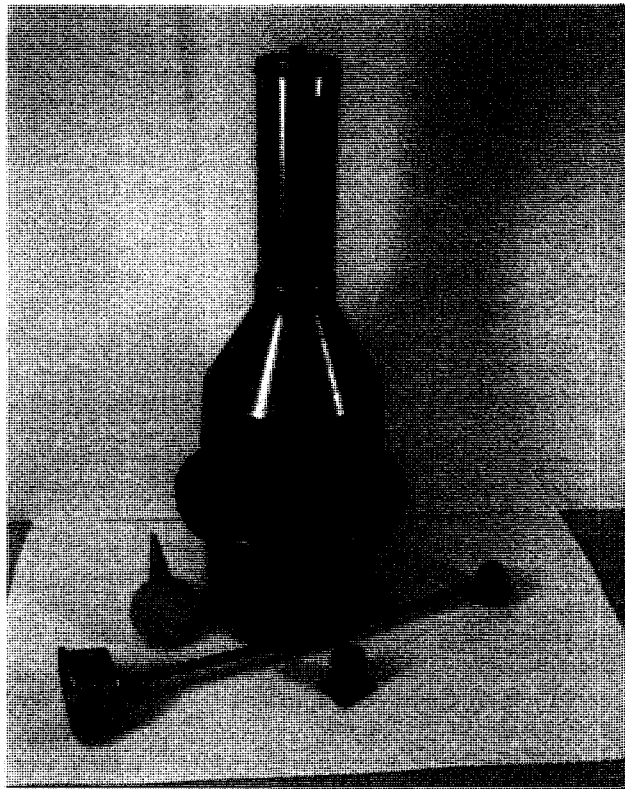
Figure 2.23: Air content apparatus (volumetric airmeter)

2.3.10   Adiabatic temperature

The ASTM C 1064[67], "Standard Test Method for Temperature of Freshly-Mixed Hydraulic Cement Concrete," was used to evaluate the adiabatic temperature of the self-consolidating concretes. A data acquisition apparatus "DI-1000 TC"[68] with 8 channels

and compatible software "WinDaq"[69] was used to record the temperature of the fresh concretes. Tap water at temperature of 21 ± 2 °C (70 ± 3 °F) was used for matrix preparation. Immediately after mixing, 104 x 208 mm (4 x 8 inches) cylindrical specimens were prepared. One end of the thermocouple was plunged halfway in the fresh concrete and the other end was connected to a channel of the apparatus. The test samples were covered with plastic sheet to prevent any water evaporation, and then stored in a laboratory room characterized by $25 \pm 5\%$ relative humidity and 21 ± 2 °C (70 ± 3 °F) temperature. The sample's adiabatic temperature was recorded every 60 seconds for 24 hours, and an average of three samples was used for each trial mixture. Figure 2.24 demonstrates a photo of the actual testing.

Figure 2.24: Adiabatic temperature test

2.3.11   Compressive strength

The ASTM C 39[70], "Standard Test Method for Compressive Strength of Cylindrical Concrete Specimens," was used to evaluate the compressive strength of the self-consolidating concretes.   A static testing compression machine (Professional Concrete Compression Machine, MC500 PR), manufactured by Gilson Company and conformed to ASTM standard testing was used to evaluate the compressive strength of the trial SCC samples.

With solid steel cross-heads from 76 to 152 mm (3 to 6 inches) thick on a standard frame, the compression machine load frames are very stiff and meet the stringent ACI 363[71] rigidity recommendations.   The bottom-mounted hydraulic ram applies compression force upward.   The lower platen and spherically seated upper platen assembly are ground plane, hardened, nickel plated and scribed with concentric circles. Locking stem holds upper platen assembly securely in place, yet allows for quick substitution of accessory.   This electric-hydraulic type machine has a capacity of 1112 to 2224 KN (250,000 to 500,000 pounds) and is equipped with state-of-art electronic controllers.   Figure 2.25 illustrates the actual the concrete compression testing machine.

After a pre-assigned curing period was completed, the compressive strength was measured by testing cylinders using the compression machine described earlier.   The test samples were capped with pads and retainers complying with the ASTM C 1231[72], as illustrated in Figure 2.25.   Reusable 70 durometer pads, which cover design strengths up to 80 MPa (12,000 psi), were used.   For quick release of pads, polysaccharide powder, a bond breaker to extend pad life, was used as a lubricant.   The specimens were placed on the top of the spherical seated bearing blocks and positioned with the centroid of upper
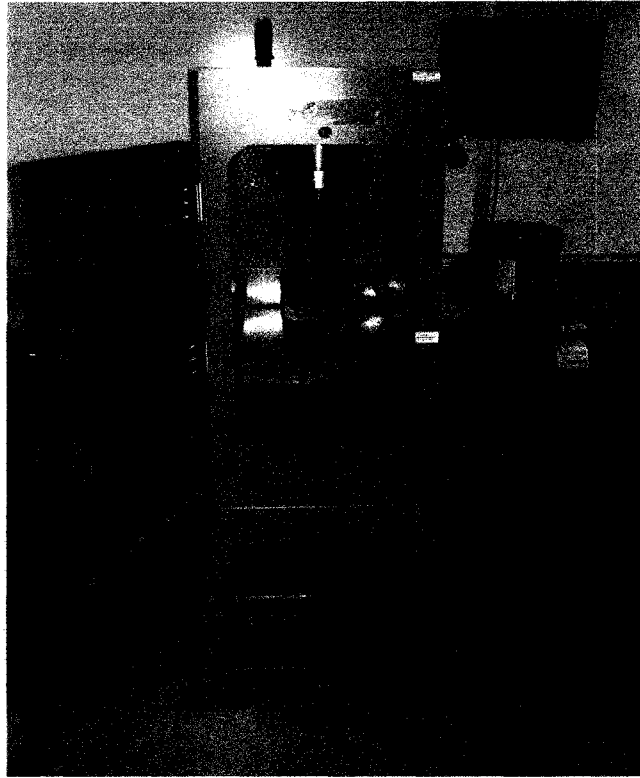
Figure 2.25: Concrete compression testing machine

platen, aligned vertically with the center of steel bearing block. The bearing side was adjusted to ensure the application of pure uniaxial compression loading, in accordance with ASTM C 39[70], at a rate of 0.138 to 0.345 MPa/sec (20 to 50 psi/sec).

2.3.12   Modulus of elasticity

The ASTM C 469[73], "Standard Test Method for Static Modulus of Elasticity and Poisson's Ratio of Concrete in Compressive," was used to evaluate the modulus of elasticity of the designed self-consolidating concretes. The modulus of elasticity and the compressive strength were obtained on the same loading. The test required an extremely accurate strain measurement system. A compressometer with a distance between the grips of 267 mm (10.5 inches) and a dial gage that measure the perpendicular linear deformation of the specimen to the nearest 0.00254 mm (0.0001 inch), mounted on the
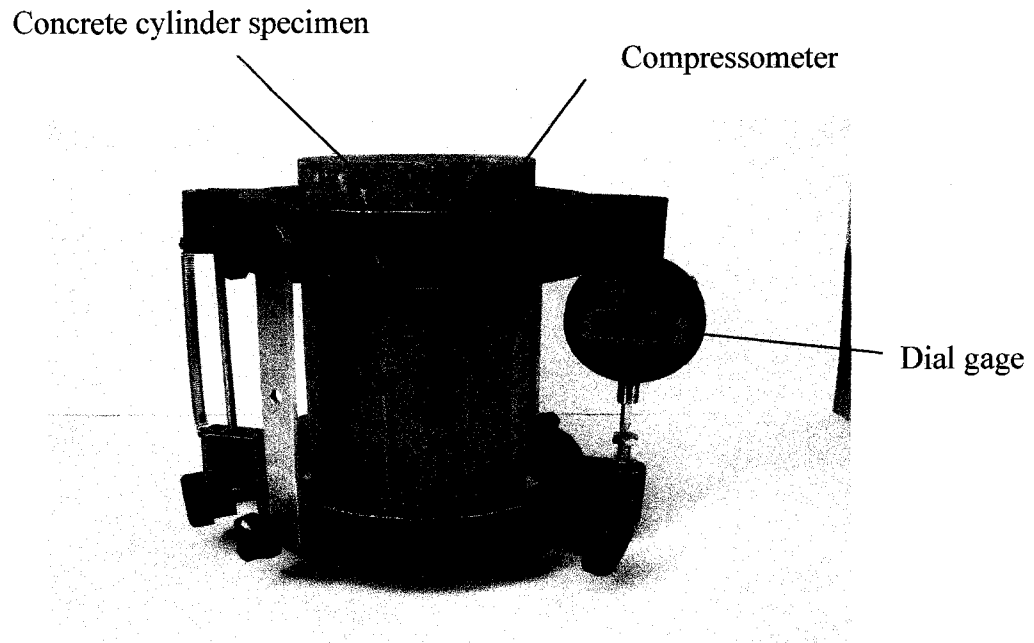
Figure 2.26: Sample set up for modulus of elasticity test

cylindrical specimen as shown in Figure 2.26, were used for the testing.

The method used in this experiment to calculate the modulus of elasticity is based upon deformation of concrete cylinders under the ultimate compressive strength load. The modulus of elasticity was calculated to the nearest 345 MPa (50,000 psi) using the following equation:

$$E_c = \frac{\sigma_2 - \sigma_1}{\varepsilon_2 - \varepsilon_1};$$

Where:

E_c = Young modulus of elasticity, psi (MPa)

σ_1 = Stress corresponding to longitudinal strain, ε_1, of 50 millionths, MPa (psi)

σ_2 = Stress corresponding to 45% of ultimate at compressive load, MPa (psi)

ε_1 = Longitudinal strain at σ_1

ε_2 = Longitudinal strain produced by stress σ_2

The longitudinal strain was the deformation that the specimen was subjected to when under compression. According to the compressometer used, each longitudinal strain (ε_1 and ε_2) was equivalent to $\frac{1}{2}$ the gage reading divided by the effective gage length, where the effective gage length was 267 mm (10.5 inches). The stress was the force exerted on the cylinder in pounds per square inch or mega Pascal. The stress was calculated by dividing the load (kilograms or pounds) by the surface area (square meters or square inches) of the cross section of the specimen.

2.3.13   Ultraviolet-visible (UV/Vis) spectroscopy

Ultraviolet-visible (UV/Vis) spectroscopy was used to investigate the adsorption of the selected polycarboxylate-based high range water-reducing admixtures in the Portland cement-water. The instrument used in ultraviolet-visible spectroscopy is called UV/Vis spectrophotometer. The spectrophotometer is basically composed of: (1) a light source (often an incandescent with tungsteen bulb for the visible wavelengths, or a deuterium arc lamp in the ultraviolet), (2) a holder for the sample, (3) a diffraction grating or monochromator to separate the different wavelengths of light, and (4) a detector. The detector is typically a photodiode or a charge-coupled device (CCD), which is an analog shift register that enables the transportation of analog signals (electric charges) through successive stages controlled by a clock signal. Photodiodes are used with monochromators, which filter the light so that only light of a single wavelength reaches the detector. Diffraction gratings are used with CCDs, which collects light of different wavelengths on different pixels. A spectrophotometer can be either single beam or double beam (see Figure 1.27).

In a single beam instrument, all of the light passes through the sample cell. This

93

was the earliest design, but is still in use in both academic and industrial laboratories. In a double-beam instrument, the light is split into two beams before it reaches the sample. One beam is used as a reference whereas the other beam passes through the sample. Some double-beam instruments have two detectors (photodiodes), and the sample and reference beam are measured at the same time. In other instruments, the two beams pass through a beam chopper, which blocks one beam at a time. The detector alternates between measuring the sample beam and the reference beam.
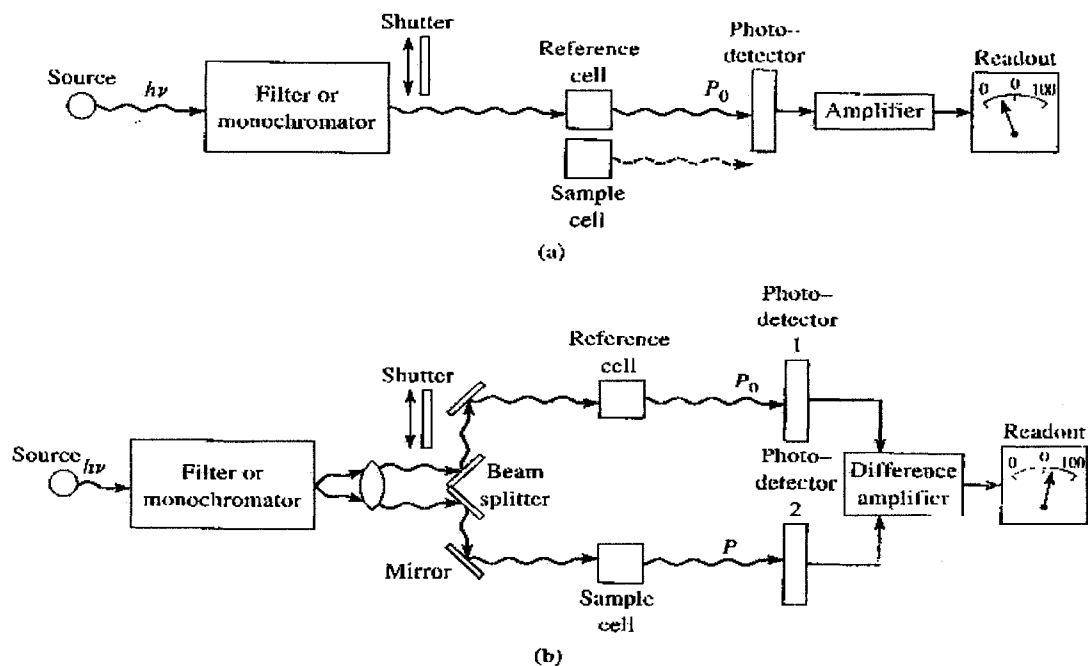
Figure 2.27: Diagram of (a) single-beam and (b) double-beam UV/Vis spectrophotometers[29]

As it can be seen from Figure 1.9 in Chapter 1, the absorption measurement requires two power measurements: each for pre- and post-entry through the medium that contains the analyte. The spectrophotometer measures the intensity of the light passing

through a sample (P) and compares it to the intensity of the light before it passes through the sample (P_o). The absorbance (A) is the logarithm of the ratio of the intensities of the incident light (P_o) and the transmitted light (P), i.e., $A = \log(P_o/P)$. The ratio P_o/P is called the transmittance (T), and is usually expressed as a percentage.

The ocean optic USB 2000 spectrophotometer with an LED boosted tungsteen bulb was used for this investigation. Figure 2.28 shows the actual UV/Vis apparatus along with the centrifuge machine and the sterilized centrifuge tubes containing the test samples used in the present study.

2.3.14   Laser diffraction particle size analysis

Laser diffraction particle size analyzer was used to study the increase of fine particle amount, and thus the specific surface area of the hauled self-consolidating concrete.

Background Laser diffraction particle size analyzer

In laser diffraction particle size analysis a representative cloud of particles passes through a broadened beam of laser light, scattering the incident light onto a Fourier lens. This lens focuses the scattered light onto a detector array and, using an inversion algorithm, a particle size distribution is inferred from the collected diffracted light data[74]. Light scattered by particles forms a series of concentric rings of alternating maximum and minimum intensities, often called the airy disk. The first minimum (closest to the center of the airy disk) provides information to determine the mean size of the distribution. Subsequent maxima and minima contain information on the shape and width of the distribution, including any shoulders and tails. It is this series of maxima and minima that needs to be accurately measured in order to report the true shape of the

95
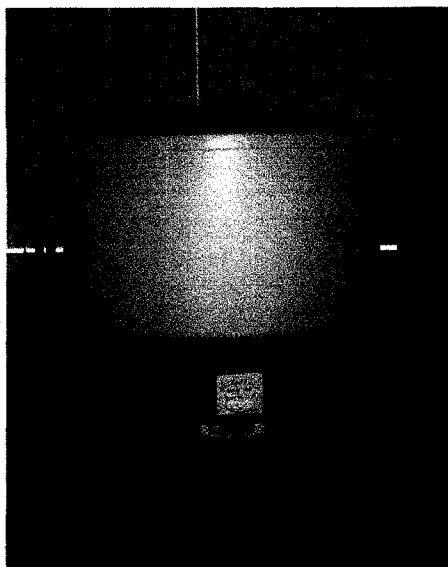
a) Centrifuge apparatus   b) Test samples in sterilized centrifuge tubes
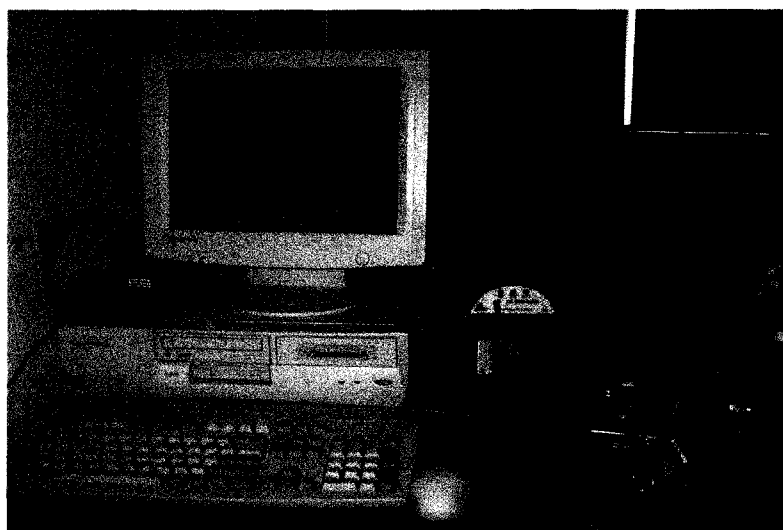
c) Actual single beam ultraviolet-visible spectrophotometer

Figure 2.28: Apparatus used for ultraviolet-visible spectroscopy test

particle size distribution.

Particles scatter light at an angle which is inversely proportional to their sizes. Therefore, as the size of the particles decreases, the scattering angle increases. Most laser diffraction instruments are only able to measure the angular intensity pattern up to a maximum angle of about 45 degrees[74]. This is because both the sample cell design and the Fourier lens size and quality limit the maximum angle of measurement. Unfortunately, sub-micrometer particles scatter most intensely at higher angles than this, limiting the collection of all scattered lights. Polarization Intensity Differential Scattering (PIDS) is a technique that overcomes the limitations of conventional laser diffraction to provide a high resolution sub-micrometer analysis. PIDS uses three different wavelengths of light (450, 600, and 900 nm) in two planes of polarization (vertical and horizontal) to irradiate the sample. The PIDS detectors are placed at angles of up to 150 degrees to collect the high angle scattered data. The resultant scatter patterns of differently sized sub micrometer particles are easily differentiated from each other to provide well resolved particle size distributions[74].

Modern laser diffraction instruments use Mie theory as the basis of their size calculations[74]. As Mie theory covers all light scatter from spherical particles, both PIDS data and laser diffraction data can be processed into a particle size distribution using one continuous algorithm.

Despite the widespread use and acceptance of the technique, three areas of concern exist for the particle size analyst who uses laser diffraction equipment, namely: inter-instrument reproducibility, resolution, and sub-micrometer characterization. In the past, there was evidence that laser diffraction particle size analyzers exhibited poor inter-

instrument reproducibility, offered limited resolution (often missing shoulders, tails, and sub-populations in particle size distributions), and gave information of limited value for sub-micrometer particles.

Particle size analysis

The laser diffraction particle size analyzer shown in Figure 2.30 was used in the present investigation. The mains steps in measuring a sample can be summarized as follows[74]:

(1) The correct range lens to fit to the instrument was selected.

(2) The program of the hardware configuration was set-up. The set-up hardware command allowed the inspection and adjustment if necessary.

(3) Precautions were taken to obtain a representative test sample. The condition for sample dispersion as suspensions in a liquid was considered carefully. The sample could have a tendency to flocculate in some media and dissolve in others. The small particles could float on the surface and the large or heavy particles might settle. Certain suspending media might promote the formation of bubbles which interfered with the measurement. The most convenient medium was water provided that the particles did not dissolve or react chemically. Some materials were not easily wetted in water and thus stick to each other rather than dispersing. Surfactant or other admixture could also be used to aid wetting and prevent particles floating.

(4) The test sample was added to the system at a suitable concentration. The concentration was adjusted by adding the sample slowly. The ideal concentration was reached when the bar on the obscuration monitor showed values between 0.1 and 0.4.

(5) The light scattered by the particles was measured at a suitable period to ensure that
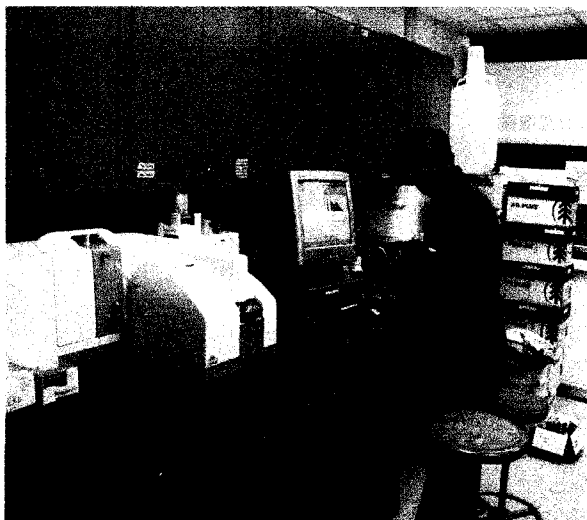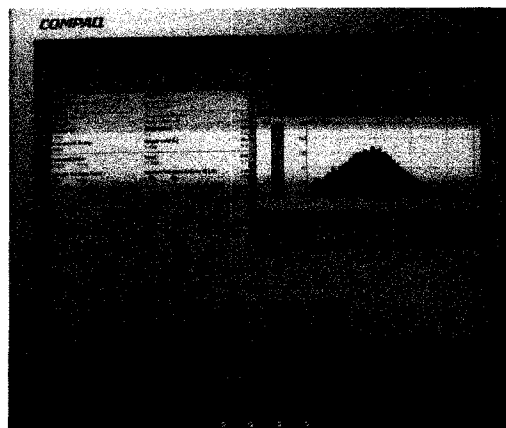
a) Testing	b) Test report at ideal sample concentration

Figure 2.29: Laser diffraction particle size analyzer

all particles were represented in the measurement and to average the fluctuations caused by the dispersing medium. A suitable measurement period was 10 to 30 seconds depending on the size range of the distribution. The setup experiment command can be used to change this time.

(6) The size distribution was obtained from the measured data by conducting the analysis.

CHAPTER 3

INFLUENCE OF ADMIXTURE SOURCE AND SLUMP FLOW ON FRESH

PROPERTIES OF DESIGNED SELF-CONSOLIDATING CONCRETE

The present chapter aims at: (1) comparing the optimum dosage requirement of four different sources of polycarboxylate-based High Range Water Reducing Admixture (HRWRA) and Viscosity Modifying Admixture (VMA) in attaining slump flows of 508 mm (20 inches), 635 mm (25 inches), and 711 mm (28 inches); and a visual stability index (VSI) of 0 (highly stable concrete) or 1 (stable concrete), (2) evaluating the flow ability/viscosity, stability, passing ability, and filling ability of three groups of self-consolidating concretes, and (3) examining the properties of the three groups of SCC as related to air content, bleeding, time of setting, adiabatic temperature, demolded unit weight, compressive strength and static modulus of elasticity.

3.1   Mixture proportion design

The mixture proportions used in the present investigation were developed based on the required engineering properties and mixture economy of various self-consolidating concretes using the raw materials described in chapter 2. Low, medium, and high slump flows, i.e., 508 mm (20 inches), 635 mm (25 inches), and 711 mm (28 inches); non-air entrained self-consolidating concretes were adopted.   For the purpose of this investigation, the moderate powder type self-consolidating concretes (see section 1.1)

100

was used to design the three groups of self-consolidating concretes. Factors that guided the selection of the matrix constituents and proportions are summarized below.

3.1.1 Engineering properties

3.1.1.1 Fresh performance

The fresh performance of self-consolidating concrete is characterized by its flow ability, passing ability, filling ability, and stability[1]. The general considerations to achieve the desired fresh performances were:

- Optimum coarse-to-fine aggregate ratio,

- Appropriate water-to-cementitious materials ratio (w/cm) to avoid formation of autogeneous shrinkage. In general, autogenous shrinkage dominates when the w/cm ratio is below 0.40. The shrinkage becomes less dependent on cement content when a w/cm ratio higher than 0.4 is used[75],

- Minimum cementitious materials content, and

- Optimum dosage of the combined HRWRA and VMA.

3.1.1.2 Hardened characteristic

- Strength was not a major consideration since high cementitious material content and low water-to-cementitious materials ratio were used.

- Sulfate durability was provided through Type V Portland cement, fly ash, and low-water-to-cementitious materials ratio. For the purpose of this study, all designed self-consolidating concretes were non-air-entrained.

In accordance with the testing standards related to the required fresh properties, and discussed in section 2.3, the followings target limits were adopted:

- Slump flow   : SF ± 25 mm (1.0 inch)

- VSI   : 0 to 1 (Highly stable to Stable)

- T_{50} : From 2 to 5 seconds

- J-ring value   : SF – J-ring $\leq$ 50 mm (2.0 inches).

- L-box   : $0.8 \leq H_2/H_1 \leq 1.0$

- U-box   : $H_1 - H_2 \leq 305$ mm (12 inches)

- V-funnel   : $t_v \leq 10$ seconds

- Column segregation   : SI (segregation index) $\leq$ 15%

3.1.2 Consideration of mixture economy

SCC is typically proportioned with a relatively high cementitious materials content and chemical admixtures, leading to a relatively high material cost. To achieve the most economical matrices, the following items were considered:

- Use of minimum possible cement content without sacrificing the desired rheological properties,

- Use of secondary cementitious material to improve fresh properties and mixture economy, and

- Use of minimum dosage of the combined admixtures to produce the intended fresh properties.

The flow chart of Figure 3.1 presents the mixture proportioning methodology of self-consolidating concrete. The mixture constituents and proportions used to produce the matrices are presented in Tables 3.1a trough 3.1c. Groups I, II, and III self-consolidating concretes were made with the aggregate groups R8, R67, and S7, respectively. All selected matrices were prepared with a constant water-to-cementitious materials ratio of 0.40 and a uniform cement factor of 390.38 kg/m^3 (658 lb/yd^3). The

102

quantities of fly ash used in the matrices were 25% of cement weight for the groups I and

II, and 20 % by weight of cement for the group III.


```
  ┌──────────────┐      ┌──────────────┐
  │ Engineering  │      │Consideration of│
  │ properties   │      │mixture economy│
  └──────────────┘      └──────────────┘
```

*Optimum coarse-to-fine aggregates ratio

**w/c

Cementitious materials content

***Chemical admixture

Perform by trial and error

Selection of performance criteria

Test of fresh properties of SCC

No

Yes

End
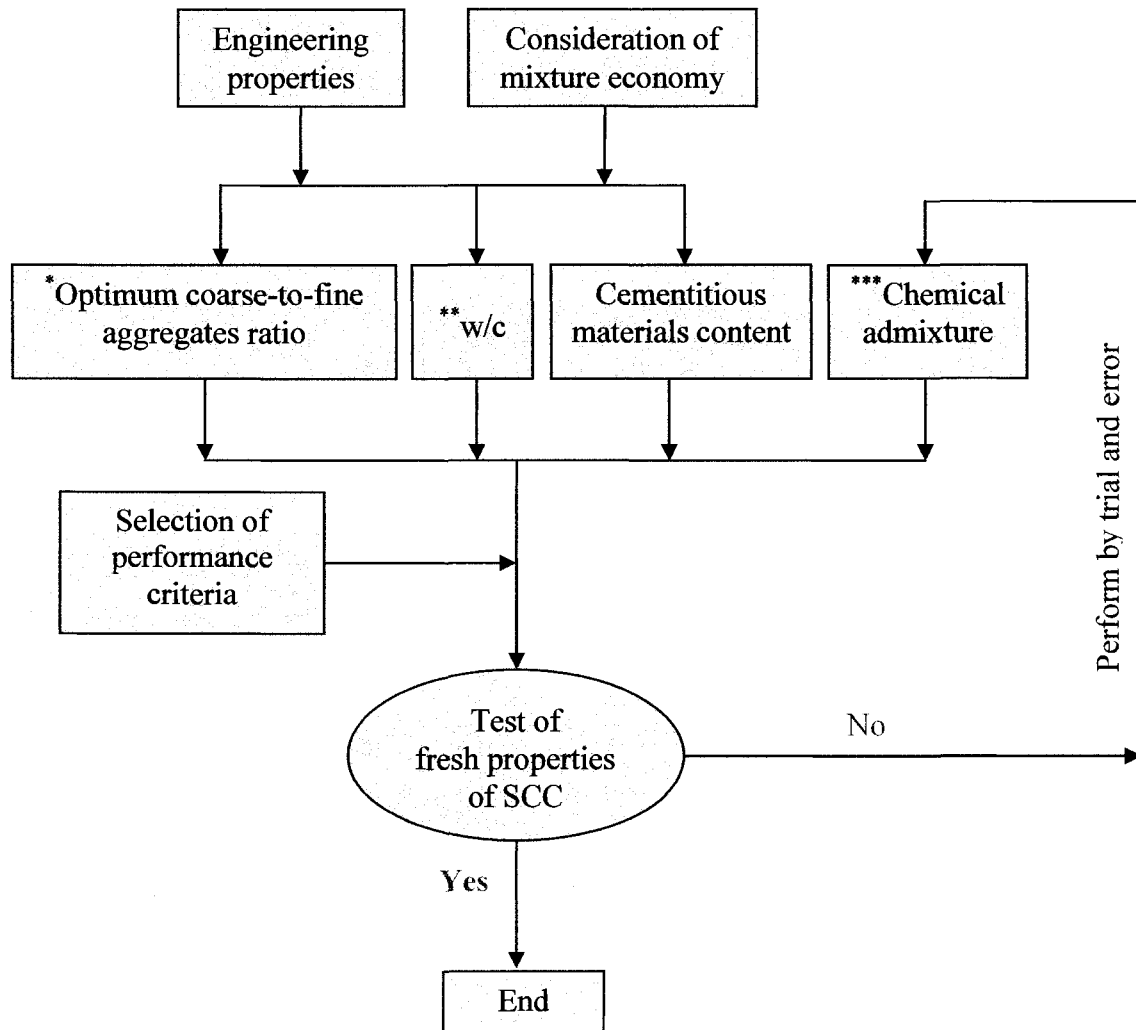
*Maximum size of aggregate not to exceed 20 mm (¾ inch)
**Water-to-cementitious materials ratio
***Start with manufacturer recommended dosage rate

Figure 3.1: Mixture proportioning methodology of self-consolidating concrete

Table 3.1a: Mixture proportion of group I self-consolidating concretes

Mix No.	Portland cement (kg/m^3)	Fly ash (kg/m^3)	w/cm[1]	Actual water (kg/m^3)	Fine aggre. (kg/m^3)	Coarse aggre. (kg/m^3)
R8.A.SF20	390.38	97.59	0.40	215.67	755.90	831.36
R8.B.SF20	390.38	97.59	0.40	215.89	755.62	831.06
R8.C.SF20	390.38	97.59	0.40	215.78	755.74	831.22
R8.D.SF20	390.38	97.59	0.40	215.89	755.61	831.06
R8.A.SF25	390.38	97.59	0.40	215.13	756.58	832.12
R8.B.SF25	390.38	97.59	0.40	215.63	755.94	831.42
R8.C.SF25	390.38	97.59	0.40	215.64	755.94	831.41
R8.D.SF25	390.38	97.59	0.40	215.67	755.90	831.37
R8.A.SF28	390.38	97.59	0.40	214.77	757.03	832.62
R8.B.SF28	390.38	97.59	0.40	215.56	756.03	831.52
R8.C.SF28	390.38	97.59	0.40	215.59	756.00	831.49
R8.D.SF28	390.38	97.59	0.40	215.60	756.07	831.47

[1]water-to-cementitious materials ratio, 1 kg/m^3 = 1.6856 lb/yd^3
1 kg/m^3 = 1.6856 lb/yd^3

Table 3.1a: Mixture proportion of group I self-consolidating concretes (cont'd)

Mix No.	ml/100 kg HRWRA[2]	VMA[3]	Paste fraction (%)	Mortar fraction (%)	Volume of coarse aggre. (%)
R8.A.SF20	411.76	0.00	36.27	66.44	32.21
R8.B.SF20	215.69	0.00	36.19	66.45	32.19
R8.C.SF20	326.80	0.00	36.24	66.44	32.20
R8.D.SF20	215.69	0.00	36.19	66.45	32.19
R8.A.SF25	555.56	326.80	36.44	66.41	32.23
R8.B.SF25	352.94	65.36	36.27	66.44	32.21
R8.C.SF25	379.08	65.36	36.28	66.44	32.21
R8.D.SF25	346.41	58.82	36.26	66.44	32.21
R8.A.SF28	673.20	522.88	36.55	66.39	32.25
R8.B.SF28	398.69	78.43	36.29	66.43	32.21
R8.C.SF28	411.76	78.43	36.30	66.43	32.21
R8.D.SF28	398.69	65.36	36.28	66.43	32.21

[2]high range water-reducing admixture, [3]viscosity modifying admixture
1 ml/100 kg = 0.0153 oz/cwt

Table 3.1b: Mixture proportion of group II self-consolidating concretes

Mix No.	Portland cement (kg/m³)	Fly ash (kg/m³)	w/cm[1]	Actual water (kg/m³)	Fine aggre. (kg/m³)	Coarse aggre. (kg/m³)
R67.A.SF20	390.38	97.60	0.40	210.50	838.15	773.29
R67.A.SF25	390.38	97.60	0.40	210.30	838.42	773.54
R67.A.SF28	390.38	97.60	0.40	209.73	839.21	774.27

[1]water-to-cementitious materials ratio, 1 kg/m³ = 1.6856 lb/yd³

Table 3.1b: Mixture proportion of group II self-consolidating concretes (cont'd)

Mix No.	ml/100 kg		Paste fraction (%)	Mortar fraction (%)	Volume of coarse aggre. (%)
	HRWRA[2]	VMA[3]			
R67.A.SF20	352.94	0.00	36.24	68.87	29.72
R67.A.SF25	457.52	65.36	36.31	68.86	29.76
R67.A.SF28	620.92	392.16	36.49	68.83	29.76

[2]high range water-reducing admixture, [3]viscosity modifying admixture
1 ml/100 kg = 0.0153 oz/cwt

Table 3.1c: Mixture proportion of group III self-consolidating concretes

Mix No.	Portland cement (kg/m³)	Fly ash (kg/m³)	w/cm[1]	Actual water (kg/m³)	Fine aggre. (kg/m³)	Coarse aggre. (kg/m³)
S7.A.SF20	390.38	78.08	0.40	197.16	848.71	922.29
S7.B.SF20	390.38	78.08	0.40	197.31	848.52	922.08
S7.C.SF20	390.38	78.08	0.40	197.23	848.63	922.20
S7.D.SF20	390.38	78.08	0.40	197.33	848.49	922.05
S7.A.SF25	390.38	78.08	0.40	197.04	848.89	922.48
S7.B.SF25	390.38	78.08	0.40	197.21	848.66	922.23
S7.C.SF25	390.38	78.08	0.40	197.16	848.72	922.29
S7.D.SF25	390.38	78.08	0.40	197.23	848.63	922.20
S7.A.SF28	390.38	78.08	0.40	196.87	849.11	922.72
S7.B.SF28	390.38	78.08	0.40	197.14	848.75	922.33
S7.C.SF28	390.38	78.08	0.40	197.10	848.80	922.38
S7.D.SF28	390.38	78.08	0.40	197.18	848.70	922.27

[1]water-to-cementitious materials ratio, 1 kg/m³ = 1.6856 lb/yd³
1 kg/m³ = 1.6856 lb/yd³

Table 3.1c: Mixture proportion of group III self-consolidating concretes (cont'd)

Mix No.	ml/100 kg		Paste fraction (%)	Mortar fraction (%)	Volume of coarse aggre. (%)
	HRWRA[2]	VMA[3]			
S7.A.SF20	281.05	0.00	34.60	65.62	33.04
S7.B.SF20	150.33	0.00	34.55	65.63	33.03
S7.C.SF20	228.76	0.00	34.58	65.63	33.03
S7.D.SF20	137.25	0.00	34.54	65.63	33.03
S7.A.SF25	326.80	65.36	34.63	65.62	33.05
S7.B.SF25	209.15	26.14	34.58	65.62	33.04
S7.C.SF25	261.44	26.14	34.60	65.62	33.04
S7.D.SF25	196.08	26.14	34.57	65.63	33.04
S7.A.SF28	431.37	104.58	34.69	65.61	33.05
S7.B.SF28	254.90	32.68	34.60	65.62	33.04
S7.C.SF28	307.19	32.68	34.62	65.62	33.04
S7.D.SF28	235.29	32.68	34.59	65.62	33.04

[2]high range water reducing admixture, [3]viscosity modifying admixture
1 ml/100 kg = 0.0153 oz/cwt

Particular attention was given to the coarse-to-fine aggregate ratio due to its critical role in generating sufficient amount of mortar for the selected self-consolidating concretes. The ASTM C 29[76] was used to determine the densified unit weight and the calculated void content using different ratios of the combined coarse and fine aggregates. As shown in Figures 3.2a through 3.2c, the optimum volumetric coarse-to-fine aggregate ratios of groups I, II, and III were found at 0.52/0.48 (or 1.083), 0.48/0.52 (or 0.923) and 0.52/0.48 (1.083), respectively. These ratios were subsequently utilized in the proportioning of the concrete constituents.

Four different sources (manufacturers) of polycarboxylate-based high range water reducing admixture (HRWRA), along with their viscosity modifying admixtures (VMA), were used. The optimum quantities of the chemical admixtures used in the selected
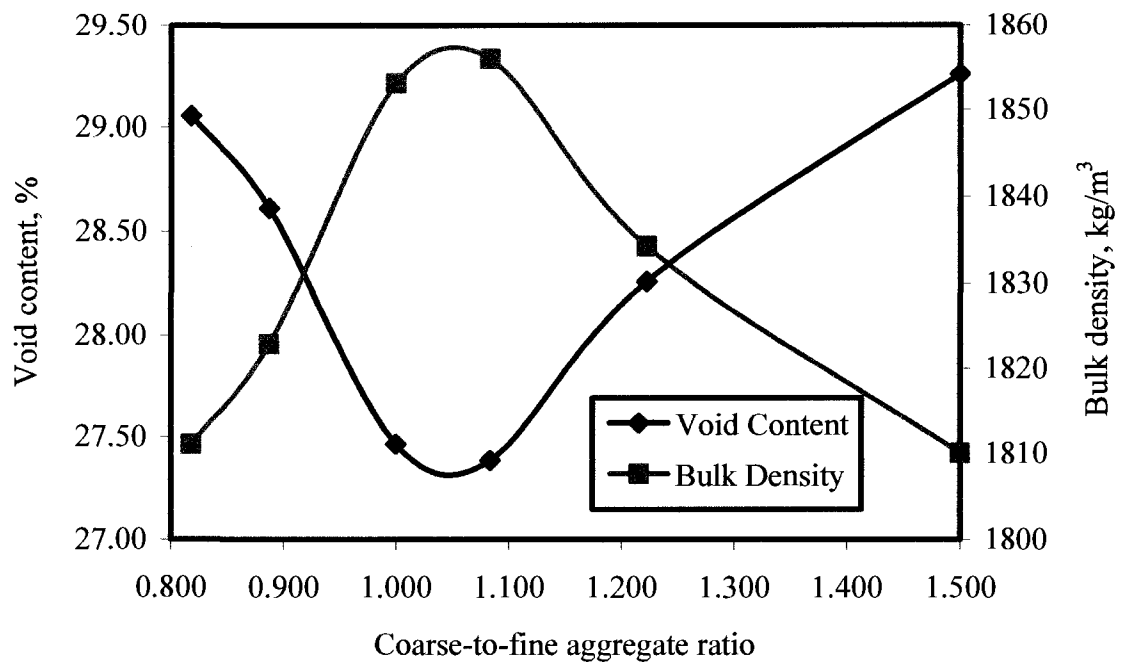
Figure 3.2a: Group I optimum volumetric coarse-to-fine aggregate ratio
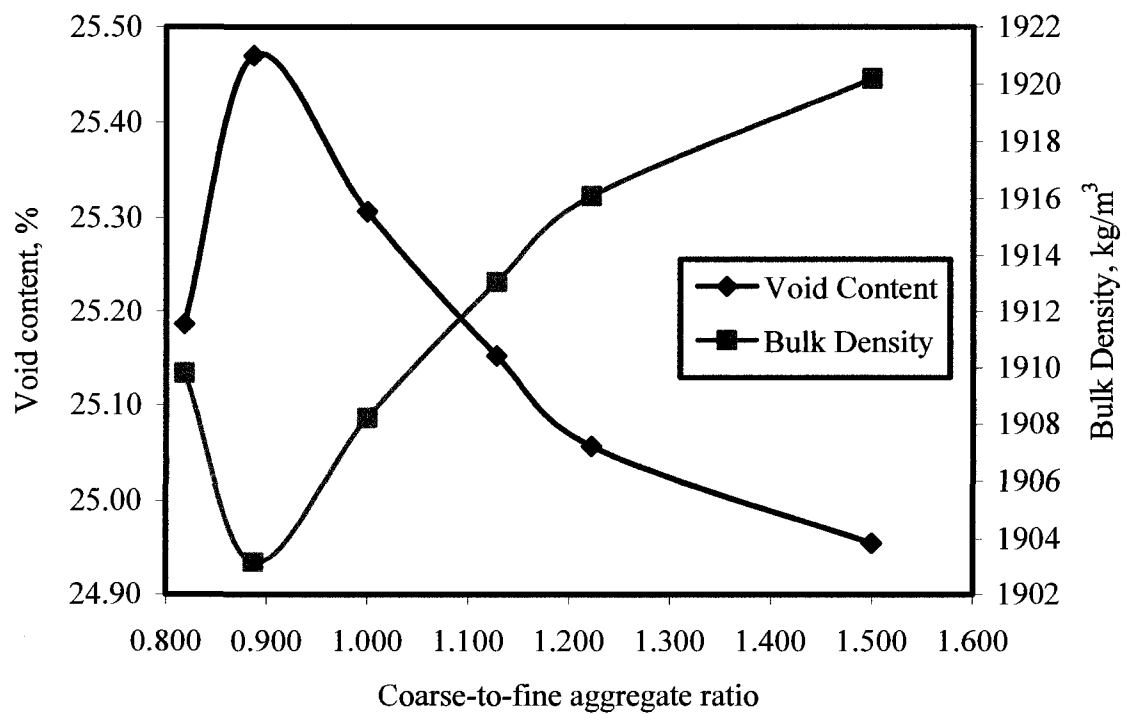
Figure 3.2b: Group II optimum volumetric coarse-to-fine aggregate ratio

107
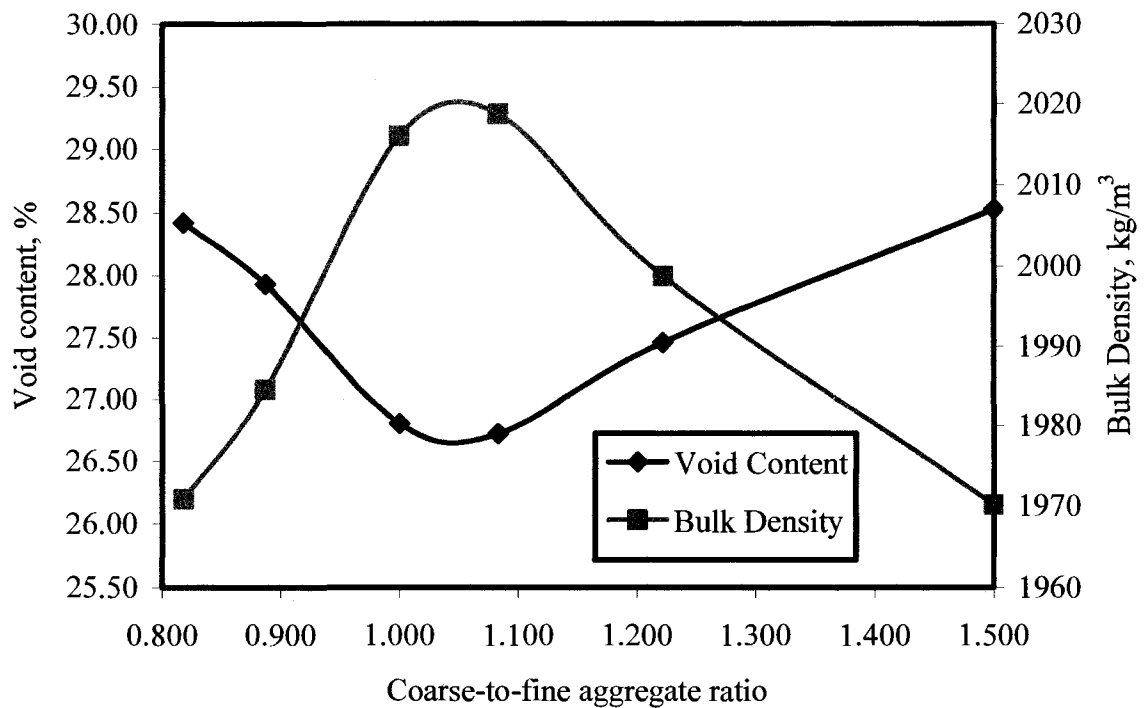
Figure 3.2c: Group III optimum volumetric coarse-to-fine aggregate ratio

self-consolidating concretes are shown in Tables 3.1a through 3.1c. They were obtained by evaluating the unconfined workability and dynamic stability of concretes using different trial batches until a satisfactory slump flow of 508 mm (20 inches), 635 mm (25 inches), and 711 mm (28 inches); and a visual stability index of 0 or 1 were attained.

Several combinations of HRWRA and VMA were tested in order to find the minimum dosage needed to achieve the above stated fresh properties. Also reported in Tables 3.1a through 3.1c, are the paste fraction, mortar fraction, and the percentage of coarse aggregate-to-total volume of concrete. These reported fractions were all within the recommended ranges as suggested by the ACI 237[1].

3.2   Mixing procedure, testing and sampling

An electric counter-current pan mixer with a capacity of 0.028 m^3 (1 ft^3) was used

to blend concrete components at a rate of 14.5 rpm. Batch volumes of 0.017 to 0.023m^3 (0.60 to 0.80 ft^3) were used for all trial mixtures. The mixing sequence consisted of blending the coarse aggregate with 1/3 of the mixing water for two minutes, followed by the fine aggregate with 1/3 of the mixing water for another two minutes, and the cementitious materials with the remaining 1/3 of the mixing water for three minutes. Finally, the HRWRA and VMA were added and blending of the matrix continued for an additional three minutes, followed by a two-minute rest and resumption of mixing for two additional minutes.

The freshly-mixed self-consolidating concretes were used to determine the unconfined workability, flow rate/plastic viscosity, passing ability, filling ability, and static and dynamic stabilities using slump flow, T_{50}, J-ring, U-box, L-box, V-funnel, visual stability index (VSI), and column segregation tests. The tests on the fresh concretes were conducted immediately after mixing to avoid any variations over time. When a significant discrepancy between two consecutives tests was observed, additional matrices were prepared and tested until reliable results were obtained. Each mixture was repeated at least three times, and the reported test results reflect the average value of a minimum of three tests.

Finally, the air content, bleeding, time of setting, adiabatic temperature, demolded unit-weight, compressive strength, and static modulus of elasticity were evaluated. Cylindrical specimens with 102 mm (4 inches) in diameter and 204 mm (8 inches) in height were cast in order to find the hardened characteristics of the self-consolidating concretes. All samples were cured in an isolated curing mold for 24 hours. Once they were removed from the molds, the test specimens were placed in a moist-curing room at

$21 \pm 2\ ^{\circ}C$ ($70 \pm 3\ ^{\circ}F$) for 7, 28 and 90 days, and then tested in compression for strength and modulus of elasticity. Prior to the curing, each cylinder was weighed to determine its unit weight upon demolding. Table 2.5, in Chapter 2, documents the evaluated fresh and hardened properties and their respective standard testing methods.

3.3   Optimum admixture dosage

The optimum admixture dosage was defined as the minimum amount of admixture required in achieving the target unconfined workability and dynamic stability. The optimized dosage requirements of HRWRA and VMA of the selected self-consolidating concretes are presented in Tables 3.1a through 3.1c. The comparisons of the test results are shown in Figures 3.3a through 3.3c. The discussion on the optimum admixture dosage, as influenced by the admixture source and slump flow, is presented below.

3.3.1   Influence of admixture source on optimum admixture dosage

The present section, devoted to the groups I and III, is intended to discuss the influence of the four selected admixture sources on the optimum admixture dosage in attaining the target slump flow of 508 mm (20 inches), 635 mm (25 inches), and 711 mm (28 inches), and a visual stability index (VSI) of 0 or 1. The test results indicate that there are differences in the dosage requirement of HRWRA and VMA in meeting the abovementioned fresh properties.

Irrespective of the SCC group, the required dosage amount of HRWRA was highest for the source A, followed by the sources C, B and D in descending order. The optimum dosages of sources B, C, and D superplasticizers in making 508 mm (20 inches) slump flow for the group I were lower by 48, 21, and 48%, respectively, when compared to that of source A. The corresponding reductions in optimum HRWRA dosages were 36,
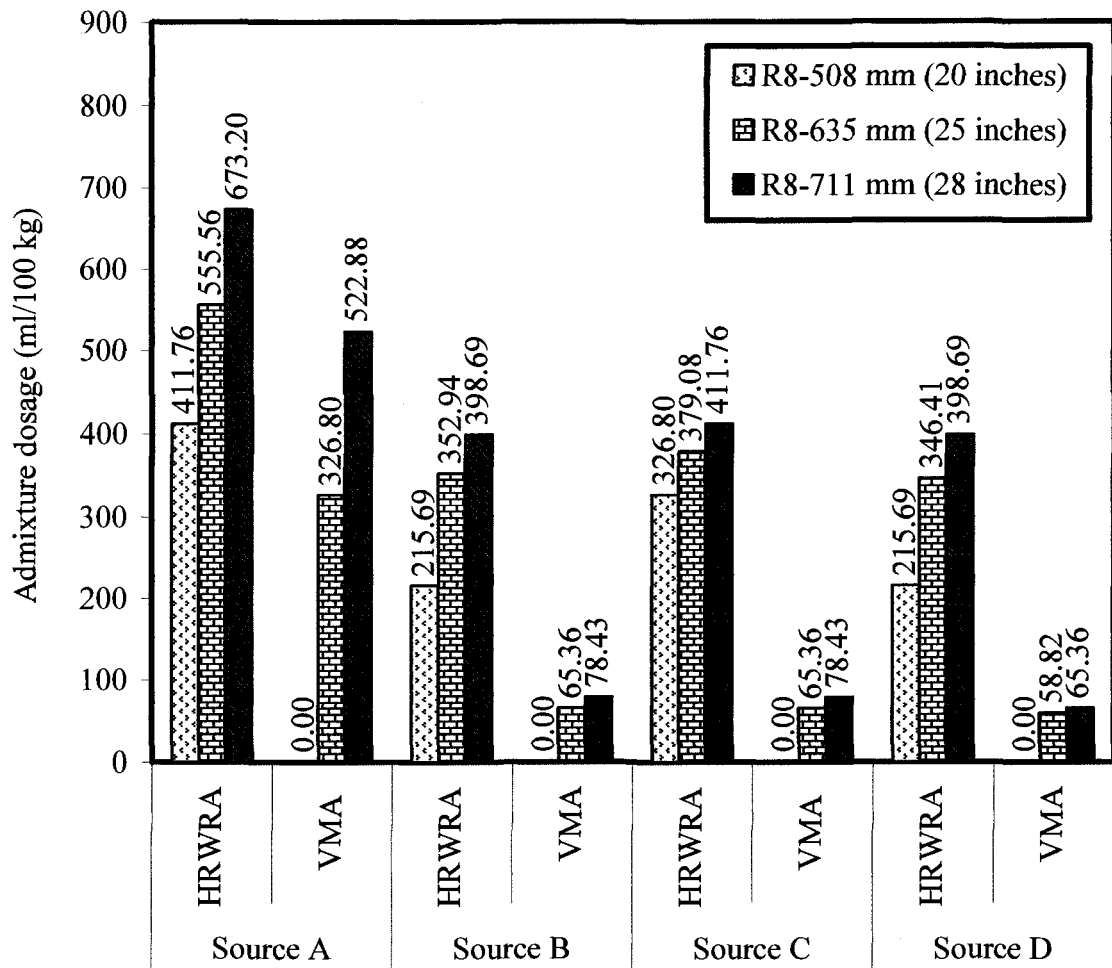
Figure 3.3a: Optimum admixture dosages for the group I self-consolidating concretes
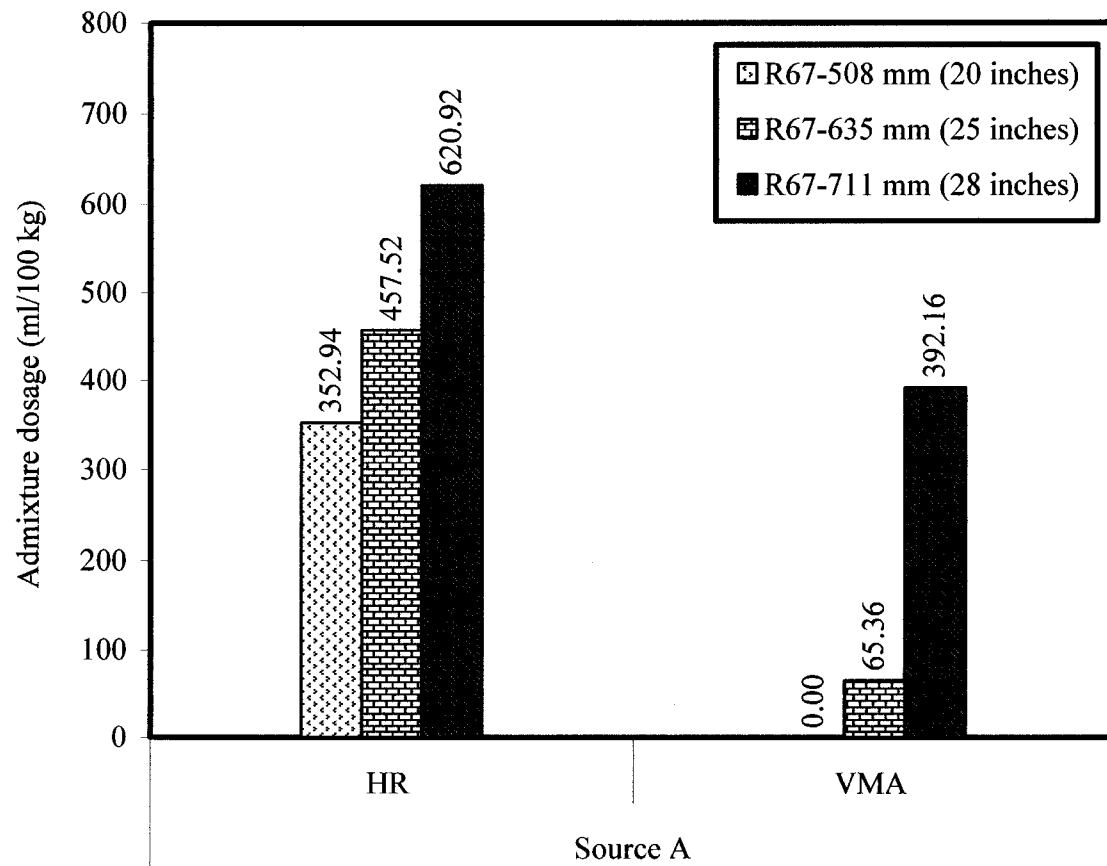
Figure 3.3b: Optimum admixture dosages for the group II self-consolidating concretes
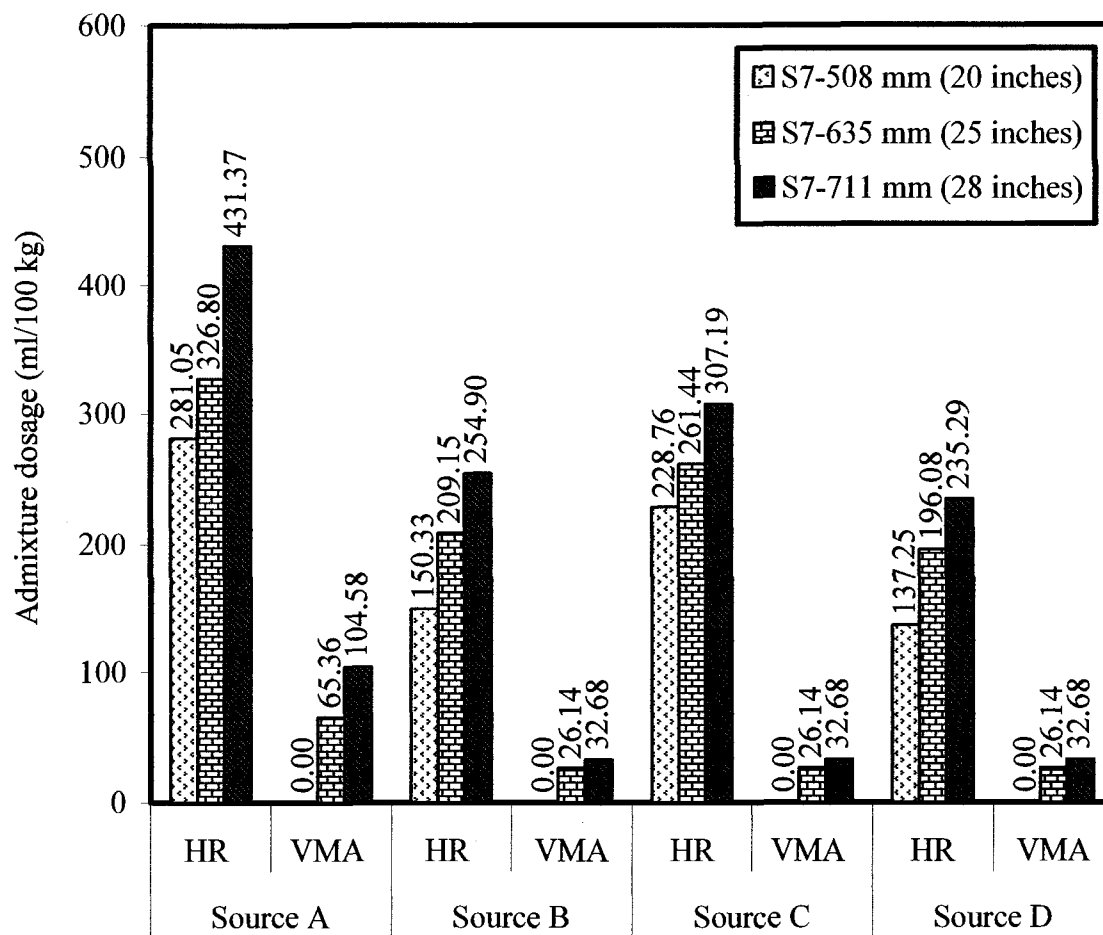
Figure 3.3c: Optimum admixture dosages for the group III self-consolidating concretes

32, and 38%; and 41, 39, and 41 % for the 635 and 711 mm (25 and 28 inches) slump flow of the group I, respectively.

All 508 mm (20 inches) slump flow group I self-consolidating concretes exhibited acceptable dynamic stability and plastic viscosity without any use of VMA. However, the SCCs prepared with slump flow of 635 and 711 mm (25 and 28 inches) required a balanced amount of viscosity modifying admixture in order to obtain the required stability and viscosity. As shown in Tables 3.1a through 3.1c and Figures 3.3a through 3.3c, the optimum VMA dosage requirement was also highest for the source A but remained uniform for the sources B, C, and D. Indeed, for the self-consolidating concretes made with 635 and 711 mm (25 and 28 inches) slump flow, sources B, C, and D required less VMA than the source A by nearly 80, 80, and 82 %; and 85, 85, and 88%, respectively.

A similar trend in the variation of admixture dosage was also observed for the group III self-consolidating concretes. The admixtures sources B, C, and D required 47, 19, and 51 %; 36, 20, and 40 %; and 41, 29, and 45 % less amount of HRWRA than the admixture source A for the mixtures prepared with 508, 635, and 711 mm (20, 25, and 28 inches) slump flow, respectively.

When compared to the admixture source A, the reductions in VMA dosage for the sources B, C, and D were fairly uniform at about 60 and 69 % for the SCCs made with 635 and 711 mm (25 and 28 inches) slump flow, respectively. All 508 mm (20 inches) slump flow of group III self-consolidating concretes displayed acceptable dynamic stability and plastic viscosity without the use of the viscosity modifying admixture.

The information concerning the exact chemical structure and molecular weight of

the HRWRA and VMA used in this investigation could not be obtained from the manufacturers. The explanation regarding the differences in optimum admixture dosages obtained during this investigation is based on the adsorption amount of HRWRA molecules in cement particles obtained from the ultraviolet-visible (UV/Vis) spectroscopy test, the information on the chemical type of the admixtures acquired from the Manufacturers Product Data (MPD) and Material Safety Data Sheet (MSDS) (see Tables 2.3 and 2.4), the related literature as summarized in Section 1.2.3, and the VMA-to-HRWRA ratios.

3.3.1.1 Adsorption of admixture on cement particles

This section is intended to explain and confirm the test results related to the trend of the optimum dosages requirement of the selected polycarboxylate-based HRWRAs (PC-HRWRA). As alluded to earlier in Section 1.2.3.3 of Chapter 1, the mechanism of action of superplasticizer in Portland cement solution involves adsorption, electrostatic repulsion, and steric hindrance repulsion. The PC-HRWRA carboxyl group (COO⁻) has to be adsorbed first to the cement calcium ions (Ca^{2+}) before being able to play a dispersing role. The UV/Vis test was used to evaluate the concentration of free admixture in the cement-water-HRWRA solution before a correlation with admixture adsorption was made. The relationship between the increase in concentration of free admixture and the increase in adsorption amount was established through the effect of slump flow on admixture dosage. As can be seen in Section 3.3.2, the higher slump flow required a higher dosage of admixture (see Figure 3.1a through 3.1c).

The UV/Vis spectroscopy absorption is not a specific test for any given compound. The nature of the solvent, the pH of the solution, temperature, high

115

electrolyte concentrations, and the presence of interfering substances can influence the absorption spectra of compounds, as can variations in effective bandwidth in the spectrophotometer[29]. However, the wavelengths of absorption peaks can be correlated with the types of bonds in a given molecule and are valuable in determining the functional groups within a molecule[29].

The UV/Vis test procedure is summarized in Chapter 2, Section 2.3.13. The experiment uses a test sample in the UV/Vis beam to determine the absorbance or transmittance at different wavelengths. Alternatively, samples are prepared in known concentrations and their absorbance determined by the UV/Vis spectrophotometer. The results are then graphed to make a calibration curve from which the unknown concentration can be determined by its absorbance.

In the present investigation, a uniform cement factor of 390.38 kg/m^3 (658 lb/yd^3) and a constant water-to-cementitious materials ratio of 0.4 were used for all trial matrices. The dosage of HRWRA was kept constant at 255 ml/100 kg (3.9 oz/cwt) for all four admixture sources, and distilled water was used throughout the study to avoid any contamination which could impair the test results. The test was performed as follows:

- First, the calibration curves for interpolation were generated. For that purpose, the selected polycarboxylate-based HRWRA were manually diluted in distilled water at different concentrations. After 10 minutes, the solutions were analyzed by the UV/Vis spectroscopy, and calibration curves of known HRWRA concentrations as a function of the recorded absorbance were plotted. Appendix III documents the absorbance spectra for the calibration curves and Figures 3.4a through 3.4d present the calibration curves for the selected admixture sources. The test results indicated a very strong relationship

116
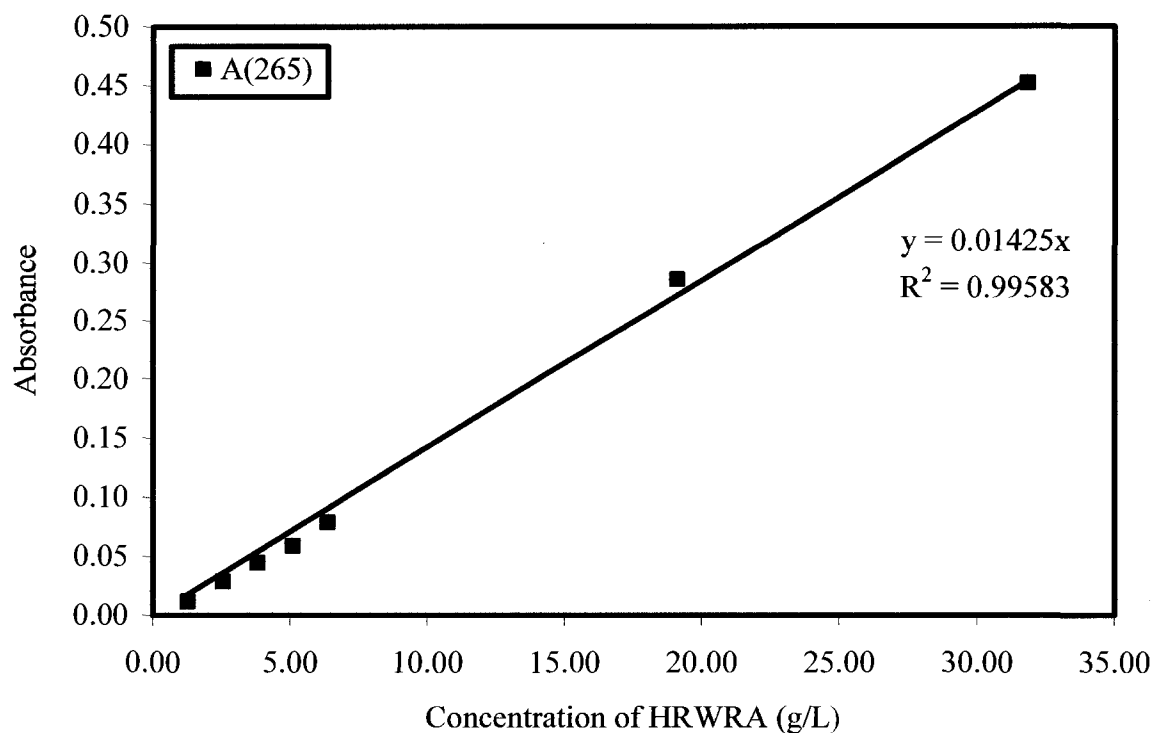
Figure 3.4a: Calibration curve of source A HRWRA at wavelength of 265 nm
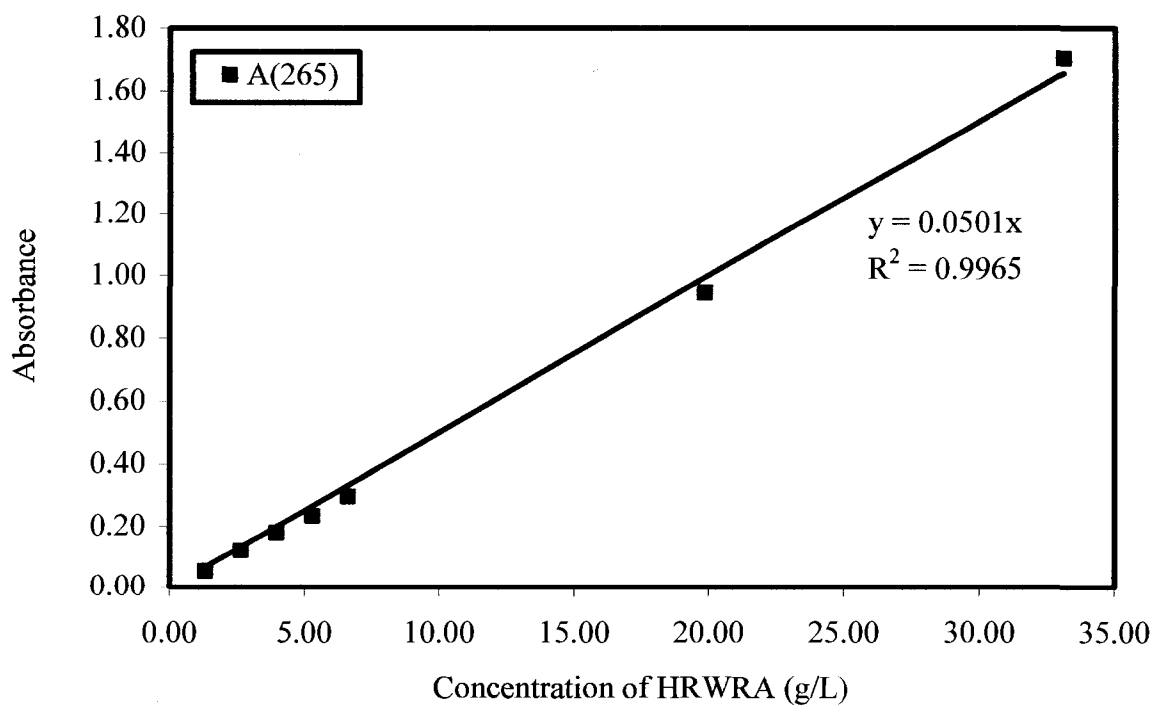
Figure 3.4b: Calibration curve of source B HRWRA at wavelength of 265 nm
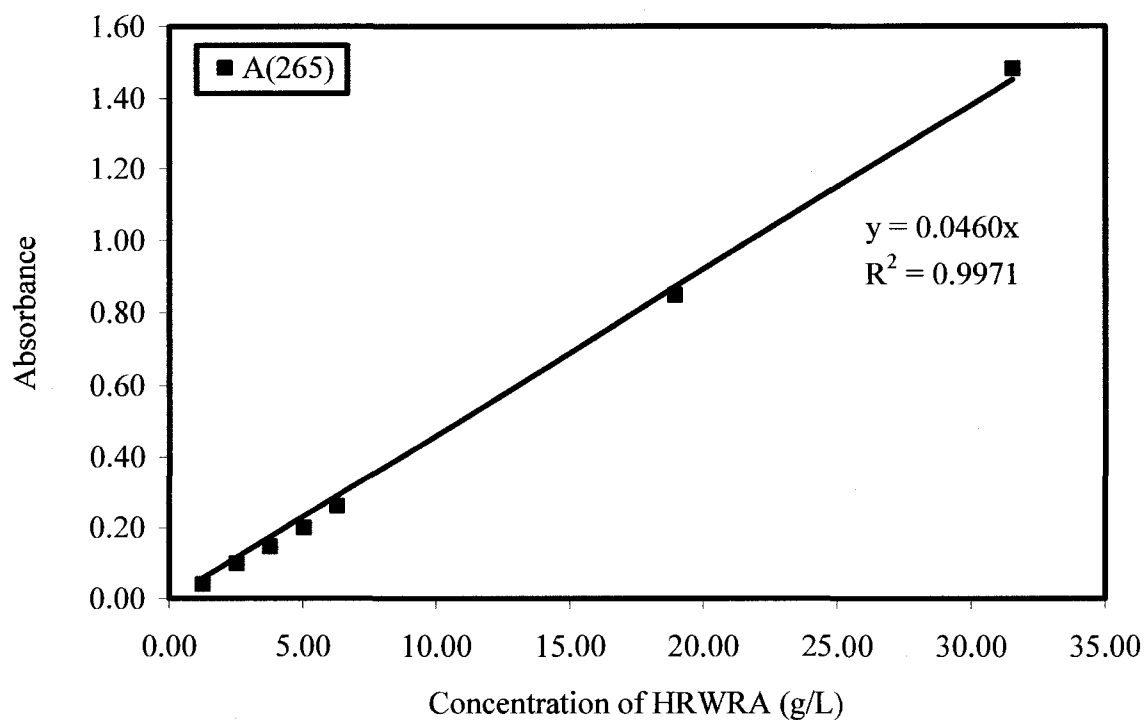
Figure 3.4c: Calibration curve of source C HRWRA at wavelength of 265 nm
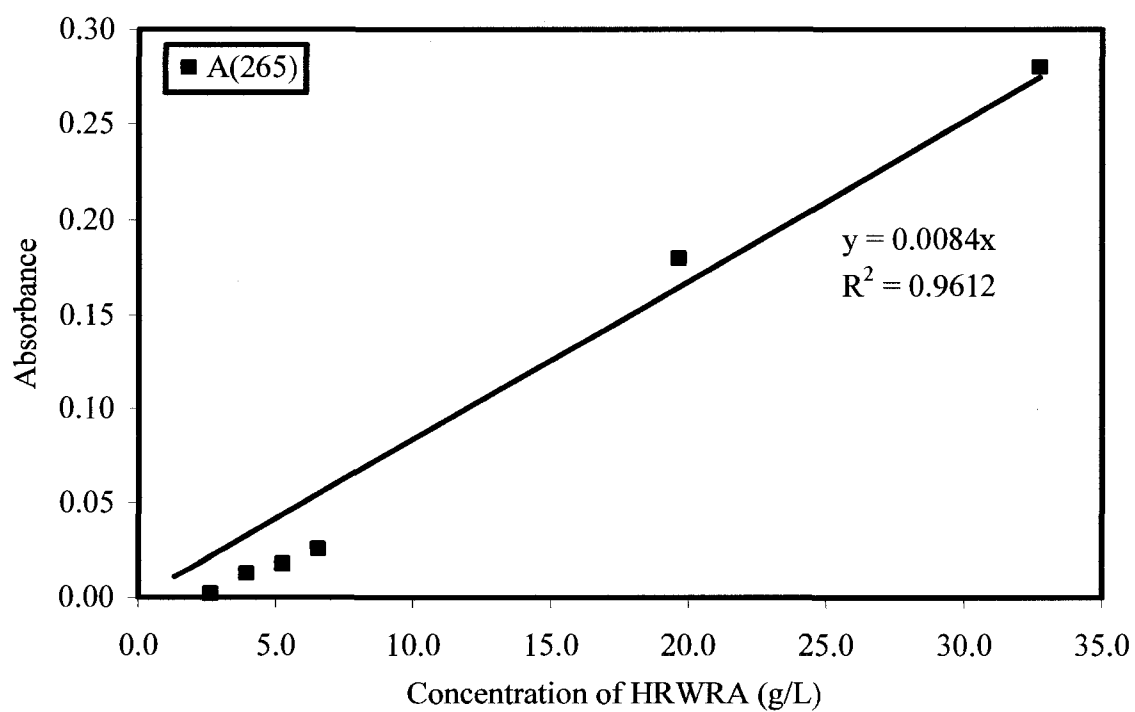
Figure 3.4d: Calibration curve of source D HRWRA at wavelength of 265 nm

118

between the concentration of HRWRA in water and the recorded absorbance, as indicated by the coefficient of multiple determinations (R^2).

- Second, the UV/Vis absorption curves for the cement-water-HRWRA solution were made. The cement and water were first mixed in a pan mixer at 14.5 rpm for 5 minutes before the pre-measured HRWRA was added and afterward the mixing continued for an additional 5 minutes. The blended paste was placed in sterilized tubes and centrifuged by ultracentrifugation for 5 minutes at 3500 rpm in order to suspend fine particles in solution. The liquid at the top of the sample was collected with a pipette and transferred into a syringe mounted on a 0.20 μm filter. The filtered liquid was then tested by the UV/Vis spectroscopy. Figure 3.5 shows typical ultraviolet absorption spectra and Figure 3.6 displays the UV/Vis absorption spectra of the four selected admixture sources.
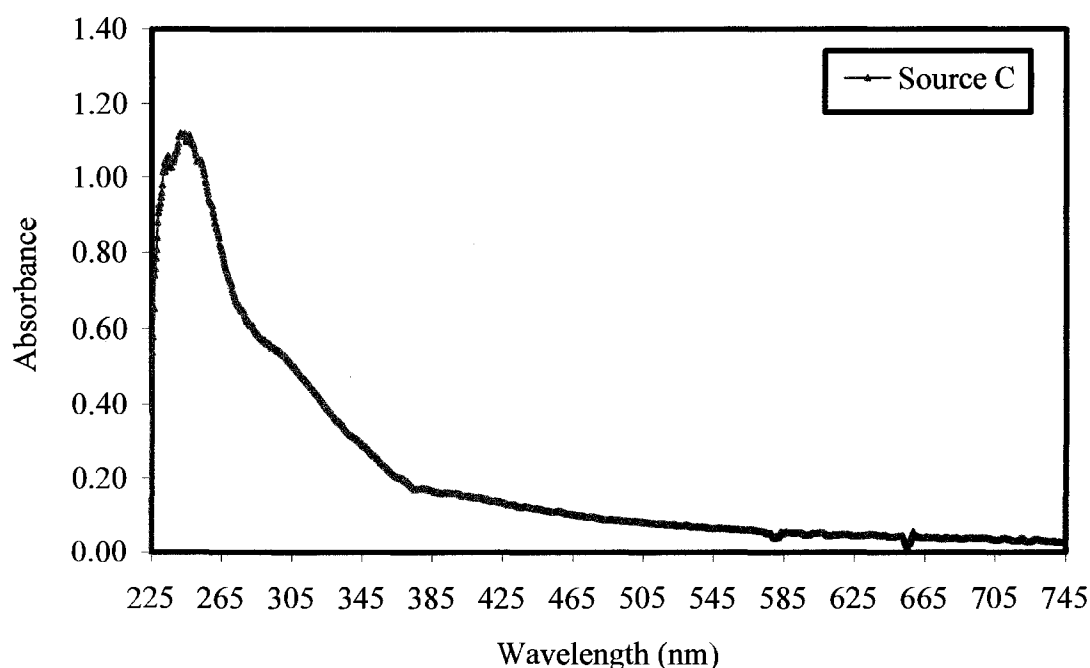
Figure 3.5: Typical ultraviolet-visible absorbance spectrum:
Case of source C HRWRA
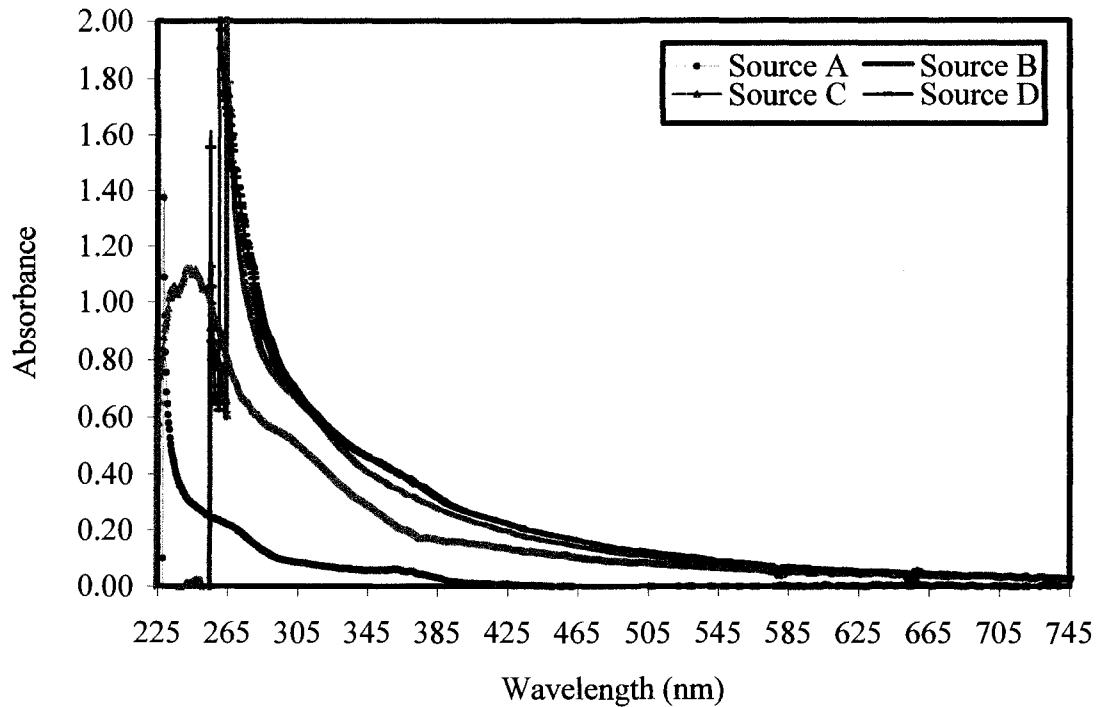
Figure 3.6: Comparison of ultraviolet-visible absorbance spectra
of sources A, B, C, and D HRWRAs

The test results indicated that the recorded absorbance peaks varied from one admixture to another as they occurred at different wavelengths (from 230 to 265 nm), indicating their differences in chemical type. The test results were also used to determine the actual concentration of free admixture in the liquid phase of cement-water-HRWRA. The calculated concentrations of the selected admixture sources are summarized in Table 3.2. It can be seen that the solution concentration of free admixture was highest for the source D, followed by the sources B, C, and A in descending order. This test results also confirms the earlier findings for the optimum dosage requirement of the four selected admixture sources as reported in Section 3.3.1.

Table 3.2: Cement-water solution's concentration of free HRWRA

Designation	*Absorbance (λ, nm)			Increase in HRWRA concentration (g/L)
	A(265)	A(700)	A(265 corr)	
Source A	1.039	0.013	1.026	15.43
Source B	2.558	0.051	2.507	33.96
Source C	1.624	0.054	1.570	16.61
Source D	2.495	0.052	2.443	194.90

*Absorbance at wavelength λ, in nanometer

3.3.1.2 Chemical type of the selected HRWRA and VMA

The difference in the selected superplasticizers dosages requirement in attaining a uniform unconfined workability, flow rate/plastic viscosity, and dynamic stability can also be explained through their chemical types. In order to support this theory, a brief review on the chemical structure of the selected admixtures and their mode of functioning is necessary.

Figure 1.11, in Chapter 1, is a typical representation of the chemical structure of a copolymer of acrylic acid and acrylic ester. The characteristic of a PC-type superplasticizer can be modified by varying the acid-to-ester ratio (modules n and m). The higher the acid ratio is, the higher is the carboxylic group content, and the higher is the adsorption ability. On the other hand, when the ester ratio is predominant, the side chains content increases and the carboxylic group content decreases, leading to a decrease in adsorption and dispersibility. Despite their relatively high dosage rate, the advantage of a high ester-to-acid ratio superplasticizer resides in its superior slump flow retention[34]. In fact, during the initial cement-polycarboxylate ester superplasticizer

(PCE) interaction the polymers which could not react immediately are adsorbed gradually to cement particles as time elapsed, resulting in better flow retention.

All four superplasticizers were acrylic polymers-based and had the same mechanism of action, namely: adsorption, electrostatic repulsion, and steric repulsion. In general, the test results showed that the difference between the optimum HRWRA dosages requirement of the sources B, C, and D in attaining the required fresh performance was marginal; indicating that they might had a similar chemical structure. On the other hand, source A produced results that were different than those of the sources B, C, and D. The behavior of the sources B, C and D superplasticizers was similar to that of a polycarboxylate-acid type (PCA), where the acid portion is predominant when compared to ester part. Source A had the highest ester-to-acid ratio and was polycarboxylate-ester type (PCE).

The difference in viscosity modifying admixture optimum dosage among the four sources can be attributed to the mechanism by which these admixtures function. Based on the reported results obtained during this study, the source A required a higher optimum VMA dosage than those of the sources B, C, and D. The source A viscosity modifying admixture functioned by thickening the concrete, making it very cohesive without significantly affecting the fluidity of the fresh matrix. The sources B, C and D performed by binding the water within the concrete mixture resulting in an increase in viscosity while reducing or eliminating concrete bleeding. The present investigation revealed that a large amount of the source A VMA was always needed to modify the viscosity of the SCC, while a small amount of the VMA belonging to the sources B, C, and D generated a noticeable improvement in the fresh performance of the selected self-

122

consolidating concretes.

3.3.1.3   VMA-to-HRWRA ratio

The minimum dosage required to achieve the stated fresh properties was obtained

by trial and error combinations of HRWRA and VMA. The analysis of the test results

obtained during this study indicated a trend for the VMA-to-HRWRA ratio, as it can be

seen in Table 3.3.   The similarity in the VMA-to-HRWRA ratios of the admixture

sources B, C, and D further affirms that these sources have a similar chemical

composition. The higher ratio seen in the source A was due to its thickening mode of

functioning which led to a higher amount of VMA required to make highly stable or

stable matrices. It can also be noted that the VMA-to-HRWRA ratio decreased for the

self-consolidating concrete made with a coarser aggregate due to its matrix incorporating

a smaller volume of paste (see Tables 3.1a through 3.1c).

Table 3.3: VMA-to-HRWRA dosage ratios

Admixture sources	Group I SCC		Group III SCC	
	Slump flow 635 mm	Slump flow 711 mm	Slump flow 635 mm	Slump flow 711 mm
A	0.59	0.78	0.20	0.24
B	0.19	0.20	0.13	0.13
C	0.17	0.19	0.10	0.11
D	0.17	0.16	0.13	0.14

1 mm = 0.03937 inch

3.3.2   Influence of slump flow on optimum admixture dosage

As shown in Tables 3.1a through 3.1c and Figures 3.3a through 3.3c, the

admixture dosages increased with an increase in slump flow, regardless of the admixture

123

sources and the selected SCC groups.

For the group I self-consolidating concretes, as the slump flow increased from 508 to 635 to 711 mm (20 to 25 to 28 inches), the optimum amount of HRWRA increased by 35 and 21%; 64 and 13%; 16 and 9%; and 61 and 15% for the admixture sources A, B, C, and D, respectively. When the slump flow increased from 635 to 711 mm (25 to 28 inches), the increases in the optimum VMA dosages became 60, 20, 20, and 11% for the admixture sources A, B, C, and D, respectively. The acceptable plastic viscosity and dynamic stability were achieved for the self-consolidating concretes prepared with 20 inches (508 mm) slump flow without the use of the viscosity modifier.

The group II self-consolidating concretes also showed an increase in the optimum admixture dosage when a higher slump flow was required. The HRWRA optimum dosage requirement for the group II self-consolidating concretes increased by 30 and 36% when the slump flow increased from 508 to 635 to 711 mm (20 to 25 to 28 inches), respectively. The VMA optimum dosage increased by nearly 500% when the slump flow changed from 635 to 711 mm (25 to 28 inches). Once again, the group II SCC prepared with 508 mm (20 inches) slump flow did not require any VMA to produce the target stability and plastic viscosity.

The trend in the optimum dosage requirement for the group III self-consolidating concretes was similar to that of the group I. For the slump flow increases from 508 to 635 to 711 mm (20 to 25 to 28 inches), the HRWRA optimum dosage for the admixture sources A, B, C, and D increased by 16 and 32 %; 39 and 22 %; 14 and 18 %; and 43 and 20 %; respectively. The increases in the VMA dosage remained at 60% for the admixture source A, and 25% for the admixture sources B, C, and D when the slump flow changed

from 635 to 711 mm (25 to 28 inches). No VMA was needed for the group III self-consolidating concretes made with 508 mm (20 inches) slump flow.

The increase in optimum dosage requirement of HRWRA and VMA in obtaining a higher slump flow can be explained through the demand in the rheological performance of the concrete. During the deflocculation system, the bond between the finer cement particles was gradually broken by the mixing water until a uniform matrix (normal slump concrete) was generated. From that moment, a superplasticizer was needed to produce a flowable matrix. The need for a higher slump flow required an increase in the amount of HRWRA. In the presence of higher amount of HRWRA, the force needed to disperse the ingredients of the fresh matrix, i.e., the yield stress, was gradually reduced as the fresh concrete was allowed to spread further. In fact, when the amount of superplasticizer was increased, the adsorbed amount of polymer molecules in cement particles increased along with the induced zeta potential (the potential difference between the dispersion medium and the stationary layer of fluid attached to the dispersed particle) leading to higher electrostatic repulsion forces. Additionally; the intensity of the steric repulsive forces (which were short-range repulsive forces caused by the overlapping of the adsorbed polymer) was also increased when a higher HRWRA dosage was used. It should be noted that the superplasticizer adsorption can show an adsorption plateau, which is also called the point of saturation. The adsorption plateau roughly corresponds to the amount of superplasticizer which allows for the optimum fluidity.

The increase in slump flow value or HRWRA dosage was usually accompanied by a decrease in plastic viscosity, and a viscosity modifying admixture was needed to overcome that problem. The addition of a VMA restored the plastic viscosity

125

deteriorated by the increase in HRWRA.

3.3.3 Predictive statistical equations of the SCC admixture dosage

As it can be seen in Tables 3.1a through 3.1c, the selected 27 trial matrices have different proportions of paste volume ratio (P), mortar volume ratio (M) and coarse aggregate absolute volume (C_{Aggr}). The matrix factor $\beta = P \cdot M \cdot C_{Aggr}$ was used to characterize each trial matrix. The equations to predict the optimum admixture dosage requirement were determined using a statistical program[59]. Analyses were conducted at a 95% confidence level. The predictive equations were tested for accuracy using R^2 (the coefficient of multiple determination) and S (average standard deviation). Correlations between the data predicted from the regression equations and the actual test results were evaluated using F and T tests. Due to the difference in their mechanism of action, admixture source A in one hand, and admixture sources B, C, and D in other hand, were analyzed separately. The HRWRA and the VMA optimum dosages were related to the target slump flow (SF) and the matrix factor (β) through the following equations:

Admixture source A

$$HR_A = 188148.26 + 0.7386SF - \frac{28390.11}{\beta} + \frac{1070.24}{\beta^2} \tag{3.1}$$

$$VMA_A = 883556.62 + 0.9014SF - \frac{134854.26}{\beta} + \frac{5141.37}{\beta^2} \tag{3.2}$$

Admixture sources B, C, and D

$$HR_{B,C,D} = 75080212.01 - \frac{45592.27}{SF} - \frac{17184249.17}{\beta} + \frac{1310935.51}{\beta^2} - \frac{33333.10}{\beta^3} \tag{3.3}$$

$$VMA_B = 88468.88 + \frac{1979137.54}{SF} - 2369377.96\beta - \frac{122606642.61}{SF^2}$$
$$+ 15826854.10\beta^2 - 21814887.75\frac{\beta}{SF} \qquad (3.4)$$

Where:

HR_A, $HR_{B,C,D}$ = optimum dosage of high range water reducing admixture, (ml/100 kg)

VMA_A, $VMA_{B,C,D}$ = optimum dosage of viscosity modifying admixture, (ml/100 kg)

SF = expected slump flow (mm), with 508 mm $\leq SF \leq$ 711 mm (tolerance $\pm$ 25 mm)

$\beta = P \cdot M \cdot C_{Aggr}$ (%),

Where: P = Paste volume ratio; M = Mortar volume ratio; and C_{Aggr} = Coarse aggregate

absolute volume.

_N.B._: - _The paste and mortar used in β do not include the admixtures._

- _No VMA is needed for slump flow SF $\leq$ 508 mm._

The regression variables R^2, S, Prob(t) and Prob(F) are given in Table 3.4. The

calculated values are indicative of a strong relationship between the dependent variable

(HRWRA or VMA) and the independent variables (slump flow value, paste volume ratio,

mortar volume ratio, and coarse aggregate absolute volume). Tables 3.5a and 3.5b shows

the actual values of the optimum admixtures dosage versus their predicted values. The

predictive equations yielded percentage errors ranging for most part from 0 to 10%

confirming a good relationship between the actual and the predicted optimum admixture

dosage.

3.4   Fresh characteristics

The results for the fresh characteristics of the selected self-consolidating concretes

are shown in Tables 3.6a through 3.6c. The discussion on the fresh performance of the

Table 3.4: Statistical regression variables

Equations	Coefficient of multiple determination R^2, %	Standard deviation S, ml/100 kg	Prob(t)						Prob (F)
			a	b	c	d	e	f	
3.1.: $HR_A = a+b*SF+c/\beta+d/\beta^2$	98.58	27.44	0.2847	0.0398	0.2897	0.2949	-	-	0.0211
3.2.: $VMA_A = a+b*SF+c/\beta+d/\beta^2$	99.53	22.61	0.0144	0.0187	0.0144	0.0146	-	-	0.0069
3.3.: $HR_{B,C,D} = a+b*SF+c/\beta+d/\beta^2+e/\beta^3$	92.68	27.16	0.0038	0.3983	0.0039	0.0039	0.0039	-	0.0000
3.4.: $VMA_{B,C,D} = a+b/SF+c*\beta+d/SF^2+e*\beta^2+f*\beta/SF$	98.40	4.44	0.2027	0.0069	0.1913	0.00142	0.1809	0.0158	0.0000

Table 3.5a: Actual and calculated optimum HRWRA dosages

SF (mm)	β (%)	Admixture source	Optimum HRWRA		
			Actual (ml/100 kg)	Calculated (ml/100 kg)	% Error
520.70	0.0776	A	411.76	410.58	0.29
644.65	0.0780	A	555.56	560.10	-0.82
727.20	0.0783	A	673.20	670.21	0.44
527.05	0.0750	A	281.05	268.59	4.43
651.00	0.0751	A	326.80	357.81	-9.49
727.20	0.0752	A	431.37	412.45	4.39
514.35	0.0774	B,C,D	215.69	240.61	-11.55
641.35	0.0776	B,C,D	352.94	353.72	-0.22
733.55	0.0777	B,C,D	398.69	428.23	-7.41
517.65	0.0749	B,C,D	150.33	143.49	4.55
641.35	0.0750	B,C,D	209.15	232.22	-11.03
723.90	0.0750	B,C,D	254.90	240.33	5.72
524.00	0.0775	B,C,D	326.80	284.37	12.98
641.35	0.0776	B,C,D	379.08	353.72	6.69
723.90	0.0777	B,C,D	411.76	427.40	-3.80
524.00	0.0750	B,C,D	228.76	216.30	5.45
651.00	0.0750	B,C,D	261.44	233.27	10.77
723.90	0.0751	B,C,D	307.19	297.75	3.07
524.00	0.0774	B,C,D	215.69	242.24	-12.31
651.00	0.0776	B,C,D	346.41	354.78	-2.42
720.85	0.0776	B,C,D	398.69	361.56	9.31
511.30	0.0749	B,C,D	137.25	142.39	-3.75
649.73	0.0750	B,C,D	196.08	233.14	-18.90
727.20	0.0750	B,C,D	235.29	240.61	-2.26

1 ml/100 kg = 0.0153 oz/cwt

Table 3.5b: Actual and calculated optimum VMA dosages

SF (mm)	β (%)	Admixture source	Optimum VMA		
			Actual (ml/100 kg)	Calculated (ml/100 kg)	% Error
520.70	0.0776	A	*	*	*
644.65	0.0780	A	326.80	301.20	7.83
727.20	0.0783	A	522.88	536.57	-2.62
527.05	0.0750	A	*	*	*
651.00	0.0751	A	65.36	69.83	-6.84
727.20	0.0752	A	104.58	103.54	0.99
514.35	0.0774	B,C,D	*	*	*
641.35	0.0776	B,C,D	65.36	59.00	9.73
733.55	0.0777	B,C,D	78.43	78.99	-0.71
517.65	0.0749	B,C,D	*	*	*
641.35	0.0750	B,C,D	26.14	28.36	-8.47
723.90	0.0750	B,C,D	32.68	31.47	3.70
524.00	0.0775	B,C,D	*	*	*
641.35	0.0776	B,C,D	65.36	59.00	9.73
723.90	0.0777	B,C,D	78.43	78.04	0.50
524.00	0.0750	B,C,D	*	*	*
651.00	0.0750	B,C,D	26.14	29.20	-11.70
723.90	0.0751	B,C,D	32.68	29.08	11.02
524.00	0.0774	B,C,D	*	*	*
651.00	0.0776	B,C,D	58.82	61.15	-3.97
720.85	0.0776	B,C,D	65.36	71.89	-9.99
511.30	0.0749	B,C,D	*	*	*
649.73	0.0750	B,C,D	26.14	29.10	-11.31
727.20	0.0750	B,C,D	32.68	31.44	3.80

1 ml/100 kg = 0.0153 oz/cwt

*The matrix does not incorporate VMA

130

Table 3.6a: Fresh properties of group I self-consolidating concretes

Mix No.	Slump Flow (mm)	T_{50} (sec.)	VSI	J Ring Value (mm)	SI (%)	L box H_2/H_1			U-Box H_1-H_2 (mm)	V-Funnel (sec.)
						H_2/H_1	T_{20} (sec.)	T_{40} (sec.)		
R8.A.SF20	520.70	2.63	0	42.67	3.47	0.57	0.68	1.56	146.05	4.86
R8.B.SF20	514.35	2.97	0	41.40	2.90	0.60	0.71	1.60	152.40	5.55
R8.C.SF20	517.65	3.09	0	41.91	2.98	0.60	0.70	1.61	154.43	5.75
R8.D.SF20	524.00	2.67	0	41.40	3.55	0.63	0.67	1.65	146.81	4.75
R8.A.SF25	644.65	2.20	0	39.37	5.65	0.86	0.57	1.48	132.08	4.55
R8.B.SF25	641.35	2.47	0	38.10	4.52	0.84	0.70	1.46	142.24	5.15
R8.C.SF25	641.35	2.52	0	38.86	4.62	0.84	0.62	1.47	144.27	5.38
R8.D.SF25	641.35	2.28	0	38.10	5.75	0.85	0.64	1.47	133.35	4.50
R8.A.SF28	727.20	1.82	1	35.05	6.37	0.92	0.53	1.38	109.22	4.27
R8.B.SF28	733.55	2.14	1	33.02	4.95	0.90	0.68	1.35	119.63	4.63
R8.C.SF28	723.90	2.11	1	34.29	5.11	0.86	0.53	1.39	123.95	4.75
R8.D.SF28	723.90	1.92	1	34.29	6.49	0.87	0.58	1.37	111.25	4.25

1 mm = 0.03937 inch

Table 3.6a: Fresh properties of group I self-consolidating concretes (continued)

Mix No.	Air content (%)	Bleeding (%)	Times of Setting (hrs.)		Initial temp. of fresh SCC (°C)	Adiabatic temperature			
			Initial	Final		Temp. difference: Initial to dormant (°C)	Temp. difference: Initial to peak (°C)	Elapsed time to dormant (hrs.)	Elapsed time to peak (hrs.)
R8.A.SF20	1.20	4.34	5.50	7.00	21.20	-1.12	1.17	3.39	11.74
R8.B.SF20	2.10	3.76	5.33	6.75	21.65	-1.18	1.27	3.14	11.48
R8.C.SF20	1.25	3.96	5.28	6.70	21.95	-1.26	1.34	3.03	11.37
R8.D.SF20	1.75	4.09	5.75	7.03	21.47	-1.15	1.20	3.29	11.58
R8.A.SF25	0.80	4.31	5.85	7.53	21.75	-1.17	1.24	3.75	12.26
R8.B.SF25	2.00	3.84	5.50	7.17	22.35	-1.28	1.35	3.49	11.98
R8.C.SF25	1.10	4.05	5.42	7.07	22.79	-1.36	1.43	3.36	11.86
R8.D.SF25	1.50	4.19	5.92	7.53	22.25	-1.25	1.33	3.64	12.11
R8.A.SF28	0.80	4.59	6.45	8.03	22.15	-1.27	1.35	4.17	12.88
R8.B.SF28	1.20	3.96	5.75	7.73	22.75	-1.34	1.45	3.88	12.58
R8.C.SF28	0.80	4.17	5.63	7.75	23.19	-1.44	1.51	3.77	12.45
R8.D.SF28	1.20	4.24	6.13	8.17	22.65	-1.30	1.43	4.08	12.74

$1°C = (5/9) (°F-32)$

Table 3.6b: Fresh properties of group II self-consolidating concretes

Mix No.	Slump Flow (mm)	T$_{50}$ (sec.)	VSI	J Ring Value (mm)	SI (%)	L box H$_2$/H$_1$			U-Box H$_1$-H$_2$ (mm)	V-Funnel (sec.)
						H$_2$/H$_1$	T$_{20}$ (sec.)	T$_{40}$ (sec.)		
R67.A.SF20	517.652	2.23	0	44.45	11.11	0.60	0.46	1.30	123.95	3.42
R67.A.SF25	641.35	1.87	0	40.13	11.66	0.84	0.42	1.09	57.15	3.18
R67.A.SF28	714.502	1.56	1	31.75	13.61	0.94	0.37	0.95	38.10	2.87

1 mm = 0.03937 inch

Table 3.6b: Fresh properties of group II self-consolidating concretes (continued)

Mix No.	Air content (%)	Bleeding (%)	Times of Setting (hrs.)		Initial temp. of fresh SCC (°C)	Adiabatic temperature			
			Initial	Final		Temp. difference: Initial to dormant (°C)	Temp. difference: Initial to peak (°C)	Elapsed time to dormant (hrs.)	Elapsed time to peak (hrs.)
R67.A.SF20	1.75	1.95	5.75	7.35	21.36	-1.29	1.35	2.96	11.32
R67.A.SF25	1.60	2.05	6.05	7.75	21.85	-1.34	1.47	3.25	11.98
R67.A.SF28	1.50	2.19	6.75	8.50	22.14	-1.40	1.50	3.53	12.64

1°C = (5/9) (°F-32)

134

Table 3.6c: Fresh properties of group III self-consolidating concretes

Mix No.	Slump Flow (in.)	T_{50} (sec.)	VSI	J Ring Value (in.)	SI (%)	L box H_2/H_1			U-Box H_1-H_2 (in.)	V-Funnel (sec.)
						H_2/H_1	T_{20} (sec.)	T_{40} (sec.)		
S7.A.SF20	527.05	2.69	0	43.94	6.37	0.65	0.55	1.62	225.55	4.82
S7.B.SF20	524.00	3.19	0	42.67	4.83	0.63	0.71	2.45	244.60	5.12
S7.C.SF20	524.00	3.15	0	45.72	5.07	0.65	0.67	1.82	247.65	5.17
S7.D.SF20	511.30	2.82	0	44.45	7.15	0.70	0.63	1.79	242.32	4.90
S7.A.SF25	651.00	2.48	0	36.83	8.12	0.84	0.52	1.61	215.90	4.35
S7.B.SF25	651.00	2.79	0	38.86	5.72	0.83	0.70	1.97	231.90	4.55
S7.C.SF25	651.00	2.69	0	37.59	5.64	0.83	0.59	1.74	231.65	4.65
S7.D.SF25	649.73	2.04	0	38.10	9.57	0.86	0.58	1.70	234.95	4.40
S7.A.SF28	727.20	1.85	1	31.75	9.11	0.88	0.48	1.48	184.15	4.07
S7.B.SF28	723.90	2.16	1	33.78	8.03	0.90	0.52	1.83	222.25	4.13
S7.C.SF28	720.85	2.15	1	32.51	8.17	0.86	0.56	1.64	225.55	4.22
S7.D.SF28	727.20	1.88	1	32.51	10.56	0.88	0.52	1.60	212.85	4.07

1 mm = 0.03937 inch

Table 3.6c: Fresh properties of group III self-consolidating concretes (continued)

Mix No.	Air content (%)	Bleeding (%)	Times of Setting (hrs.)		Initial temp. of fresh SCC (°C)	Adiabatic temperature			
			Initial	Final		Temp. difference: Initial to dormant (°C)	Temp. difference: Initial to peak (°C)	Elapsed time to dormant (hrs.)	Elapsed time to peak (hrs.)
S7.A.SF20	1.50	3.01	5.12	6.83	21.84	-1.12	1.25	3.17	11.17
S7.B.SF20	2.20	2.55	4.63	6.13	22.58	-1.26	1.39	2.97	10.85
S7.C.SF20	1.25	2.69	4.60	6.15	22.97	-1.41	1.48	2.85	10.73
S7.D.SF20	1.75	2.88	4.95	6.25	22.39	-1.23	1.26	3.02	11.01
S7.A.SF25	1.25	3.18	5.58	7.28	22.20	-1.15	1.34	3.45	11.70
S7.B.SF25	1.50	2.62	5.10	6.65	22.82	-1.30	1.53	3.23	11.37
S7.C.SF25	1.10	2.73	5.07	6.55	23.39	-1.44	1.56	3.10	11.20
S7.D.SF25	1.50	3.04	5.38	6.75	22.38	-1.29	1.40	3.30	11.57
S7.A.SF28	1.00	3.23	6.02	7.75	23.40	-1.21	1.45	3.66	12.49
S7.B.SF28	1.00	2.73	5.48	7.02	24.16	-1.37	1.62	3.45	12.17
S7.C.SF28	0.90	2.81	5.45	6.95	24.47	-1.48	1.71	3.33	12.00
S7.D.SF28	1.20	3.13	5.92	7.42	23.85	-1.35	1.55	3.50	12.34

1°C = (5/9) (°F-32)

selected self-consolidating concretes as related to their flow ability, viscosity, stability, passing ability, and filling ability is presented below.

3.4.1 Slump flow

The slump flow test as a measure of the unconfined workability was carried out using a traditional slump cone, by which the horizontal spread of the fresh concrete was measured. The test result is a mean value of the concrete spread determined from the measurements of diameters of the spread concrete at two perpendicular directions. It can be seen from the Tables 3.6a through 3.6c that all selected self-consolidating concretes were within the target uniform slump flow of 508 ± 25 mm (20 ± 1 inches), 635 ± 25 mm (25 ± 1 inches), or 711 ± 25 mm (28 ± 1 inches).

3.4.2 Flow ability/Viscosity

Slump flow values were used to describe the flow ability of the fresh concrete in an unconfined condition and the slump flow (SF) test is the preferred test method for flow ability. The flow ability of a given fresh SCC is related to its viscosity. The flow times of T_{20}, T_{40}, and T_{50} and V-funnel flow time (t_v) can be used to measure both the flow ability and the viscosity. The flow times reported in Tables 3.6a through 3.6c do not measure the viscosity of SCC, but they are related to it by describing the rate of flow. A T_{50} time of 2 seconds or less characterizes self-consolidating concrete with a low viscosity, and a T_{50} of 5 seconds and more is generally considered a high-viscosity SCC mixture[1]. A V-funnel time of 10 seconds is acceptable. Currently there is no agreement on the suitable values for the T_{20} and T_{40} times.

The tests results expressed in second are very small in nature and highly operator sensitive. A minimum of two operators are needed to perform these tests. The variations

137

in test results can be caused by the admixture source or by one of the followings: moisture condition of the base plate, L-box or V-funnel apparatus; angle of slope of the base plate or L-box apparatus, the speed of lifting of the cone or the gates of L-box and V-funnel apparatus, the mixing action, the batching temperature, and the material preparation. Precautionary steps were taken in all phases of the experiments in order to minimize the potential influence due to the above-mentioned factors. Since there is no consensus on the acceptable T_{20} and T_{40} times, the discussion related to the flow ability (or viscosity per inference) is confined to the results obtained for the T_{50} and V-funnel tests.

3.4.2.1   Influence of admixture source on flowability/viscosity

The test results indicate that; for the slump flows of 508, 635, and 711 mm (20, 25, and 28 inches); the group I self-consolidating concretes made with sources B and C admixtures displayed similar T_{50} times which were on average 14, 11 and 14%, respectively, higher than those of the concretes prepared with the admixture sources A and D. The corresponding increases in T_{50} time were 15, 21, and 16%, respectively, for the group III SCCs. For the V-funnel test results, the pair sources B and C displayed on average 18, 16, and 10% reductions in t_v when compared to the pair sources A and D for the group I SCC prepared with slump flows of 508, 635, and 711 mm (20, 25, and 28 inches), respectively. For the group III SCCs, the corresponding flow ability losses as related to the V-funnel were 6, 5, and 3%, respectively.

In summary it can be concluded that the T_{50} time and V-funnel flow time varied among the selected self-consolidating concretes and were all within the acceptable values recommended by the ASTM committee C09.47[51]. Irrespective of the SCC groups, the

admixture sources B and C displayed similar flowability which was lower than that of the sources A and D; or by inference, sources B and C showed higher viscosity when compared to sources A and D.

3.4.2.2   Influence of slump flow on flowability/viscosity

The increase in the flow ability of the selected self-consolidating concretes led to reductions in the T_{50} and V-funnel flow times. For the group I SCCs, when the slump flow increased from 508 to 635 to 711 mm (20 to 25 to 28 inches), the T_{50} and V-funnel flow times decreased on average by 17 and 6 %, and 16 and 8 %, respectively. The corresponding decreases were 19 and 8 %, and 20 and 11 % for the groups II SCCs; and 16 and 10 %, and 19 and 8 % for the group III SCCs. This, by no means, is a statistically rigorous comparison, but it gives a good idea of the trend in flow ability/viscosity as related to the increase in slump flow values. The loss in viscosity (or gain in flowability) induced by an increase in slump flow can be attributed to increases in adsorption of admixture leading to an increase in dispersion of cement flocs and the break down of the bond between the cement particles due to increases in the amount of superplasticizer. The incorporation of VMA helped to partially restore the loss in viscosity by elevating the T_{50} and V-funnel flow times to the acceptable values.

3.4.3   Stability

The stability of the self-consolidating concrete is defined as its ability to maintain homogeneous distribution of its ingredients during its flow and setting. Dynamic and static stabilities are the two most common stability characteristics of self-consolidating concretes. Their methods of testing and evaluation of the result are presented in the Chapter 2. The section below presents the test results obtained for the dynamic and static

139

stabilities of the trial self-consolidating concretes.

3.4.3.1   Dynamic segregation resistance

Dynamic segregation resistance refers to the resistance of the SCC to separation of its constituents during placement into formwork[1]. It was evaluated by visual examination of the fresh concrete and reported as visual stability index (VSI). A visual assessment for any indication of mortar/paste separation at the circumference of the flow and any aggregate separation in the central area gives an indication of dynamic segregation resistance.

3.4.3.1.1   Influence of admixture source on dynamic segregation resistance

All selected self-consolidating concretes were designed to attain a visual stability index of 0 (highly stable concrete) or 1 (stable concrete) by balanced proportioning of HRWRA and VMA once sufficient cementitious materials content and an appropriate coarse-to-fine aggregate ratio were determined. As reported in Tables 3.6a through 3.6c, irrespective of the admixture source and aggregate type and size, the target VSI of 0 or 1 was obtained for all trials matrices. No evidence of segregation or bleeding in slump flow was observed in any of the selected self-consolidating concretes, indicating that stable matrices were attained with all four admixture sources.

3.4.3.1.2   Influence of slump flow on dynamic segregation resistance

Highly stable mixtures (VSI = 0) were achieved for the selected self-consolidating concretes made with 508 and 635 mm (20 and 25 inches) slump flows. When the slump flow was increased from 635 to 711 mm (25 to 28 inches), the attainment of a highly stable matrix was not possible without the utilization of excessive and impractical amount of admixtures. Consequently, in order to maintain a practical design in searching for the

optimum dosage and proportioning of the admixtures, the ranking of stable dynamic segregation resistance (VSI = 1) was adopted for the 28-inch (711 mm) slump flow self-consolidating concretes. HRWRA and VMA were used in the selected concretes to decrease their yield stress and increase their plastic viscosity, respectively. The reduction in dynamic stability for the 711-mm (28-inch) slump flow self-consolidating concretes was primarily due to the increase in the amount of HRWRA leading to a gain in dispersibility and a reduction in the homogeneity of the matrix. For all three SCC groups, and irrespective of admixture source, the selected self-consolidating concretes made with 508 and 635 mm (25 and 28 inches) slump flows required the use of VMA to obtain an acceptable visual stability index.

3.4.3.2   Static segregation resistance

Static stability or static segregation resistance refers to the resistance of self-consolidating concrete to bleeding, accumulation of paste at the top, and settling of aggregates on the bottom after casting while the concrete is still in a plastic state[1]. Such heterogeneity can results in considerable variations in the hardened properties across the concrete. Self-consolidating concrete which experiences a dynamic segregation (segregation during placement) also sees static segregation, but lack of dynamic segregation does not necessary imply that the mixture is definitely stable[2]. In this investigation, the static segregation resistance of self-consolidating concrete was determined using column segregation test. The top-to-bottom retained #4 sieve coarse aggregate mass (weight) ratio was measured to find the segregation resistance of the SCC. The detail testing procedure is summarized in the Chapter 2. This section discusses the static stability of the 27 designed self-consolidating concretes as related to

admixture sources and slump flow.

3.4.3.2.1 Influence of admixture source on static segregation resistance

The segregation indices (SI) of the 27 trial matrices, as reported in Tables 3.6a through 3.6c, were lower than the maximum recommended value of 15%. Irrespective of the SCC group, the admixture sources A and D exhibited similar segregation indices which were higher than those of the admixture sources B and C. This is indicative of a better static segregation resistance of SCCs made with the admixture sources B and C as compared to those made with the admixture sources A and D. On average, groups I and III self-consolidating concretes incorporating the admixture sources A and D experienced reduction in static stability of 20 and 26 %, respectively, when compared to those obtained when admixture sources B and C were used. The increase in static segregation resistance due to admixture sources B and C may be attributed to their relative higher viscosity (by inference) as can be seen from the results of the T_{20}, T_{40}, T_{50} and V-funnel times reported in Tables 3.6a through 3.6c.

3.4.3.2.2 Influence of slump flow on static segregation resistance

The segregation indices of the selected self-consolidating concretes increased as the slump flow increased irrespective of admixture source and SCC group. When the slump flows increased from 508 to 635 to 711 mm (20 to 25 to 28 inches), the static stability decreased on average by 59 and 11%, 5 and 14 %, 23 and 27%; for groups I, II, and III, respectively. This is mainly due to the reduction in the viscosity (by inference) of the higher slump flow concrete.

The static stability mechanism of action can be explained through aggregate sedimentation which is related to the viscosity and the density of the mixture, the size and

the density of the aggregate, and the flow velocity of the mixture. Bonen and Shah[2] reported that the sedimentation velocity of aggregate is proportional to the radius square of the aggregate, the differences in the specific densities of the aggregate and the matrix, and inversely related to the viscosity of the mixture. The explanation is presented through equations 3.5a, 3.5b, and 3.5c; and Figure 3.7. Laminar flow was assumed. Considering the gravitational force (F_g), the buoyancy force (F_a) and the frictional force (F_r) acting on aggregate particles as shown in Figure 3.7; and the specific gravity of common aggregate being greater than that of the concrete paste, the velocity of the aggregate will increase until there is equilibrium of forces. At this point the net forces acting on the aggregate become zero. This is translated in equations 3.5a and 3.5b (note that aggregate are assumed to have spherical shape).

$$F_r = 6\pi\eta r v_e \qquad\qquad 3.5a$$

$$F_r = F_g - F_a \qquad\qquad 3.5b$$

Substituting F_g and F_a for F_r

$$v_e = \frac{2gr^2\left(\rho_{agg} - \rho_m\right)}{9\eta} \qquad\qquad 3.5c$$

Where: v_e = equilibrium sedimentation velocity,

g = gravitational force,

r = sphere radius of coarse aggregate,

ρ_{agg} and ρ_m = specific densities of the aggregate and the matrix, respectively,

η = plastic viscosity.

143
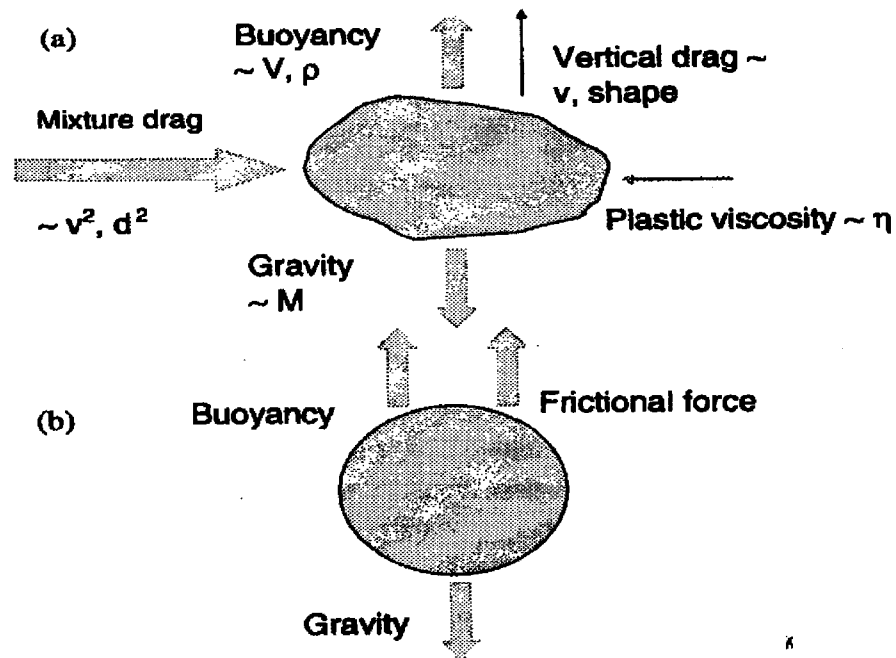
Figure 3.7: Force acting on particles: (a) horizontal flow; (b) sedimentation[2]

While comparison of the segregation resistance among the three SCC groups was not critical to the objective of this investigation, a few observations can be noted. It is shown in Tables 3.6a through 3.6c that irrespective of admixture source, the group I trial matrices displayed the highest resistance to static segregation (lowest segregation index (SI) value), followed by the group III and then the group II in descending order. This can be mainly attributed to the combination of the following three factors:

• The differences in the size of the coarse aggregate: The lowest static segregation resistance of the group II matrices stems mainly from the larger size of the coarse aggregate used in their composition (see section 2.1.1 for the selected aggregates nominal maximum sizes).

• The specific densities of the fine and coarse aggregates: The group III self-consolidating concretes were manufactured with heavier type of fine and coarse

144

aggregates (about 8% more) when compared to those of the groups I and II (see Table 2.1 for the selected aggregates specific density).

- The matrix's paste viscosity: The viscosity of the paste is influenced by its water-to-cementitious materials ratio and cementitious materials content. The group III self-consolidating concretes were manufactured with less amount of fly ash (about 20% less) when compared to that of the groups I and II (see Table 3.1a through 3.1c for the selected matrices design and proportion).

The abovementioned observations confirmed that the sedimentation theory, as alluded to earlier, can validate the variation in static segregation resistance of the selected self-consolidating concretes.

3.4.4   Passing ability

The passing ability or the capacity of the fresh matrix to flow through confined spaces and narrow opening without blocking was measured by the J-ring, L-box and U-box tests. The blocking develops more easily when the size of aggregate is large relative to the size of the opening; the total content of the aggregate is high; and when the shape of the particles deviates from spherical. It is also likely that the friction between the flowing concrete and the surface of the obstacle/confinement, e.g. the reinforcement and formwork, as well as the type of the material used in the J-ring and L-box, will influence the blocking and thus the passing ability of a fresh self-consolidating concrete[9]. In the present study, standard J-ring, L-box and U-box testing apparatus as described in Chapter 2 were used.

The passing ability as related to the J-ring test was conducted to assess the blocking of fresh self-consolidating concretes. The passing ability as related to the L-box

145

was determined by the flow height ratio H_2/H_1, where H_1 is the height of the concrete flow at the sliding gate and H_2 at the end of the horizontal portion of the L box. The passing ability as related to the U-box was evaluated by the filling height H_1-H_2, the difference in height between the left and right compartments of the U-box. For an acceptable SCC, a J-ring value between 0 and 51 mm (0 and 2 inches), an L-box flow height ratio H_2/H_1 of 0.8 to 1, and a U-box filling height H_1-H_2 lower than 305 mm (12 inches) are recommended. The current section is intended to discuss the influence of the four selected admixture sources and the three slump flow values on the passing ability of the designed self-consolidating concretes.

3.4.4.1   Influence of admixture source on passing ability

As shown in Tables 3.6a and 3.6c it can be seen that for both groups I and III SCCs, the measured J-ring values of the four admixture sources were between 25 and 50 mm (1 and 2 inches), indicating a moderate passing ability (passing ability rate of 1) or minimal to noticeable blocking of the selected self-consolidating concretes.

The test results as related to the L-box and U-box are also presented in Tables 3.6a through 3.6c. The flow height ratios H_2/H_1 of the 508 mm (20 inches) slump flow self-consolidating concretes were less than the minimum recommended value of 0.8, indicating their extreme blocking ability. However, regardless of the admixture source and SCC group, for concretes made with slump flow of 635 and 711 mm (25 and 28 inches), the flow height ratios remained near the bottom third-point of the recommended limits, indicating their moderate passing ability.

The results pertaining to the U-box test were also indicative of a moderate passing ability for the 27 selected SCC mixtures. The U-box filling height H_1-H_2 values of the

group I SCCs were near the middle point of the allowable 305 mm (12 inches) value. The corresponding results for the group III SCCs were also less than the maximum recommended value, but remained near its upper limit of 305 mm (12 inches).

Overall, with proper proportioning, self-consolidating concrete with acceptable passing ability can be achieved with any of the four selected admixture sources.

While it is not intended to compare the three SCCs groups, since their aggregate type and size were different, a few observations are worth mentioning. All four admixture sources exhibited similar flow height ratio H_2/H_1 independently of the selected SCC groups. The flow height ratio of the groups I, II and III self-consolidating concretes made with 635 and 711 mm (25 and 28 inches) slump flows represented on average 87, 89 and 86%, respectively, of the recommended upper limit of passing ability for the L-box test (the 508 mm (20 inches) slump flow matrices were excluded in this comparison because they failed to pass the L-box test). On the other hand, there was a noticeable difference in the U-box filling height H_1-H_2 values among the three trial self-consolidating concretes groups. The average U-box filling height H_1-H_2 values of the groups I, II and III 635 and 711 mm (25 and 28 inches) slump flow SCCs were 42, 16 and 72%, respectively, of maximum recommended value of 305 mm (12 inches) for the passing ability of the U-box test. The findings of the two passing ability test methods (L-box and U-box) highlighted the difference in the test mechanism that exists between them.

3.4.4.2   Influence of slump flow on passing ability

Irrespective of the admixture source and SCC group, the passing ability of the selected matrices improved with an increase in slump flow. When the slump flow

147

increased from 508 to 635 to 711 mm (20 to 25 to 28 inches), the J-ring passing ability improved by an average of 8 and 12%, 11 and 21%, and 14 and 14% for the groups I, II, and III, respectively. Similar gains in passing ability were observed when the assessment included the L-box or U-box tests. The corresponding improvements in L-box passing ability were 41 and 5%, 29 and 11%, and 28 and 5% for the groups I, II, and III, respectively; and 8 and 16%, 117 and 50%, and 5 and 8% for the same groups respectively, when the U-box test was used. This behavior can be attributed to a decrease in the yield point and an increase in the viscosity of the higher slump flow self-consolidating concretes, allowing an ease of movement around blocking rebars.

3.4.5   Filling ability

V-funnel and U-box tests were also utilized to assess the filling ability of the selected concretes. As reported above, the test results for all four admixture sources as related to the V-funnel times and U-box filling heights were indicative of their good filling ability, for the groups I and II, and moderate filling ability for the group III SCCs.

3.4.6   Air content

The results pertaining to the air content of the selected self-consolidating concretes are shown in Tables 3.6a through 3.6c. Although no air-entraining admixture was used, the test results indicated that the admixture sources B and D were able to produce more air than the sources A and C. In fact, for the groups I and III SCCs, admixture sources B and D entrained on average, approximately 0.60 % and 0.35 %, respectively, more air than the admixture sources A and C.

Additionally, irrespective of admixture source and SCC group, the air content decreased as the slump flow increased. When the slump flow increased from 508 to 635

to 711 mm (20 to 25 to 28 inches), the average air content of groups I, II, III SCCs decreased by 16 and 22%, 9 and 7%, and 19 and 23%, respectively.

The use of AEA to make air-entrained self-consolidating concrete was not part of the present investigation. However, a companion investigation made by Ghafoori N., and Barfield M.,[77] revealed that the source of air entrainment admixture (AEA) dictates the dosage requirement to produce similar air content and air void characteristics. They found that: (1) The smallest and closely spaced air voids were produced by the synthetic detergent type AEA of source A; (2) the AEA containing tall oil (source B) produced the best air void characteristics, followed by the saponified wood rosin/resin-acid combination (source C), and the natural wood rosin (source D); and (3) the increase in the matrix fluidity engendered a deterioration of the self-consolidating concrete's air void characteristics because of the increased ability of the air voids to move in the cement paste, causing bubble coalescence.

3.4.7   Bleeding

Tables 3.6a through 3.6c present the test results pertaining to the bleeding of the selected self-consolidating concretes. The four admixture sources produced self-consolidating concretes with a relatively similar bleedings values which were about 4, 2 and 3% for groups I, II and III, respectively; indicating that the four admixture sources had marginal influence on the bleeding of the self-consolidating concretes.

Irrespective of the admixture source, when the slump flow increased from 508 to 635 to 711 mm (20 to 25 to 28 inches), the group I SCCs exhibited increases in bleeding by nearly 2 and 3%, respectively. For the groups II and III SCCs, the corresponding increases were 5 and 6%, and 4 and 3%, respectively. The marginal variation between

the bleeding of different slump flows was due to the high cementitious material content and low water-to-cementitious materials ratio used for the trials matrices.

3.4.8 Setting time

The test results pertaining to the setting times of the selected self-consolidating concretes are shown in Tables 3.6a through 3.6c. The admixture sources A and D displayed similar initial setting times which were, on average, higher than those of the admixture sources B and C by about 6.8 and 7.5% for the groups I and III SCCs, respectively. The corresponding increases in the final setting times were 4.2 and 6.8%, respectively. On the whole, the differences in setting times between the pair sources A and D in one side, and the pair sources B and C in the other side were less than 30 minutes, indicating that the source of polycarboxylate-based admixture used had little impact on the setting times of the selected self-consolidating concretes.

In general, independently of the admixture source and the matrix group, the selected self-consolidating concretes produced higher setting times when the slump flow increased. On average, as the slump flow increased from 508 to 635 to 711 mm (20 to 25 to 28 inches), groups I, II, and III SCCs displayed rises in the initial setting time of 4 and 6%, 5 and 10%, and 10 and 8%, respectively. The corresponding increases in the final setting times were 7 and 8%, 5 and 9%, and 7 and 7.0%, respectively. These delays in setting times can be attributed to the increase in the bleeding water generated by the increase in the dosages requirement of HRWRA in attaining a higher slump flow.

3.4.9 Adiabatic temperature

Tables 3.6a through 3.6c display the adiabatic test results of the selected self-

consolidating concretes. A typical sample of temperature evolution of a trial matrices over the period of 24 hours is presented in Figure 3.8. The figure documents the occurrence of the four different stages involved in Portland cement hydration process, namely: initial hydration (from 0 to 1), induction or dormant period (from 1 to 2), acceleration and setting period (from 2 to 3) and deceleration period (from 3 to 4).

3.4.9.1   Influence of admixture source on adiabatic temperature

Irrespective of the admixture source; groups I, II and III self-consolidating concretes displayed induction periods lasting about 3.4, 3.0, and 3.0 hours, respectively. The corresponding periods for the acceleration and setting stage were 8.3, 8.5, and 8.1 hours. These hydration characteristics indicated that both the induction and the acceleration stages displayed durations close to the upper end of the recommended ranges (15 minutes to 4 hours for the induction stage, and 4 to 8 hours for the acceleration stage) for conventional concrete. Moreover, the tests results indicated a relatively insignificant influence of admixture source on the temperature evolution of the self-consolidating concretes.

Irrespective of the SCC group and slump flow, the selected polycarboxylate-based superplasticizers produced similar temperature evolution trend in which an analogous temperature drop of about 1.1 $^{\circ}$C (2.3 $^{\circ}$F) during the initial and dormant hydration (from point 1 to 2) and an increase of roughly 2.3 $^{\circ}$C (4.7 $^{\circ}$F) in the acceleration and setting phase (from point 2 to 3) were observed. Marginal differences, less than 0.5 $^{\circ}$C (1 $^{\circ}$F), among dormant or peak temperatures of the four admixture sources were also recorded.

In comparing the four selected admixture sources, there were slight differences in elapsed times from the beginning of the hydration to the end of induction or acceleration
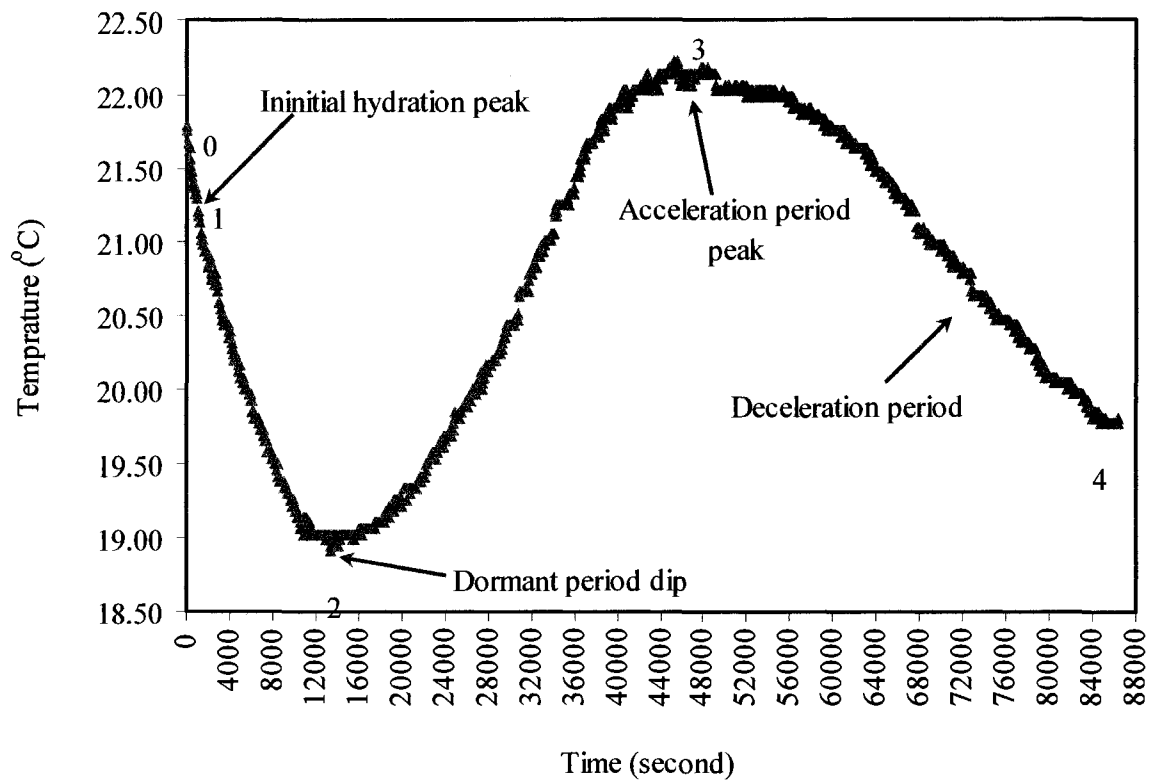
Figure 3.8: Temperature evolution over 24-hour of group I and admixture source A-SCC

stages. When admixture sources changed from A to B, C and D, the elapsed times to the

dormant stage of groups I and III SCCs decreased by 16, 23, and 6 minutes; and 13, 20,

and 9 minutes, respectively. The corresponding reductions for the acceleration and

setting phase became 17, 24, and 9 minutes; and 19, 29, and 9 minutes, respectively.

These results indicate a delay in hydration time of the admixture sources A and D when

compared to the admixture sources B and C, pointing out that admixture sources A and D

generated similar hydration time which was longer than that of the admixture sources B

and C.

3.4.9.2   Influence of slump flow on adiabatic temperature

As shown in Tables 3.6a through 3.6c, regardless of the admixture source, all the

trial self-consolidating concrete groups displayed negligible increases in the dormant and peak temperatures when the slump flow increased. On average, as the slump flow increased from 508 to 635 to 711 mm (20 to 25 to 28 inches), all three SCC groups experienced less than 0.5 °C (1 °F) increase in the dormant and peak temperatures. This relative conservation of temperature may be due to the chemical type of the HRWRA and VMA which does not induce any temperature increase when a higher dosage is used. However, the increase in slump flow led to increases in elapsed times to the dormant and peak point. Irrespective of the admixture sources, when the slump flow increased from 508 to 635 to 711 mm (20 to 25 to 28 inches), the delay in reaching the dormant temperature of groups I, II and SCCs were on average 21 and 25 minutes, 17 and 17 minutes, and 16 and 13 minutes, respectively. The corresponding delay for reaching the peak temperature became 31 and 37 minutes, 40 and 40 minutes, and 31 and 47 minutes, respectively. As was the case for the setting time, the delays in adiabatic temperature are the consequences of the increase in the bleeding water caused by the increase in HRWRA dosages requirement in attaining the higher slump flow.

3.5   Bulk characteristics

Tables 3.7a through 3.7c present the mean demolded unit weight, compressive strength and modulus of elasticity of the trial matrices. In the following sections, the results of the bulk characteristics as influenced by different admixture sources and slump flows are discussed.

3.5.1   Demolded unit weight

The unit weight of conventional normal-weight concrete used in pavements, buildings, and other structures ranges between 2240 to 2400 kg/m³ (140 to 150 pcf). The

Table 3.7a: Bulk characteristics of group I self-consolidating concretes

Mix No.	Demolded unit weight (kg/m³)	Modulus of elasticity (MPa)		Compressive strength (MPa)		
		28-day	90-day	7-day	28-day	90-day
R8.A.SF20	2287	26199	28515	35.76	48.75	62.29
R8.B.SF20	2287	26723	29085	36.59	49.94	63.70
R8.C.SF20	2287	27029	29394	36.90	50.42	64.32
R8.D.SF20	2287	26471	28829	36.32	49.35	63.32
R8.A.SF25	2287	26322	28835	36.77	49.63	63.08
R8.B.SF25	2287	26877	29430	37.63	50.72	64.69
R8.C.SF25	2287	27153	29742	37.92	51.04	65.28
R8.D.SF25	2287	26673	29163	37.33	50.20	64.14
R8.A.SF28	2287	26587	29339	37.44	50.27	65.20
R8.B.SF28	2287	27160	29954	38.32	51.62	66.80
R8.C.SF28	2287	27415	30259	38.69	51.99	67.49
R8.D.SF28	2287	26906	29671	37.97	50.97	66.12

1 kg/m³ = 0.0624 pcf, 1 MPa = 145 psi

Table 3.7b: Bulk characteristics of group II self-consolidating concretes

Mix No.	Demolded unit weight (kg/m³)	Modulus of elasticity (MPa)		Compressive strength (MPa)		
		28-day	90-day	7-day	28-day	90-day
R67.A.SF20	2287	25662	28918	36.99	47.51	58.86
R67.A.SF25	2287	26150	29597	37.08	48.50	60.76
R67.A.SF28	2287	26444	29880	38.10	48.95	61.07

1 kg/m³ = 0.0624 pcf, 1 MPa = 145 psi

Table 3.7c: Bulk characteristics of group III self-consolidating concretes

Mix No.	Demolded unit weight (kg/m³)	Modulus of elasticity (MPa)		Compressive strength (MPa)		
		28-day	90-day	7-day	28-day	90-day
S7.A.SF20	2452	39001	46469	44.21	55.50	69.24
S7.B.SF20	2452	39794	47522	45.13	56.68	70.85
S7.C.SF20	2452	40262	48013	45.67	57.42	71.62
S7.D.SF20	2452	39478	47099	44.79	56.22	70.16
S7.A.SF25	2452	40554	47275	44.72	56.32	70.13
S7.B.SF25	2452	41405	48292	45.58	57.41	71.64
S7.C.SF25	2452	41812	48753	46.13	57.92	72.48
S7.D.SF25	2452	41101	47892	45.39	56.99	71.04
S7.A.SF28	2452	41517	47607	45.55	57.08	70.43
S7.B.SF28	2452	42429	48700	46.41	58.30	71.98
S7.C.SF28	2452	42809	49073	47.02	59.03	72.87
S7.D.SF28	2452	41999	48306	46.19	57.86	71.31

1 kg/m³ = 0.0624 pcf, 1 MPa = 145 psi

amounts of air, water and cementitious materials, which in turn are influenced by the maximum size and the density of the aggregates, have a direct impact on the unit weight of concrete. The ASTM C 138[65], "Test Method for Density (Unit Weight), Yield, and Air Content (Gravimetric) of Concrete," was used to evaluate the unit weight of the trial mixtures. The one-day unit weights of the selected matrices, immediately after demolding, are shown in Tables 3.7a through 3.7c. These values represent the average of four samples. Both the groups I and II self-consolidating concretes exhibited demolded unit weights within the 2240 - 2400 kg/m³ (140 - 150 pcf) range of normal-weight concrete. On the other hand, the group III self-consolidating concretes displayed demolded unit weights slightly above the upper limit of that reported for normal-weight concrete due to the relatively high specific gravity of its coarse and fine aggregates (2.79

and 2.78, respectively), when compared to that of most natural aggregates (2.4 to 2.9)[10,78].

In general, irrespective of the self-consolidating concrete's constituent and proportions, the unit weight of all selected trial matrices remained at the level equal to (groups I and II) or above (group III) that is required to produce normal- weight concrete. The recorded demolded unit weights were affected neither by the selected admixture sources nor by the slump flow value.

3.5.2 Compressive strength

The ASTM C 39[70], "Standard Test Method for Compressive Strength of Cylindrical Concrete Specimens," was used to evaluate the compressive strength of the designed self-consolidating concretes. The compressive strength test results of the selected trial mixtures at different curing ages are shown in Tables 3.7a through 3.7c. Each of these values is the average of four tested cylinders.

3.5.2.1 Influence of admixture source on compressive strength

Typical representations of compressive strength as a function of admixture source and curing age are displayed in Figures 3.9a and 3.9b, respectively. In comparison to the admixture source C, both groups I and III self-consolidating concretes incorporating admixture sources A, B, and D showed reductions in compressive strength of 3, 1 and 2%, respectively, regardless of the slump flow and curing age. These relatively small variations indicate that the four selected polycarboxylate-based HRWRA and their corresponding VMA had the type of chemical composition that did not interfere with hydration reaction and did not alter the compressive strength development of concrete. The increase in strength at 28 and 90 days is attributed to the availability of more calcium

156
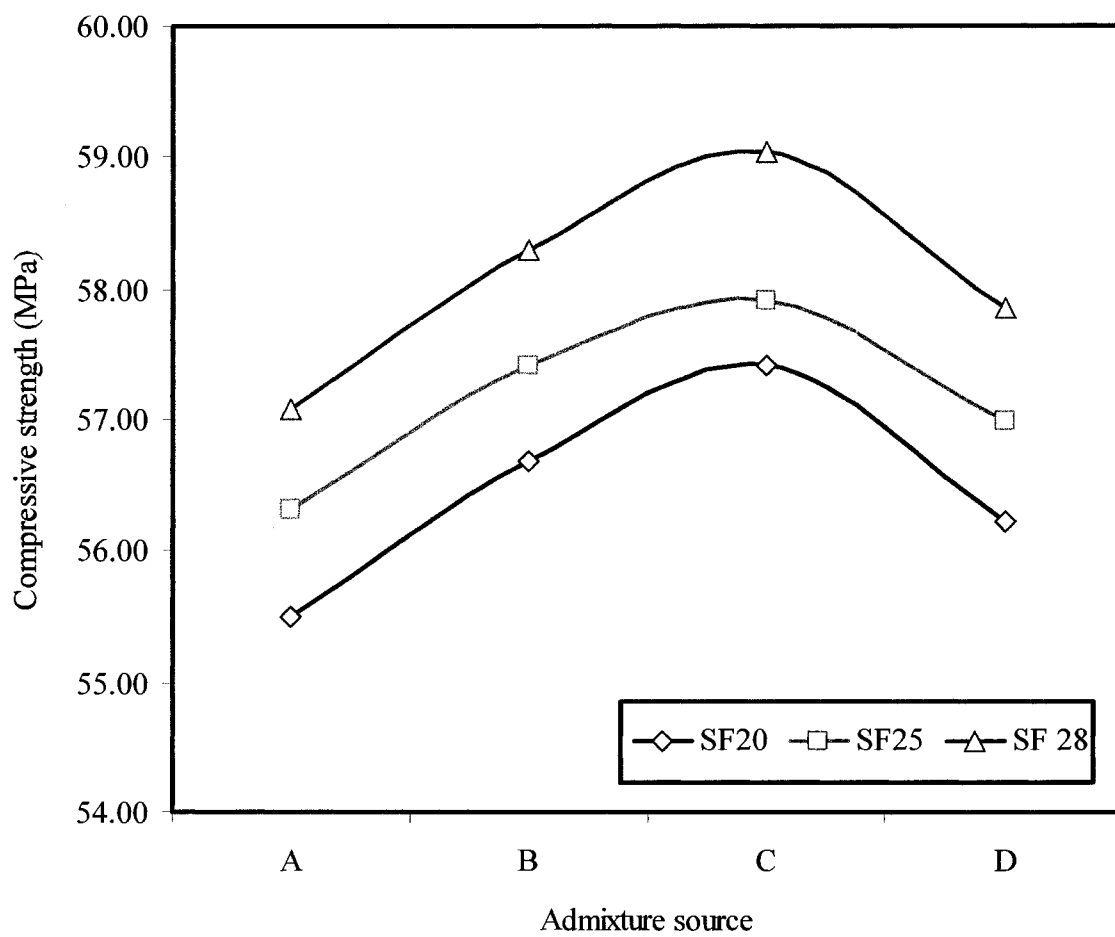
Figure 3.9a: Influence of admixture source on the 28-day compressive strength

of group III self-consolidating concretes
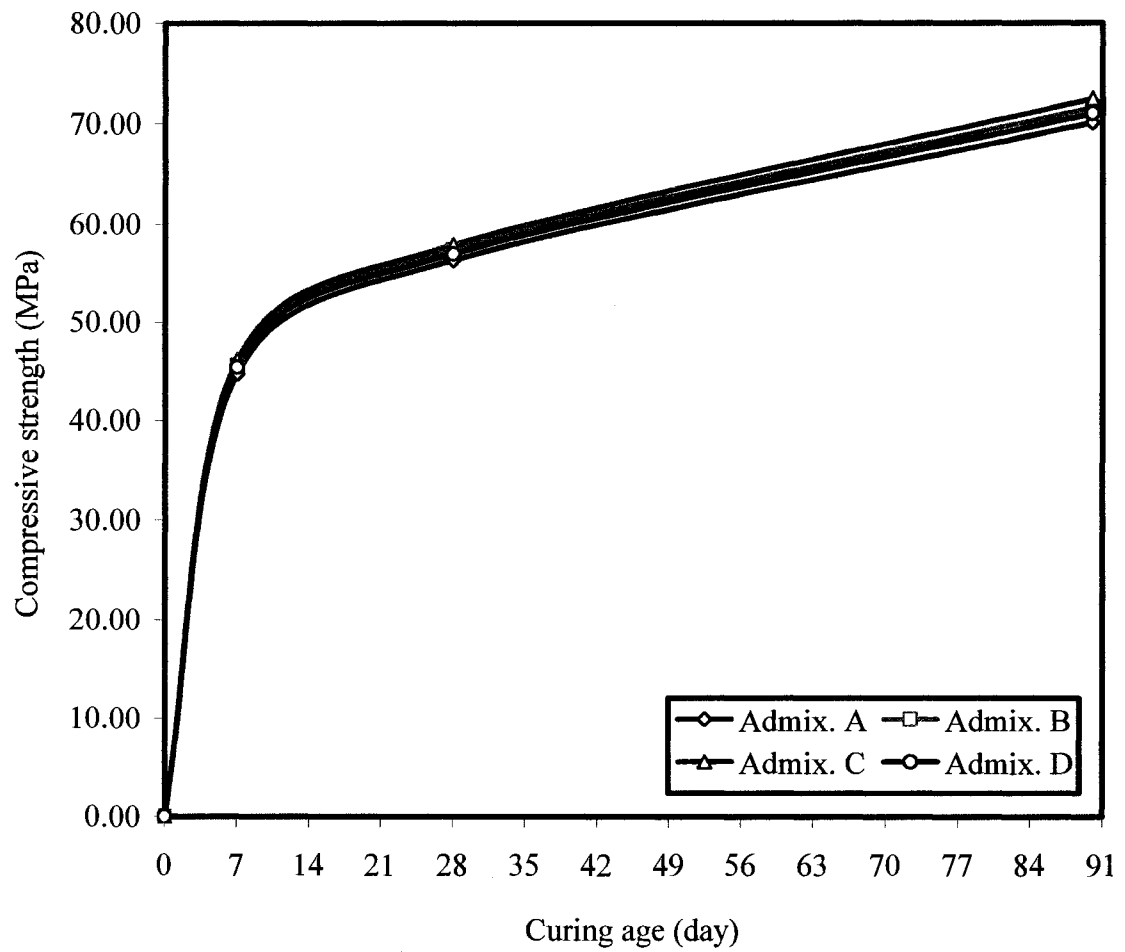
Figure 3.9b: Influence of admixture source and curing age on the compressive strength of

group III-635 mm (25 inches) slump flow self-consolidating concretes

silicate hydrate (C-S-H) binder, due to the pozzolanic reaction of fly ash with lime, and the continued hydration of the cement paste.

3.5.2.2   Influence of slump flow on compressive strength

Figure 3.9c is a typical representation of the compressive strength as a function of slump flow. On the whole, when the slump flow increased from 508 to 635 to 711 mm (20 to 25 to 28 inches), irrespective of admixture source and curing age, all three SCC groups displayed similar compressive strength improvement of less than 3% variation. This marginal difference in compressive strength indicated the insignificant influence of increased in fluidity of self-consolidating concrete due to increases in slump flow through additional dosage of admixtures.

3.5.2.3   Strength and aggregate correlation

It can be seen from Tables 3.7a through 3.7c, that irrespective of admixture source and curing age, the group III SCCs exhibited a higher compressive strength than group I, which in turn yielded stronger concrete than group II. Using the group III SCC as reference, the groups I and II SCCs experienced reductions in their 28-day compressive strength of about 12 and 16%, respectively. The corresponding losses in strength were 9 and 12% at 90 days of curing. The three SCC groups were totally independent from each other. The groups I and II SCCs were made of the aggregate source R which had different size, shape, surface texture, grading and mineralogy than the source S used to produce group III self-consolidating concretes. While both groups I and II had richer paste than that of group III concretes, the increase in paste quality was not sufficient enough to overcome the higher quality aggregates used to produce group III self-consolidating concretes.

159
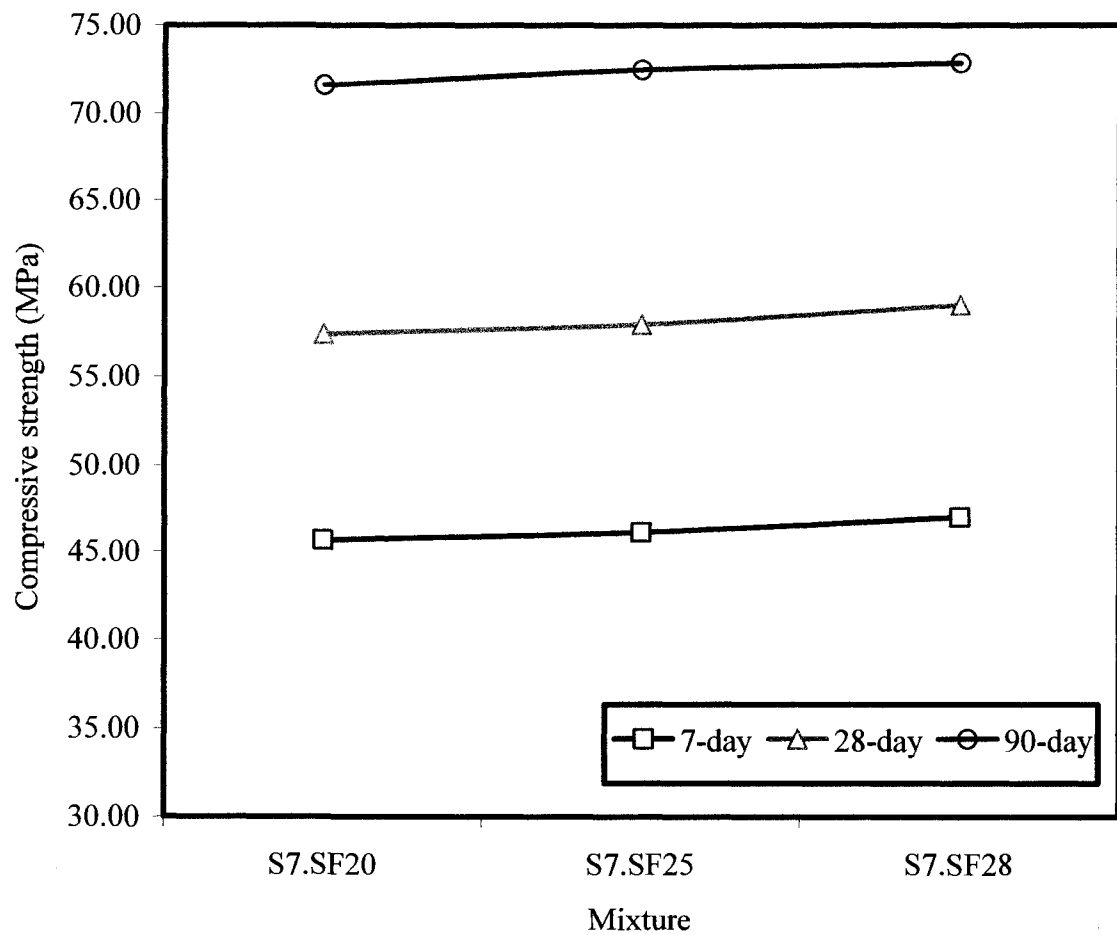
Figure 3.9c: Influence of slump flow value on the compressive strength of group III

self-consolidating concretes made with admixture source C

3.5.2.4 Predictive statistical equations of the compressive strength of the selected SCCs

A statistical program[79] was used to determine the best-fit predictive equations for compressive strength of the groups I and III SCCs at different curing ages. Analyses were conducted at 95% confidence level. The predictive equations were tested for accuracy using R^2 (the coefficient of multiple determination) and S (average standard deviation). Correlations between the data predicted from the regression equations and the actual results obtained from the compressive strength test results of the selected trial matrices at various curing ages were evaluated using F and T tests. The compressive strength can be related to the slump flow and the curing age in the form of $CS = a\left(SF^b\right)\left(CA^c\right)$ as follow:

Group I self-consolidating concrete

$$CS_I = 11.47817\left(SF^{0.11818}\right)\left(CA^{0.21537}\right) \tag{3.6}$$

Group III self-consolidating concrete

$$CS_{III} = 20.96944\left(SF^{0.06634}\right)\left(CA^{0.17581}\right) \tag{3.7}$$

Where:

CS_I and CS_{III} = Compressive strength of the groups I and III SCCs, (MPa)

SF   = Slump flow (mm), with 508 mm $\leq SF \leq$ 711 mm (tolerance $\pm$ 25 mm)

CA   = Curing age (day), with 7 days $\leq$ CA $\leq$ 90 days

The regression equations 3.6 and 3.7 produced R^2 and S values of 99.6% and 0.74 MPa; and 99.38% and 0.86 MPa, respectively, indicating a strong relationship between the dependent variable (compressive strength) and the independent variables (slump flow and curing age). F and T tests were performed to confirm the significance of coefficients a, b, and c in the regression model. Both equations 3.6 and 3.7 displayed Prob(t) = 0.000

for all the coefficients, and Prob(F) = 0, indicating that the slump flow and curing age had a similar influence on the predicted compressive strength. Tables 3.8a and 3.8b represent the actual versus the calculated compressive strengths of the groups I and III SCCs, respectively. The predictive equations yielded percentage errors less than 3% confirming a strong relationship between the actual and the predicted compressive strengths.

3.5.3 Static modulus of elasticity

The elastic characteristics of a material are a measure of its stiffness. The term pure elasticity is used when the strains appear and disappear immediately. Four main categories of stress-strain response exist: (a) linear and elastic, such as in steel; (b) non-linear and elastic, such as in timber and some plastics; (c) linear and non-elastic, such as in brittle materials like glass and most rocks; and (d) non-linear and non-elastic, in which a permanent deformation remain after removal of load. This behavior is typical of concrete in compression or tension loaded to moderate and high stresses but is not very pronounced at very low stresses. The nonlinearity of concrete stems from its composite nature. While both hydrated cement paste and aggregates show linear elastic properties, their combined material, namely concrete, does not[12]. The slope of the relation between stress and strain of concrete under uniaxial loading gives the static modulus of elasticity, but the term Young's modulus can be applied strictly only to linear categories[10]. Since the curve for concrete is nonlinear, the following three methods for computing the modulus of elasticity are used: (a) the tangent modulus, given by the slope of a line drawn tangent to the stress-strain curve at any point on the curve; (b) the secant modulus, given by the slope of a line drawn from the origin to a point on the curve corresponding to a 40 percent stress of the failure load; and (c) the chord modulus, given by the slope of

162

Table 3.8a: Actual versus calculated compressive strength, Group I SCC

Actual slump flow (mm)	Curing age (Day)	Compressive strength (Mpa)		% Error
		Actual	calculated	
520.70	7	35.76	36.55	-2.22
520.70	28	48.75	49.27	-1.07
520.70	90	62.29	63.36	-1.72
514.35	7	36.59	36.50	0.24
514.35	28	49.94	49.20	1.48
514.35	90	63.70	63.27	0.68
517.65	7	36.90	36.53	1.01
517.65	28	50.42	49.24	2.35
517.65	90	64.32	63.32	1.56
524.00	7	36.32	36.58	-0.72
524.00	28	49.35	49.31	0.08
524.00	90	63.32	63.41	-0.14
644.65	7	36.77	37.49	-1.95
644.65	28	49.63	50.53	-1.82
644.65	90	63.08	64.98	-3.01
641.35	7	37.63	37.46	0.44
641.35	28	50.72	50.50	0.43
641.35	90	64.69	64.94	-0.39
641.35	7	37.92	37.46	1.20
641.35	28	51.04	50.50	1.06
641.35	90	65.28	64.94	0.52
641.35	7	37.33	37.46	-0.36
641.35	28	50.20	50.50	-0.60
641.35	90	64.14	64.94	-1.25
727.20	7	37.44	38.03	-1.56
727.20	28	50.27	51.26	-1.96
727.20	90	65.20	65.91	-1.09
733.55	7	38.32	38.06	0.67
733.55	28	51.62	51.31	0.60
733.55	90	66.80	65.98	1.23
723.90	7	38.69	38.00	1.77
723.90	28	51.99	51.23	1.47
723.90	90	67.49	65.88	2.39
723.90	7	37.97	38.00	-0.09
723.90	28	50.97	51.23	-0.51
723.90	90	66.12	65.88	0.37

Table 3.8b: Actual versus calculated compressive strength, Group III SCC

Actual slump flow (mm)	Curing age (Day)	Compressive strength (Mpa)		% Error
		Actual	Calculated	
527.05	7	44.21	44.74	-1.21
527.05	28	55.50	57.09	-2.87
527.05	90	69.24	70.10	-1.24
524.00	7	45.13	44.73	0.90
524.00	28	56.68	57.07	-0.69
524.00	90	70.85	70.07	1.10
524.00	7	45.67	44.73	2.07
524.00	28	57.42	57.07	0.61
524.00	90	71.62	70.07	2.16
511.30	7	44.79	44.65	0.31
511.30	28	56.22	56.98	-1.35
511.30	90	70.16	69.96	0.29
651.00	7	44.72	45.37	-1.46
651.00	28	56.32	57.90	-2.80
651.00	90	70.13	71.09	-1.37
651.00	7	45.58	45.37	0.45
651.00	28	57.41	57.90	-0.85
651.00	90	71.64	71.09	0.77
651.00	7	46.13	45.37	1.64
651.00	28	57.92	57.90	0.04
651.00	90	72.48	71.09	1.92
649.73	7	45.39	45.37	0.05
649.73	28	56.99	57.89	-1.58
649.73	90	71.04	71.08	-0.06
727.20	7	45.55	45.71	-0.35
727.20	28	57.08	58.32	-2.18
727.20	90	70.43	71.61	-1.68
723.90	7	46.41	45.69	1.54
723.90	28	58.30	58.31	-0.01
723.90	90	71.98	71.59	0.54
720.85	7	47.02	45.68	2.85
720.85	28	59.03	58.29	1.25
720.85	90	72.87	71.57	1.78
727.20	7	46.19	45.71	1.04
727.20	28	57.86	58.32	-0.80
727.20	90	71.31	71.61	-0.43

a line drawn between two points on the stress-strain curve. To further modify the secant modulus, the origin of the line is drawn from a point representing a longitudinal strain of 50 μin/in. to the point that corresponds to 40 percent of the ultimate load. Shifting the base line by 50 micro strains is recommended to correct for the slight concavity that is often observed at the beginning of the stress-strain-curve. Figure 3.10 represents a typical stress-strain curve of concrete along with the tangent and secant moduli.
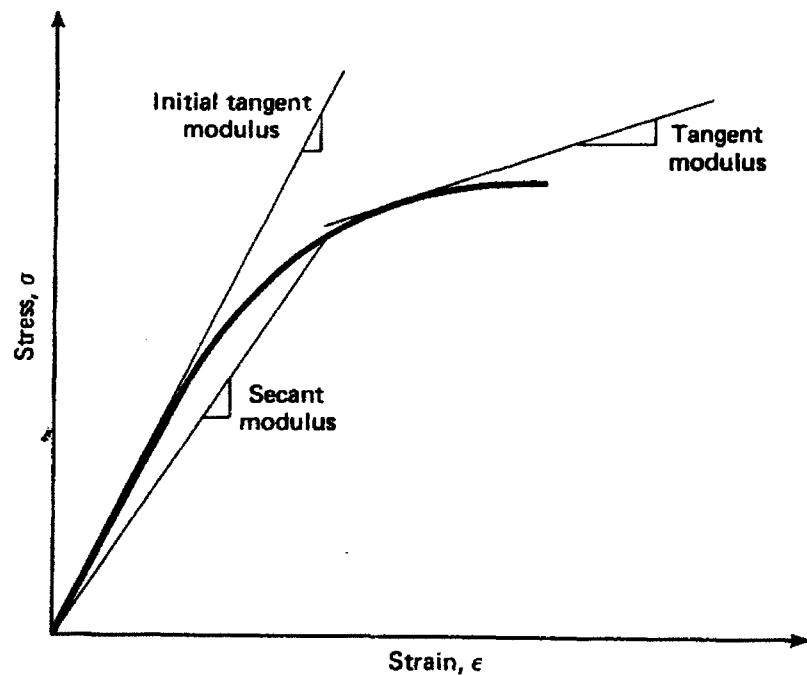
Figure 3.10: Tangent and secant moduli of concrete[80]

The elastic modulus is defined as the ratio between the applied stress and instantaneous strain within an assumed proportional limit. In spite of the nonlinear behavior of concrete, an estimate of the elastic modulus is necessary for determining the stress induced by strains associated with environmental effects. It is also needed for

computing the design stress under load in simple element, and moments and deflections in complicated structures. It is usually estimated from empirical expressions that assume direct dependence of the elastic modulus on the strength and density of concrete. According to the ACI Building Code 318[81], the secant modulus of elasticity can be determined from:

$$E_c = 33w_c^{1.5}\sqrt{f_c'} \text{, in psi} \tag{3.8}$$

$$E_c = 0.0143w_c^{1.5}\sqrt{f_c'} \text{, in MPa} \tag{3.9}$$

for concrete with a unit weight between 90 and 155 lb/ft^3 (1442 and 2432 kg/m^3)

$$\text{or } E_c = 57000\sqrt{f'} \text{, in psi} \tag{3.10}$$

$$\text{or } E_c = 4730\sqrt{f'} \text{, in N/mm}^2 \tag{3.11}$$

for normal-weight concrete

Where E_c is the static modulus of elasticity, w_c the unit weight, and f_c' the 28-day compressive strength of standard cylinder. Equations 3.8 through 3.11 are valid only for normal-strength concretes with characteristic strengths up to 6000 psi (41 MPa).

High strength concrete (with f_c' from 41 to 82 MPa (6000 to 12000 psi)) behaves in fundamentally different ways from normal strength concrete, more like a homogeneous material[82]. Its stress-strain curves are steeper and more linear to a higher stress-strength ratio than in normal-strength concretes. When using high strength concrete ACI proposed a modified version of equation 3.8 or 3.9 for computing the static modulus of elastic normal weight concrete of strength up to 83 MPa (12000 psi) and lightweight concrete up to 62 MPa (9000 psi), based on expression due to Carrasquillo et al.[83] as follow:

166

$$E_c = \left(40000\sqrt{f_c'} + 1x10^6\right)\left(\frac{w_c}{145}\right)^{1.5}, \text{in psi} \qquad (3.12)$$

$$E_c = \left(3.2\sqrt{f_c'} + 6895\right)\left(\frac{w_c}{2320}\right)^{1.5}, \text{in MPa} \qquad (3.13)$$

The ASTM C 469[73], "Standard Test Method for Static Modulus of Elasticity and Poisson's Ratio of Concrete in Compression," was used to evaluate the modulus of elasticity of the selected self-consolidating concretes. In the present study, the static modulus of elasticity E_c as the slope of the line drawn from the stress of zero to the compressive strength of $0.45f_c'$ was adopted. The test results of the E_c for the selected trial mixtures at 28 and 90 days curing ages are shown in Tables 3.7a through 3.7c. Each of these values is the average of four tested samples.

3.5.3.1 Influence of admixture source on static modulus of elasticity

Figures 3.11a and 3.11b are the typical representations of static modulus of elasticity of the trial matrices as function of admixture sources and curing ages, respectively. A similar trend and behavior to that of the compressive strength was observed for the static modulus of elasticity of the selected self-consolidating concretes. In comparison to the admixture source C, admixture sources A, B, and D displayed the overall percentage reduction of about 3, 1 and 2%, respectively, for the groups I and III self-consolidating concretes. This similarity is normal because the modulus of elasticity is simply the ratio between the resistance of the compressive stress and the strain within the assumed stress limit. Like the compressive strength, the change in the admixtures source did not affect the static modulus of elasticity of the selected self-consolidating concretes. The increase in static modulus of elasticity at 28 and 90 days is due to the improvement in compressive strength during the same period.
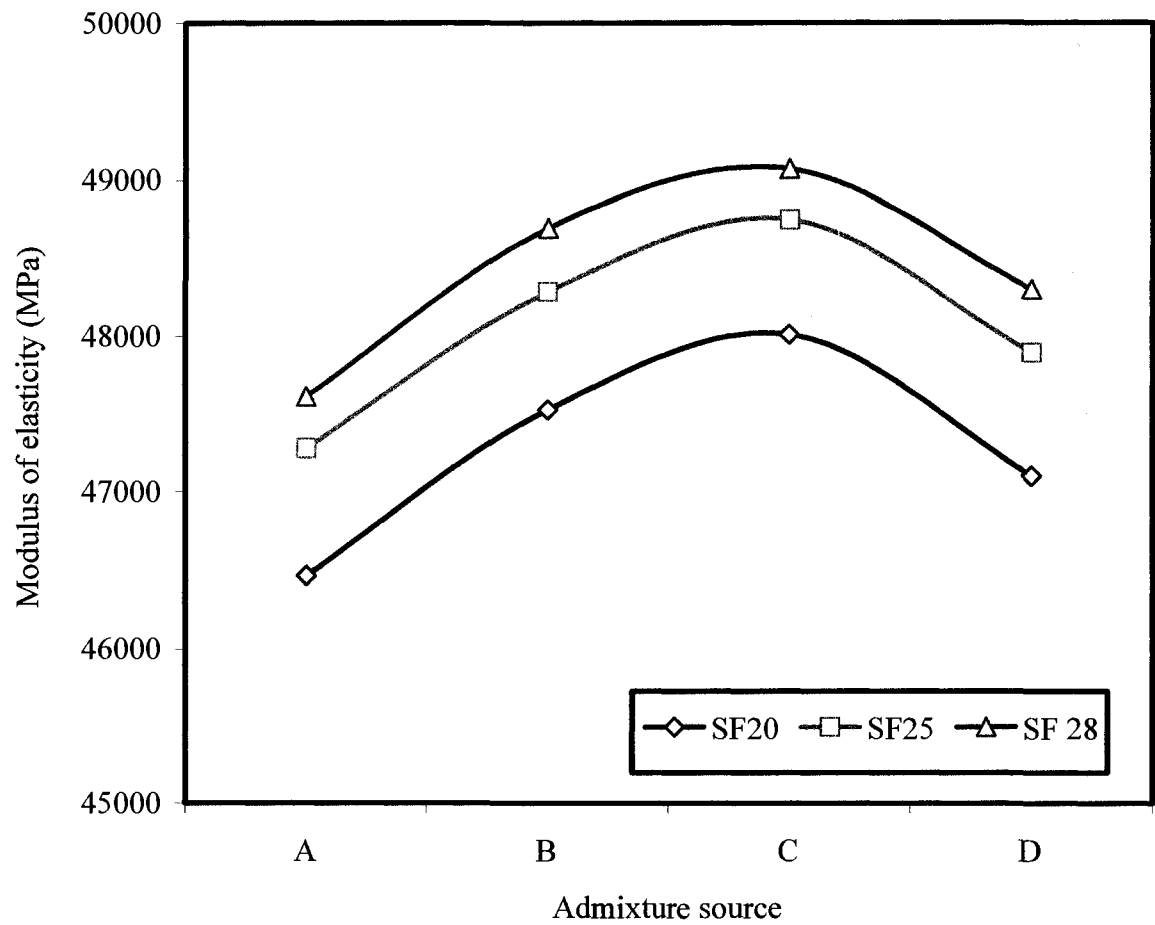
Figure 3.11a: Influence of admixture source on the 28-day modulus of

elasticity of the group III self-consolidating concretes
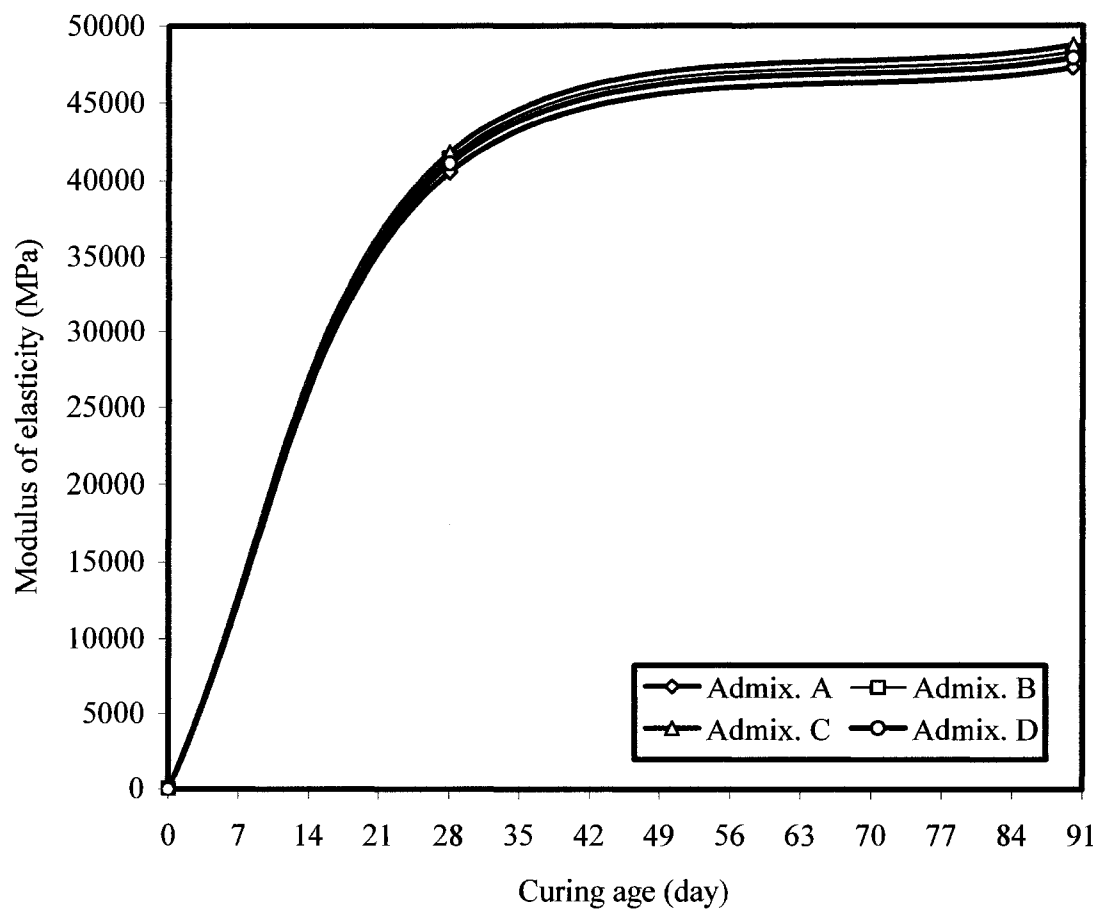
Figure 3.11b: Influence of admixture source and curing age on the modulus of elasticity

of the group III-635 mm (25 inches) slump flow SCCs

3.5.3.2   Influence of slump flow on static modulus of elasticity

The influence of slump flow value on static modulus of elasticity can be seen in Tables 3.7a through 3.7c. When the slump flow increased from 508 to 635 to 711 mm (20 to 25 to 28 inches), irrespective of the admixture source and curing age, marginal improvements in static moduli of elasticity of less than 3% were recorded for all three SCC groups, indicating that the increases in slump flow had virtually no influence on the modulus of elasticity of the trial self- consolidating concretes.

3.5.3.3   Measured versus specified modulus of elasticity

The modulus of elasticity is usually estimated from empirical expressions that assume direct dependence of the elastic modulus on the strength and density of concrete. Since all the three SCC groups are normal weight concretes which exhibited compressive strength at 28 and 90 days between 62 to 83 MPa (6000 and 12000 psi), equation 3.10 or 3.11 was used to determine the ACI specified modulus of elasticity where f'_c is the 28-day compressive strength of the selected matrix. For the groups I and II SCCs, the experimental static moduli of elasticity were on average 11% lower than that obtained from equation 3.12 or 3.13. The group III SCCs displayed an opposite trend and produced moduli of elasticity which on average were higher than that obtained from equation 3.10 or 3.11 by 15 %. On whole, all selected trial SCCs exhibited moduli of elasticity within the typical range of 120 to 80% recommended by the ACI 318[81].

In addition to the compressive strength and the unit weight reflected in equations 3.8 and 3.12, the modulus of elasticity of concrete is very sensitive to the modulus of the aggregate. Considering that the group I matrices had 4% more cementitious materials content than group III matrices, and both groups I and III had identical water-to-

170

cementitious materials and coarse-to-fine aggregate ratios, it can be concluded that the

aggregate S used in the group III had a higher modulus of elasticity than the aggregate R

used in the group I matrices.

3.6   Conclusions

For the test results of this study the following conclusions can be drawn:

a)   Irrespective of the self-consolidating concrete groups, the optimum dosages

requirement in obtaining a uniform slump flow and visual stability index varied among

the four selected admixture sources. As shown in Table 3.9, the required dosage amount

of HRWRA was highest for the source A, followed by the sources C, B, and D in

descending order. On the other hand, the required VMA dosage was highest for the

source A and remained uniform for the sources B, C, and D. For all four admixture

sources, the self-consolidating concretes made with slump flow of 508 ± 25 mm (20 ± 1

inches) did not require VMA to yield a satisfactory unconfined workability and dynamic

stability. An increase in the slump flow generated a higher dosage demand for all

admixture sources.

Table 3.9: Influence of admixture sources on optimum dosage requirement

	Low High			
Optimum dosage of HRWRA	← →			
	D	B	C	A
Optimum dosage of VMA	Low High			
	← →			
	B, C, D			A

The differences among admixture sources can be explained through the ultraviolet-visible (UV/Vis) spectroscopy test, the chemistry of admixture, and the calculated VMA-to-HRWRA ratios.

- The relationship between the cement-water-superplasticizer solution concentration of free admixture and the fluidity of the matrix was studied. The increase in the solution concentration of free admixture produced higher adsorption of the PC-HRWRA carboxyl group (COO^-) on the cement calcium ions (Ca^{2+}), generating more electrostatic and steric hindrance repulsions which favored greater dispersibility of the mixture. The UV/Vis test results indicated that the concentration of the PC-HRWRA was highest for the source D, followed by the sources B, C, and A in descending order, supporting the results obtained for the optimum dosage requirement of the four admixture sources.

- The difference in the admixture sources can also be attributed to their chemical type. The behavior of the sources B, C, and D superplasticizers was similar to that of a polycarboxylate-acid type (PCA), where the acid portion was predominant when compared to the ester part (PCE). The higher acid ratio increased the adsorption of the polymer to cement particles resulting in further dispersion of the fresh matrix. On the other hand, source A was polycarboxylate-ester type and for the same dosage, it was unable to disperse cement grains at a rate similar to that of polycarboxylate acid type. The gradual adsorption of the polycarboxylate-ester type superplasticizer increased the slump flow retention of freshly-mixed self-consolidating concrete.

- The test results also indicated a trend for the VMA-to-HRWRA ratio. The similarity of the VMA-to-HRWRA ratios of the admixture sources B, C, and D led to the conclusion that these sources had to have a similar chemical composition. The higher

172

VMA-to-HRWRA ratio of the source A admixture was due to its thickening mode of functioning which led to a higher demand for the source A VMA to produce a highly stable or stable fresh matrix.

b)   With proper proportioning, self-consolidating concrete with acceptable flow ability, plastic viscosity, dynamic and static stabilities, passing ability, and filling ability can be achieved with any of the four selected admixture sources. However, the performance of the selected admixtures in attaining a uniform fresh property varied among the admixture sources. The ranking of the four admixture sources as related to their influence on the fresh performance of the trial self-consolidating concrete is presented in Table 3.10.

Table 3.9: Influence of admixture sources on the fresh properties of SCC

Flowability/viscosiy	Low/High ←————————————→ High/Low B, C A,D
Dynamic stability	Similar ←————————————→ A B C D
Static stability	Best Worst ←————————————→ B,C A,D
Passing ability	Similar ←————————————→ A B C D
Filling ability	Similar ←————————————→ A B C D

c)   The 508 mm (20 inches) slump flow SCCs exhibited very low plastic viscosity, very high dynamic stability, moderate filling ability, low passing ability, and high static stability. As a result, the 508 mm (20 inches) slump flow was found unsuitable for congested reinforced structures. All 635 mm (25 inches) and 711 mm (28 inches) slump flow self-consolidating concretes displayed high flow ability, low plastic viscosity (by inference) , high dynamic stability, moderate static stability, moderate passing ability, and moderate to high filling ability, indicating their suitability for most civil engineering applications. The formwork for the 711 mm (28 inches) slump flow SCCs may be subjected to a higher than expected pressure due to the flow ability that remained near the lower bond of the acceptable limit.

d)   The data pertaining to the air content, bleeding, time of setting, adiabatic temperature, demolded unit weight, compressive strength and modulus of elasticity revealed marginal differences among the selected self-consolidating concretes made with different sources of admixtures and various slump flows.

e)   Predictive equations to correlate HRWRA or VMA dosages or compressive strength with concrete paste content, aggregate sizes, and target slump flow showed significant statistical relationships between the dependant variables and independent variables.

CHAPTER 4

INFLUENCE OF HAULING TIME ON FRESH PERFORMANCE

OF SELF CONSOLIDATING CONCRETE

The present chapter is intended to evaluate the influence of hauling time on the

fresh performance of selected self-consolidating concretes. Nine different hauling times,

namely: 10, 20, 30, 40, 50, 60, 70, 80, and 90 minutes, were used to evaluate the change

in unconfined workability, flow ability rate, and dynamic segregation resistance of

freshly-mixed self-consolidating concretes. Additionally, the overdosing approach

(sufficient initial optimum admixture dosage) was selected to revert the adverse influence

of hauling time on the fresh characteristics of the selected matrices.

4.1   Background on mixing and hauling concrete

Immediately after or during its mixing, concrete is transported from its mixing

location to the final destination. During its transportation, concrete should remain

cohesive and workable within acceptable tolerances. Transportation methods which

promote segregation should be avoided. Since hauling generally includes mixing, a

presentation detailing the method and equipments involved in mixing concrete is

necessary.

4.1.1   Concrete mixers

To produce concrete with consistent quality, an appropriate mixer should be used.

The concrete mixers are classified into two main categories: batch mixers and continuous

mixers.

4.1.1.1   Batch mixers

The batch mixers can be divided into two categories depending on the orientation

of the axis of rotation: horizontal or inclined (drum mixer) and vertical (pan mixer)[10,12,84].

a. Drum mixers: Drum mixers are composed of blades attached to the inside of the

movable drum. The role of the blades is to lift the materials as the drum rotates.

Depending on the speed of rotation of the drum and the angle of inclination of the

rotation axis, the drum mixers can be classified in three main categories, namely: non-

tilting drum, tilting drum, and reversing drum.

• Non-tilting drum mixer: For this type of mixer, the orientation of the drum is fixed.

The materials are added at one end and discharged at the other.

• Tilting drum mixer: For this type of mixer the inclination can be varied. A horizontal

inclination provides more energy for mixing concrete, because more concrete is lifted to

the full diameter of the drum before dropping. If the axis of rotation is almost vertical the

blades cannot lift the concrete and the concrete is not well mixed. Axis at an angle of 15

degrees generally provides efficient mixing[84]. The tilting drum is the most common type

of drum mixer for small batches (less than 0.5 m^3 (18 ft^3) both in the laboratory and in the

field.

• Reversing drum mixer: This type of mixer is similar to the non-tilting drum mixer

except that the same opening is used to add the constituents and discharge the concrete.

The drum rotates in one direction for mixing and in the opposite direction for discharging

concrete. The blades have a spiral arrangement to obtain the desired effect for discharge

and mixing. The truck mixers belong to the reversing category of drum mixers. In the

176

United States, most ready-mixed concretes are mixed in trucks and not premixed in plant. When a truck mixer is used, 70 to 100 revolutions of the drum or blades at the rate of rotation designated by the manufacturer as mixing speed are usually required to produce the specified uniformity of concrete. The mixing speed is generally 6 to 18 rpm. Any additional revolutions beyond the 100 are classified as agitating speed, which are usually about 2 to 6 rpm[10,11,78].

b. Pan mixers: Pan mixers are forced-action mixers. They consist essentially of a cylindrical pan (fixed or rotating) which contains the concrete to be mixed, one or two sets of blades which rotate inside the pan to mix the materials, and a blade which scrapes the wall of the pan. The concrete in every part of the pan is generally thoroughly mixed, and scraper blades ensure that the mortar does not stick to the sides of the pan. To discharge the mixer, the pan is usually emptied through a trap on the bottom. For small mixers (less than 28 liters or 0.028 m^3 (1 ft^3)), the blades are lifted and the pan can be removed to empty the mixer. Pan mixers are particularly efficient with stiff and cohesive mixes and often preferred for mixing small quantities of concrete or mortar in the laboratory[12].

4.1.1.2 Continuous mixers

For continuous mixers, the materials are continuously fed into the mixer at the same rate as the concrete is discharged. They are usually no-tilting drums with screw-type blades rotating in the middle of the drum. These mixers are used for applications that require a short working time, long unloading time, remote sites (not suitable for ready-mix) and small deliveries[84]. A major use of these types of mixers is for zero or low slump (i.e. roller compacted cement concrete pavements).

4.1.2 Batching concrete

Batching is the process of measuring concrete mix ingredients by either mass or volume and introducing them into the mixer[10]. Concrete batching can be characterized by the order of loading the constituents into the mixer and the duration of the loading period. The loading period is extended from the time when the first constituent is introduced in the mixer to when all the constituents are in the mixer. ASTM C 94[85] and AASHTO M 157[48] require batching to be done by mass rather than by volume. Volumetric method (ASTM C 685[86] or ASASHTO M 241[87]) is used for batching concrete in a continuous mixer[10].

RILEM[88] (Réunion Internationale des Laboratoires d'Essais et de Recherches sur les Matériaux et les Constructions) divides the loading period into two parts: dry mixing and wet mixing. Dry mixing is the mixing that occurs during loading but before water is introduced. Wet mixing is the mixing after or while water is being introduced, but still during mixing. The loading period is important because some of the concrete properties will depend on the order in which the constituents are introduced in the mixer. It is well known that the delayed addition of high range water-reducing admixture leads to a better dispersion of cement[23,34].

Specifications generally require the following batching delivery tolerances: cementitious material ± 1% by weight, aggregates ± 2% by weight, water ± 1% by weight (or volume at central mix plants only), and admixtures ± 3% by weight (or volume ± 30 milliliters (1 ounce)), whichever is greater)[10,89].

4.1.3 Mixing concrete

Mixing concrete consists of blending its constituents until it is uniform in

appearance with all ingredients evenly distributed. In many countries the mixing is performed in the truck where water and then dry materials are dosed into the truck. The truck mixing is not as efficient as the plant mixing, where much longer times, up to 20 minutes, are needed[9]. The required mixing time varies depending on the equipment, materials used, gradations of aggregates, amount and types of admixtures, temperature, etc. However, if factors such as segregation, bleeding, finishing and others are of concern, the first and easiest solution is to adjust the mixing time or speed. The mixing time requirements are recommended by the manufacturer of the mixer. Each mixer has attached in a prominent place a manufacturer's plate showing the capacity of the drum in terms of volume of mixed concrete and the speed of rotation of mixing drum or blades.

Generally, the mixing time is defined as the elapsed time between the loadings of the first constituent to the final discharge of the concrete[10,12]. RILEM[88] defines mixing time as the time between the loading of all constituents and the beginning of concrete discharge. In any case, it is important to fully describe the mixing process for each batch of concrete. *In the current study, the mixing time is defined as the elapsed time between the loading of the first ingredient to the beginning of concrete discharge, and during the mixing time the mixer is operated at the mixing speed.*

4.1.4 Ready-mixed concrete

In a ready-mixed plant, concrete is generally mixed using one or a combination of the following operations: (1) central mixing: the batched (weighed or metered) ingredients are added into a stationary mixer, completely mixed, and then delivered either in a truck agitator, a truck mixer operating at agitating speed, or a nonagitating truck for transporting to the point of discharge. (2) shrink mixing: concrete is partially mixed in a

stationary mixer and the mixing is complete en route in a truck mixer; and (3) truck mixing: concrete is mixed entirely in the truck mixer[10]. Nowadays, ready-mixed plants are largely used in concrete industry due to the numerous related advantages, such as: close quality control, use in congested sites, use of agitator trucks to prevent segregation and maintain workability[11], etc. The cost of ready-mixed concrete may be higher than that of site-mixed concrete, but the in-place concrete cost can be cheaper by saving in construction time, organization, labor and cement content.

4.1.5   Hauling concrete

Several methods for transporting and handling concrete exist and the most important are: wheelbarrows or handcarts, dumpers, lorries, buckets, chutes, belts conveyors, pneumatic placers with pipeline, concrete pumps with pipelines, and truck mixers[10,12,78]. The choice of the transportation method depends on economic consideration and the quantity of concrete to be transported. In most cases truck mixers are used for mixing and hauling concrete, and truck agitators are used for hauling central-mixed concrete. In some cases nonagitating (e.g., flatbed) trucks can be also used for delivering concrete (e.g., pavement). *The hauling time, which can be defined as the elapsed time between the first contact of water and cement to the beginning of concrete discharge*, ranges usually between 30 minutes (when the concrete is hauled in nonagitating trucks) to 90 minutes (when the concrete is hauled in truck mixers or truck agitators). In the case of hot weather or under other conditions contributing to quick stiffening of concrete, the maximum allowable time may be reduced[89]. Short mixing periods will reduce the amount of entrained air and will likely lead to a non-uniform mixture. During the hauling time the mixer is operated at the agitating speed.

4.1.6   Mixing and hauling of self-consolidating concrete

Self-consolidating concrete requires special attention in the mixing and delivery method due to its low water content relative to the high cementitious materials content. Shrink mixing or truck mixing can be used. Several researchers have reported that the length of mixing and the time of addition of superplasticizers to SCC can influence both its fresh and hardened properties. Due to its high fluidity, the volume of SCC placed into a truck should not exceed 80% of the drum capacity. This type of monitoring will prevent the SCC from spilling out of the drum during hauling. Concrete truck operators should keep the drum revolving in a mixing rotational direction while in transport. Self-consolidating concrete can also be made from conventional concrete by adding admixtures at the discharge site to bring the mixture to the desired consistency[1].

In general, slump flow loss occurs when the free concrete's mixing water is absorbed by the hydration reactions, adsorbed on the surfaces of cement hydrated products, or by evaporation[10,11]. It can be defined as the loss of consistency in fresh concrete with elapsed time. It is a normal phenomenon which is related to the intrinsic nature of concrete. Mixing at a high speed or for a long period of time (about one or more hours); and high temperature due to excessive heat of hydration in mass concreting, and/or the use of hot materials can result in slump loss[10,11,12,78]. The slump flow loss can lead to an unusual rate of stiffening in fresh concrete and cause loss of entrained air, strength and durability; difficulty in pumping and placing; and excessive effort in placement and finishing operation[10,12].

To overcome the slump flow loss, two main remediation methods are generally practiced. They consist of starting with a higher initial slump than needed (overdosing),

or adding extra water or admixtures just before placement which is referred to as retempering. The progressive increase use of chemical admixture in concrete industry has facilitated the control of slump loss. Superplasticizers or high range water-reducing admixtures were developed in order to improve the dispersibility and the slump retention of melamine and naphthalene type admixtures. Their extended life can impart up to 2 hours longer working life of concrete[33]. Overdosing the admixture amount in attaining the target slump flow at job site or retempering with admixture instead of water are the preferred methods in remediation of the slump flow loss. The use of extra water in retempering or in making a higher initial slump can induce side effects on the properties and serviceability of the hardened concrete (i.e. decrease in strength and durability, increase in permeability and drying shrinkage, etc.)[10,11,12].

4.2   Experimental programs

The self-consolidating concretes S7.B.SF20, S7.B.SF25 and S7.B.SF28 were used. Their mixture constituents and proportions are presented in Table 3.1c. The detail of design proportioning procedure is shown in section 3.1. Laboratory trial mixtures were used to produce all SCCs. An electric counter-current pan mixer with a capacity of 0.028 m^3 (1 ft^3) was used to blend concrete components. A pan mixer was preferred because it is particularly efficient for mixing small quantities of concrete in a laboratory. In simulating the influence of hauling time on the fresh SCCs, a realistic concrete mixing tool with changeable velocity was needed. Therefore, a speed control box was designed and mounted on the mixer to control its rotational velocity during hauling. Figure 4.1 documents the actual mixing apparatus used in this study. The aggregates, cement, fly ash, water and chemical admixtures were prepared as reported in the Chapter 2,

Agitation speed
control box ————

Pan mixer
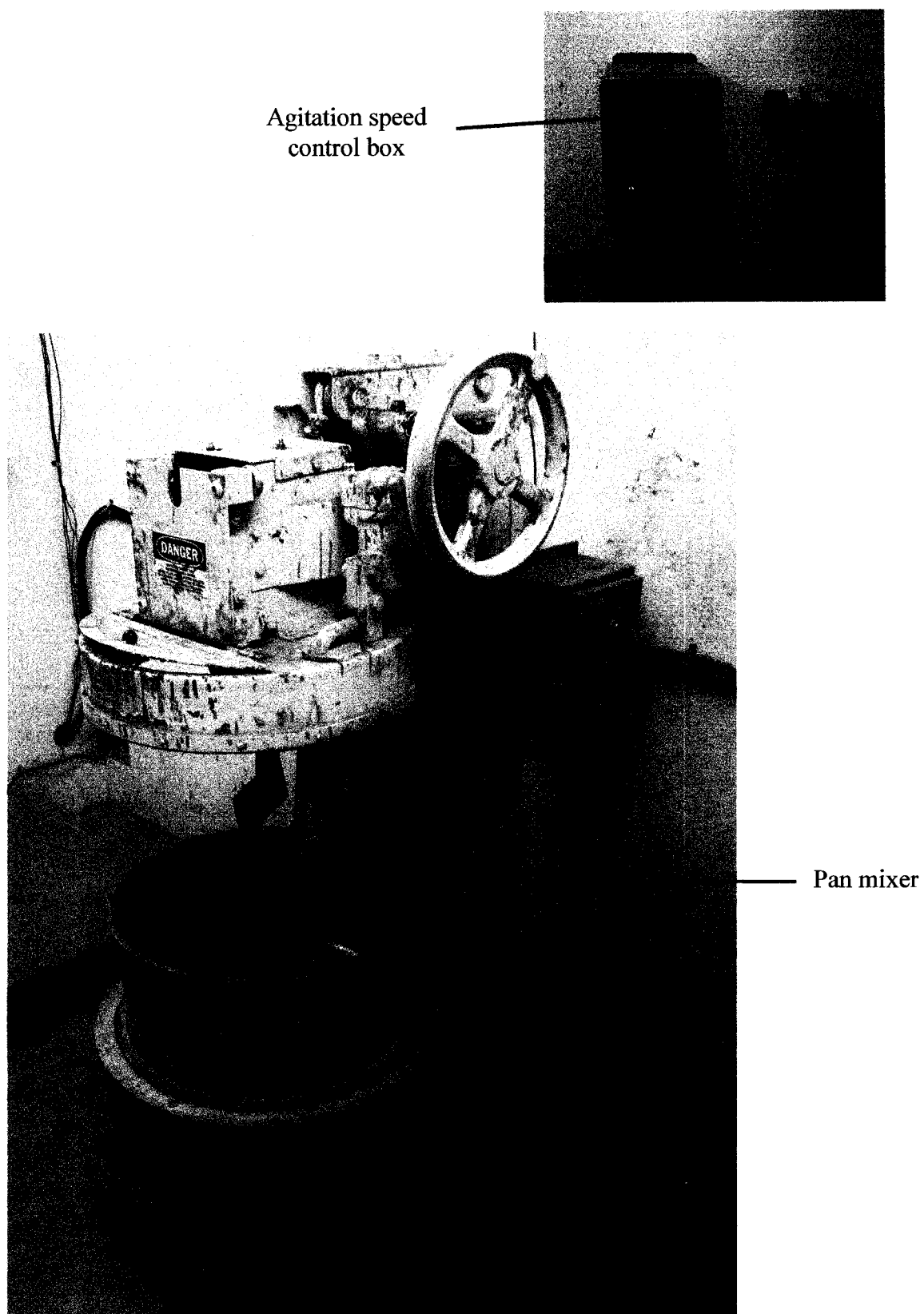
Figure 4.1: Mixing tool and agitation speed control box

Section 2.1; and stored in the laboratory prior to their use. The laboratory room condition was always maintained at 25±5% relative humidity and 21 ± 2 °C (70 ± 3 °F) temperature. The concrete mixtures at the end of hauling time were used to determine the unconfined workability, flow rate or plastic viscosity per inference, segregation resistance, and J-ring passing ability in accordance with the ASTM C 1611[55] and C 1621[58]. The test results were measured immediately after the hauling time to avoid any variation in the concrete properties over time.

The workability of concrete is influenced by the mixing tool, velocity and time. Because of its low water content relative to the amount of cementitious materials, self-consolidating concrete requires a higher mixing energy than conventional concrete to thoroughly distribute the ingredients. In fact, when water is added to dry matrix, the inter-particle forces are increased due to the water surface tension and the capillarity pressure inside the fluid bond. In the presence of superplasticizer, the fluidity of the matrix further increases, resulting in a lower required mixing energy. The need for transporting concrete to its final place of deposit requires additional mixing time. In order to reflect the high energy level followed by a lower energy needed in the production and transport of SCC, a mixing and hauling procedure as shown in Figure 4.2 was adopted. *As it can be seen, the hauling time was defined as the elapsed time between the first contact of water and cementitious materials to the beginning of concrete discharge.*

4.3   Discussion of results

4.3.1   Influence of hauling time on fresh performance of SCC

During the present study, the effect of hauling time on the unconfined workability

184
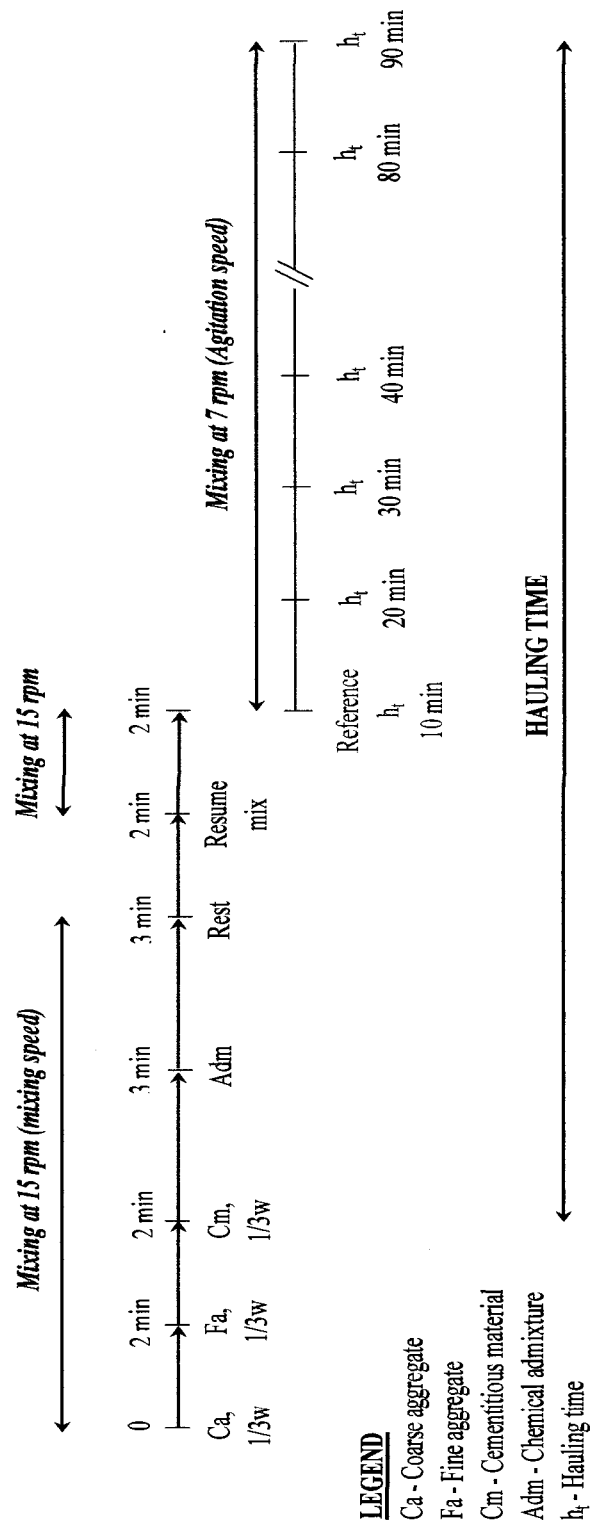
Figure 4.2: Mixing and hauling sequences

185

(measured by the slump flow), the flow rate (evaluated by the T_{50} time), and the dynamic segregation resistance (assessed by the VSI) was investigated. Tables 4.1, 4.2 and 4.3 document the test results.

4.3.1.1 Unconfined workability

The measured slump flows at the end of 20, 30, 40, 50, 60, 70, 80, and 90 minutes of hauling time were compared to that of the reference (control) hauling time of 10 minutes. Figure 4.3 represents the slump flow losses of the selected trials matrices as a function of hauling times. It can be seen from the abovementioned tables and figure that all three selected self-consolidating concretes lost slump flow as early as 20 minutes hauling time. In comparing to 10 minutes hauling time, mixtures made with 508 mm (20 inches) slump flow displayed slump flow losses of 16, 21, 23, 26, 30, 35, 36, and 38% at 20, 30, 40, 50, 60, 70, 80, and 90 minutes hauling time, respectively. The corresponding slump flow losses were 14, 17, 20, 24, 29, 34, 36, and 38%; and 7, 12, 17, 21, 25, 31, 35, and 37% for the mixtures prepared for 635 and 711 mm (25 and 28 inches) slump flows, respectively. The decrease in slump flow can be translated to the loss in ability of self-consolidating concrete to flow through unconfined areas or formwork.

4.3.1.2 Flow rate or viscosity per inference

As an index of viscosity, the T_{50} times of the selected self-consolidating concretes were also recorded and compared to that of the reference hauling time. Irrespective of the slump flow value, the T_{50} always increased with an increase in hauling time. At hauling time of 20 minutes and more, the T_{50} of the mixtures S7.B.SF20 could not be measured since the concrete spread was less than the 508 mm (20 inches) recommended value. In comparison with the 10-minute reference hauling time, the T_{50} time of the

186

Table 4.1: Fresh properties of hauled SCC mixture S7.B.SF20

Hauling Time (min)	Slump flow (mm)	T_{50} (sec.)	VSI	Slump flow loss (mm)
10	524	3.19	0	0
20	438	-	0	-86
30	413	-	0	-111
40	402	-	0	-122
50	387	-	0	-137
60	368	-	0	-156
70	343	-	0	-181
80	337	-	0	-187
90	324	-	0	-200

1 ml/100 kg = 0.0153 oz/cwt, 1 mm = 0.03937 inch

Table 4.2: Fresh properties of hauled SCC mixture S7.B.SF25

Hauling Time (min)	Slump flow (mm)	T_{50} (sec.)	VSI	Slump flow loss (mm)
10	651	2.79	0	0
20	559	2.92	0	-92
30	540	3.10	0	-111
40	521	3.28	0	-130
50	495	-	0	-156
60	464	-	0	-187
70	432	-	0	-219
80	419	-	0	-232
90	406	-	0	-245

1 ml/100 kg = 0.0153 oz/cwt, 1 mm = 0.03937 inch

Table 4.3: Fresh properties of hauled SCC mixture S7.B.SF28

Hauling Time (min)	Slump flow (mm)	T_{50} (sec.)	VSI	Slump flow loss (mm)
10	724	1.85	1	0
20	643	2.20	0	-81
30	635	2.55	0	-89
40	603	2.67	0	-121
50	572	2.80	0	-152
60	546	3.00	0	-178
70	502	-	0	-222
80	470	-	0	-254
90	457	-	0	-267

1 ml/100 kg = 0.0153 oz/cwt, 1 mm = 0.03937 inch
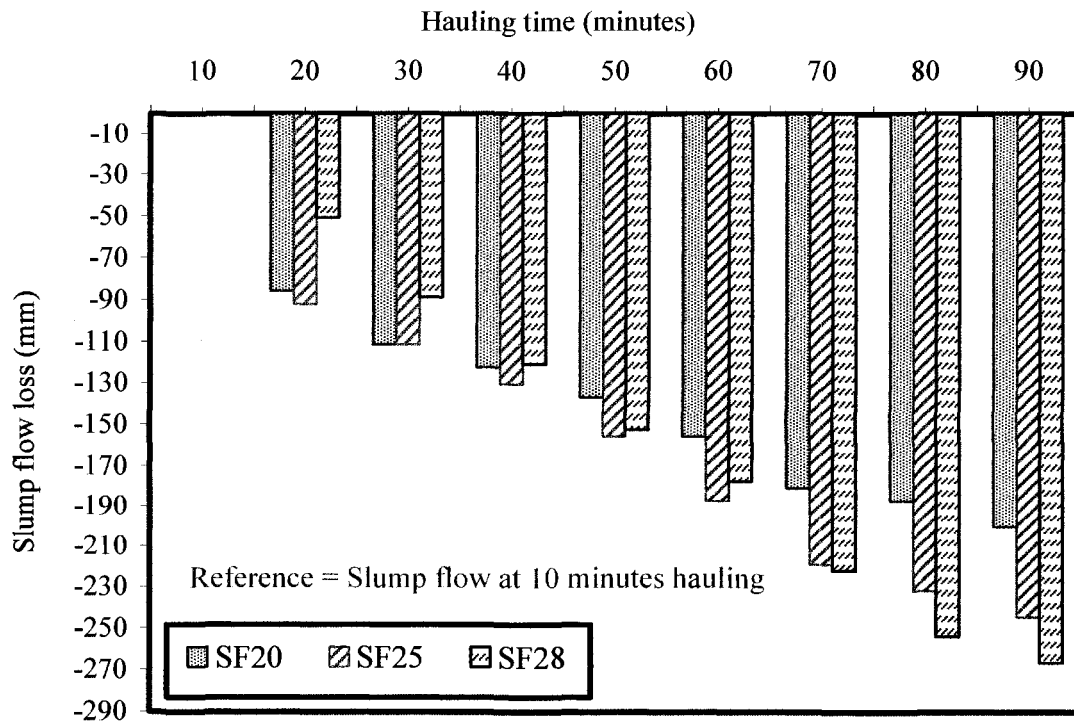
Figure 4.3: Slump flow loss of self-consolidating concretes as a function of hauling time

mixture made with 635 mm (25 inches) slump flow increased by 0.13, 0.31, and 0.49 second after 20, 30, and 40 minutes hauling times, respectively. Beyond that time, the T_{50} could not be measured due to the severe loss in slump flow. For the mixture made with 711 mm (28 inches) slump flow, the increases in T_{50} time were 0.35, 0.70, 0.82, 0.95, and 1.15 seconds after 20, 30, 40, 50, and 60 minutes hauling time, respectively; after which the mixture displayed a significant loss in slump flow. An increase in T_{50} time is indicative of enhanced viscosity. It is to note that the T_{50} times of the selected self-consolidating concretes were all within the recommended value of 2 to 5 seconds.

4.3.1.3   Dynamic segregation resistance

The influence of hauling time on dynamic segregation resistance of the selected matrices was also evaluated through the visual stability index (VSI). Irrespective of slump flow value, all selected self-consolidating concretes displayed high stability (VSI = 0) for the selected hauling times.

4.3.2   Mechanism of slump flow loss due to hauling time

The fundamental mechanism of slump loss of concrete during the hauling process has been established and reported by several studies. It mainly involves the additional fines brought to the concrete mortar by the grinding of aggregates and cement particles, the growth of the cement hydrated products, and the adsorption of the superplasticizer on the cement hydrates throughout the hauling time[16,23,90,91,92,93]. The flow chart of Figure 4.4 presents the phases and actions involved in aggregate-cement-admixture mechanical interaction during mixing and hauling.

Since the fluidity of concrete is mostly controlled by the fluidity of the mortar portion[1,92,94], the slump flow losses recorded during the present investigation can be

189
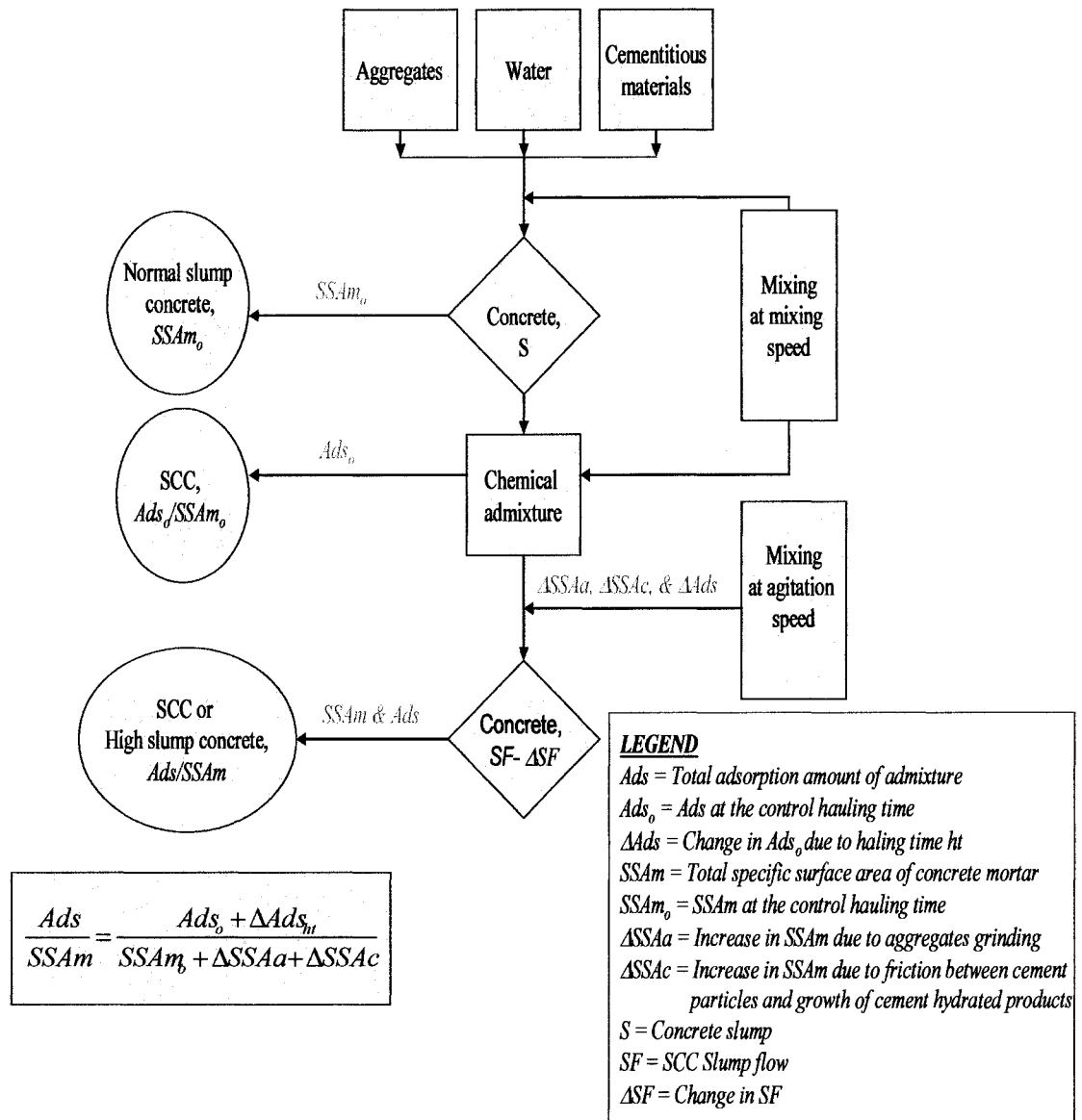
Figure 4.4: Self-consolidating concrete production and slump flow loss

mechanism during hauling

explained through the specific surface area of concrete mortar (*SSAm*) and adsorption amount of chemical admixtures (*Ads*). The ratio *Ads/SSAm* will be used to characterize the fresh performance of self-consolidating concrete.

4.3.2.1   Specific surface area of concrete mortar (*SSAm*)

The specific surface area (SSA) can be defined as a material property which measures the total surface area per unit of mass (with units of m²/kg), solid or bulk volume (units of m²/m³ or m⁻¹). It has a particular importance in the case of adsorption and reactions on surfaces. The value of the specific surface area depends critically upon the method of measurement. The SSA can be calculated from a particle size distribution, making some assumption about the particle shape. This method, however, fails to account for surface associated with the surface texture of the particles.

In the current study, laser diffraction particle size distribution was used to investigate the SSAm, in order to illustrate qualitatively the increase in specific surface area of the self-consolidating concrete mortar due to hauling times. It was by no mean intended to quantify the exact amount of increase in SSA. Particle size analyzer described in section 2.3.14 was used for that purpose. The adopted apparatus was suitable for wet condition, and particle sizes ranging between 0.2 to 2000 μm. Suspending mediums which promote the formation of bubbles and interfere with the measurement, were avoided. The most convenient medium is water, because the concrete's particles do not dissolve in water. Consequently, water was used as a suspending medium. The self- consolidating concrete mixture S7.B.SF25 was tested. At the end of the selected hauling times, a representative sample of fresh self-consolidating concrete was obtained. The sample was added to the system at a suitable concentration,

191

about 1 gram (0.0022 lb). The ideal concentration was reached when the bar on the obscuration monitor showed a value between 0.1 and 0.4. The light scattered by the particles was measured in a period of 10 to 30 seconds as recommended by the manufacturer.

The test reports on the particle size distribution analysis at the selected hauling times are given in Appendix IV. Figure 4.5 presents the relationship between particles size and hauling times. It can be see that the volume of fine particles ranging from 1 to 250 μm (39×10^{-6} to 9843×10^{-6} inch) increased as the hauling time increased from 10 to 20, 40, 60, and 80 minutes, supporting the proposed hypothesis that SSAm increases with an increase in hauling time.
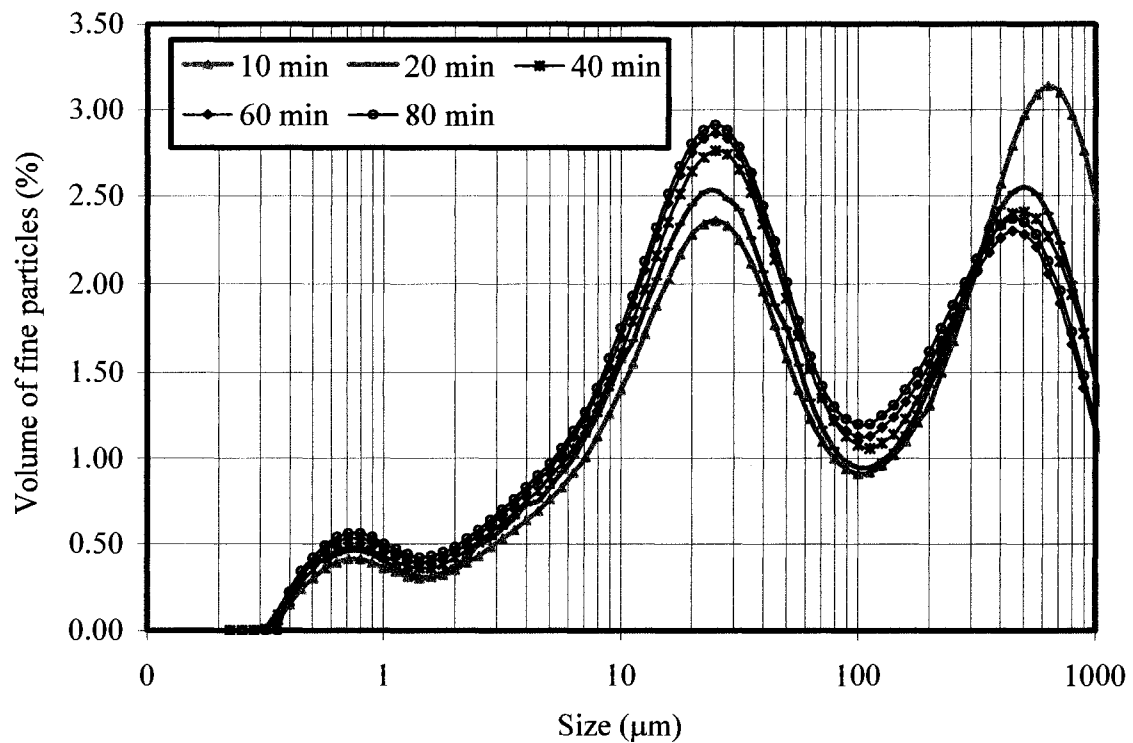
Figure 4.5: Particle size distribution of SCC at different hauling times

The increase in the specific surface area of SCC mortar due to hauling can be attributed to the combined effect of three factors, namely: aggregate grinding, cement particles' grinding, and growth of cement hydrated products.

- *Aggregate grinding*

During the hauling process of concrete further collisions between aggregate particles; as well as between them and the wall and blades of the mixing pan took place. This phenomenon resulted in additional fine particles from the abraded aggregates; and led to an increase in specific surface area of the concrete mortar (*ΔSSAa*). The resulting matrix contributed to an increase in the SCC slump flow loss.

- *Cement particles' grinding*

Similarly to the aggregates, abrasion of the cement particles during the hauling also contributed to the increase in specific surface area of concrete mortar (*ΔSSAc*). The friction between the cement particles as well as between the cement particles and mixing tool disaggregated cement clinker into finer cement particles with higher specific surface areas. During the flocculation system, the finer cement particles bond thicker and stickier necessitating higher repulsive forces (through additional admixture dosages) for their dispersion.

- *Growth of cement hydrated products*

Cements are reactive multimineral powders whose particle's surface grows with time mainly in the presence of water where the surface area of ordinary Portland cement can increase by 2 to 2.5 times[95]. The growth of the cement hydrated product can be attributed to the tricalcium aluminate's (C_3A) final hydrated product and the formation of ettringite compound (calcium aluminate trisulfate, $C_3A \cdot 3C_s \cdot H_{32}$)[16,23,92]. In fact, in the

presence of mixing water, the C_3A compound hydrates very rapidly (during the initial hydration) as it first converts into unstable phases and then into stable calcium aluminate hydrate phase (C_3AH_6) which has a larger surface area than the original C_3A (see equation 1.3). Additionally, in the presence of the dissolved Ca^{2+} and SiO_4^{2-}, the C_3A is converted into ettringite which has also larger specific surface area than other cement hydrated phases such as: gypsum ($CaSO_4$), portlandine (CH), calcium silicate hydrate (CSH), and calcite (stable polymorph of $CaCO_3$)[92]. These progressive growths of cement hydrated products throughout the hauling process ($\Delta SSAc$) contributed to the slump flow loss by affecting the overall specific surface area of the concrete mortar.

4.3.2..2   Adsorption of HRWRA during the hauling of SCC

The mechanism of action of Portland cement-superplasticizer involves adsorption first, and then electrostatic and steric hindrance repulsions. In concrete, the most important parameter in cement-admixture interaction is not the adsorption amount per mass of clinker minerals, but it is the adsorption amount per surface area of hydrated cement paste[90]. Due to the repulsive electrostatic and steric hindrance forces created between cement particles by the adsorbed polycarboxylate molecules on cement particles, the fluidity of the system significantly increases in the presence of the admixture. The amount of admixture molecules adsorbed in cement particles (*Ads*) characterizes the intensity of that fluidity. In the presence of a uniform SSAm, the higher *Ads* is, the higher fluidity becomes.

The direct measure of adsorption is beyond the scope of this investigation. However, in Chapter 3, it was found that the production of higher slump flow matrices required increases in the amount of polycarboxylate-based high range water-reducing

admixture (PC-HRWRA) dosages. In another word, the higher amount of the superplasticizer resulted in a higher rate of adsorption on cement grains which, in turn, provided a more fluid fresh matrix.

The ultraviolet-visible (UV/Vis) spectroscopy was used to determine the cement-water-superplasticizer solution concentration of free admixture, from which correlations between hauling time and the amount of adsorption were made. The experimental program including the testing methodology and procedure are described in Chapter 2, Section 2.3.13, and Chapter 3 Section 3.3.3. The UV/Vis absorbance spectra at the selected hauling times are presented in Appendix IV. As it can be seen from the figures of appendix 4, the liquid phase of the matrices obtained at 10, 20, 40, 60, 80, 100, 140, and 180 minutes of hauling time displayed maximum UV/Vis absorption at wavelength of 264, 253, 314, 320, 310, 323, 295, and 298 nm, respectively. These differences in the absorbance peaks indicate a variation in solutions concentrations from one hauling time to another. For comparison purpose, the wavelength of 320 nm (at which all solutions were absorbed) was chosen. The calculated concentrations do not represent the actual amount of adsorbed HRWRA on cement particles. However, as explained earlier, they provide a good indication of the evolution of HRWRA adsorption at various hauling times. The UV/Vis test results are shown in Figure 4.6. It can be seen that the concentration of free admixture in cement-water solution increased as hauling time increased up to 80 minutes. Beyond that time, gradual decreases were recorded as longer hauling times of 100, 140, and 180 minutes were used. The increase or decrease in admixture concentration led to an increase or decrease in admixture adsorption on cement particle. This finding is in line with the theory of Ads variation with hauling time used to
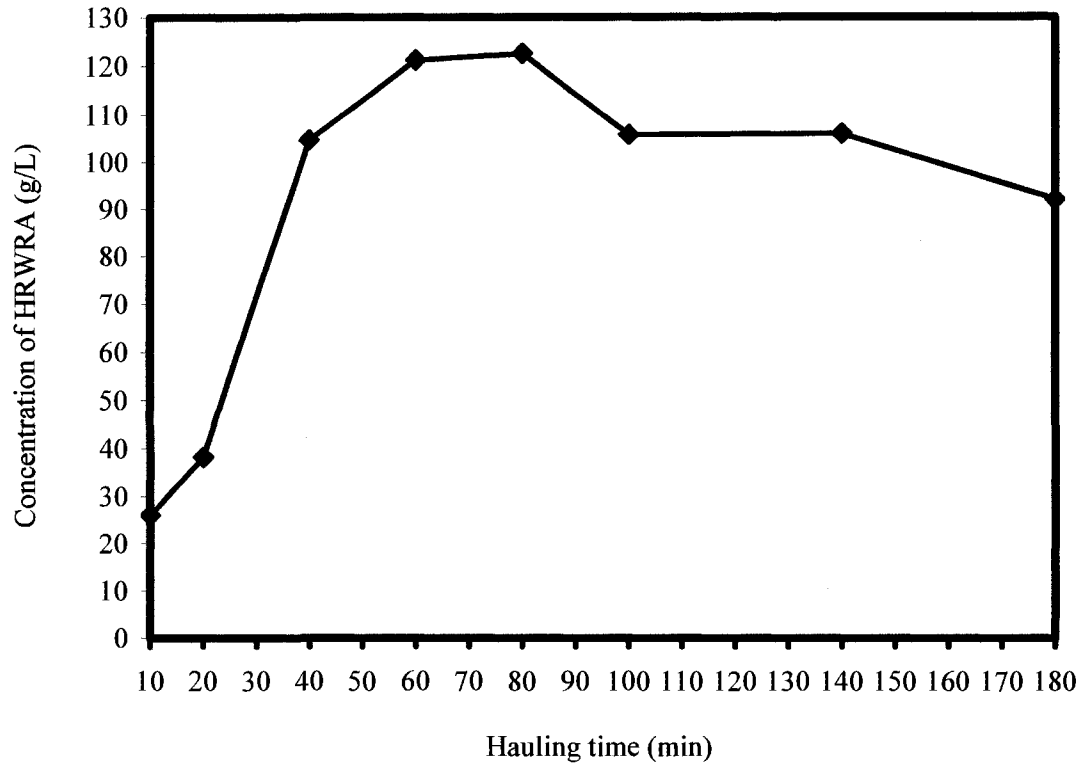
Figure 4.6: Influence of hauling time on adsorption of HRWRA

characterize the fresh performance of self-consolidating concrete through the expression Ads/SSAm in the flow chart of Figure 4.4.

From the beginning of the mixing up to the end of the hauling, not only do the hydrating minerals evolve, but the chemical composition of the solution also changes. During the hydration of Portland cement, the dissolved Ca^{2+} and $H_2SiO_4^{2-}$ ions are hydrolyzed from C_3A and C_3S. These Ca^{2+} ions produce positive charged surface-adsorbed layer around the cement particles. In the presence of a superplasticizer, the hydrophilic end of the molecule chain (i.e. COO^-) is adsorbed to the cement particles, and the admixture adsorption rate is higher during the first few minutes of the hydration reaction. Beyond the rapid initial adsorption (to saturate the most reactive phases), the

admixture uptake by the hydrating cement continues at a reduced rate. Continuing adsorption occurs, mainly due to the growth and abraded product of new hydrated particles. During the induction period of cement hydration, the solution concentration of free admixture decreases, and simultaneously the sulfate ion (SO_4^{2-}) concentration increases with elapsed time. The increase in sulfate ion concentration is due to the solubility product of gypsum. The adsorption of polycarboxylate-based superplasticizer on cement particles by the carboxylic group may be prevented by the competitive adsorption between the sulfate ions and the dissociated carboxylic group on cement particles. The reduction in the adsorption amount of admixture contributed to the loss in fluidity of the trial matrices[16,23,92].

In summary it can be concluded that the fresh performance of SCC, such as: flow ability, flow rate, and dynamic stability can be characterized by *Ads/SSAm*. While both Ads and SSAm increased with hauling time (up to 80 min for the Ads), the contribution of SSAm on the slump flow loss was greater than that of Ads. In fact, the ratio Ads/SSAm decreases with increase in hauling time and can be expressed as follows:

$$\frac{Ads}{SSAm} = \frac{Ads_o + \Delta Ads_{ht}}{SSAm_o + \Delta SSAa + \Delta SSAc} \tag{4.1}$$

The terms *Ads*, *Ads_o*, ΔAds_{ht}, *SSAm* , *SSAm_o*, $\Delta SSAa$, and $\Delta SSAc$ are defined in Figure 4.5.

4.3.3   Predictive statistical equation of hauling time's slump flow loss

Predictive statistical analysis at a 95% confidence level was conducted to determine the slump flow loss due to hauling time. The predictive equation was tested for accuracy using R^2 (the coefficient of multiple determination) and S (average standard

deviation). The slump flow loss can be related to the initial slump flow and the hauling time as follows:

$$SF_{loss} = -273.0366 - 1.7838h_t + 1.2853SF - 0.0049h_t^2 - 0.0013SF^2 + 0.0074h_tSF \quad (4.2)$$

$$\text{Or } SF_{loss} = a + bh_t + cSF + dh_t^2 + eSF^2 + fh_tSF$$

Where:

SF_{loss} = Slump flow loss at the end of the hauling time (mm)

SF = Initial slump flow (mm), with 508 mm $\leq SF \leq$ 711 mm

h_t = Target hauling time (minute), with 10 minutes $\leq h_t \leq$ 90 minutes

The regression equation 4.2 produced R^2 and S values of 98.93% and 6.89 mm (0.27 inch), respectively, indicating a very strong relationship between the dependent variable (slump flow loss) and the independent variables (initial slump flow and hauling time). F and T tests were performed to confirm the significance of coefficients a, b, c, d, e, and f in the regression model. The following results were found: Prob(t) = 0.0446, 0.0067, 0.0054, 0.1248, 0.0010, and 0.0000 for a, b, c, d, e, and f, respectively, and Prob(F) = 0.0000, indicating that both the slump flow value and the hauling time have similar influence on the predictive slump flow loss induced by the hauling process. Table 4.4 represents the actual versus the calculated slump flow losses of the selected self-consolidating concretes. The predictive equations yielded percentage errors ranging for the most part from 1 to 5% confirming a very strong relationship between the actual and the calculated slump flow losses.

4.3.4 Remediation of slump flow loss

A remediation method based on admixture overdosing was adopted to attain the target fresh properties at the completion of each selected hauling time. Tables 4.5, 4.6

198

Table 4.4: Actual versus calculated slump flow loss

Haul time (min)	Target slump flow (mm)	Actual slump flow loss (mm)	Calculated slump flow loss (mm)	% Error
20	524.00	85.85	88.99	-3.66
30	524.00	111.25	107.70	3.19
40	524.00	122.30	125.42	-2.55
50	524.00	136.65	142.16	-4.03
60	524.00	155.70	157.90	-1.41
70	524.00	181.10	172.65	4.66
80	524.00	187.45	186.42	0.55
90	524.00	200.15	199.20	0.47
20	651.00	92.20	79.92	13.32
30	651.00	111.25	108.08	2.85
40	651.00	130.30	135.26	-3.80
50	651.00	155.70	161.45	-3.69
60	651.00	187.45	186.65	0.43
70	651.00	219.20	210.86	3.81
80	651.00	231.90	234.08	-0.94
90	651.00	244.60	256.32	-4.79
20	723.90	50.80	56.03	-10.29
30	723.90	88.90	89.62	-0.81
40	723.90	120.65	122.23	-1.31
50	723.90	152.40	153.84	-0.95
60	723.90	177.80	184.47	-3.75
70	723.90	222.25	214.11	3.66
80	723.90	254.00	242.76	4.42
90	723.90	266.70	270.43	-1.40

1 mm = 0.03937 inch

and 4.7 present the required optimum dosages of admixtures along with the recorded slump flows, T_{50} times, VSI ratings, and J-ring values at different hauling times.

4.3.4.1   HRWRA dosage requirement for the remediation of slump flow loss

Figure 4.7 presents the optimum dosages requirement of HRWRA for the remediation of slump flow loss due to hauling time. Irrespective of the SCC mixtures, the optimum dosage of HRWRA in attaining the required workability increased as the hauling time increased. In comparing to the optimum dosage at the control 10 minutes hauling time, the mixture made for 508 mm (20 inches) of slump flow required 13, 22, 30, 39, 48, 52, 65, and 74% more HRWRA at 20, 30, 40, 50, 60, 70, 80, and 90 minutes hauling times, respectively. The corresponding increases in HRWRA optimum dosages. were 16, 22, 25, 31, 38, 44, 50, and 56 %; and 8, 13, 21, 28, 33, 38, 46, and 51 % for the SCCs prepared for 635 and 711 mm (25 and 28 inches) of slump flow, respectively.

The higher demand for the superplasticizer in contesting the slump flow loss of the selected SCCs, induced by the hauling process, can be explained through Figure 4.4 and Equation (4.1). The idea behind the adopted remediation technique was to find by trial and error an initial admixture dosage in which $(Ads/SSAm)_{ht}$ at the end of hauling time became identical or nearly identical to $(Ads/SSAm)_{10}$ at the control 10 minutes hauling time. The term h_t refers to the hauling at time (t = 20 to 90 minutes). This was achieved by admixture overdosing and is explained through the equations 4.3 and 4.4.

- *At 10 minutes hauling time:*

$$\left(\frac{Ads}{SSAm} \right)_{10} = \frac{Ads_o}{SSAm_o} \tag{4.3}$$

Table 4.5: Admixtures dosages and fresh properties of remediated SCC mixture S7.B.SF20

Hauling time (min)	HRWRA (ml/100 kg)	VMA (ml/100 kg)	Slump Flow (mm)	T_{50} (sec.)	VSI	J-ring value (mm)
10	149.96	0.00	524	3.19	0	28
20	169.52	0.00	521	3.25	0	29
30	182.56	0.00	518	3.48	0	38
40	195.60	0.00	521	3.10	0	22
50	208.64	0.00	519	3.69	0	21
60	221.67	0.00	519	3.79	0	21
70	228.19	0.00	518	3.08	0	29
80	247.75	0.00	514	3.11	0	29
90	260.79	0.00	518	3.00	0	19

1 ml/100 kg = 0.0153 oz/cwt, 1 mm = 0.03937 inch

Table 4.6: Admixtures dosages and fresh properties of remediated SCC mixture S7.B..SF25

Hauling time (min)	HRWRA (ml/100 kg)	VMA (ml/100 kg)	Slump Flow (mm)	T_{50} (sec.)	VSI	J-ring value (mm)
10	209.15	26.14	651	2.70	0	22
20	241.83	26.14	643	2.29	0	33
30	254.90	26.14	641	2.22	0	32
40	261.44	26.14	638	2.33	0	29
50	274.51	26.14	645	2.24	0	19
60	287.58	26.14	638	2.34	0	35
70	300.65	26.14	645	2.30	0	35
80	313.73	26.14	645	2.33	0	35
90	326.80	26.14	641	2.30	0	29

1 ml/100 kg = 0.0153 oz/cwt, 1 mm = 0.03937 inch

Table 4.7: Admixtures dosages and fresh properties of remediated SCC mixture
S7.B.SF28

Hauling time (min)	HRWRA (ml/100 kg)	VMA (ml/100 kg)	Slump Flow (mm)	T_{50} (sec.)	VSI	J-ring value (mm)
10	254.90	32.68	724	1.85	1	32
20	274.51	32.68	718	1.97	1	16
30	287.58	32.68	711	2.03	1	19
40	307.19	32.68	714	2.13	1	14
50	326.80	39.22	718	1.98	1	13
60	339.87	39.22	724	2.02	1	16
70	352.94	45.75	719	1.94	1	8
80	372.55	52.29	718	2.02	1	16
90	385.62	58.82	714	2.13	1	14

1 ml/100 kg = 0.0153 oz/cwt, 1 mm = 0.03937 inch
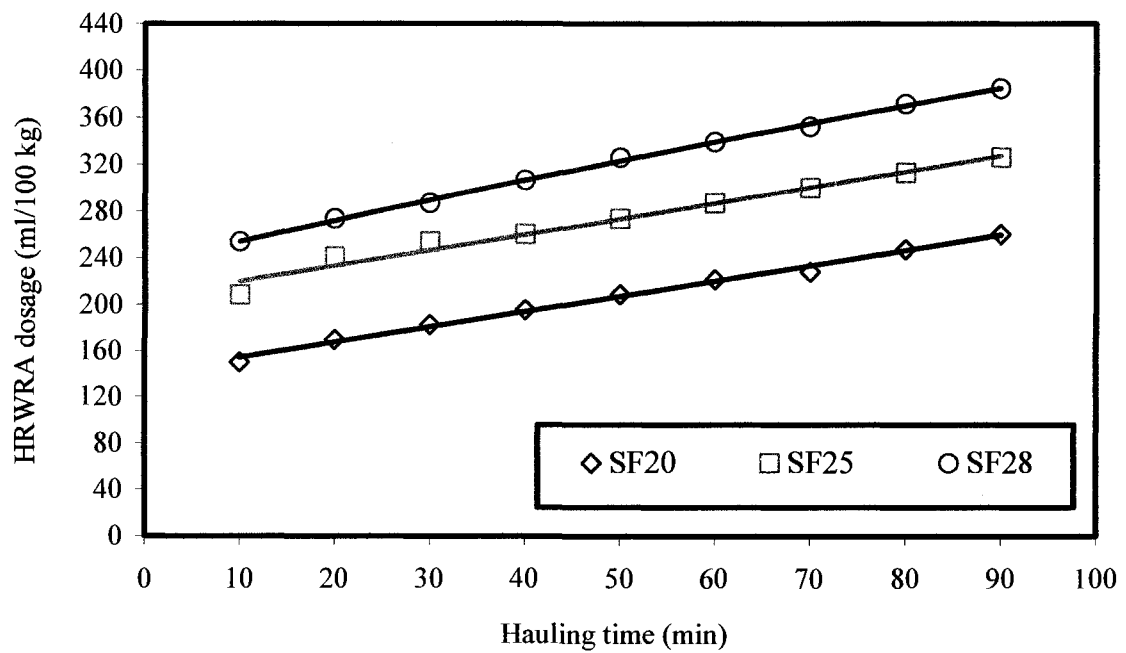
Figure 4.7: Optimum dosage of HRWRA for remediation

of slump flow loss due to hauling time

- *During the remediation, at hauling time h_t:*

$$\left(\frac{Ads}{SSAm}\right)_{ht} = \underbrace{\frac{Ads_o + \Delta Ads_{ht1}}{SSAm_o + \Delta SSAa + \Delta SSAc}}_{\text{A}} + \underbrace{\frac{\Delta Ads_{ht2}}{SSAm_o + \Delta SSAa + \Delta SSAc}}_{\text{B}} \approx \left(\frac{Ads}{SSAm}\right)_{10} \quad (4.4)$$

(A) Characterizes the slump flow loss

(B) Characterizes the slump flow restoration

ΔAds_{ht1} and ΔAds_{ht2} in Equation 4.4 correspond to the increases in adsorption amount of admixture during the hauling time and brought by the additional superplasticizer used for the remediation purpose, respectively. The term "$\Delta SSAa + \Delta SSAc$" reflects the increase in specific surface area of concrete mortar due to the additional fines brought by the grinding of aggregates and cement particles, and the growth of the cement hydrated products. While Ads and SSAm increased with hauling time (up to 80 min for the Ads), the contribution of SSAm on the slump flow loss was greater than that of Ads.

In remediating the slump flow loss, the designed optimum dosages of HRWRA at h_t were sufficient to maintain the solution concentration of free admixture and sulfate ion at the level that produced adequate amount of adsorption to meet the target fluidity at the end of the hauling time h_t. ΔAds_{ht2} generated additional repulsive electrostatic and steric hindrance forces between the cement particles to further disperse the cement agglomerations provoked by the grinding and hydration of cement particles in the course of hauling time.

The rate of HRWRA dosage increment was higher at 20 minutes hauling time (20, 33, and 20 ml/100 kg (0.3, 0.5, and 0.3 oz/cwt) for 508, 635, and 711 mm (20, 25, and 28

inches) slump flows, respectively, and became constant thereafter at about 13 ml/100 kg (0.2 oz/cwt) per 10 minutes hauling time increment, irrespective of the slump flow target. In remediating the slump flow loss, the higher demand of HRWRA during the first 20 minutes hauling time may be attributed to the rapid ettringite formation (during the first 15 minutes of cement hydration). As discussed in section 1.2.2.2, the hydrated phase of ettringite is formed around the C_3A grains and protects them from further rapid hydration during the dormant period. The larger specific surface area of ettringite required higher superplasticizer dosages to restore the SCC fluidity back to its initial level. The decrease in the rate of superplasticizer dosage can be attributed to the availability of a lower amount of C_3A found in Type V Portland cement in producing ettringite compounds at the higher hauling times.

4.3.4.2 VMA dosage requirement for the remediation of workability loss

Figure 4.8 shows the optimum dosages of VMA used to remediate the slump flow loss for different hauling times. Irrespective of the hauling time, self-consolidating concretes prepared with slump flows of 508 and 635 mm (20 and 25 inches) did not require any adjustments in their initial VMA dosage in reaching the target fresh properties. However, the matrices made with 711 mm (28 inches) slump flow required 0, 0, 0, 20, 20, 40, 60, and 80% augmentation at 20, 30, 40, 50, 60, 70, 80, and 90 minutes of hauling times, respectively, when compared to the required optimum dosage of VMA needed for the control hauling time. The results for the mixtures produced with 508 and 635 mm (20 and 25 inches) of slump flows can be explained through the increase in specific surface area of the concrete mortar (*SSAm*) induced by the hauling process as noted earlier. The viscosity modifying admixture is mainly used in SCC to increase its
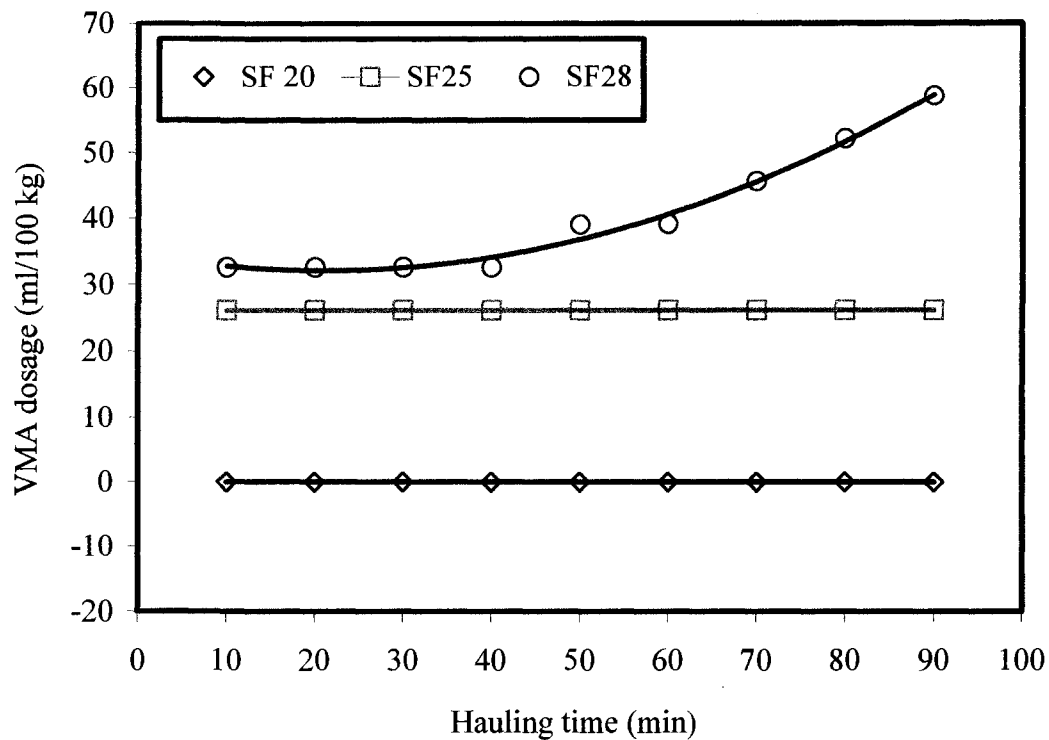
Figure 4.8: Optimum dosage of VMA for remediation of slump loss due to hauling time

viscosity and stability. Despite a higher demand for HRWRA, the increase in *SSAm* during hauling may have been sufficiently effective in enriching and thickening the cement paste, resulting in a higher viscosity (T_{50} time between 2 and 5 seconds) and a higher VSI (0 or 1) of the trial self-consolidating concretes. On the other hand, after 40 minutes of hauling time, the increase in *SSAm* of the mixtures made of 711 mm (28 inches) slump flow may not have been enough to repair the destabilized viscosity and reduced stability generated by a higher dosage requirement of HRWRA. The additional VMA used in these mixtures helped the viscosity and stability by reverting them to their acceptable levels.

4.3.4.3 Fresh properties of remediated self-consolidating concretes

As reported in Tables 4.5, 4.6, and 4.7, the test results showed that independently

of hauling time, all trial self-consolidating concretes were within the target slump flows ±
1.0 inch (25 mm), VSI of 0 (highly stable) or 1 (stable), T_{50} time of 2 to 5 seconds, and J-
ring value of 25 to 50 mm (1 to 2 inches).

In comparing the slump flow values at different hauling times to that measured at
the 10 minutes hauling time, the remediated fresh SCCs displayed an insignificant
difference of less than 2%. All T_{50} times decreased as the slump flow increased, and
within the same group of concrete remained similar to that of the reference hauling time.
No evidence of segregation or bleeding in slump flow was observed in any of the selected
self-consolidating concretes, indicating that a stable matrix condition was achieved
through the adopted overdosing remediation method.

Irrespective of the hauling time, the measured J-ring values of all trial matrices
were within the allowable limit of 25 to 50 mm (1 to 2 inches) indicating a moderate
passing ability or minimal to noticeable blocking of the selected self-consolidating
concretes. As was the case for the unconfined workability and resistance to dynamic
segregation, the overdosing method of remediation was effective in obtaining a passing
ability which was similar to that of the control hauling time (10 minutes).

4.3.4.4   Predictive statistical equations of HRWRA and VMA optimum dosages for
            remediation of slump flow loss due to hauling time

The most suitable predictive relationships between the HRWRA or VMA
optimum dosage, and the slump flow and hauling time of the remediated self-
consolidating concretes were determined at 95% confidence level. The predictive
equations were tested for accuracy using R^2 (regression value) and S (standard deviation).
The relationships are as follows:

$$HR = 0.02081\left(SF^{1.34247}\right)\left(h_t^{0.21595}\right) \tag{4.5}$$

$$\text{Or } HR = a\left(SF^b\right)\left(h_t^c\right)$$

$$VMA = 0.00987\left(SF^{1.46405}\right)\left(h_t^{0.20344}\right) \tag{4.6}$$

$$\text{Or } VMA = a\left(SF^b\right)\left(h_t^c\right)$$

Where:

HR = High range water-reducing admixture required dosage (ml/100 kg)

VMA = Viscosity modifying admixture required dosage (ml/100 kg)

SF = Target slump flow at the end of the hauling time (mm)

Equation 4.5 is valid for 508 mm ≤ SF ≤711 mm ± 25 mm

Equation 4.6 is valid for 635 mm ≤ SF ≤711 mm ± 25 mm

h_t = Target hauling time (min), with 10 minutes ≤ h_t ≤ 90 minutes

The regression equations 4.5 and 4.6 produced R^2 and S values of 98.06% and 8.88 ml/100 kg (0.14 oz/cwt); and 97.51 and 7.87 ml/100 kg (0.12 oz/cwt), respectively The calculated values are indicative of a strong relationship between the dependent variable (HRWRA or VMA dosage) and the independent variables (slump flow and hauling time). F and T tests were performed to confirm the significance of coefficients a, b, and c in the regression model. The following results were found:

- Equation 4.5: Prob(t) = 0.0069, 0.0000, and 0.0000 for a, b, and c, respectively; and Prob(F) = 0.

- Equation 4.6: Prob(t) = 0.1945, 0.0000, and 0.0000 for a, b, and c, respectively; and Prob(F) = 0.

These values indicate that both slump flow and hauling time have similar influence on predicting the required admixture dosages. The actual and calculated required HRWRA and VMA dosages are shown in Tables 4.8 and 4.9, respectively. As can be seen, the predictive equations yielded percentage errors ranging for the most part from 1 to 5% confirming a strong relationship between the dependent and independent variables of equations 4.5 and 4.6.

Table 4.8: Actual versus calculated VMA dosage for slump flow remediation

Target slump flow (mm)	Haul time (min)	Actual VMA* dosage (ml/100 kg)	Calculated VMA* dosage (ml/100 kg)	% Error
642.94	20	241.83	234.54	3.02
641.35	30	254.90	253.78	0.44
638.18	40	261.44	267.13	-2.18
644.53	50	274.51	283.62	-3.32
638.18	60	287.58	290.10	-0.88
644.53	70	300.65	303.72	-1.02
644.53	80	313.73	312.08	0.53
641.35	90	326.80	317.34	2.89
723.90	10	254.90	242.31	4.94
717.55	20	274.51	275.43	-0.34
711.20	30	287.58	295.25	-2.67
714.38	40	307.19	315.10	-2.57
717.55	50	326.80	331.88	-1.55
723.90	60	339.87	348.89	-2.65
718.82	70	352.94	356.31	-0.96
717.55	80	372.55	365.18	1.98
714.38	90	385.62	371.62	3.63

* Viscosity modifying admixture

1 mm = 0.03937 inch; 1 ml/ 100 kg = 0.0153 oz/cwt

Table 4.9: Actual versus calculated HRWRA dosage for slump flow remediation

Target slump flow (mm)	Haul time (min)	Actual HRWRA* dosage (ml/100 kg)	Calculated HRWRA* dosage (ml/100 kg)	% Error
524.00	10	150.33	153.08	-1.83
520.70	20	169.93	176.29	-3.74
517.53	30	183.01	190.85	-4.29
520.70	40	196.08	204.76	-4.43
519.18	50	209.15	214.02	-2.33
519.43	60	222.22	222.76	-0.24
517.53	70	228.76	229.17	-0.18
514.35	80	248.37	233.93	5.81
517.53	90	261.44	241.95	7.45
651.00	10	209.15	204.85	2.06
642.94	20	241.83	233.98	3.25
641.35	30	254.90	254.54	0.14
638.18	40	261.44	269.06	-2.92
644.53	50	274.51	286.12	-4.23
638.18	60	287.58	293.69	-2.12
644.53	70	300.65	307.69	-2.34
644.53	80	313.73	316.69	-0.94
641.35	90	326.80	322.70	1.25
723.90	10	254.90	236.22	7.33
717.55	20	274.51	271.14	1.23
711.20	30	287.58	292.44	-1.69
714.38	40	307.19	313.05	-1.91
717.55	50	326.80	330.47	-1.12
723.90	60	339.87	347.83	-2.34
718.82	70	352.94	356.22	-0.93
717.55	80	372.55	365.77	1.82
714.38	90	385.62	372.97	3.28

* High range water reducing admixture

1 mm = 0.03937 inch; 1 ml/ 100 kg = 0.0153 oz/cwt

4.4   Conclusions

The results of this section of the investigation revealed the following conclusions:

a)   The fresh performance of self-consolidating concrete was affected by hauling time. The effects were manifested in the form of loss in flow ability, and gain in plastic viscosity and dynamic stability.

b)   The change in fresh properties can be characterized by the adsorption amount of admixture per specific surface area of concrete mortar Ads/SSAm. The increase in hauling time increased both Ads and SSAm. The contribution of SSAm on the slump flow loss was greater than that of Ads.

Increases in specific surface area of concrete mortar (SSAm) were due to the grinding of aggregates and cement particles, and the growth of the cement hydrated products. This hypothesis was supported by the test results from a laser diffraction particle size analysis. The analysis performed on representative samples of freshly-mixed SCC, showed that the volume of fine particles ranging from 1 to 250 μm (39×10^{-6} to 9843×10^{-6} inch) increased as the hauling time increased from 10 to 20, 40, 60, and 80 minutes.

Since an actual measurement of adsorption was beyond the scope of this investigation, an indirect method of evaluation was used. The UV/Vis spectroscopy test was utilized to determine the concentration of free admixture in cement-water-superplasticizer solution at different hauling times. Afterward, the results were used to find the level of admixture adsorption on cement particles as function of hauling time. It is well established that the production of a higher slump flow matrices required increases in the amount of polycarboxylate-based high range water-reducing admixture (PC-

HRWRA) dosages (see Chapter 3, Section 3.3.1). The test result of the UV/Vis spectroscopy test indicated that the solution concentration of free admixture increased up to 80 minutes. The increase in the admixture concentration led to an increase in the admixture adsorption on cement particles. During the 10 to 80 minutes intervals the admixture adsorption rate was higher during the first few minutes of the hydration reaction. Beyond the rapid initial adsorption (to saturate the most reactive phases), the admixture uptake by the hydrating cement continued at a reduced rate. The continuation of adsorption occurred mainly due to the growth and abraded product of new hydrated particles. Past 80 minutes of hauling time, the solution concentration of free admixture decreased, and simultaneously the sulfate ion (SO_4^{2-}) concentration increased with elapsed time, as was the case during the induction period of cement hydration. The adsorption of PC-HRWRA on cement may have been prevented by the competitive adsorption between the sulfate ions and the dissociated carboxylic group on cement particles.

c) Regardless of the slump flow value, the losses in slump flow due to hauling time were observed as early as 20 minutes, and increased with increasing hauling time. For the selected self-consolidating concretes made with slump flow of 508, 635, and 711 mm (20, 25, and 28 inches), the T_{50} could not be measured after 20, 40, and 60 minutes of hauling time, respectively, due to the severe loss in slump flow.

d) A remediation technique consisting of admixture overdosing was able to produce SCCs with a similar flow ability, plastic viscosity, dynamic stability, and passing ability to those obtained at the control hauling time. The rate of HRWRA dosage increment was higher at 20 minutes hauling time (20, 33, and 20 ml/100 kg (0.3, 0.5, and 0.3 oz/cwt) for

211

508, 635, and 711 mm (20, 25, and 28 inches) slump flows, respectively) and became constant thereafter at about 13 ml/100 kg (0.2 oz/cwt) per 10 minutes hauling time increment, independently of the slump flow. The additional amount of admixtures increased admixture adsorption and generated supplementary repulsive electrostatic and steric hindrance forces between cement particles. These forces further dispersed cement agglomerations provoked by the grinding and hydration of the cement constituents during hauling time.

e) The predictive equations to correlate: (1) the slump flow loss with the initial slump flow value and hauling time, and (2) the required amount of overdosed admixtures (HRWRA and VMA) with the target slump flow and hauling time showed significant statistical relationships between the dependent and independent variables.

CHAPTER 5

INFLUENCE OF EXTREME TEMPERATURES ON FRESH PERFORMANCE

OF SELF CONSOLIDATING CONCRETE

The goal of the Chapter 5 is to study the influence of extreme temperatures on the

fresh performance of self-consolidating concrete. Seven different temperatures, namely:

43, 36, 28, 21, 14, 7, and -0.5 °C (109, 96, 83, 70, 57, 44, and 31 °F) to simulate hot and

cold temperatures were used to evaluate the unconfined workability, the rate of flow

ability or viscosity per inference, and the dynamic stability of the trial matrices.

Additionally, the overdosing approach (sufficient initial optimum admixture dosage) was

used to remediate the adverse influence of hot and cold temperatures on the fresh

performance of the selected self-consolidating concretes.

5.1   Background on concrete in extreme temperatures

During the last half of the twenty century, the world climate has been unusual and

unnatural due to a phenomenon called global warming. Warmer, colder, drier and wetter

climate than the climatic average have been recorded all over the world. Scientific

literatures and popular media have extensively reported the cause and consequence of the

global warming.

The operation of the concrete industry is not immune from the adverse effect of

extreme climatic conditions. Particularly, mixture proportioning, mixing, transporting,

placing, and curing are all negatively impacted. The hot or cold weather can adversely

213

affect the fresh and hardened properties of concrete by accelerating or retarding the rate of moisture loss and the rate of cement hydration.

5.1.1   Hot concrete temperature

Hot concrete temperature is mainly caused by hot weather or mass concreting. ACI Committee 305[96] defines hot weather as any combination of high air temperature, low relative humidity, and high wind velocity tending to impair the quality of fresh and hardened concrete or otherwise resulting in abnormal properties.   The Standard Specification for Ready Mixed Concrete, ASTM C 94[85], reports that some difficulties may be encountered when concrete temperatures approach 32 °C (90 °F). Admissible hot concrete should have a temperature between 29 °C to 32 °C (85 °F to 90 °F) in the time of its placement[9].

The hot weather condition is transferred to the concrete through the concrete ingredients. High temperature of fresh concrete than normal results in a fast hydration of cement leading to an accelerated rate of setting and a lower long term strength and hardened properties. If the high temperature is accompanied by a low relative humidity, rapid evaporation of some mixing water takes place, causing loss of workability[10,11,78]. Other problems which can be induced by high concrete temperature are the tendency to plastic shrinkage, the potential for thermal cracking, and difficulty in controlling entrained-air.   High temperature is also detrimental when placing large volume concrete[10,11,78]. During mass concreting, for instance in gravity dam, the hot concrete temperature is associated with possible cracking due to restraint to contraction on cooling from temperature rise provoked by the heat of hydration of cement[78].

Precaution can be taken in remediation to hot weather concreting. Starting with a

higher initial slump than needed, or retempering the fresh concrete by adding water at the job site is frequently used to restore the loss of workability induced by the hot temperature. However, the extra water in concrete mixture may cause adverse effects in its hardened properties. The development and increase use of plasticizers and superplasticizers admixtures can make them a best overdosing or retempering material in hot weather condition at job site instead of water. Supplementary cementitious materials such as fly ash and ground granulated blast furnace slag are often used in hot concreting to slow down the rate of setting as well as the rate of slump loss[10]. Injection of liquid nitrogen into the mixer is performed if a greater temperature reduction is required. Liquid nitrogen can be added directly into a central mixer drum or the drum of a truck mixer to lower concrete temperature. It does not in itself influence the amount of mix water requirement[10]. Lowering the temperature of the concrete ingredients is also used to combat the undesirable effects of hot concreting[10,11,78]. The contribution of each ingredient in the freshly matrix temperature is related to the temperature, specific heat, and quantity of each material. Among all concrete material, water is the easiest to cool. Cooling the mix water temperature by 2.0 °C (3.5 °F to 4 °F) will usually lower the concrete temperature by about 0.5 °C (1 °F). Mixing water can be cooled by refrigeration, liquid nitrogen, or ice. Aggregates temperatures have more pronounced effect on the concrete temperature since they represent 70 to 85% of the total mass of concrete. In order to lower the temperature of concrete by 0.5 °C (1 °F), it is necessary to reduce the aggregate temperature by only 0.8 °C to 1.1 °C (1.5 °F to 2 °F). Aggregates can be cooled by shading the stockpile or keeping them moist by sprinkling. Refrigeration, circulation of cooled air through the storage bin can also be used to lower

the aggregate temperature. Cement temperature has only a minor effect on the temperature of the freshly mixed concrete because of cement's low specific heat and the relatively small amount of cement in a concrete mixture. A cement temperature change of 5 °C (9 °F) generally will change the fresh concrete temperature by only 0.5 °C (1 °F)[10]. Retarding admixtures may also be beneficial in delaying the setting time.

5.1.2 Cold concrete temperature

Cold concrete temperature is usually caused by cold weather. ACI Committee 306[97] defines cold weather as a period when for more than 3 successive days the average daily air temperature drops below 5 °C (40 °F) and stays below 10 °C (50 °F) for more than one-half of any 24-hour period. Cold temperature affects the rate of cement hydration by retarding the setting, hardening and strength gain of concrete. As the temperature of concrete decreases, the rate of setting and hardening, and the development of strength decrease progressively until the freezing point is reached[10,11,78]. If concrete is frozen and remains frozen at -10 °C (14 °F) it will gain strength slowly. Below that point the cement hydration and concrete setting and hardening process cease[10]. When the temperature rises again, thawing takes place and the setting and hardening resume. Ultimate compressive strength reduction of up to 50% can occur if concrete is frozen within a few hours after placement or before it attains a compressive strength of 3.5 MPa (500 psi)[10].

In order to alleviate or eliminate the adverse effect of cold temperature on concrete, the water and the aggregates can be heated or a heater can be applied in the mixer. The simplest and cheapest method consists of heating water, and water can hold five times the amount of heat held by aggregate or cement[11]. Water heated to 50 °C (122

216

°F) can produce a temperature of 61 °F (16 °C) in the resulting concretes even when the cement and aggregates have an initial temperature of only -15 °C (4 °F). The approximate temperature of concrete can be calculated from the following equation[9]:

$$T = \frac{0.22(T_a M_a + T_c M_c) + T_w M_w + T_{wa} M_{wa}}{0.22(M_a + M_c) + M_w + M_{wa}}$$ (5.1)

Where,

T = temperature of the freshly mixed concrete, °C (°F)

T_a, T_c, T_w, and T_{wa} = temperature in °C (°F) of aggregates, cements, added mixing water, and free water on aggregates, respectively.

M_a, M_c, M_w, and M_{wa}= mass, kg (lb), of aggregates, cementing material, added mixing water, and free water on aggregates, respectively.

The use of ASTM C 150[13] Type III cement (high-early strength cement), additional cement content and chemical accelerators constitute also an alternative to increase the rate of initial hydration and, consequently produce high early-strength concrete. The increase in cost induced by high early-strength concrete can be tolerated in high-value added applications, especially when cost savings can be realized from the earlier reuse of forms and shore, earlier setting times that allows the finishing, and earlier use of structure[10].

The use of air entrainment admixture is strongly recommended in cold temperature concreting. The incorporation of suitable entrained air will help prevent strength loss and internal as well as surface damage resulting from the concrete freezing and thawing.

5.2   Experimental programs

Similarly to the Chapter 4, the self-consolidating concrete mixtures S7.B.SF20,

S7.B.SF25 and S7.B.SF28 were used in the study of Chapter 5. Their mixture constituents and proportions are presented in Chapter 3, Table 3.1.c. Laboratory trial mixtures were used to produce the required self-consolidating concretes. An electric counter-current pan mixer with a capacity of 0.028 m^3 (1 ft^3) was used to blend concrete components. An environmental chamber to simulate hot or cold temperature conditions was built around the mixing apparatus. The walls, roof and floor of the room were made with plywood and insulated with polystyrene foam to maintain a uniform temperature throughout the experiments. The hot temperatures were generated by a heater while a cooling unit was used to produce the cold temperatures. A temperature regulator, which was connected to the heating and cooling units and assisted by multiple probes, maintained the target temperature within ±2 °C (3 °F) margins. A separate control unit also monitored and recorded the relative humidity of the environmental chamber. Figure 5.1 shows the actual environmental chamber.

The concrete's dry ingredients (i.e., aggregate, cement and fly ash) were prepared as reported in Chapter 2, Section 2.1. Prior to the actual mixing, they were stored in the environmental chamber, as shown in Figure 5.1, for 24 hours or until they reached the target temperature. The effect of the mixing water temperature on the fresh performance of the selected matrices was not part of this study. Thus, the mixing water was kept at a constant temperature of 21 ± 2 °C (70 ± 3 °F) to avoid any interference with the rate of cement hydration. The HRWRA and the VMA were also kept at the normal laboratory conditions as recommended by the manufacturer. Table 5.1 presents the materials' temperatures and the chamber's environmental conditions at the time of mixing.

The mixing sequence was identical to that reported in Chapter 3, Section 3.1.
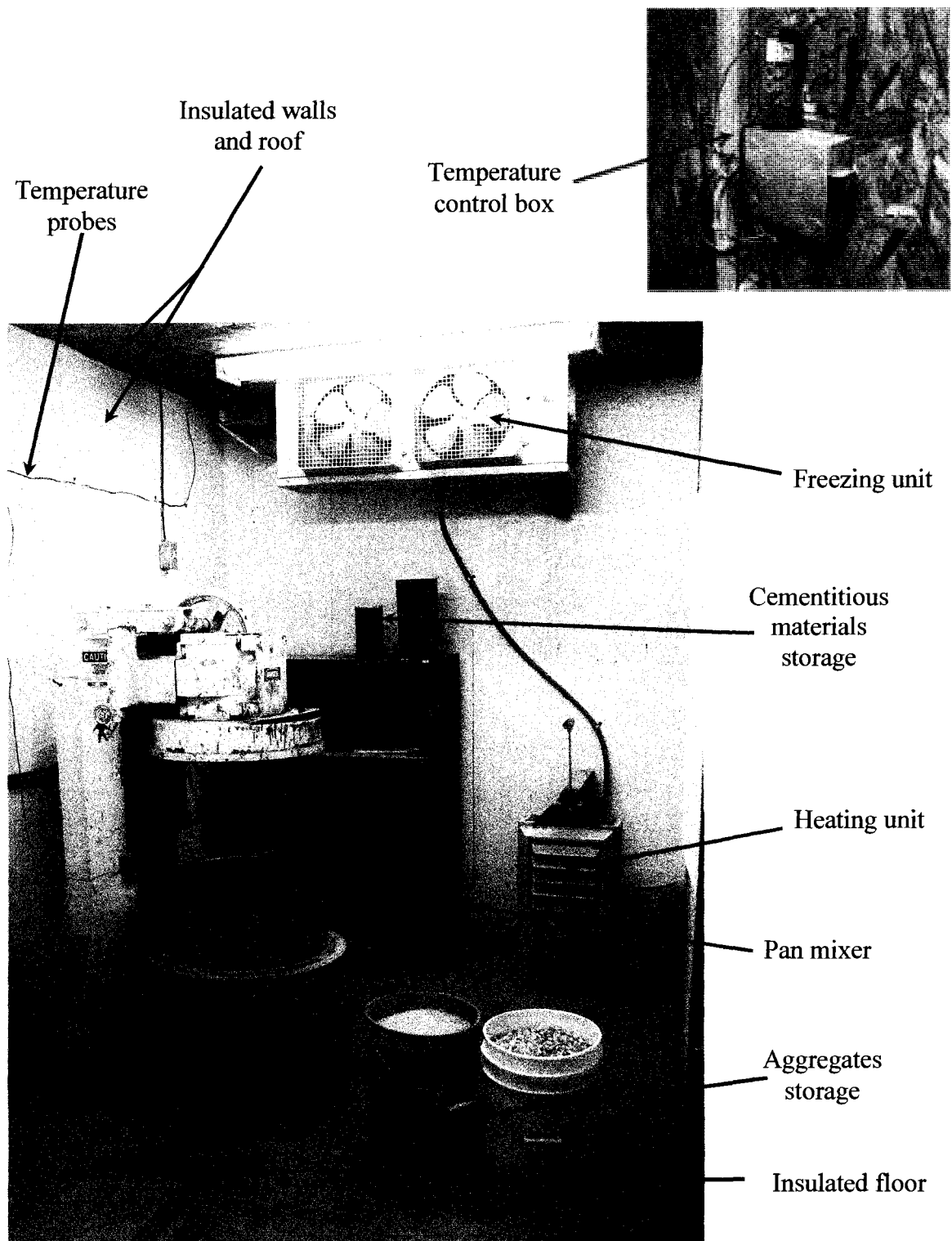
Figure 5.1: Environmental room and equipments

Table 5.1: Materials and mixing room environmental conditions

Mix No.	Target temp. (°C)	Coarse aggr. (°C)	Fine aggr. (°C)	Cement & fly ash (°C)	Water (°C)	Admixtures (°C)	Air temp. (°C)	Relative humidity (%)
S7.B.SF20		44.14	42.11	44.67	20.89	21.94	43.86	
S7.B.SF25	43.00	43.33	42.39	44.17	21.22	21.88	43.83	18.00
S7.B.SF28		43.50	42.00	44.67	21.00	22.72	43.72	
S7.B.SF20		35.33	35.56	37.22	21.22	21.14	37.00	
S7.B.SF25	36.00	35.61	35.83	36.89	21.22	21.28	36.72	19.00
S7.B.SF28		36.47	35.94	37.11	21.28	21.22	36.69	
S7.B.SF20		29.11	28.67	29.44	21.22	20.56	30.00	
S7.B.SF25	28.00	29.31	29.67	29.61	21.17	21.06	29.33	20.00
S7.B.SF28		28.31	29.36	29.61	21.22	21.22	29.72	
S7.B.SF20		21.89	21.83	21.33	21.11	21.78	21.33	
S7.B.SF25	21.00	27.11	21.67	21.44	21.00	21.67	21.44	26.00
S7.B.SF28		21.78	21.56	21.67	20.83	21.78	21.39	
S7.B.SF20		14.72	14.72	14.78	21.06	21.11	14.22	
S7.B.SF25	14.00	14.22	14.33	13.94	21.17	21.11	13.78	45.00
S7.B.SF28		14.11	14.33	13.78	21.22	20.56	13.72	
S7.B.SF20		7.22	7.06	6.72	21.11	20.00	7.11	
S7.B.SF25	7.00	7.50	7.44	6.83	21.22	20.56	7.33	54.00
S7.B.SF28		7.22	7.22	6.89	20.89	20.28	7.06	
S7.B.SF20		-0.22	-0.64	-0.47	21.22	20.56	-0.50	
S7.B.SF25	-0.50	0.33	0.00	-0.44	21.11	20.28	-0.89	70.00
S7.B.SF28		0.17	0.19	-0.03	21.17	20.00	-0.78	

°C = 5/9(°F-32)

Immediately upon completion of the mixing, the fresh self-consolidating concretes were evaluated for the unconfined workability (measured by the slump flow), the flow rate or viscosity by inference (evaluated by T_{50} time), the dynamic segregation resistance (evaluated by VSI), and J-ring passing ability in accordance with the ASTM C 1611[55], and C 1621[58].

In the present study, laboratory conditions characterized by a temperature of 21 ± 2 °C (70 ± 3 °F) and a relative humidity of 25 ± 5%, was used as the control condition. The selected hot temperatures were 43, 36, and 28 °C (109, 96, and 83 °F) while the cold temperatures were characterized by 14, 7, and -0.5 °C (57, 44, and 31 °F). The relatives humidity reported in Table 5.1 were generated by heating or cooling of the environmental chamber. The impact of hot and cold temperatures on the performance of the selected self-consolidating concretes as related to the unconfined workability, flow rate, and dynamic stability is discussed below.

5.3   Discussion of results

5.3.1   Influence of hot temperature on fresh performance of SCC

Table 5.2 presents the fresh properties; namely: slump flows, T_{50}, and VSI of the trial self-consolidating concretes at the selected hot temperatures. Figure 5.2 displays the slump flow losses caused by the elevated temperature. In general, the hot temperature adversely affected the unconfined workability in the form of slump flow loss. In comparing to the control slump flow, the selected self-consolidating concretes displayed average slump flow losses of about 25, 12, and 5% at 43, 36, and 28 °C (109, 96, and 83 °F), respectively. As it can be seen from Figure 5.2, the losses were small at the lower hot temperatures and increased progressively as the temperature moved toward the

Table 5.2: Fresh properties of SCCs at various hot and cold temperatures

Mix No.	Target temp. (^{o}C)	Matrix temp. (^{o}C)	Measured slump flow (mm)	T_{50} (sec.)	VSI	Slump flow loss (mm)
S7.B.SF20		41.22	391	-	0	-133
S7.B.SF25	43.00	41.19	480	-	0	-171
S7.B.SF28		41.28	540	2.82	0	-184
S7.B.SF20		34.72	457	-	0	-67
S7.B.SF25	36.00	34.56	572	2.98	0	-80
S7.B.SF28		34.56	635	2.74	0	-89
S7.B.SF20		26.61	495	-	0	-29
S7.B.SF25	28.00	26.78	616	2.83	0	-35
S7.B.SF28		27.00	681	2.59	0	-42
S7.B.SF20		21.89	524	3.19	0	0
S7.B.SF25	21*	22.00	651	2.79	0	0
S7.B.SF28		22.17	724	1.85	1	0
S7.B.SF20		18.56	548	2.95	0	24
S7.B.SF25	14.00	19.11	673	2.51	0	22
S7.B.SF28		18.50	746	1.80	1	22
S7.B.SF20		13.33	546	2.90	0	22
S7.B.SF25	7.00	13.44	670	2.49	0	19
S7.B.SF28		13.33	743	1.81	1	19
S7.B.SF20		7.78	543	3.00	0	19
S7.B.SF25	-0.50	7.50	673	2.50	0	22
S7.B.SF28		7.89	743	1.80	1	19

^{o}C = 5/9(^{o}F-32), 1 mm = 0.03937 in.

*Reference temperature

222
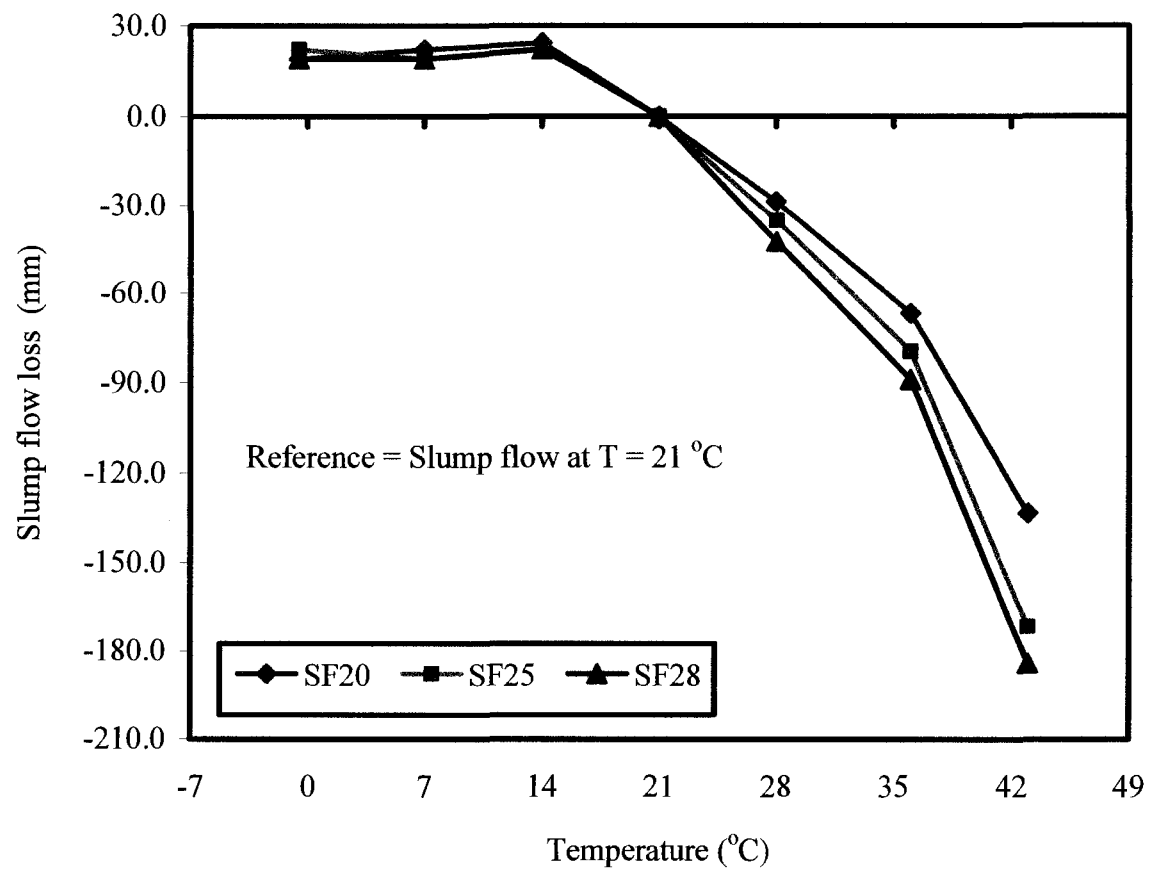
Figure 5.2: Influence of hot and cold temperatures on slump flow of SCC

elevated ones.

The T_{50} time was used to determine the flow rate or plastic viscosity per inference of the self-consolidating concretes. Overall, regardless of the slump flow, all selected hot temperatures adversely influenced the flow rate of the trial matrices by increasing the T_{50} times. The increases in T_{50} times were indicative of gains in plastic viscosity (by inference), or decrease in flow rate. The flow rate further increased as the temperature increased. The T_{50} times of the mixtures made for 508 mm (20 inches) slump flow could not be measured in any of the selected hot temperatures since their flow spreads were below the established limit of 508 mm (20 inches). At the temperatures of 36 and 28 °C (96 and 83 °F), the mixtures made for 635 mm (25 inches) slump flow displayed relatively small increases in T_{50} time of about 1 and 1%, respectively, when compared to that of the control temperature. The same concrete ceased to be self-consolidating at 43 °C (109 °F) and its T_{50} could not be measured. For the mixture prepared for the slump flow of 711 mm (28 inches), significant increases in flow rate were induced by hot temperatures. In comparing to the control temperature, the augmentations in flow rate were 52, 48 and 40% at 43, 36, and 28 °C (109, 96, and 83 °F), respectively.

The influence of elevated temperatures on dynamic stability of the selected self-consolidating concretes was also evaluated. As shown in Table 5.2, the effect of hot temperatures on the dynamic stability of the selected SCCs was manifested by an improvement in the visual stability index (VSI), from 1 (stable matrix) to 0 (highly stable matrix) for the mixtures made with 711 mm (28 inches) slump flow. The others two SCC types (slump flows of 508 and 635 mm (20 and 25 inches)) remained highly stable at the selected elevated temperatures.

5.3.2 Influence of cold temperature on fresh performance of SCC

Table 5.2 and Figure 5.2 also document the effect of cold temperatures on the fresh performance of self-consolidating concrete. In general, cold temperatures marginally increased the unconfined workability, slightly reduced the flow rate (increased the plastic viscosity by inference), and barely affected the dynamic stability of freshly-mixed self-consolidating concretes. In comparing to the control temperature, the self-consolidating concretes exposed to the selected cold temperatures experienced less than 1 inch (25 mm) gain in slump flow. The decreases in T_{50} times were on average less than 30 seconds; while the dynamic stabilities remained highly stable for the 508 and 635 mm (20 and 25 inches) SCCs, and stable for the 711 mm (28 inches) matrices.

5.3.3 Mechanism of slump flow loss and gain in hot and cold temperatures

The slump flow loss and gain induced by the hot and cold temperatures, respectively, may be explained through the adsorption amount of admixture per specific surface area of concrete paste (Ads/SSAp), the change in the aggregates' moisture content, and the partial evaporation of mixing water (in the case of elevated temperatures). The flow chart of Figure 5.3 documents the mechanism of slump flow loss and gain in extreme temperatures.

There are general consensuses that increase in concrete temperature leads to an increase in the amount of cement hydrated products (SSAp) mainly at early ages[98,99]. However, there is no extensive literature regarding the adsorption behavior of polycarboxylate-based high range water-reducing admixture in hot temperatures. Burg[100] and Klieger[101] found that, in ordinary concrete, a slump loss of 20 to 25 mm (0.8 to 1 inch) was observed for each 11 °C (20 °F) temperature increase. Nawa[99] reported that the

$$\frac{Ads_o + \Delta Ads_{hot}}{SSAp_o + \Delta SSAp_{hot}} + (w_o + \nabla w_{hot})$$

$$\frac{Ads_o}{SSAp_o} + (w_o)$$

$$\frac{Ads_o - \Delta Ads_{cold}}{SSAp_o} + (w_o + \Delta w_{cold})$$

LEGEND

Ads_o = Adsorptions at control temperature

∇Ads_{hot} and ΔAds_{cold}= Change in Ads_o at hot and cold temperatures, respectively

$SSAp_o$ = Specific surface area of concrete paste at control temperature

$\Delta SSAp_{hot}$ = Increase in $SSAp_o$ due to hot temperature

w_o = Water contribution to the initial fluidity of the concrete at control temperature

∇w_{hot} = Decrease in w_o due to low relative humidity and hot temperature

Δw_{cold} = Increase in w_o due to high relative humidity and cold temperature

SF_o = Slump flow at control temperature

ΔSF = Change in SF

RH = Relative humidity

Figure 5.3: Mechanism of slump flow loss and gain in hot and cold temperatures

226

superplasticizer adsorption (Ads) on cement particle increased as the fresh concrete temperature increased. Flatt[31] et al. investigated the effect of temperature on the adsorption of Polycarboxylic-Ester (PCE) and Polycarboxylic Acid-polymers (PCA). The model powders used in the study was dead burnt MgO and $Mg(OH)_2$ which are chemically similar to $Ca(OH)_2$ and CaO, respectively. They found that in MgO at the pH of 12, the PCE adsorption plateau concentrations increased significantly with temperature, while with the PCA no effect was found. Moreover, in the $Mg(OH)_2$ medium, at a pH level of 11.3, the adsorption of polycarboxylic acid-polymers remained unaffected by the elevated temperature.

In the current literature, to our best knowledge, there is no investigation on the effect of cold temperature on the fresh performance of self-consolidating concrete. The existing literature in cold weather concreting mostly deals with the strength loss and freeze-thaw. Burg[100] reported that concrete made with the cement containing 5% of C_3A displayed over 100% slump increase when the temperature decreases from 23 to 10 °C (73 to 50 °F) indicating that the vibratory-placed slump concrete can gain slump with the increase in cold temperature.

In short, it appears that additional studies on the adsorption of admixture on cement particles are warranted in order to determine the extent to which the ratio Ads/SSAp can affect the fluidity of self-consolidating concrete in a hot temperature condition.

5.3.3.1   Influence of extreme temperatures on adsorption of PC-based HRWRA

In an attempt to investigate the evolution of the adsorption amount of the selected polycarboxylate-based high range water-reducing admixtures (PC-based HRWRA) in

water-cement solution at the selected temperatures, the ultraviolet-visible (UV/Vis) spectroscopy test was used. Detailed descriptions of the UV/Vis spectroscopy test are presented in Chapter 2, Section 2.3.13, and Chapter 3 Section 3.3.3.

The UV/Vis absorbance spectra of the matrices at the selected temperatures are summarized in Appendix V. The recorded spectra indicate that the maximum UV/Vis absorption wavelengths increased from 236 to 245, 262, 265, 271, and 292 nm when the temperatures increased from -0.5 to 7, 14, 21, 28, and 36 °C (31 to 44, 57, 70, 83, and 96 °F), respectively. Beyond that point, gradual drops of wavelength at 241 and then 237 nm were recorded as the temperature was increased to 43 and then 50 °C (109 and then 122 °F), respectively. For comparison purpose, the wavelength of 265 nm of the solution at the control temperature (21 °C (70 °F)) was selected, and the solution concentration of free admixture interpolated using the calibration curve at the selected wavelength of 265 nm (see Chapter 3, Section 3.3.3 and Appendix 5).

It can be seen from Figure 5.4 that the PC-based HRWRA free concentration in cement-water system was affected by a change in material or solution temperatures. While the concentration remained fairly uniform at temperatures ranging from 14 to 36 °C (57 to 96 °F), it decreased as the temperature moved toward the extreme cold and hot temperatures. It should be noted that the calculated concentrations do not represent the actual amounts of adsorbed HRWRA on cement particles. However, their increases in Portland cement-water solution leads to an augmentation of the adsorbed amount of admixture' molecules on cement grains, favoring further electrostatic repulsion and steric hindrance effects. This finding confirms the theory presented through the flow chart of Figure 5.2 to explain the mechanism of slump flow loss or gain in hot or cold

temperature, respectively.
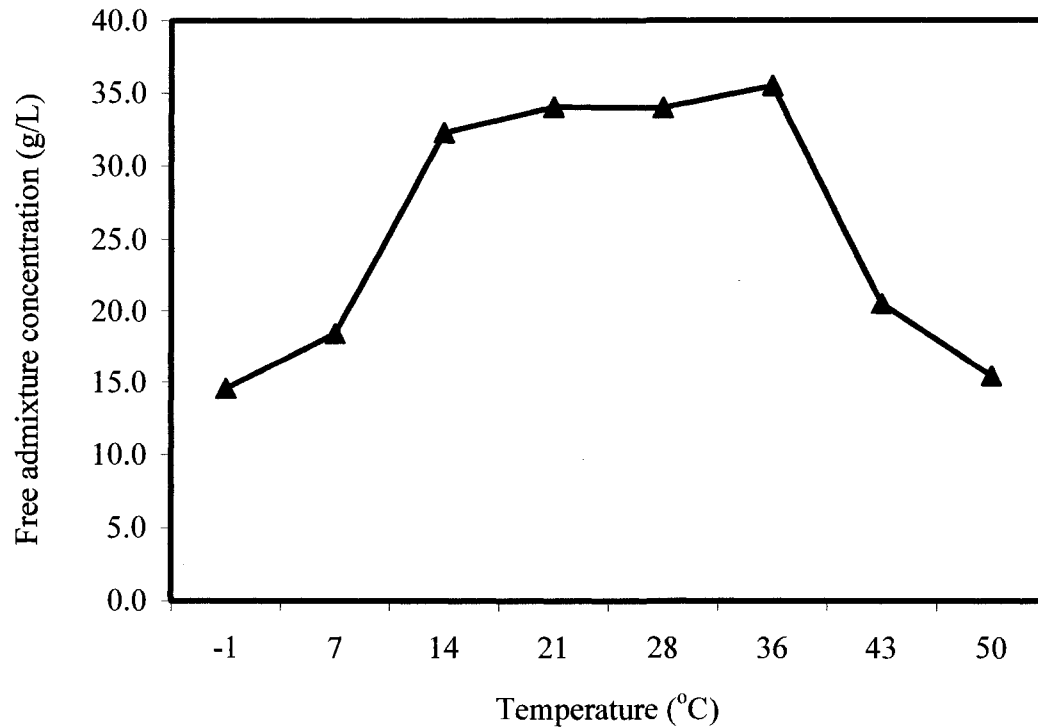
Figure 5.4: Influence of hot and cold temperatures on Portland cement-water solution's

concentration of free admixture

The pH of the cement paste was measured at the selected extreme temperatures. It remained uniform at about 12.5. In an attempt to explain and confirm the decrease/increase in free concentration of the PC-HRWRA in extreme cold and hot temperatures, the UV/Vis test was used to investigate the behavior of PC-HRWRA in a different solution with a pH similar to that of the cement paste. The sodium hydroxide (NaOH) was used for that purpose. An adequate amount of liquid NaOH was used with distilled water to make a solution of pH 12.5. Then, the selected dosage of PC-HRWRA used to prepare the self-consolidating concrete mixture S7.B.SF28 was diluted in a

prepared NaOH solution and brought to the target temperature. The UV/Vis was used to test the samples in order to determine their concentrations in free admixture. As it can be seen from Figure 5.5, the HRWRA-water-sodium hydroxide (NaOH) solution concentration of free admixture was highest at the control temperature of 21 °C (70 °F) and decreased as the temperature of the solution was elevated to 43 °C (109 °F) or moved toward the extreme cold temperatures of -0.5 °C (31 °F), respectively.
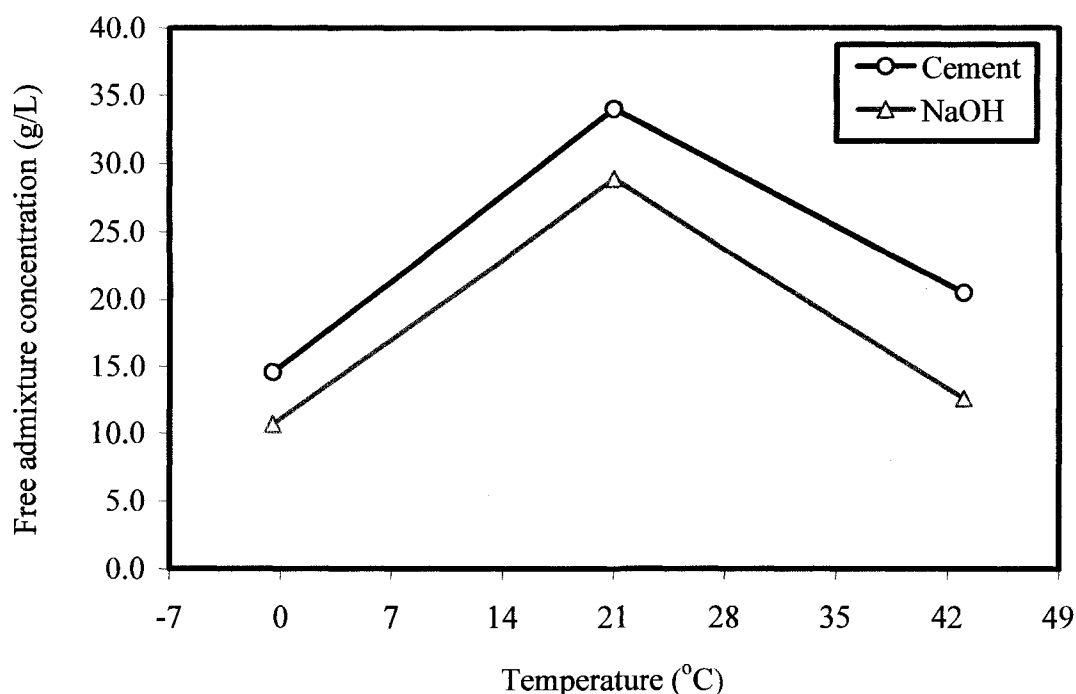
Figure 5.5: Comparison of free admixture concentration of cement-PCA and sodium hydroxide-PCA solutions

Although the cement solution exhibited a higher amount of concentration than the sodium hydroxide, an analogous trend in the superplasticizer concentration was observed for the two mediums. It is suspected that the polycarboxylate-acid (PCA) polymer was hydrolyzed in extreme temperatures. Hydrolysis is a chemical reaction during which

molecules are split into hydrogen and hydroxide ions which may go on to participate in further reactions[102]. This type of reaction is used to break down certain polymers, especially those made by step-growth polymerization. Such polymer degradation is usually catalyzed by either acid or alkali attack, often increasing with their strength or pH. This finding further corroborates the test results discussed earlier[102].

5.3.3.2   Influence of extreme temperatures on aggregates' moisture content

For the most part a segment of loss or gain in SCC workability may be credited to the available moisture in aggregates. The study of the moisture content of aggregates in extreme temperatures was not part of this investigation. However, throughout the course of this investigation it was observed that the fresh properties of self-consolidating concrete were very sensitive to the fluctuation in moisture content of aggregates. Therefore, a closer look at the aggregates' water contribution to the concrete mixture became necessary in understanding the slump flow loss or gain phenomenon.

As noted in Table 5.1, the selected elevated temperatures generated reduction in relative humidity of the mixing environmental chamber, leading to a decrease in the moisture condition of the coarse and fine aggregates, whereas the contrary was observed in cold temperatures. Table 5.3 displays the influence of the environmental room condition (i.e. temperature and relative humidity) on the aggregates' moisture content.

The coarse and fine aggregates' moisture contents were evaluated in accordance with ASTM C 127 and C 128, respectively. As it can be seen from Table 5.3, when the temperature of the mixing room increased from -0.5 to 21 to 43 °C (31 to 70 to 109 °F), the contribution of aggregates' moisture content to the total mixing water also augmented. In another word, an increase in aggregates' temperature from -0.5 to 21 to

Table 5.3: Influence of environment condition on aggregates' moisture content

Room temperature (°C)	Generated relative humidity (%)	Coarse aggregate moisture content (%)	Fine aggregate moisture content (%)	Aggregates' water contribution (kg/m³)
43.00	17.00	0.05	0.10	12.00
21.00	26.00	0.15	0.20	10.00
-0.50	70.00	0.30	0.35	7.00

1 kg/m³ = 1.6856 lb/yd³

43 °C (31 to 70 to 109 °F), required about 3 to 2 kg/m³ (5 to 3 lb/yd³) of additional mixing water to maintain the same slump flow. Otherwise accounted in the design of the matrices at extreme temperatures, the corresponding aggregates' moisture contribution can affect significantly the mixing water requirement, and thus the yield stress and plastic viscosity of concrete in general and self-consolidating concrete in particular. Similar trends were found by Kosmatka et al.[10], who reported that an increase from 10 to 38 °C (50 to 100 °F) in fresh concrete temperature requires 20 kg/m³ (33 lb/yd³) of additional water to maintain the same slump. It should be noted that the difference in water requirement found by Kosmatka et al.[10] could stem from the difference in aggregates' absorption, the contribution of cement in mixing water requirement at elevated temperature, and the temperature of the mixing water.

5.3.3.3   Evaporation of mixing water in elevated temperatures

As reported in Section 5.1.1, if the high temperature is accompanied by a low relative humidity, rapid evaporation of some mixing water takes place, resulting in the loss of workability[9,10,16]. A quick review of the various states of water in hydrated

cement paste is necessary to comprehend the fluidity loss of concrete matrix as related to the evaporation of water. Concrete paste is capable of holding a significant amount of water depending on the environmental humidity and the porosity, and there is a continuous loss of water from saturated cement paste as the relative humidity decreases[12]. Capillary water, adsorbed water, interlayer water, and chemically combined water are the main states of water present in hydrated cement paste[12]. The capillary water or bulk water is free from the influence of the attractive forces exerted by the solid surface. It is divided into free water, which the removal does not cause a volume change, and water held by capillary tension, which the removal may cause shrinkage. The adsorbed water is the water that is under the influence of attractive forces water molecules. This water is generally adsorbed onto the surface of hydrated cement paste. The loss of adsorbed water is mainly responsible for the shrinkage of hydrated cement paste in drying. The interlayer water is associated with the calcium silicate hydrate, (C-S-H) structure. The C-S-H structure shrinks considerably when the interlayer water is lost. The chemically combined water is also an integral part of various cement hydrated products. It is not lost on drying and it is evolved when the hydrates decompose on heating[12]. The capillary and adsorbed waters are of interest in a freshly-mixed matrix. The interlayer and chemically combined waters are mostly important for the strength, shrinkage, and durability aspect of hardened concretes[12].

Although not measured, based on the above-mentioned discussion, it is suspected that a portion of the mixing water was evaporated and/or absorbed once it become in contact with the hot aggregates and cementitious materials, thus reducing the amount of water necessary to assist the admixture in dispersing cement particles. It is also

suspected that during the cement hydration process, the capillary tension and the adsorbed water of the hydrated cement paste partially evaporated due to the low relative humidity and elevated temperature (see Table 5.1), contributing to the overall loss in slump flow.

5.3.3.4 Influence of extreme temperatures on specific surface area of hydrated cement

It is well established that the performance of fresh concrete is influenced by the amount of Portland cement hydration and its internal structure, which in turn are influenced by the environmental conditions such as temperature, relative humidity, and wind velocity[10,11,78]. The decrease in self-consolidating concrete's workability, induced by elevated temperatures, was partially attributed to the increase in specific surface area of the concrete paste (ΔSSAp), manifested in the form of growth of cement hydrated products. During the initial hydration, water wets the cement particles and solubilizes the cement phases. Various reactions occur through several types of bonding interaction. Ca^{2+} and SiO_4^{2-} are hydrolyzed from the most reactive cement particles C_3A and C_3S, and C_3A is converted into ettringite (calcium aluminate trisulfate). Ettringite has larger specific surface area than other cement hydrated phases such as: gypsum ($CaSO_4$), portlandine (CH), calcium silicate hydrate (CSH), and calcite (stable polymorph of $CaCO_3$)[92]. As a result, the cement particles' surface can increase by to 2 to 2.5 times[95]. These chemical reactions increase with temperature rise, along with the kinetic energy per mole, as translated in the Arrhenius equation[103]: $R_1 = Ae^{-E/RT}$, where R_1, R, E, T, and A are the reaction rate, the gas constant, the absolute temperatures, the activation energy, and a constant, respectively. The opposite is valid in cold temperatures, where the cement particles' don't expand when compared to that of the control condition.

The determination of the specific surface area of cement hydration products was not part of this investigation. However, the finding of Ludwig and Pence[104] who determined that the 7-day specific surface areas of Portland cement hydration products at 27 and 66 °C (81 and 151 °F) were equal to 103.4 and 122 m^2 g^{-1}, respectively, can confirm the theory adopted herein. The progressive growth of cement hydration products in elevated temperatures ($\Delta SSAp$) was a contributing factor to the slump flow loss.

In view of the above discussions, the slump flow loss of SCC in hot temperatures and gain in cold temperatures can be expressed in the following mathematically forms:

$$Slump\ flow\ loss = f\left\{\frac{Ads}{SSAp}, w\right\} = \frac{Ads_o + \Delta Ads_{hot}}{SSAp_o + \Delta SSAp_{hot}} + (w_o + \nabla w_{hot}) \tag{5.2}$$

$$Slump\ flow\ gain = f\left\{\frac{Ads}{SSAp}, w\right\} = \frac{Ads_o - \Delta Ads_{cold}}{SSAp_o} + (w_o + \Delta w_{cold}) \tag{5.3}$$

Where, $Ads/SSAp$ is the adsorption amount of admixture per specific surface area of concrete paste at the target temperature. The terms Ads_o, ΔAds_{hot}, ΔAds_{cold}, $SSAp_o$, $\Delta SSAp_{hot}$, w, w_o, ∇w_{hot}, and Δw_{cold} are defined in Figure 5.2.

It seems that the contribution of SSAp in the slump flow loss was greater than that of the admixture adsorption and its related electrostatic repulsion and steric hindrance effect. In fact, despite the augmentation in Ads, as discussed earlier in Section 5.1.3.1, the increase in SSAp induced by the hot temperatures was able to reduce the overall workability of the concrete mixture. On the other hand, it is suspected that the selected cold temperatures did not affect significantly the specific surface area of the Portland cement hydrated products as the hydration continued in cold temperatures, but at a slower rate. In this case, Ads nearly overtook on the SSAp, and little to no change in the concrete workability was observed.

5.3.4 Prediction of SCC slump flow loss and gain in hot and cold temperatures

Predictive statistical analysis, at 95% level confidence, was used to relate the slump flow losses or gains of the selected self-consolidating concretes to the temperatures and initial slump flows as follows:

In hot temperature:

$$SF_{loss} = -904.10 - 0.65SF + \frac{64060.40}{t_h} + 7.63x10^{-5}SF^2 - \frac{1066402.06}{t_h^2} + 14.32\frac{SF}{t_h} \quad (5.4)$$

$$\text{Or } SF_{loss} = a + bSF + \frac{c}{t_h} + dSF + \frac{e}{t_h^2} + f\frac{SF}{t_h}$$

In cold temperature:

$$SF_{gain} = 23.16 - 6.14x10^{-3}SF - 1.37t_c + 0.31t_c^2 - 1.36x10^{-2}t_c^3 \quad (5.5)$$

$$\text{Or } SF_{gain} = a + bSF + ct_c + dt_c^2 + et_c^3$$

Where:

SF_{loss} = Slump flow loss in hot temperature conditions (mm)

SF_{gain} = Slump flow gain in cold temperature conditions (mm)

SF = Initial slump flow (mm), with 508 mm $\leq SF \leq$ 711 mm $\pm$ 25 mm

t_h = Hot temperature ($^{\circ}$C) with 28 $^{\circ}$C $\leq t_h \leq$ 43 $^{\circ}$C $\pm$ 2 $^{\circ}$C

t_c = Cold temperature ($^{\circ}$C) with -0.5 $^{\circ}$C $\leq t_c \leq$ 14 $^{\circ}$C $\pm$ 2 $^{\circ}$C

The regression equations 5.4 and 5.5 produced coefficients of multiple determination, R^2, and standard deviations, S, values of 99.6% and 6.08 mm (0.24 inch), and 98.8% and 1.33 mm (0.05 inch), respectively, indicating a very strong relationship between the dependent variable (slump flow loss or slump flow gain) and the independent variables (initial slump flow and hot or cold temperature). F and T tests

were performed to confirm the significance of coefficients a, b, c, d, e, and f in the regression models. The following results were found.

For Equation 5.4:

Prob(t) = 0.0274, 0.3552, 0.0038, 0.8814, 0.0031, and 0.0574 for a, b, c, d, e, and f, respectively; and Prob(F) = 0.00089.

For Equation 5.5:

Prob(t) = 0.0001, 0.2287, 0.0076, 0.0004, and 0.0000 for a, b, c, d, and e, respectively; and Prob(F) = 0.0000.

The F and T tests results indicated that both the slump flow value and the temperature had a similar influence on the predicted slump flow loss or gain. Table 5.4 shows the actual versus the calculated slump flow loss or gain values. The predictive equations yielded percentage errors less than 5%, for the most part, confirming a very strong relationship between the actual and the predicted slump flow loss or gain.

5.3.5   Remediation of slump flow loss induced by extreme temperature

Several studies have reported that both the hot and cold temperatures affected the fresh and hardened properties of concrete[10,12,96,97]. Various remediation methods to mitigate the adverse effect of extreme temperatures on concrete have been proposed. Among them, cooling or heating the materials, retempering in job site with water or superplasticizer, overdosing in mixing plant with water or superplasticizer, and others can be noted. In the present chapter only the remediation of the hot temperature condition was studied since the increased slump flow in cold temperature was relatively marginal at less than ± 25 mm (1.0 inch), well within the established limit of tolerance. The adopted remediation method consisted of overdosing the admixtures in order to eliminate the

237

adverse impact of hot temperatures on the unconfined workability, flow rate/plastic viscosity, dynamic stability, and passing ability of the trial freshly-mixed self-consolidating concretes.

Table 5.4: Actual versus calculated slump flow loss or gain

Target slump flow (mm)	Target temperature (°C)	Actual slump flow loss or gain (mm)	Calculated slump flow loss or gain (mm)	% Error
524.00	43.00	-133.35	-138.17	-3.62
651.00	43.00	-171.45	-167.52	2.29
723.90	43.00	-184.15	-183.25	0.49
524.00	36.00	-66.80	-60.65	9.21
651.00	36.00	-79.50	-81.77	-2.85
723.90	36.00	-88.90	-92.78	-4.37
524.00	28.00	-28.70	-30.03	-4.62
651.00	28.00	-35.05	-36.71	-4.73
723.90	28.00	-42.42	-39.43	7.04
524.00	21.00	0.00	0.48	0.00
651.00	21.00	0.00	-0.42	0.00
723.90	21.00	0.00	-0.06	0.00
524.00	14.00	24.38	23.82	2.29
651.00	14.00	22.10	22.40	-1.38
723.90	14.00	22.35	22.60	-1.14
524.00	7.00	22.10	22.18	-0.37
651.00	7.00	19.05	19.16	-0.55
723.90	7.00	19.05	18.86	0.99
524.00	-0.50	19.05	19.05	0.01
651.00	-0.50	22.10	22.11	-0.04
723.90	-0.50	19.05	19.04	0.04

1 mm = 0.03937 inch, °C = 5/9(°F - 32)

238

5.3.5.1 HRWRA dosage requirement for the remediation of slump flow loss

Table 5.6 presents the optimum dosages of HRWRA for the remediation of slump loss induced by the elevated temperatures, and Figure 5.5 shows the required HRWRA dosages as a function of temperatures. In comparing to the control optimum dosage at 21 °C (70 °F), an average increase of only 3% in the HRWRA optimum dosage was sufficient to combat the adverse effect of the 28 °C (83 °F) temperature. On the other hand, significant increases in HRWRA optimum dosage requirement of about 13, 19 and 13%; and 26, 47, and 54% at the temperatures of 43 and 36 °C (96 and 109 °F) were obtained for the self-consolidating concretes prepared for 508, 635, and 711 mm (20, 25 and 28 inches) of slump flow, respectively.

The higher superplasticizer demand in contesting the slump flow loss of the selected SCCs, induced by the elevated temperatures, can be explained through Equations 5.5 and 5.6. The idea behind the adopted remediation technique in the present study was to find by trial and error an initial admixtures dosage so that $(Ads/SSAp)_t$ at the target temperature became equivalent to $(Ads/SSAp)_o$ at the control temperature; with the term "t" referring to the elevated temperatures (t = 28, 43 or 36 °C (83, 96 or 109 °F)).

- *At the control temperature of 21 °C (70 °C):*

$$\left(\frac{Ads}{SSAp}\right)_o = \frac{Ads_o}{SSAp_o} + w_o \tag{5.6}$$

- *At the target hot temperature "t":*

$$\left(\frac{Ads}{SSAp}\right)_t = \underbrace{\left[\frac{Ads_o + \Delta Ads_{hot}}{SSAp_o + \Delta SSAp_{hot}} + (w_o + \nabla w_{hot})\right]}_{A} + \underbrace{\left[\frac{\Delta Ads_{overd}}{SSAp_o + \Delta SSAp_{hot}}\right]}_{B} = \left(\frac{Ads}{SSAp}\right)_o \tag{5.7}$$

Table 5.5: Optimum overdosed amounts of admixtures and fresh properties of remediated SCCs at various temperatures

Mix No.	Target temp. (°C)	HRWR (ml/100 kg)	VMA (ml/100 kg)	Slump flow (mm)	T_{50} (sec.)	VSI	J ring value (mm)
S7.E.SF20		189.54	0.00	521	4.72	0	44
S7.E.SF25	43.00	307.19	39.22	648	2.28	0	38
S7.E.SF28		392.16	58.82	724	2.05	1	38
S7.E.SF20		169.93	0.00	521	3.09	0	44
S7.E.SF25	36.00	248.37	32.68	648	2.19	0	38
S7.E.SF28		287.58	45.75	721	2.00	1	35
S7.E.SF20		153.59	0.00	521	3.41	0	37
S7.E.SF25	28.00	215.69	26.14	648	2.35	0	34
S7.E.SF28		261.44	32.68	715	2.25	1	32
S7.E.SF20		150.33	0.00	524	3.19	0	35
S7.E.SF25	21.00	209.15	26.14	651	2.79	0	29
S7.E.SF28		254.90	32.68	724	1.85	1	25

°C = 5/9(°F-32), 1 ml/100 kg = 0.0153 oz/cwt, 1 mm = 0.03937 in.
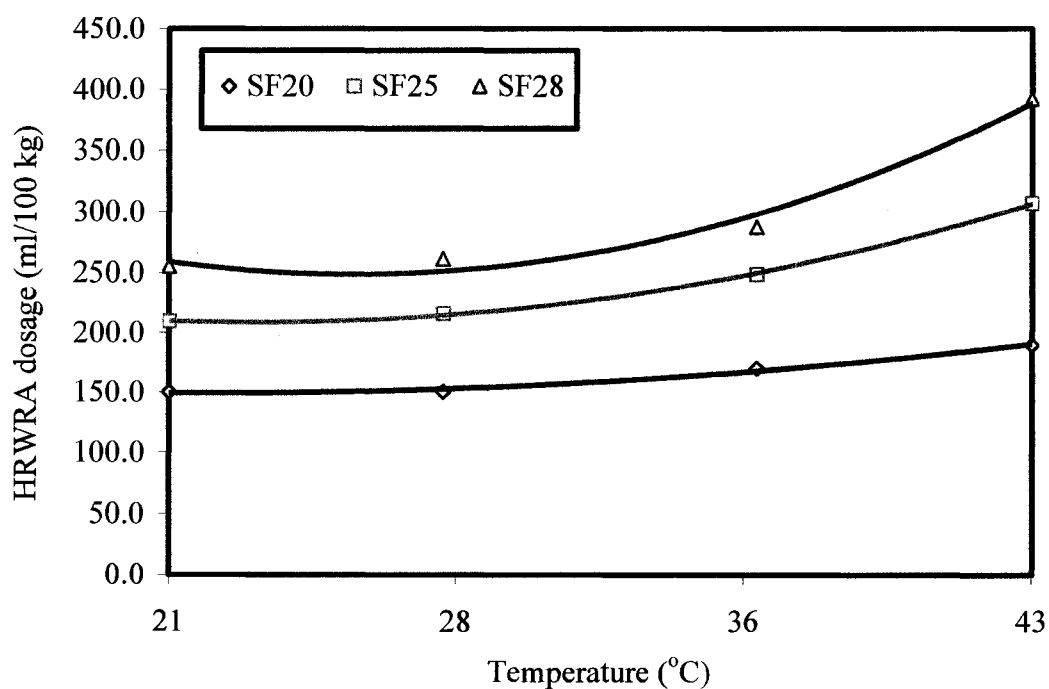
Figure 5.6: Optimum dosage of HRWRA for the overdosing remediation of slump loss at various elevated temperatures

$\left(\textbf{A}\right)$ Characterizes the slump flow loss

$\left(\textbf{B}\right)$ Characterizes the slump flow restoration

Ads_o, ΔAds_{hot}, $SSAp_o$, $\Delta SSAp_{hot}$, w_o, and ∇w_{hot} are defined in Figure 5.2. The term ΔAds_{overd} corresponds to the increase in adsorption amount of admixture brought by the additional superplasticizer to compensate for the increase in specific surface area of concrete paste, $\Delta SSAp_{hot}$, and the loss of mixing water, ∇w_{hot}, due to hot temperature and low relative humidity. ΔAds_{overd} generated additional repulsive electrostatic and steric hindrance forces between the cement particles to make-up for the loss of repulsive forces caused by the growth of the cement hydrated products due to hot temperatures. The designed optimum dosages of HRWRA for the temperature "t" were sufficient to produce the target fluidity at the target temperature.

5.3.5.2   VMA dosage requirement for the remediation of slump flow loss

Table 5.5 and Figure 5.7 display the optimum dosages of VMA for the remediation of slump loss due to elevated temperatures. At the temperature of 28 °C (83 °F), the three selected slump flow mixtures did not required any adjustment in their initial VMA dosage in attaining similar fresh performance to those of the control temperature. At the temperature of 36 and 43 °C (96 and 109 °F), the matrices made with 508, 635, and 711 mm (20, 25, and 28 inches) slump flow required 0, 25, and 40%, and 0, 50, and 80% augmentation of the dosage of VMA, respectively, when compared to that of the control temperature.

The viscosity modifying admixture is mainly used to increase the plastic viscosity and stability of self-consolidating concrete. In hot temperatures, the increase in SSAp was effective in thickening the paste, resulting in a higher plastic viscosity (T_{50} time between 2
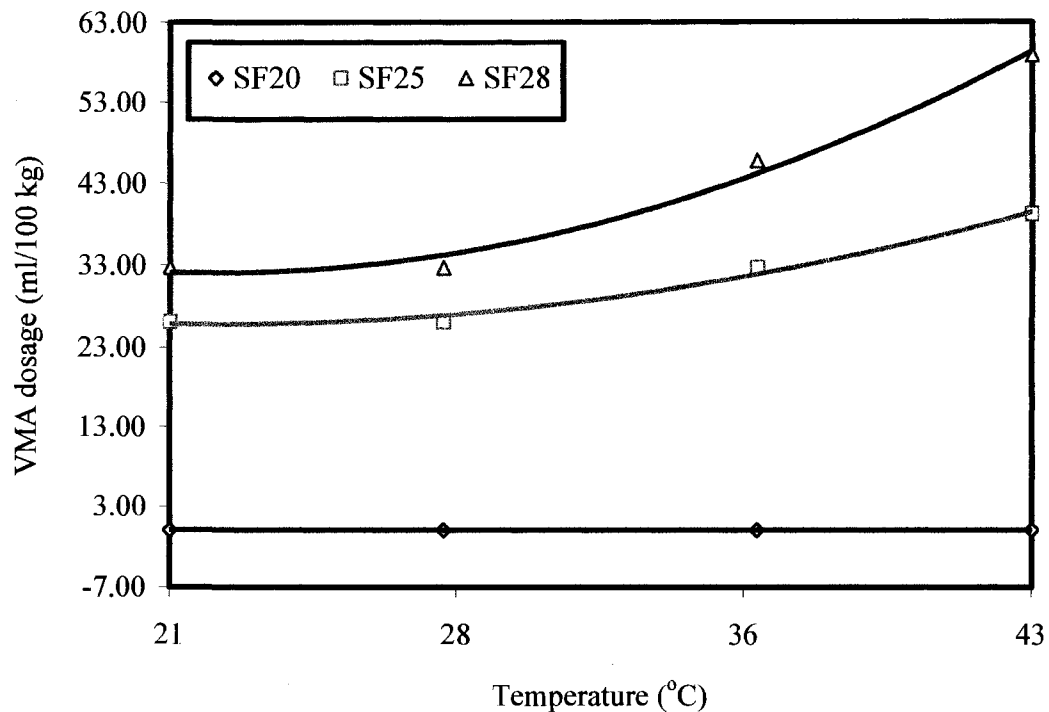
Figure 5.7: Optimum dosage of VMA for the overdosing remediation
of slump loss at various elevated temperatures

and 5 seconds) and a higher VSI (0 or 1) of fresh self-consolidating concretes. This was the case for the selected matrices made with 508 mm (20 inches) of slump flow. However, in the case of mixtures made for 635 and 711 mm (25 and 28 inches) of slump flows; the increase in SSAp was insufficient to restore the reduced plastic viscosity and dynamic stability generated by the higher dosage of HRWRA. The additional VMA used in these mixtures helped the viscosity and stability to revert back to their acceptable levels.

5.3.5.3   Fresh properties of the remediated self-consolidating concretes

The slump flow, T_{50}, and VSI tests were used to determine the unconfined workability, the flow rate or plastic viscosity (per inference), and the dynamic stability of

242

the remediated self-consolidating concretes at elevated temperatures. As reported in Table 5.5, the test results showed that irrespective of the selected hot temperatures, all remediated self-consolidating concretes were within the assigned target slump flows ± 25 mm (1 inch), T_{50} time between 2 and 5 seconds, and VSI of 0 (highly stable) or 1 (stable). In comparing the slump flow values at various hot temperature conditions to that measured at the control temperature, the selected remediated fresh SCCs displayed an insignificant difference of less than 1%. All T_{50} times decreased as the slump flow increased and, within the same group, remained similar to that of the reference temperature. No evidence of segregation or bleeding in slump flow was observed in any of the remediated self-consolidating concretes, indicating that a stable matrix condition was achieved through the adopted overdosing method.

The passing ability of the remediated self-consolidating concrete was determined by the J-ring value (the diameter of the unobstructed slump flow minus the diameter of the obstructed slump flow). As shown in Table 5.5, similar J-ring values to that of the control temperature were recorded. Irrespective of the hot temperatures, the calculated J-ring values of all remediated matrices were within the allowable limit of 25 to 50 mm (1 to 2 inches) indicating a moderate passing ability or minimal to noticeable blocking of the selected self-consolidating concretes.

5.3.5.4   Predictive statistical equations of HRWRA and VMA optimum dosages for remediation of slump flow loss due to elevated temperatures

The most suitable predictive relationships among the HRWRA or VMA optimum dosages, slump flow, and elevated temperatures for the remediation of slump flow loss induced by the elevated temperature were determined using a 95% confidence level. The

predictive equations were tested for accuracy using R^2 (regression value) and S (standard deviation). The relationships are as follows:

$$HR = 5.0126 x 1.0030^{SF} \left(t_h^{0.5592} \right)$$ (5.8)

$$\text{Or } HR = a \cdot b^{SF} \left(t_h^{c} \right)$$

$$VMA = -141.3107 + 0.5313SF - 4.7307t_h - 4.0479SF^2 + 0.0268t_h^{2} + 0.0058SFt_h$$ (5.9)

$$\text{Or } VMA = a + bSF + ct_h + dSF^2 + et_h^{2} + fSFt_h$$

Where:

HR = High range water-reducing admixture initial optimum dosage (ml/100 kg)

VMA = Viscosity modifying admixture initial optimum dosage (ml/100 kg)

SF = Target slump flow in hot temperature condition (mm),

       with 508 mm $\leq SF \leq$ 711 mm $\pm$ 25 mm

t_h = Hot temperature ($^{\circ}$C), with 21 $^{\circ}$C $\leq t_t \leq$ 43 $^{\circ}$C $\pm$ 2 $^{\circ}$C

The regression equations 5.8 and 5.9 produced R^2 and S values of 92.83% and 20.94 ml/100 kg (0.32 oz/cwt), and 99.36% and 2.17 ml/100 kg (0.03 oz/cwt), respectively, indicating a good relationship between the dependent variable (HRWRA or VMA optimum dosage) and the independent variables (initial slump flow and hot temperature). F and T tests were performed to confirm the significance of coefficients a, b, c, d, e, and f in the regression models. The following results were found.

For Equation 5.8:

Prob(t) = 0.0384, 0.0000, and 0.0003 for a, b, and c, respectively; and Prob(F) = 0.00005.

For Equation 5.9:

Prob(t) = 0.0523, 0.0267, 0.0027, 0.0319, 0.0653, and 0.0007 for a, b, c, d, e, and f,

Table 5.6: Actual versus calculated HRWRA required dosage for remediation

Target slump flow (mm)	Target temperature (°C)	Actual HRWRA (ml/100 kg)	Calculated HRWRA (ml/100 kg)	% Error
520.70	43.00	189.54	196.45	-3.65
647.70	43.00	307.19	287.76	6.33
723.90	43.00	392.16	361.82	7.74
520.70	36.00	169.93	177.87	-4.67
647.70	36.00	248.37	260.54	-4.90
720.85	36.00	287.58	324.61	-12.87
520.70	28.00	153.59	154.55	-0.62
647.70	28.00	215.69	226.38	-4.96
714.50	28.00	261.44	276.71	-5.84
524.00	21.00	150.33	132.89	11.60
651.00	21.00	209.15	194.66	6.93
723.90	21.00	254.90	242.34	4.93

1 mm = 0.03937 inch, °C = 5/9(°F-32)

Table 5.7: Actual versus calculated VMA required dosage for remediation

Target slump flow (mm)	Target temperature (°C)	Actual VMA (ml/100 kg)	Calculated VMA (ml/100 kg)	% Error
520.70	43.00	*	*	*
647.70	43.00	39.22	40.20	-2.49
723.90	43.00	58.82	57.31	2.56
520.70	36.00	*	*	*
647.70	36.00	32.68	32.26	1.28
720.85	36.00	45.75	45.82	-0.16
520.70	28.00	*	*	*
647.70	28.00	26.14	26.41	-1.04
714.50	28.00	32.68	35.88	-9.79
524.00	21.00	*	*	*
651.00	21.00	26.14	24.53	6.15
723.90	21.00	32.68	31.54	3.48

1 mm = 0.03937 inch, °C = 5/9(°F-32)
*The matrix does not incorporate VMA

respectively. Prob(F) = 0

The F and T tests results indicated that both the slump flow value and the temperatures had a similar influence on the predictive HRWRA and VMA optimum dosages. Tables 5.6 and 5.7 present the actual versus the calculated required admixtures dosages for the slump flow loss remediation. The predictive equations yielded percentage errors ranging from 1 to 7% for the most part, confirming a good relationship between the actual and the predicted admixture dosages.

5.4   Conclusions

a)   The fresh performance of self-consolidating concrete was affected by both hot and cold temperatures.

In hot temperatures, the influence was manifested in the form of significant decrease in unconfined workability, substantial increase in flow rate or plastic viscosity per inference, and improvement in dynamic stability of the freshly-mixed SCCs. In comparing to the control temperature of 21 °C (70 °F), the losses in slump flow induced by the elevated temperatures were only 5% at 28 °C (83 °F), but increased significantly to about 12 and 25%, at 36 and 43 °C (96 and 109 °F), respectively.

The cold temperature affected the fresh performance of the selected self-consolidating concretes by a marginal gain in flow ability (averaging 3%), small variation in flow rate (averaging 6%), and an increase in the resistance to segregation from VSI of 1 to 0 for the matrices only made with slump flow of 711mm (28 inches), when compared to those obtained under the control temperature. The VSI of the trial SCCs prepared with slump flows of 508 and 635 mm (20 and 25 inches) were unaffected by the selected cold temperatures.

b)   The change in the fresh properties due to elevated and cold temperatures can be characterized by the adsorption amount of admixture per specific surface area of concrete paste (Ads/SSAp), the change in the aggregate's moisture content, and the partial evaporation of mixing water in the case of elevated temperatures.

• The ultraviolet-visible spectroscopy test determined that the free concentration of polycarboxylate-based high range water-reducing admixture cement-water solution changed with material temperatures. The concentration was relatively uniform at temperatures ranging from 14 to 36 °C (57 to 96 °F) and beyond that range, it decreased as the temperature moved toward the extreme cold and hot temperatures. While the calculated concentrations do not represent the actual amounts of adsorbed HRWRA on cement particles, their increases in the solution leads to an augmentation of the adsorbed amount of the PC-HRWRA carboxylic group (COO^-) on cement grains, favoring further increase or decrease in electrostatic repulsion and steric hindrance forces.

• In cold temperatures, the relative humidity increased the moisture content of the aggregates and, thus, contributed to the augmentation of slump flow. The contrary was observed in hot temperatures. Indeed, an increase in aggregate's temperature from -0.5 to 43 °C (31 to 109 °F), required about 5 kg/m^3 (8 lb/yd^3) of additional mixing water to maintain the same slump flow. Additionally, the mixing water was partially evaporated and/or absorbed by the elevated temperatures and low relative humidity.

• Through the increase rate of hydration, the hot temperatures increased the specific surface area of concrete paste. The contribution of the specific surface area of concrete paste, SSAp, to the slump flow loss was greater than that of the admixture adsorption through increases/decreases in electrostatic repulsion and steric hindrance forces.

Despite the augmentation in adsorption, Ads, the increase in SSAp induced by hot temperatures was able to reduce the overall workability of the fresh concrete. On the other hand, the selected cold temperatures did not significantly impact the specific surface area of the Portland cement hydrated products, since continued hydration in cold temperature was at a lower rate. In this case, Ads nearly gained on SSAp, as little to no change in the workability of the fresh matrix was observed.

c)   A remediation method by way of admixture overdosing was successful to reverse the change in fresh properties of the selected self-consolidating concretes in elevated temperatures. The additional amount of admixtures increased workability (up to 36 °C (96 °F)) through generation of supplementary repulsive electrostatic and steric hindrance forces between the cement particles and was able to offset the loss of workability caused by the growth of the cement hydrated products engendered during hot temperatures. The selected remediation method was able to produce SCCs with a similar unconfined workability, flow rate or plastic viscosity per inference, dynamic stability, and passing ability to those obtained for the equivalent matrices at the control temperature.

d)   The selected self-consolidating concretes did not require any remediation in cold temperatures of 14, 7, and -0.5 °C (57, 44, and 31 °F). The gains in slump flow of the trial self-consolidating concretes in cold temperatures were less than 25 mm (1.0 inch), and both the flow rate and dynamic segregation resistance were unaffected by the selected cold temperatures.

e)   The predictive equations to correlate the slump flow loss or gain with the initial slump flow value and the selected hot and cold temperatures showed significant statistical relationships between the dependent and independent variables. For the remediation

purpose in hot temperature, the required optimum admixtures dosages (HRWRA and VMA) were also predicted for the selected target slump flows and elevated temperatures. A strong significant statistical relationship between the dependent and independent variables of the remediated concretes were also obtained.

CHAPTER 6

INFLUENCE OF COMBINED HAULING TIME AND EXTREME TEMPERATURE

ON FRESH PERFORMANCE OF SELF CONSOLIDATING CONCRETE

The investigation presented herein is intended to study the influence of combined hauling time and hot and cold temperatures on the fresh properties of selected self-consolidating concretes. Seven different temperatures (43, 36, 28, 21, 14, 7, and -0.5 °C (109, 96, 83, 70, 57, 44, and 31 °F)) to simulate hot and cold weathers were used to evaluate the unconfined workability, flow rate (or plastic viscosity per inference), and dynamic stability of the self-consolidating concretes hauled for 10, 20, 40, 60, and 80 minutes. Additionally, the fresh performance of the remediated self-consolidating concretes by way of admixture overdosing (using sufficient admixture dosage during mixing) and retempering (adjusting admixture dosage at the end of hauling) under the influence of the combined hauling time and extreme temperatures was investigated.

6.1   Introduction

Nowadays, ready-mixed plants are predominantly used in concrete industry for the manufacture of concrete, due to their suitability for close quality control, use in congested sites, and use of agitator trucks to prevent segregation and maintain workability[11]. In general, lengthy hauling time and extreme temperature (due to excessive hot or cold weather) can adversely affect the fresh and hardened properties of concrete by accelerating or retarding the rate of moisture loss and the rate of cement

250

hydration. Owing to its high fluidity, the mixing and delivery of self-consolidating concrete from the ready-mixed to the job site requires a suitable mixture proportioning and design, and adequate preparation and monitoring in extreme weather. The influence of combined hauling time and extreme temperature on the fresh performance of selected self-consolidating concrete, along with the remediation solutions, is presented in the subsequent sections.

6.2 Experimental programs

The self-consolidating concrete mixtures S7.B.SF25 and S7.B.SF28 were used. Their mixture constituents and proportions are presented in Chapter 3, Table 3.1c. The aggregates, cement, fly ash, water, and chemical admixtures used to manufacture the matrices were prepared as reported in Sections 2.1 and 5.1. The mixing tool and the environmental chamber as shown in Figure 5.1 were used. The mixing sequence presented in Figure 4.2 was adopted. At the completion of each mixing and hauling, the fresh self-consolidating concretes were evaluated for the unconfined workability (measured by the slump flow), the flow rate or viscosity by inference (evaluated by the T_{50} time), the dynamic segregation resistance (assessed by the visual stability index (VSI)), and J-ring passing ability (determined by the J-ring test); in accordance with the ASTM C 1611[55] and C 1621[58].

6.3 Discussion of results

6.3.1 Influence of combined hauling time and extreme temperature on fresh performance of self-consolidating concrete

The characteristics of plastic self-consolidating concrete were affected by both hauling time and extreme temperature. In order to understand the combined influence of

251

the two above-mentioned construction-related variables on the fresh self-consolidating concrete, an overview on the influence of each variable is presented.

6.3.1.1 Hauling time

The study of the effect of hauling time on fresh performance of self-consolidating concrete is useful in simulating batching and transporting concrete at different times under control room temperature and relative humidity $(21 \pm 2\ ^{\circ}C\ (70 \pm 3\ ^{\circ}F)$ and 25 ± 5 %). The influence of the selected hauling times on the fresh properties of the designed self-consolidating concretes is discussed in Chapter 4. In comparing to the control hauling time of 10 minutes, the selected self-consolidating concretes exhibited progressive losses in workability as the hauling time increased. The changes in fresh performance of the matrices were manifested in the form of decrease in flow ability, increase in flow rate/plastic viscosity, and increase in dynamic stability. The decreases in workability were explained through reduction in the adsorbed amount of admixture per specific surface area of concrete mortar (Ads/SSAm).

6.3.1.2 Extreme temperature

The effect of extreme temperature on fresh performance of self-consolidating concrete can be used to simulate mixing concrete during extreme temperature conditions. The influence of selected hot and cold temperatures on the fresh properties of the designed self-consolidating concrete is discussed in Chapter 5. The weather condition characterized by a temperature of $21 \pm 2\ ^{\circ}C\ (70 \pm 3\ ^{\circ}F)$ and a relative humidity of $25 \pm$ 5% was adopted as the control environment. The performance of plastic self-consolidating concrete was adversely affected by both hot and cold temperatures. The influence of hot temperature was manifested in the form of flow ability loss, and flow

rate/plastic viscosity and dynamic stability gains; while the selected cold temperatures affected the fresh characteristics of SCC by a marginal gain in flow ability, a small difference in flow rate/plastic viscosity, and a slight to no improvement in resistance to dynamic segregation. These findings were attributed to the decrease in the adsorbed amount of admixture per specific surface area of concrete paste (Ads/SSAp).

6.3.1.3 Combined hauling time and extreme temperature

The understanding of the effect of the combined hauling time and extreme temperature on freshly-mixed self-consolidating concrete is useful in simulating concrete mixing and hauling by the mean of a concrete truck mixer during extreme temperatures. For the purpose of this study, the combination of hauling times of 10, 20, 40, 60, and 80 minutes and temperatures of 43, 36, 28, 21, 14, 7, and -0.5 °C (109, 96, 83, 70, 57, 44, and 31 °F) were considered. The term "TxHy" is used throughout the report to indicate the mixing condition and environment. "Tx" stands for the temperature "x", and "Hy" represents the hauling time "y." The test results for the slump flow, T_{50} time, and visual stability index (VSI) at the selected combined hauling time and temperature are presented in Tables 6.1 through 6.4.

6.3.1.3.1 Slump flow loss

6.3.1.3.1.1 TxHy versus T21H10

In this section, the slump flow of the selected self-consolidating concretes exposed to the combination of hauling time and temperature are compared to the control matrices hauled for 10 minutes under the reference temperature of 21 ± 2 °C (70 ± 3 °F) (T21H10 condition). The slump flows at the control condition are given in Chapter 4, Tables 4.2 and 4.3. These values are 651 and 724 mm (25.63 and 28.50 inches) for the

Table 6.1: Influence of temperature on fresh properties of SCC hauled for 20 minutes

Temperature (^{o}C)	Mix designation	Measured slump flow (mm)	T_{50} (sec.)	VSI	Slump flow loss (mm)
43.00	S7.B.SF25	451	-	0	-200
	S7.B.SF28	508	-	0	-216
36.00	S7.B.SF25	495	-	0	-156
	S7.B.SF28	613	3.02	0	-111
28.00	S7.B.SF25	527	3.91	0	-124
	S7.B.SF28	635	2.81	0	-89
21.00	S7.B.SF25	559	2.92	0	-92
	S7.B.SF28	673	2.20	0	-51
14.00	S7.B.SF25	594	2.65	0	-57
	S7.B.SF28	711	2.33	0	-13
7.00	S7.B.SF25	591	2.68	0	-60
	S7.B.SF28	711	2.38	0	-13
-0.50	S7.B.SF25	588	2.60	0	-63
	S7.B.SF28	710	2.35	0	-14

^{o}C = 5/9(^{o}F - 32), 1 ml/100 kg, 1 mm = 0.03967 inch

Table 6.2: Influence of temperature on fresh properties of SCC hauled for 40 minutes

Temperature (°C)	Mix designation	Measured slump flow (mm)	T_{50} (sec.)	VSI	Slump flow loss (mm)
43.00	S7.B.SF25	387	-	0	-264
	S7.B.SF28	429	-	0	-295
36.00	S7.B.SF25	425	-	0	-226
	S7.B.SF28	540	3.95	0	-184
28.00	S7.B.SF25	451	-	0	-200
	S7.B.SF28	559	2.90	0	-165
21.00	S7.B.SF25	521	3.28	0	-130
	S7.B.SF28	603	2.67	0	-121
14.00	S7.B.SF25	559	3.00	0	-92
	S7.B.SF28	654	2.83	0	-70
7.00	S7.B.SF25	556	3.00	0	-95
	S7.B.SF28	667	2.84	0	-57
-0.50	S7.B.SF25	552	3.03	0	-99
	S7.B.SF28	670	2.87	0	-54

°C = 5/9(°F - 32), 1 ml/100 kg, 1 mm = 0.03967 inch

Table 6.3: Influence of temperature on fresh properties of SCC hauled for 60 minutes

Temperature (°C)	Mix designation	Measured slump flow (mm)	T_{50} (sec.)	VSI	Slump flow loss (mm)
43.00	S7.B.SF25	292	-	0	-359
	S7.B.SF28	368	-	0	-356
36.00	S7.B.SF25	343	-	0	-308
	S7.B.SF28	470	-	0	-254
28.00	S7.B.SF25	375	-	0	-276
	S7.B.SF28	502	-	0	-222
21.00	S7.B.SF25	464	-	0	-187
	S7.B.SF28	546	3.00	0	-178
14.00	S7.B.SF25	505	-	0	-146
	S7.B.SF28	610	3.00	0	-114
7.00	S7.B.SF25	502	-	0	-149
	S7.B.SF28	613	2.97	0	-111
-0.50	S7.B.SF25	502	-	0	-149
	S7.B.SF28	616	2.97	0	-108

°C = 5/9(°F - 32), 1 ml/100 kg, 1 mm = 0.03967

Table 6.4: Influence of temperature on fresh properties of SCC hauled for 80 minutes

Temperature (°C)	Mix designation	Measured slump flow (mm)	T_{50} (sec.)	VSI	Slump flow loss (mm)
43.00	S7.B.SF25	229	-	0	-422
	S7.B.SF28	279	-	0	-445
36.00	S7.B.SF25	292	-	0	-359
	S7.B.SF28	394	-	0	-330
28.00	S7.B.SF25	330	-	0	-321
	S7.B.SF28	419	-	0	-305
21.00	S7.B.SF25	419	-	0	-232
	S7.B.SF28	470	-	0	-254
14.00	S7.B.SF25	464	-	0	-187
	S7.B.SF28	546	3.47	0	-178
7.00	S7.B.SF25	464	-	0	-187
	S7.B.SF28	549	3.44	0	-175
-0.50	S7.B.SF25	462	-	0	-189
	S7.B.SF28	549	3.57	0	-175

°C = 5/9(°F - 32), 1 ml/100 kg, 1 mm = 0.03967 inch

mixtures S7.B.SF25 and S7.B.SF28, respectively. Figures 6.1 and 6.2 document the slump flow losses due to the combined hauling time and temperature, for the matrices prepared with 635 and 711 mm (25 and 28 inches) slump flows, respectively. In comparing to the control condition, the 635 mm (25 inches) self-consolidating concretes hauled for 20 minutes experienced 31, 24, and 19% decreases in slump flow at the elevated temperatures of 43, 36, and 28 °C (109, 96, and 83 °F), respectively. The corresponding slump flow losses were 30, 15, and 12% for the 711 mm (28 inches) matrices. When transportation time was progressively increased to 80 minutes, both self-consolidating concrete types exhibited an average reduction in slump flow of about 10% per 20 minutes increment in hauling time for the selected temperatures of 28 through 43 °C (83 through 109 °F).

The combined transportation duration and cold temperature (i.e., 14, 7, and -0.5 °C (57, 44, and 31 °F)), also caused decreases in slump flow when compared to T21H10, but to a lesser extend. On average, the losses were about 9 and 2% for the 635 and 711 mm (25 and 28 inches) slump flow SCCs, respectively, after 20 minutes of hauling time. Beyond that time, an average increase of about 7% were experienced for each 20-minute increment in hauling time ranging from 40 to 80 minutes.

6.3.1.3.1.2   TxHy versus T21Hy

This section is intended to compare the slump flows obtained for the matrices transported for the same duration under different temperatures to those obtained under the control temperature (21 ± 2 °C (70 ± 3 °F)) of the equivalent hauling time.

As shown in Figures 6.3 and 6.4, when the hauling time varied from 20 to 40, 60, and 80 minutes, the self-consolidating concretes manufactured and hauled in different
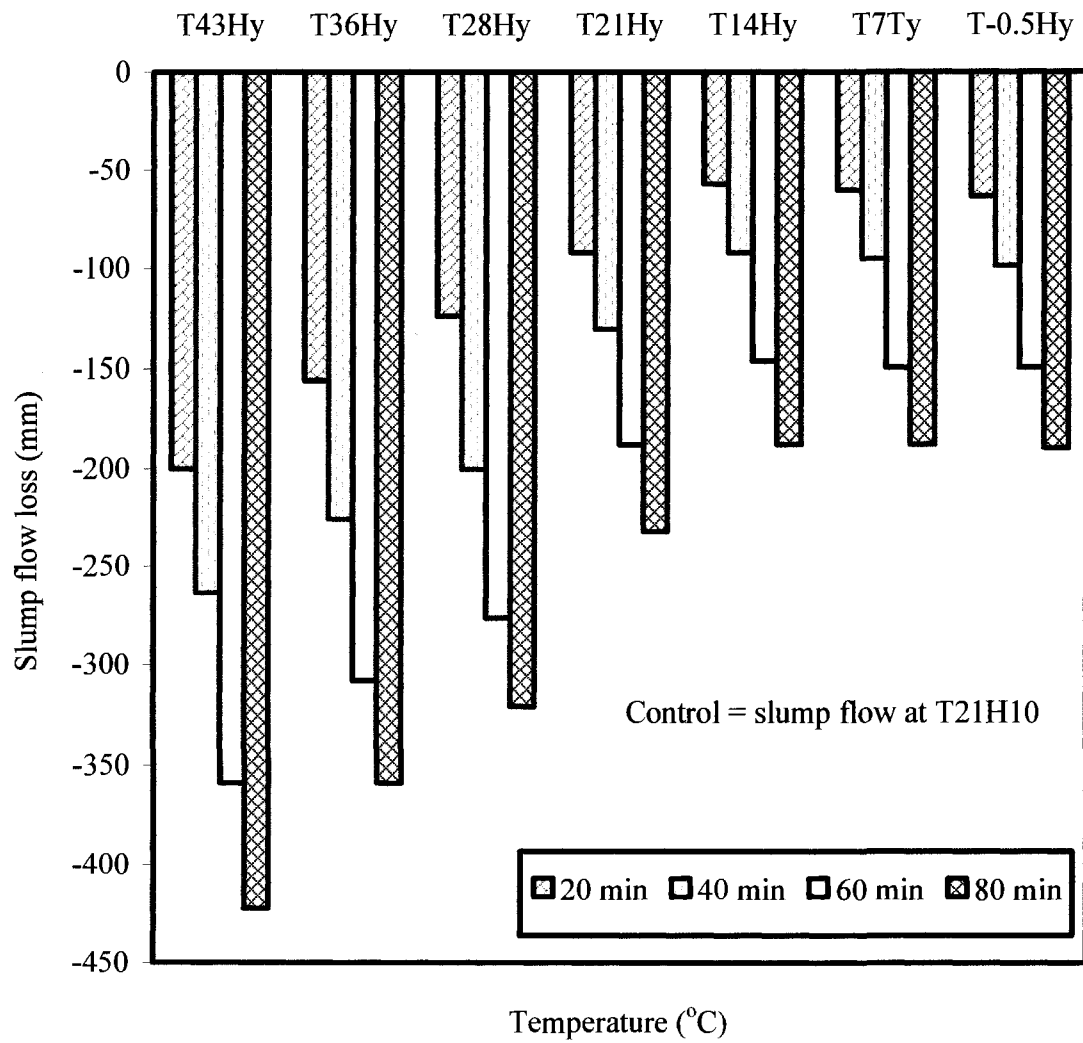
Figure 6.1: Slump flow loss of self-consolidating concrete mixture S7.B.SF25

at various TxHy conditions with respect to T21H10
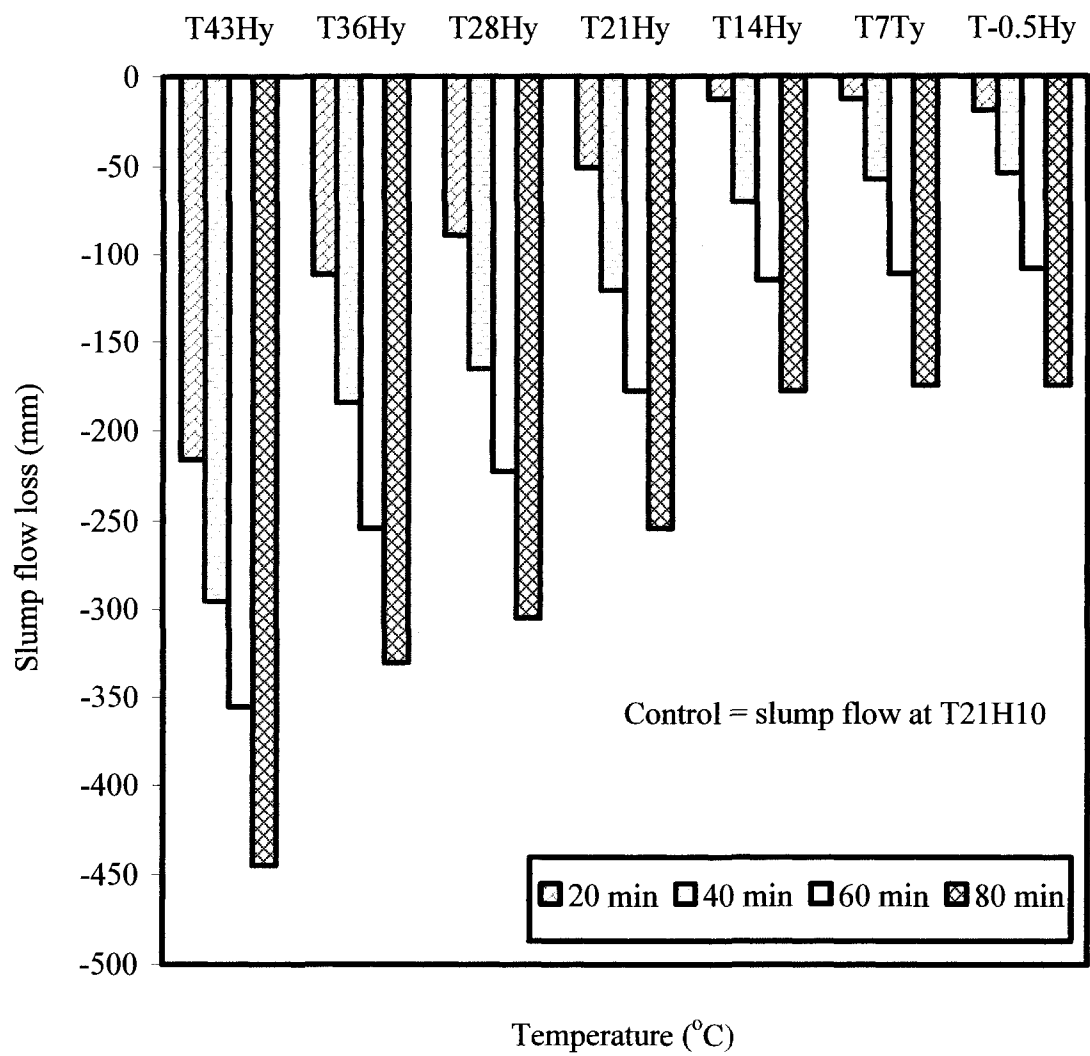
Figure 6.2: Slump flow loss of self-consolidating concrete mixture S7.B.SF28

at various TxHy conditions with respect to T21H10
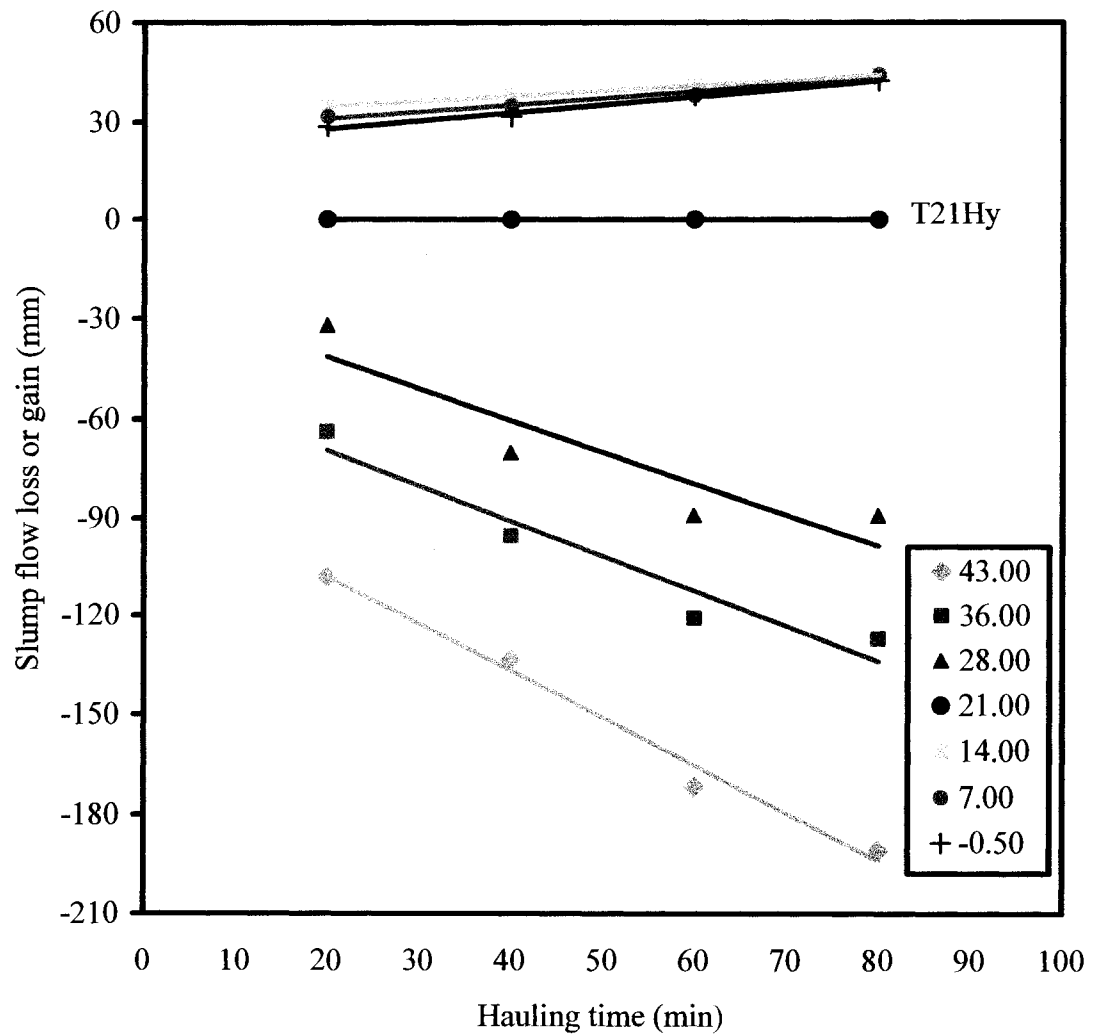
Figure 6.3: Slump flow loss or gain of self-consolidating concrete mixture S7.B.SF25

at various TxHy conditions with respect to T21Hy
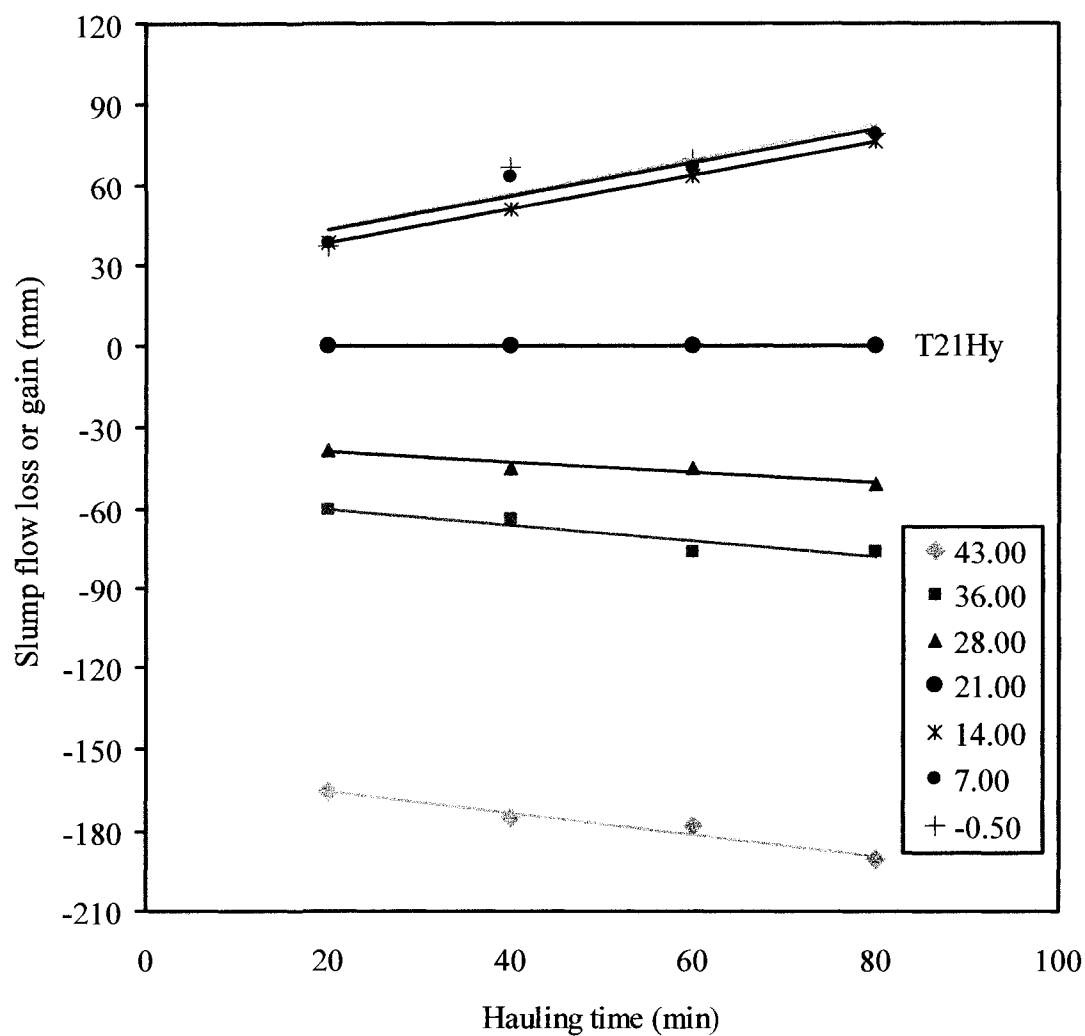
Figure 6.4: Slump flow loss or gain of self-consolidating concrete mixture S7.B.SF28

at various TxHy conditions with respect to T21Hy

temperatures experienced slump flow losses in hot conditions and gains in cold environments when compared to the equivalent concretes produced at control temperature. The reduction in slump flow increased with increases in hot temperature and hauling time.

When the self-consolidating concrete made for 635 mm (25 inches) slump flow was hauled for 20, 40, 60, and 80 minutes under 28 °C (83 °F), it experienced reductions in slump flow of about 5, 11, 14, and 14%, respectively, when compared to the slump flow of the equivalent matrix under T21Hy condition. Regardless of the hauling time, as the temperature of the materials and the mixing environment increased from 28 to 36 to 43 °C (83 to 96 to 109 °F), the same fresh matrices displayed additional losses of 5 and 8% in slump flow, respectively. The 711 mm (28 inches) slump flow concrete was less sensitive to hauling time. In comparing to the control condition, it exhibited average reductions in slump flow of 6, 10, and 25% at the temperatures of 28, 36, and 43 °C (83, 96, and 109 °F), respectively, at each selected hauling time.

Contrary to the results of hot temperatures, the unconfined workability of the selected self-consolidating concretes improved during mixing and hauling under a cold environment when compared to that of the control matrix in T21Hy. As it can be seen from Figures 6.3 and 6.4, the improvement in slump flow remained unaffected by the selected cold temperatures but slightly increased with hauling time. The increase was about 5% when the matrices were hauled for 20 minutes hauling time. Past that time, a marginal percentage increment of 1.5% per 20 minutes of hauling time was observed.

6.3.1.3.2 Change in flow rate

In general, the flow rate of the selected self-consolidating concretes increased

when the mixture was exposed to the combination of hauling time and temperature. The discussion on the flow rate was confined to TxHy versus T21H10 because, for the most part, the T_{50} times could not be measured when the transportation time was prolonged to 40 minutes or more in hot temperature due to severe losses in slump flow.

In the current section, the T_{50} times of self-consolidating concretes at TxHy condition were compared to those obtained at the control condition of T21H10, i.e. 2.79 and 1.85 seconds, for the 635 and 711 mm (25 and 28 inches) slump flow SCCs, respectively. Figures 6.5 and 6.6 document the effect of combined hauling time and temperature on the flow rate (or plastic viscosity per inference).

In elevated hot temperatures of 43 and 36 °C (109 and 96 °F) the T_{50} times of the selected self-consolidating concretes made for 635 mm (25 inches) were not available for measurement since their spreads were less than the recommended 508 mm (20 inches). At 28 °C (83 °F) the same mixture experienced 40% decrease in flow rate at 20 minutes of hauling time, when compared to the control T_{50} time. After that point, the spread of the concrete was less than 508 mm (20 inches) and the flow rate could not be measured. On the other hand, the 711 mm (28 inches) slump flow matrices prepared under 28 °C (83 °F) temperature condition displayed increases in flow rate of 52 and 57% after 20 and 40 minutes hauling, respectively, when compared to the control T_{50} time. The corresponding gains in flow rate were 63 and 114% at 36 °C (96 °F). Beyond the 40 minutes hauling time, the T_{50} times of the 711 mm (28 inches) slump flow mixture could not be measured due to severe losses in flow ability.

When self-consolidating concretes were hauled in cold environments the flow rate of the matrix decreased at the hauling times of 20 minutes or less. However, the longer
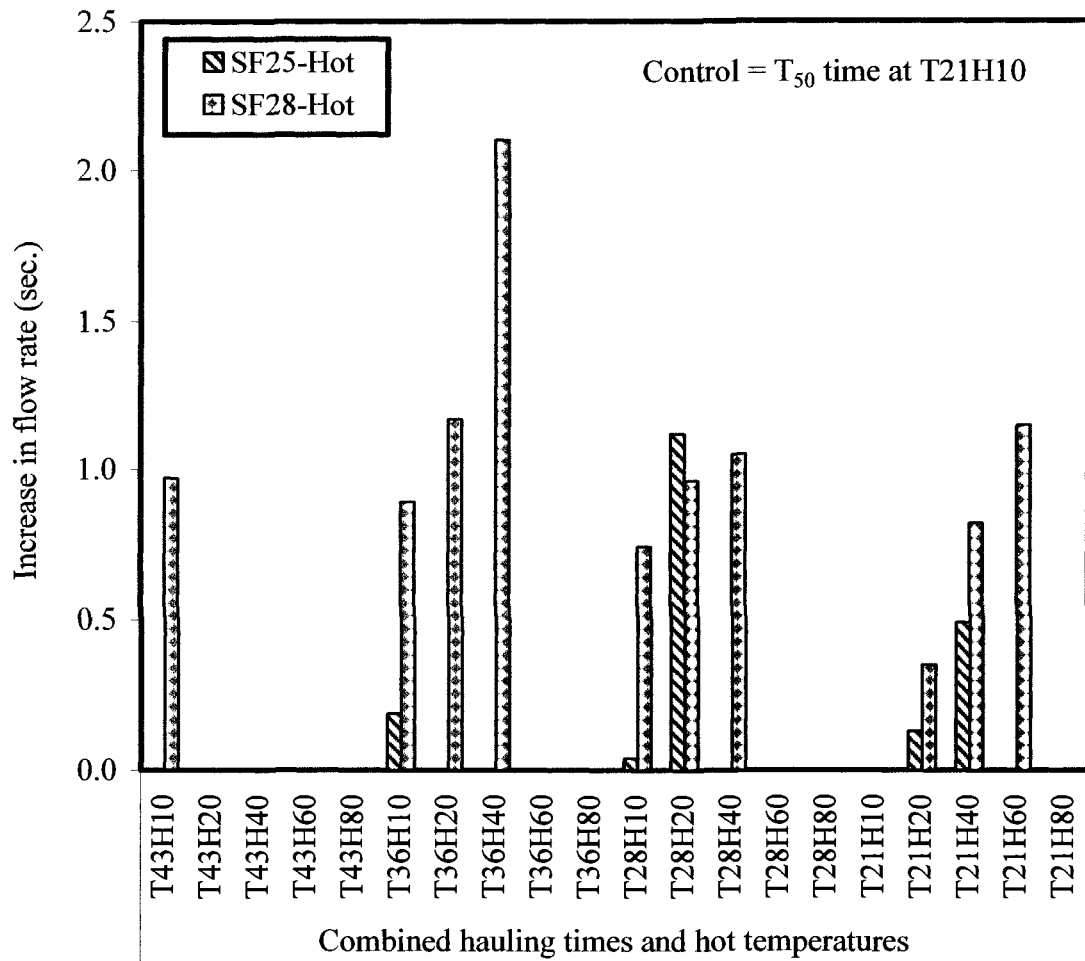
Figure 6.5: Influence of combined hauling time and hot temperature on the flow rate

of self-consolidating concrete
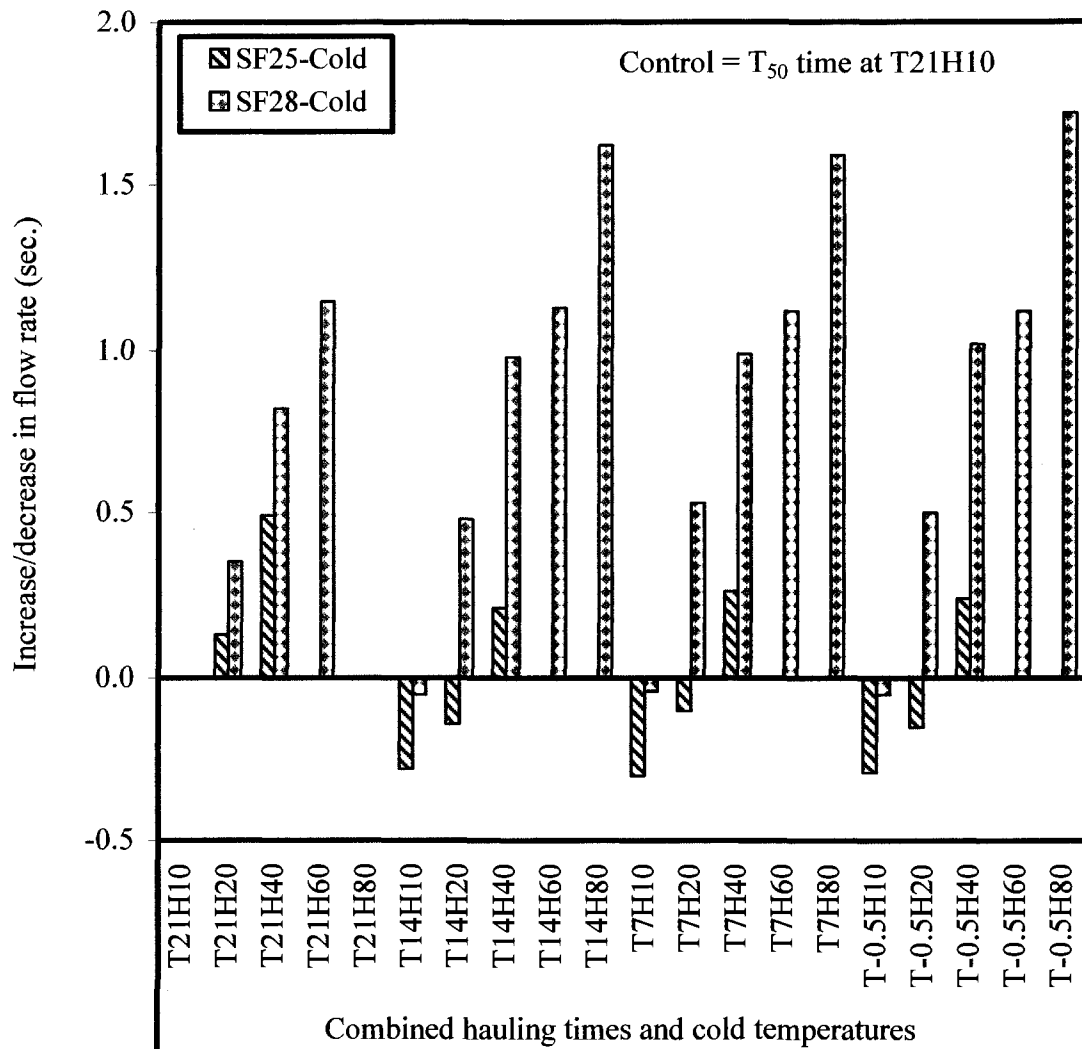
Figure 6.6: Influence of combined hauling time and cold temperature on the flow rate

of self-consolidating concrete

transportation times (i.e., from 20 to 80 min) induced significant increases in plastic viscosity. For the 635 mm (25 inches) slump flow concretes, the changes in flow rate were about -5 and 9 % after 20 and 40 minutes of hauling when compared to the T_{50} time of the equivalent concrete at the control condition of T21H10. The negative sign indicates a decrease in flow rate. As the transportation time was increased to 60 and 80 minutes, the T_{50} could not be measured due to severe losses in the mixture. The 711 mm (28 inches) slump flow concretes experienced 27, 54, 61, and 89% augmentations in flow rate at 20, 40, 60, and 80 minutes hauling times under cold temperature, respectively.

6.3.1.3.3   Change in dynamic stability

In general, the combination of the selected hauling times and temperatures variables enhanced the dynamic stability by changing the stability of the 711 mm (28 inches) matrices from stable (VSI = 1) to highly stable (VSI = 0). The 635 mm (25 inches) SCCs were not affected by the cold temperatures and always remained highly stable.

6.3.2   Mechanism of slump flow loss or gain

The fundamental mechanism of slump flow loss or gain induced by the combination of hauling time and hot or cold temperatures is illustrated by the flow chart of Figure 6.7. It can be explained through the increase or decrease in adsorption amount of admixture per specific surface area of concrete mortar (Ads/SSAm), the contribution of aggregate's moisture content, and the partial evaporation of mixing water.

As reported in Chapters 4 and 5, both the hauling time and temperature affected the specific surface area of concrete mortar, SSAm. The contribution of the hauling time to the increase in SSAm was attributed to the grinding of aggregate and cement particles,

267

Hot temperature

$$\dfrac{Ads_o + \Delta Ads_{tempHot}}{SSAp_o + \Delta SSAc_{tempHot}} - w$$

SCC or High slump concrete, $Ads_{hot}/SSAm_{hot}$

$$\dfrac{Ads_o + \Delta Ads_{haul}}{SSAm_o + \Delta SSAa + \Delta SSAc}$$

Hauling time

$$\dfrac{Ads_o + \Delta Ads_{haul}}{SSAm_o + \Delta SSAa + \Delta SSAc}$$

Cold temperature

$$\dfrac{Ads_o + \nabla Ads_{tempCold}}{SSAp_o + \Delta SSAc_{tempCold}} + w$$

SCC, $Ads_{cold}/SSAm_{cold}$
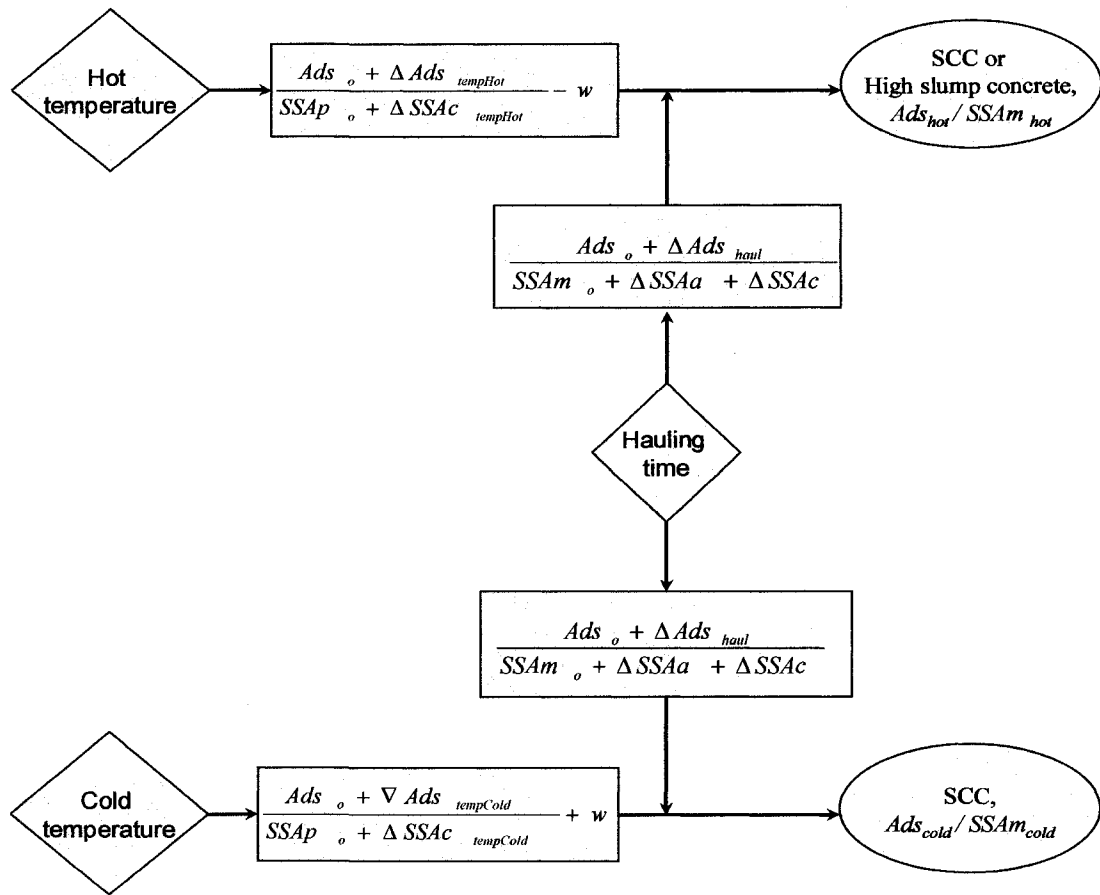
LEGEND

Ads_o = Adsorption amount of admixture at the control condition of T21H10

$SSAm_o$ = Specific surface area of concrete mortar at T21H10

$SSAp_o$ = Total specific surface area of concrete paste at T21H10

$\Delta SSAa$ = Increase in SSAm due to the grinding of aggregates and cement during hauling

$\Delta SSAc$ = Increase in SSAm or SSAp due to the growth of cement hydrated products

$\Delta Ads_{tempHot}$ = Increase in adsorption due to hot temperature

$\nabla Ads_{tempCold}$ = Decrease in adsorption due to cold temperature

$\Delta SSAc_{tempHot}$ = Increase in SSAm due to hot cement hydration

$\Delta SSAc_{tempCold}$ = Increase in SSAm due to cold cement hydration

w = mixing water contribution

Figure 6.7: Mechanism of slump flow loss induced by the combined hauling time

and temperature

and the growth of cement hydrated products, whereas the role of the temperature was explained through the growth of cement hydrated products.

The evolution of free admixture concentration in cement-water-superplasticizer solution at various hauling times or temperatures was determined by the ultraviolet-visible (UV/Vis) spectroscopy test. The test description and methodology are presented in Sections 2.3.13 and 3.3.1.1. Table 6.5 documents the UV/Vis test results.

Table 6.5: HRWRA concentration at various hauling times and temperatures

Hauling		Temperature		Mixing condition	Total concentration of admixture (g/L)
Time (min)	Concentration of admixture (g/L)	(°C)	Concentration of admixture (g/L)		
10	10.22	-0.5	14.70	T-0.5H80	63.42
20	15.06	7	18.78		
40	41.62	14	32.66		
60	48.18	21	34.27	T21H10	44.49
80	48.72	28	34.32		
100	42.04	36	35.83		
140	42.12	43	20.65	T43H80	69.37
180	36.57	50	15.57		

1 g = 0.0022 lb, 1 l = 33.814 oz, 1 °C = 9/5(°F - 32)

It summarized the influence of the selected hauling times and temperatures on HRWRA free concentration in a cement paste. As it can be seen from this table, for a given TxHy condition, the contribution of Ads to the fresh performance of the trial matrix could be derived from the superposition of Ads_{haul} from hauling time and Ads_{temp} from the temperature. Despite the increase in free admixture concentration, the total released carboxylic group (COO⁻) from the PC-HRWRA could not produce enough electrostatic

269

and steric hindrance repulsive forces in dispersing cement particles to avoid the loss in slump flow. Based on the prior evidence on the role of hauling time on specific surface area of concrete mortar, it can be concluded that the increase in SSAm was sufficient to overtake the increase in Ads. As a result, decreases in fresh properties of the fresh self-consolidating concretes were observed, indicating that the contribution of the specific surface area in slump flow loss was greater than that of the admixture adsorption.

The contribution of aggregate's moisture content to the final mixing water and the evaporation of a portion of the mixing water in presence of elevated temperatures are detailed in Sections 5.3.3.2 and 5.3.3.3, respectively.

Considering the abovementioned discussions, the slump flow loss or gain of self-consolidating concrete exposed to the combination of hauling times and extreme temperatures can be expressed in the following mathematical form:

$$Slump\ flow\ loss\ or\ gain = f\left\{\frac{Ads}{SSAm}, w\right\} = \frac{Ads_{haul} + Ads_{temp}}{SSAm_{haul} + SSAm_{temp}} + (w_o + w_t)_{temp} \qquad (6.1)$$

Where:

$\dfrac{Ads}{SSAm}$ = Adsorption amount of admixture per specific surface area of concrete mortar

Ads_{haul} = Adsorption amount of admixture induced by hauling time

Ads_{temp} = Adsorption amount of admixture induced by temperature

$SSAm_{haul}$ = Specific surface area of concrete mortar generated by hauling time

$SSAp_{temp}$ = Specific surface area of concrete paste generated by temperature

w = Contribution of the mixing water

w_o = Contribution of the mixing water at the control temperature

w_t = Contribution of the mixing water at the target temperature (could be ±)

6.3.3 Prediction of SCC slump flow at TxHy

The measured slump flow at the TxHy condition can be related to the target slump flow, the hauling time and the temperature by determining the most suitable statistical predictive equation using a 95% confidence level. The relationships are as follows:

In hot temperature:

$$SF_{measured} = -3.4021h_t - 7.0002t_h + 0.2354SF \tag{6.2}$$

$$\text{Or } SF_{measured} = ah_t + bt_h + cSF$$

In cold temperature:

$$SF_{measured} = -2.5162h_t - 0.2070t_c + 1.0314SF \tag{6.3}$$

$$\text{Or } SF_{measured} = ah_t + bt_c + cSF$$

Where:

$SF_{measured}$ = Slump flow measured at TxHy condition (mm)

h_t = Hauling time (minute), with 10 minutes $\leq h_t \leq$ 80 minutes

t_h = Hot temperature ($^{\circ}$C) with 21 $^{\circ}$C $\leq t_h \leq$ 43 $^{\circ}$C $\pm$ 2 $^{\circ}$C

t_c = Cold temperature ($^{\circ}$C) with -0.5 $^{\circ}$C $\leq t_c \leq$ 14 $^{\circ}$C $\pm$ 2 $^{\circ}$C

SF = Target slump flow (mm), with 635 mm $\leq SF \leq$ 711 mm $\pm$ 25 mm

The predictive equations were tested for accuracy using R^2 (regression value) and S (standard deviation). Correlations between the data predicted from the regression equations and the actual results were evaluated using F and T tests. The regression equations 6.2 and 6.3 produced R^2 and S values of 96.7% and 20.82 mm (0.82 inch); and 95% and 18.32 mm (0.72 inch), respectively, indicating a good relationship between the dependent variable (slump flow loss) and the independent variables (initial slump flows,

hauling times and hot or cold temperatures). F and T tests were performed to confirm the significance of coefficients a, b, c, and d in the regression models. The following results were found.

For Equation 6.2:

Prob(t) = 0.0000, 0.0000 and 0.0000, for a, b and c, respectively; Prob(F) = 0.0000.

For Equation 6.3:

Prob(t) = 0.000, 0.7458 and 0.000 for a, b and c, respectively; Prob(F) = 0.000.

In general, the F and T tests results indicated that all independent variables, i.e. hauling time, temperature, and initial slump flow had a similar influence on the predicted slump flow losses. The higher value of Prob(t) for the coefficient b of equation 6.3 indicates that the magnitude of the cold temperature has little influence in the prediction of the slump flow loss. Tables 6.6 and 6.7 present the actual versus the calculated slump flow loss values. The predictive equations yielded percentage errors less than 15%, for the most part, confirming a good relationship between the actual and the predicted slump flow loss.

6.3.4   Remediation of slump flow loss

The progressive use of new generation of plasticizers and superplasticizers in concrete industry has facilitated the control of slump loss caused by harsh mixing and hauling conditions. Several methods of remediation have been proposed by several investigations. Cooling or heating the concretes raw materials exposed to severe cold or hot weather, making concrete with a higher initial slump than required (overdosing), retempering with water or superplasticizer upon arrival of the concrete in a job site, and others can be noted[10,11,12]. For the purpose of this study, remediations by way of

Table 6.6: Actual versus calculated slump flow loss in combined hauling time and hot temperatures

Hauling time (min)	Temperature (°C)	Target slump flow (mm)	Actual slump flow (mm)	Calculated slump flow (mm)	% Error
20	43	651	451	435	3.53
20	43	724	508	525	-3.46
20	36	651	495	484	2.21
20	36	724	613	574	6.27
20	28	651	527	540	-2.47
20	28	724	635	630	0.71
20	21	651	559	589	-5.37
20	21	724	673	679	-0.97
40	43	651	387	367	5.15
40	43	724	429	457	-6.66
40	36	651	425	416	2.11
40	36	724	540	506	6.20
40	28	651	451	472	-4.66
40	28	724	559	562	-0.63
40	21	651	521	521	0.01
40	21	724	603	611	-1.41
60	43	651	292	299	-2.41
60	43	724	368	389	-5.85
60	36	651	343	348	-1.46
60	36	724	470	438	6.70
60	28	651	375	404	-7.73
60	28	724	502	494	1.50
60	21	651	464	453	2.38
60	21	724	546	543	0.47
80	43	651	229	231	-0.87
80	43	724	279	321	-15.23
80	36	651	292	280	4.12
80	36	724	394	370	5.97
80	28	651	330	336	-1.80
80	28	724	419	426	-1.78
80	21	651	419	385	8.13
80	21	724	470	475	-1.15

1 mm = 0.03937 inch, °C = 5/9(oF-32)

Table 6.7: Actual versus calculated slump flow loss in combined hauling time and cold temperatures

Hauling time (min)	Temperature (°C)	Target slump flow (mm)	Actual slump flow (mm)	Calculated slump flow (mm)	% Error
20	14	651	594	618	-4.07
20	14	724	711	693	2.46
20	7	651	591	620	-4.85
20	7	724	711	695	2.26
20	-0.5	651	588	621	-5.65
20	-0.5	724	710	696	1.90
40	14	651	559	568	-1.59
40	14	724	654	643	1.66
40	7	651	556	569	-2.40
40	7	724	667	645	3.36
40	-0.5	651	552	571	-3.42
40	-0.5	724	670	646	3.56
60	14	651	505	518	-2.49
60	14	724	610	593	2.81
60	7	651	502	519	-3.39
60	7	724	613	594	3.05
60	-0.5	651	502	521	-3.70
60	-0.5	724	616	596	3.27
80	14	651	464	467	-0.70
80	14	724	546	543	0.64
80	7	651	464	469	-1.01
80	7	724	549	544	0.92
80	-0.5	651	462	470	-1.78
80	-0.5	724	549	546	0.63

1 mm = 0.03937 inch, °C = 5/9(oF-32)

overdosing and retempering were adopted. The target remediated fresh properties were those obtained at control condition T21H10. The HRWRA and VMA optimum dosages at the control condition were 209.15 and 26.14 ml/100 kg (3.2 and 0.4 oz/cwt), and 254.90 and 32.68 ml/100 kg (3.9 and0.5 oz/cwt) for the mixtures S7.B.SF25 and S7.B.SF28, respectively.

6.3.4.1   Overdosing method of remediation

The overdosing method of remediation consisted of using a higher initial amount of admixtures than usually required under the control condition in order to compensate for the increased yield stress and decreased plastic viscosity created by the combined hauling time and extreme temperature. The discussion on the optimum HRWRA and VMA dosages necessary for the overdosing remediation is presented below.

6.3.4.1.1   Optimum HRWRA requirement for the overdosing remediation

Tables 6.8 through 6.11 present the optimum overdosed amount of HRWRA needed to remediate the adverse effect of the combined hauling time and temperature on plastic self-consolidating concrete. Figures 6.8 and 6.9 present the required HRWRA dosages for different combinations of hauling time and temperature.

In cold temperature the HRWRA dosages necessary for the overdosing remediation were unaffected by the magnitude of the selected temperature, but increased with hauling time. In comparing to the equivalent control dosage, the optimized amount of HRWRA for the overdosing remediation of 635 mm (25 inches) slump flow SCCs increased on average by 6, 9, 19, and 28% after 20, 40, 60, and 80 minutes of hauling, respectively. The corresponding augmentations for the matrices prepared for 711 mm (28 inches) slump flow were 5, 8, 15, and 23%, respectively.

Table 6.8: Overdosing remediation of fresh properties of SCC hauled for 20 minutes at various temperatures

Temperature (°C)	Mix designation	HRWRA (ml/100 kg)	VMA (ml/100 kg)	Measured slump flow (mm)	T_{50} (sec.)	VSI	J ring value (mm)
43.00	S7.B.SF25	326.80	45.75	652	2.18	0	49
	S7.B.SF28	411.76	71.90	718	2.30	1	32
36.00	S7.B.SF25	267.97	39.22	648	2.28	0	49
	S7.B.SF28	307.19	58.82	718	2.12	1	44
28.00	S7.B.SF25	241.83	26.14	652	2.45	0	30
	S7.B.SF28	281.05	32.68	721	2.25	1	29
21.00	S7.B.SF25	241.83	26.14	638	2.29	0	29
	S7.B.SF28	273.83	32.68	711	2.20	1	25
14.00	S7.B.SF25	222.22	26.14	645	2.50	0	22
	S7.B.SF28	267.97	32.68	718	2.38	1	19
7.00	S7.B.SF25	222.22	26.14	648	2.54	0	25
	S7.B.SF28	267.97	32.68	721	2.25	1	22
-0.50	S7.B.SF25	222.22	26.14	638	2.75	0	10
	S7.B.SF28	267.97	32.68	718	2.60	1	19

°C = 5/9(°F - 32), 1 ml/100 kg = 0.0153 oz/cwt, 1 mm = 0.03967 inch

Table 6.9: Overdosing remediation of fresh properties of SCC hauled for 40 minutes at various temperatures

Temperature (°C)	Mix designation	HRWRA (ml/100 kg)	VMA (ml/100 kg)	Measured slump flow (mm)	T_{50} (sec.)	VSI	J ring value (mm)
43.00	S7.B.SF25	352.94	45.75	648	2.28	0	46
	S7.B.SF28	437.91	84.97	724	2.20	1	38
36.00	S7.B.SF25	294.12	39.22	641	2.16	0	51
	S7.B.SF28	346.41	71.90	718	2.18	0	47
28.00	S7.B.SF25	274.51	26.14	648	2.31	0	25
	S7.B.SF28	307.19	32.68	724	2.12	1	25
21.00	S7.B.SF25	260.79	26.14	638	2.31	0	29
	S7.B.SF28	306.43	32.68	711	2.19	1	25
14.00	S7.B.SF25	228.76	26.14	648	2.25	0	25
	S7.B.SF28	274.51	32.68	718	2.28	1	19
7.00	S7.B.SF25	228.76	26.14	648	2.38	0	25
	S7.B.SF28	274.51	32.68	718	2.10	1	25
-0.50	S7.B.SF25	228.76	26.14	645	2.92	0	10
	S7.B.SF28	274.51	32.68	721	2.50	1	22

°C = 5/9(°F - 32), 1 ml/100 kg = 0.0153 oz/cwt, 1 mm = 0.03967 inch

Table 6.10: Overdosing remediation of fresh properties of SCC hauled for 60 minutes at various temperatures

Temperature (^{o}C)	Mix No.	HRWRA (ml/100 kg)	VMA (ml/100 kg)	Measured slump flow (mm)	T_{50} (sec.)	VSI	J ring value (mm)
43.00	S7.B.SF25	385.62	52.29	648	2.03	0	44
	S7.B.SF28	464.05	91.50	711	2.48	1	25
36.00	S7.B.SF25	320.26	45.75	635	2.16	0	41
	S7.B.SF28	379.08	78.43	718	2.25	1	44
28.00	S7.B.SF25	294.12	26.14	648	2.26	0	9
	S7.B.SF28	339.87	39.22	728	2.09	1	30
21.00	S7.B.SF25	286.87	26.14	641	2.38	0	32
	S7.B.SF28	339.03	39.22	724	2.22	1	32
14.00	S7.B.SF25	248.37	26.14	648	2.38	0	13
	S7.B.SF28	294.12	39.22	718	2.35	1	19
7.00	S7.B.SF25	248.37	26.14	645	2.22	0	3
	S7.B.SF28	294.12	39.22	721	2.31	1	26
-0.50	S7.B.SF25	248.37	26.14	648	3.05	0	13
	S7.B.SF28	294.12	39.22	715	2.54	1	3

^{o}C = 5/9(^{o}F - 32), 1 ml/100 kg = 0.0153 oz/cwt, 1 mm = 0.03967 inch

Table 6.10: Overdosing remediation of fresh properties of SCC hauled for 80 minutes at various temperatures

Temperature (^{o}C)	Mix designation	HRWRA (ml/100 kg)	VMA (ml/100 kg)	Measured slump flow (mm)	T_{50} (sec.)	VSI	J ring value (mm)
43.00	S7.B.SF25	418.30	58.82	635.00	2.25	0	44.45
	S7.B.SF28	503.27	104.58	717.55	2.15	1	38.10
36.00	S7.B.SF25	352.94	52.29	644.65	2.19	0	41.40
	S7.B.SF28	418.30	91.50	714.50	2.25	1	41.40
28.00	S7.B.SF25	320.26	26.14	652.27	2.08	0	29.97
	S7.B.SF28	372.55	52.29	723.90	2.05	1	34.80
21.00	S7.B.SF25	312.95	26.14	641.35	2.32	0	31.75
	S7.B.SF28	371.63	52.29	711.20	2.25	1	25.40
14.00	S7.B.SF25	267.97	26.14	647.70	2.50	0	12.70
	S7.B.SF28	313.73	45.75	714.50	2.25	1	22.35
7.00	S7.B.SF25	267.97	26.14	647.70	2.44	0	19.05
	S7.B.SF28	313.73	45.75	720.85	2.31	1	26.16
-0.50	S7.B.SF25	267.97	26.14	647.70	2.60	0	3.05
	S7.B.SF28	313.73	45.75	717.55	2.50	0.5	12.70

Figure 6.8: Optimum dosage of HRWRA for the overdosing remediation of slump flow
loss due to the combined hauling time and temperature: Mixture S7.B.SF25

Figure 6.9: Optimum dosage of HRWRA for the overdosing remediation of slump flow
loss due to the combined hauling time and temperature: Mixture S7.B.SF28

In hot temperatures, the demand in superplasticizer for the overdosing remediation increased with increases in both hauling time and temperature. When the trial self-consolidating concretes were transported for 20 minutes, the remediation of the 635 and 711 mm (25 and 28 inches) slump flow matrices necessitated increases in HRWRA dosage of 16, 28, and 57%; and 10, 21, and 62% at 28, 36, and 43 °C (83, 96, and 109 °F), respectively, when compared to the required superplasticizer dosages obtained under the adopted control condition. The corresponding increases were 32, 41 and 69%, and 21, 36, and 72% after 40 minutes of hauling time; 41, 54, and 85% and 34, 49, and 83% after 60 minutes of hauling time; and 54, 70, and 100%; and 47, 65, and 98% after 80 minutes of hauling time.

The increase in demand for HRWRA amount was basically due to the decrease in the ratio Ads/SSAm. As was the case for the hauling time, or when temperature is considered separately, the overdosing remediation consisted to achieve by trial and error the optimum admixture dosage so that (Ads/SSAm) at the end of the mixing and hauling time became equal or similar to (Ads$_o$/SSAm$_o$) at the control condition T21H10. The idea is translated mathematically through Equations 6.4 and 6.5 given below:

- *At the control condition T21H10:*

$$\left(\frac{Ads}{SSAm}\right)_{control} = \frac{Ads_o}{SSAm_o} \tag{6.4}$$

- *At the target condition TxHy:*

$$\left(\frac{Ads}{SSAm}\right) = \underbrace{\frac{Ads_{haul} + Ads_{temp}}{SSAm_{haul} + SSAp_{temp}} + (w_o + w_t)_{temp}}_{A} + \underbrace{\frac{\Delta Ads_{haul+temp}}{SSAm_{haul} + SSAp_{temp}}}_{B} \tag{6.5}$$

$\boxed{A}$ Characterizes the slump flow loss

$\boxed{B}$ Characterizes the slump flow restoration

The terms Ads, Ads_o, SSAm, $SSAm_o$, Ads_{haul}, Ads_{temp}, $SSAm_{haul}$, $SSAp_{temp}$, and $(w_o + w_t)_{temp}$ are defined in equation 6.1. $\Delta Ads_{haul+temp}$ corresponds to the increase in adsorption amount of HRWRA generated by the additional amount of superplasticizer with respect to the control dosage. This supplementary adsorption was required to compensate for the increased in specific surface area $(SSAm_{haul} + SSAp_{temp})$ and the variation in aggregate's water content, $(w_o + w_t)_{temp}$. The additional amount of adsorption enhanced electrostatic and steric hindrance repulsive forces between cement particles to meet the target fresh properties of the self-consolidating concrete at the completion of mixing and hauling in extreme temperatures.

6.3.4.1.2   Optimum VMA requirement for the overdosing remediation

The optimum dosage of viscosity modifying admixture required for the overdosing remediation are displayed in Tables 6.8 through 6.11. Figures 6.10 and 6.11 present the increase in VMA optimum dosages as related to the selected hauling times and temperatures.

In comparing to the equivalent control VMA dosage, the 635 mm (25 inches) self-consolidating concrete did not required any change in its initial VMA dosage in attaining the target fresh properties, when temperatures were between -0.5 and 28 $^{\circ}$C (31 and 83 $^{\circ}$F), for any of the selected hauling times. However, when the temperatures were elevated to 36 or 43 $^{\circ}$C (96 or 109 $^{\circ}$F) the demand in VMA increased by 50 and 75% at 20 and 40 minutes hauling times, respectively. Further increases in VMA dosages were required as the hauling times were prolonged in these elevated temperatures. Indeed,
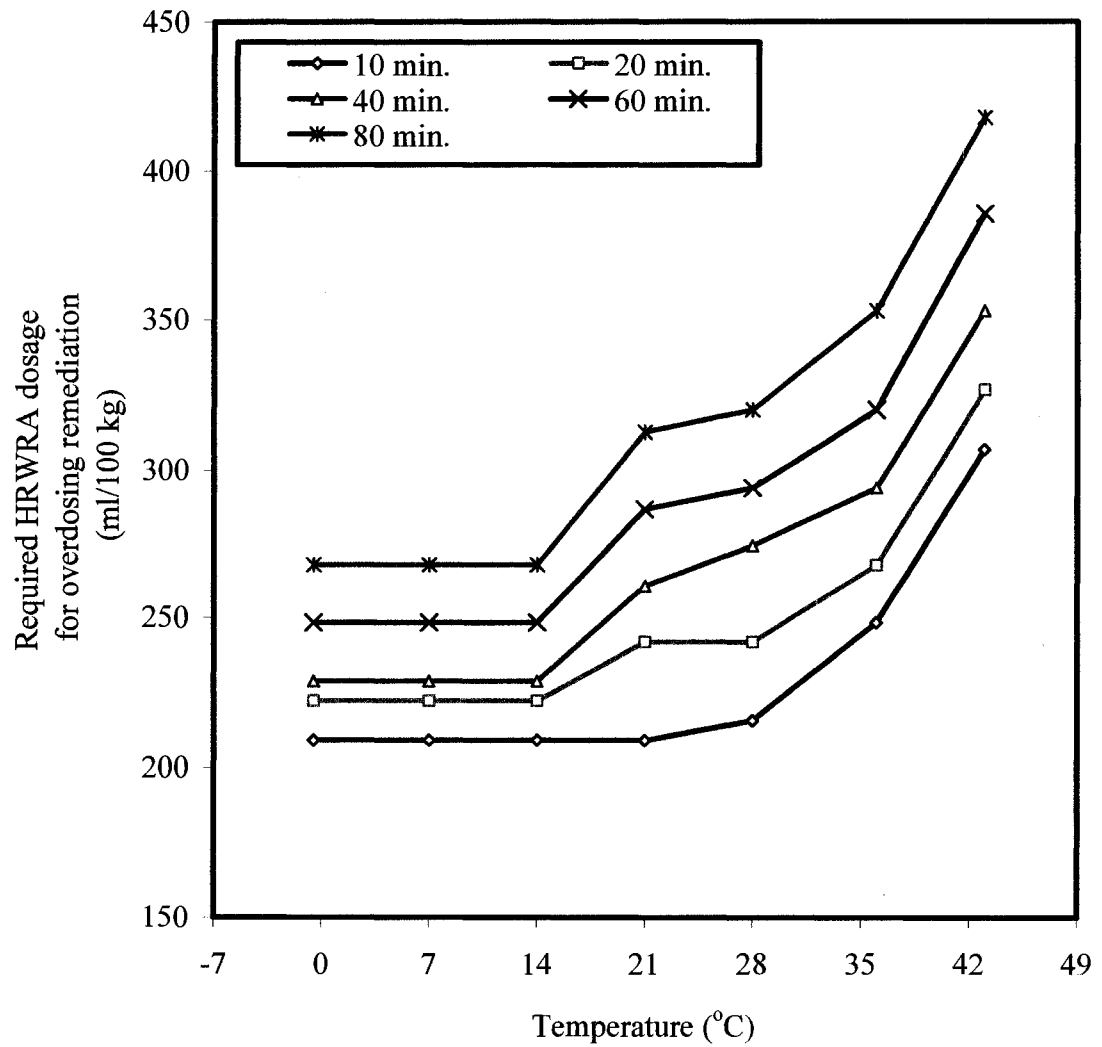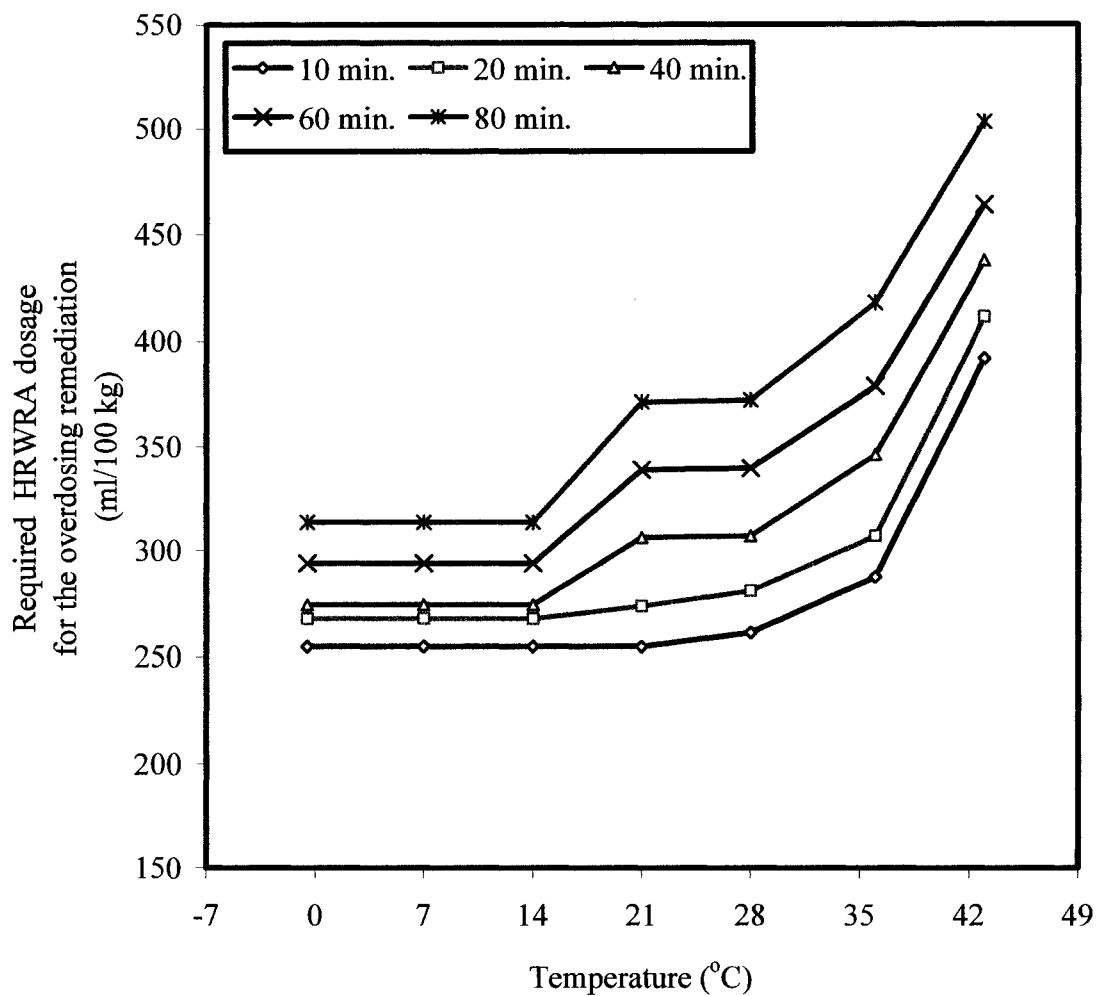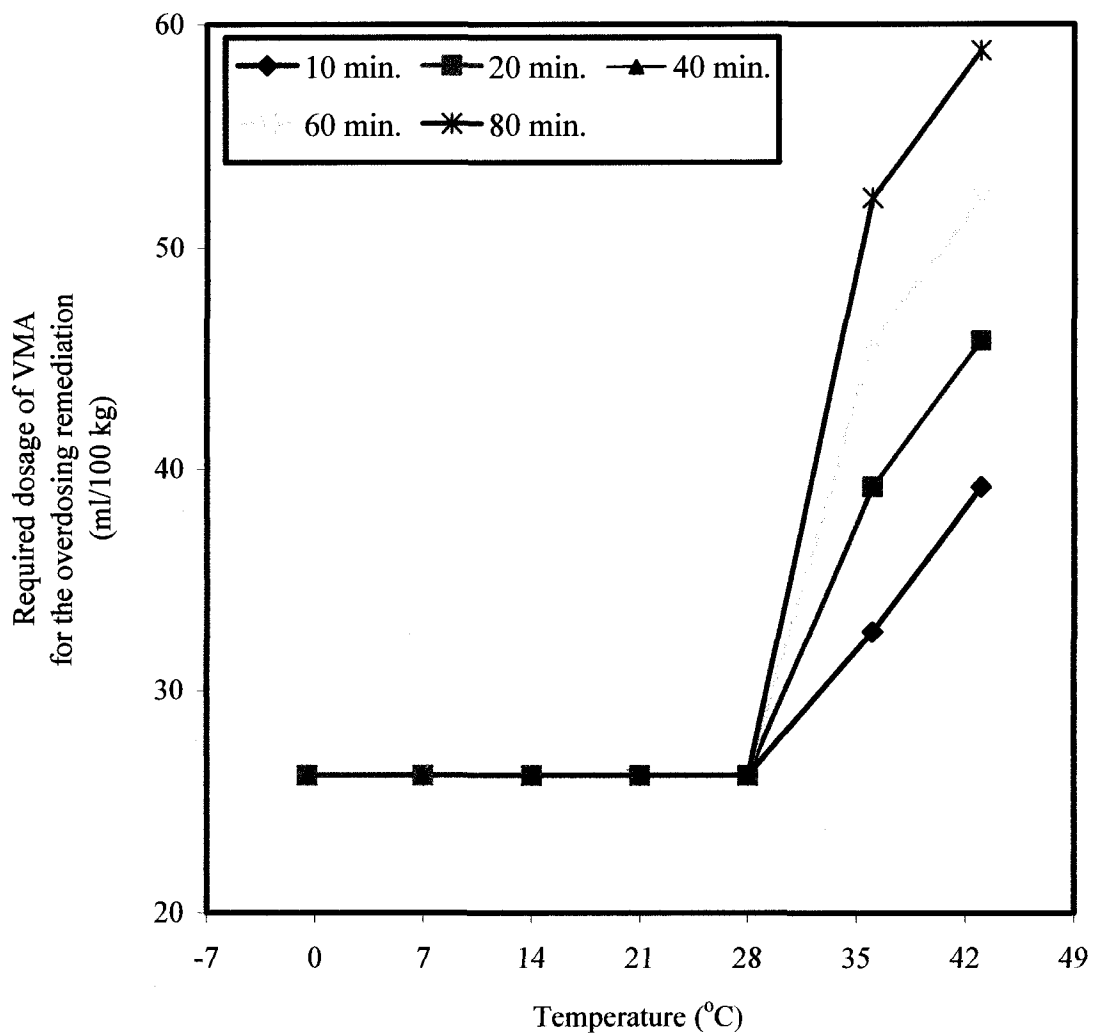
Figure 6.10: Optimum dosage of VMA for the overdosing remediation of slump flow loss
due to the combined hauling time and temperature: Mixture S7.B.SF25
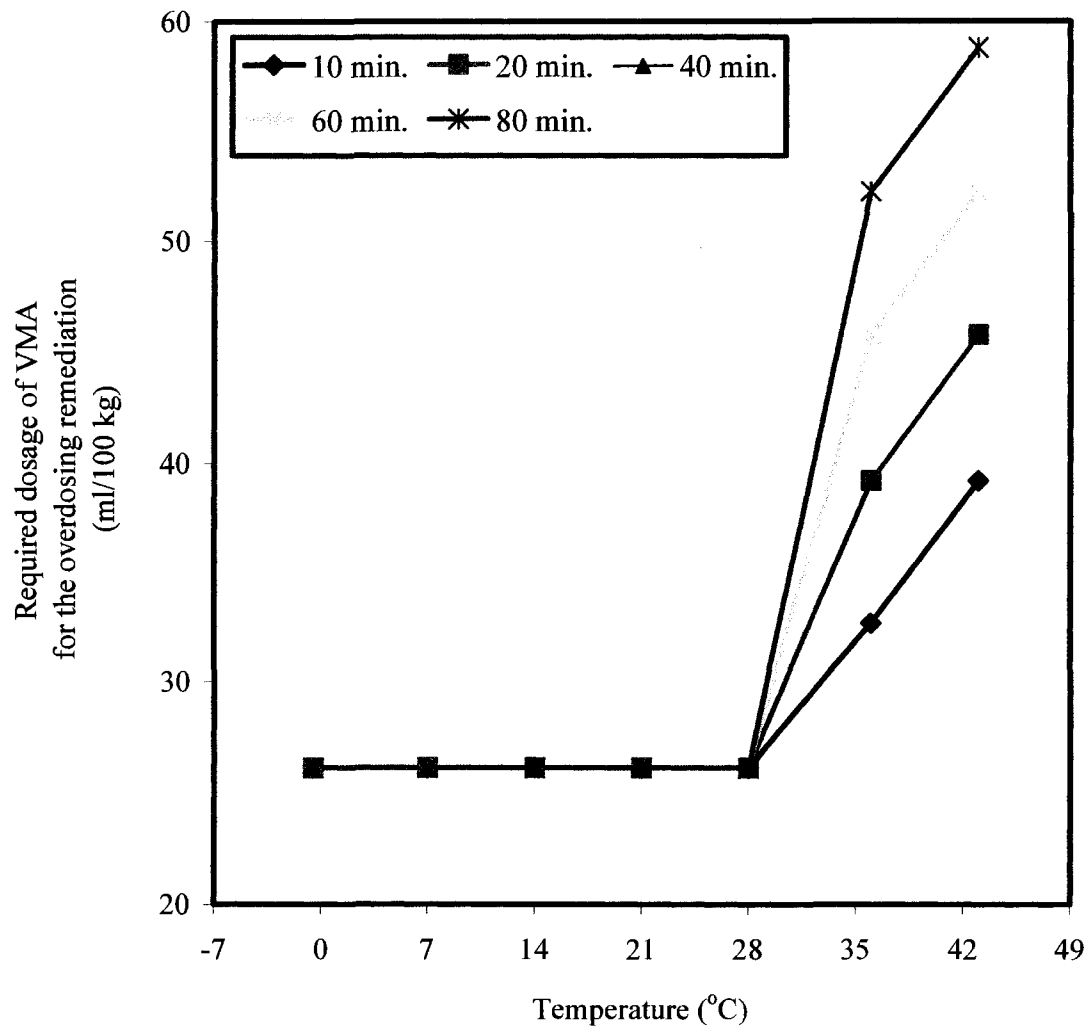
Figure 6.11: Optimum dosage of VMA for the overdosing remediation of slump flow loss
due to the combined hauling time and temperature: Mixture S7.B.SF28

increases of 75 and 100%; and 100 and 126% in VMA amount were needed for the overdosing remediation of the same matrix hauled for 60 and 80 minutes at temperature of 36 and 43 °C (96 and 109 °F), respectively.

Similar findings were observed as the slump flow was increased to 28 inches (711 mm). In comparing to the equivalent control VMA dosage, the trial self-consolidating concretes did not require any additional VMA at 20 and 40 minutes hauling times when prepared in temperatures ranging from -0.5 to 28 °C (31 to 83 °F). However, the demand in VMA to compensate for the increased plastic viscosity and decreased dynamic segregation resistance augmented as the hauling times were increased. After 60 and 80 minutes of hauling times, the increases in VMA dosage were 20 and 50%, respectively. When the temperature were elevated to 36 and 43 °C (96 and 109 °F), the remediation of fresh properties necessitated increases of about 80 and 121%, 121 and 162%, 141 and 181%, and 181 and 221% at 20, 40, 60, and 80 minutes of hauling times, respectively, when compared to the equivalent control VMA dosage.

6.3.4.1.3   Prediction of optimized overdosed amount of HRWRA and VMA

The dosages requirement of admixtures for the overdosing remediation of slump flow loss induced by the combined hauling time and temperature were predicted using statistical modeling. The most suitable predictive relationships between the optimized dosages of HRWRA or VMA, as dependent variables, and the target slump flow, hauling time and hot or cold temperatures, as independent variables, are as follows:

In hot temperature

$$HR_{overd}hot = \exp(0.004367h_t + 0.015477t_h + 0.00234SF + 3.483835) \qquad (6.6)$$

$$\text{Or } HR_{overd}hot = \exp(ah_t + bt + cSF + d)$$

286

$$VMA_{overd}hot = \exp(0.00624h_t + 0.04027t_h + 0.00719SF - 2.75206) \qquad (6.7)$$

Or $VMA_{overd}hot = \exp(ah_t + bt + cSF + d)$

In Cold temperature

$$HR_{overd}cold = \exp(0.002839h_t - 0.002410t_c + 0.002353SF + 3.83327) \qquad (6.8)$$

Or $HR_{overd}cold = \exp(ah_t + bt + cSF + d)$

$$VMA_{overd}cold = \exp(0.004252h_t - 9x10^{-17}t_c + 0.005169SF - 0.330418) \qquad (6.9)$$

Or $VMA_{overd}cold = \exp(ah_t + bt + cSF + d)$

Where:

$HR_{overd}hot$ and $HR_{overd}cold$ = Required dosages of HRWRA for the overdosing remediation of slump flow loss in hot and cold temperatures (ml/100 kg),.

$VMA_{overd}hot$ and $VMA_{overd}cold$ = Required dosages of VMA for the overdosing remediation of slump flow loss in hot and cold temperatures (ml/100 kg), respectively.

SF = Target slump flow in hot temperature condition (mm),

        with 635 mm $\leq$ SF $\leq$ 711 mm $\pm$ 25 mm

t_h = Hot temperature (°C), with 21 °C $\leq$ t_t $\leq$ 43 °C $\pm$ 2 °C

t_c = Cold temperature (°C), with -0.5 °C $\leq$ t_t $\leq$ 14 °C $\pm$ 2 °C

The predictive equations were tested for accuracy using R^2 (the coefficient of multiple determination) and S (average standard deviation). Correlations between the data predicted from the regression equations and the actual test results were evaluated using F and T tests. The following results were found.

- *For Equation 6.6:*

R^2 = 92.35%, S = 18.82 ml/100 kg (0.29 oz/cwt)

287

Prob(t) = 0.000, 0.000, 0.000, and 0.000 for a, b, c, and d, respectively; Prob(F) = 0.000.

- *For Equation 6.7:*

R^2 = 93.00%, S = 6.29 ml/100 kg (0.096 oz/cwt)

Prob(t) = 0.000, 0.000, 0.000, and 0.000 for a, b, c, and d, respectively; Prob(F) = 0.000.

- *For Equation 6.8:*

R^2 = 98.07%, S = 4.42 ml/100 kg (0.068 oz/cwt)

Prob(t) = 0.000, 0.000, 0.000, and 0.000 for a, b, c, and d, respectively; Prob(F) = 0.000.

- *For Equation 6.9:*

R^2 = 88.00%, S = 2.61 ml/100 kg (0.04 oz/cwt)

Prob(t) = 0.000, 1.000, 0.000, and 0.000 for a, b, c, and d, respectively; Prob(F) = 0.000.

Equations 6.6, 6.7, 6.8, and 6.9 produced R^2 and S values indicative of good relationship between the dependent variable (HRWRA or VMA optimum dosage). In general, the F and T tests results indicated that the hauling time, the temperature and the target slump flow had similar influence on the predictive HRWRA and VMA optimum dosages. In equation 6.9, Prob (t) = 1.0 for the coefficient b, indicates that the predicted slump flow loss was independent from the selected cold temperatures. Tables 6.12 through 15 document the actual versus the calculated required optimized admixtures dosages for the overdosing remediation of slump flow loss. The predictive equations yielded percentage errors ranging from 1 to 10% for the HRWRA, and 1 to 13% for the VMA, confirming a good relationship between the actual and calculated admixture dosages.

6.3.4.2   Retempering method of remediation

Retempering concrete consists of adding extra water or admixtures just before its

288

Table 6.12: Actual versus calculated HRWRA optimum dosage for the
overdosing remediation in combined hauling time and hot temperatures

Hauling time (min)	Temperature (^{o}C)	Target slump flow (mm)	Actual HRWRA dosage (ml/100	Calculated HRWRA dosage (ml/100 kg)	% Error
20	43	651	326.8	317	2.93
20	43	724	411.76	376	8.61
20	36	651	267.97	285	-6.22
20	36	724	307.19	338	-9.92
20	28	651	241.83	251	-4.00
20	28	724	281.05	298	-6.15
20	21	651	241.83	226	6.68
20	21	724	273.83	268	2.24
40	43	651	352.94	346	1.92
40	43	724	437.91	411	6.23
40	36	651	294.12	311	-5.61
40	36	724	346.41	368	-6.37
40	28	651	274.51	274	0.02
40	28	724	307.19	326	-5.98
40	21	651	260.79	246	5.57
40	21	724	306.43	292	4.67
60	43	651	385.62	378	2.03
60	43	724	464.05	448	3.43
60	36	651	320.26	339	-5.85
60	36	724	379.08	402	-6.08
60	28	651	294.12	300	-1.83
60	28	724	339.87	355	-4.53
60	21	651	286.87	269	6.32
60	21	724	339.03	319	5.97
80	43	651	418.3	412	1.44
80	43	724	503.27	489	2.83
80	36	651	352.94	370	-4.81
80	36	724	418.3	439	-4.90
80	28	651	320.26	327	-2.06
80	28	724	372.55	388	-4.07
80	21	651	312.95	293	6.28
80	21	724	371.63	348	6.39

1 mm = 0.03937 inch; 1 ml/ 100 kg = 0.0153 oz/cwt

Table 6.13: Actual versus calculated VMA optimum dosage for the overdosing remediation in combined hauling time and hot temperatures

Hauling time (min)	Temperature (°C)	Target slump flow (mm)	Actual VMA dosage (ml/100	Calculated VMA dosage (ml/100 kg)	% Error
20	43	651	45.75	43.90	4.04
20	43	724	71.90	74.21	-3.22
20	36	651	39.22	33.12	15.56
20	36	724	58.82	55.98	4.82
20	28	651	26.08	24.00	7.99
20	28	724	32.60	40.56	-24.43
20	21	651	26.08	18.10	30.59
20	21	724	32.60	30.60	6.14
40	43	651	45.75	49.54	-8.28
40	43	724	84.97	83.74	1.45
40	36	651	39.22	37.37	4.72
40	36	724	71.90	63.17	12.15
40	28	651	26.08	27.08	-3.82
40	28	724	32.60	45.77	-40.40
40	21	651	26.08	20.42	21.69
40	21	724	32.60	34.53	-5.91
60	43	651	52.29	55.89	-6.89
60	43	724	91.50	94.48	-3.26
60	36	651	45.75	42.16	7.84
60	36	724	78.43	71.27	9.12
60	28	651	26.08	30.55	-17.14
60	28	724	39.22	51.64	-31.67
60	21	651	26.08	23.05	11.63
60	21	724	39.22	38.96	0.67
80	43	651	58.82	63.07	-7.22
80	43	724	104.58	106.61	-1.94
80	36	651	52.29	47.57	9.02
80	36	724	91.50	80.42	12.11
80	28	651	26.08	34.47	-32.17
80	28	724	52.29	58.27	-11.44
80	21	651	26.08	26.00	0.29
80	21	724	52.29	43.96	15.94

1 mm = 0.03937 inch; 1 ml/ 100 kg = 0.0153 oz/cwt

Table 6.14: Actual versus calculated HRWRA optimum dosage for the overdosing remediation in combined hauling time and cold temperatures

Hauling time (min)	Temperature (°C)	Target slump flow (mm)	Actual HRWRA dosage (ml/100	Calculated VMA dosage (ml/100 kg)	% Error
20	14	651	209.15	219	-4.66
20	14	724	254.9	260	-1.98
20	7	651	222.22	223	-0.18
20	7	724	267.97	264	1.35
20	-0.5	651	228.76	227	0.91
20	-0.5	724	274.51	269	1.94
40	14	651	228.76	232	-1.28
40	14	724	274.51	275	-0.22
40	7	651	235.29	236	-0.14
40	7	724	281.05	280	0.44
40	-0.5	651	241.83	240	0.79
40	-0.5	724	287.58	285	0.93
60	14	651	248.37	245	1.27
60	14	724	294.12	291	0.99
60	7	651	248.37	249	-0.41
60	7	724	294.12	296	-0.69
60	-0.5	651	254.9	254	0.37
60	-0.5	724	300.65	302	-0.30
80	14	651	267.97	260	3.14
80	14	724	313.73	308	1.76
80	7	651	261.44	264	-0.97
80	7	724	307.19	313	-2.04
80	-0.5	651	267.97	269	-0.30
80	-0.5	724	313.73	319	-1.73

1 mm = 0.03937 inch; 1 ml/ 100 kg = 0.0153 oz/cwt

Table 6.15: Actual versus predicted VMA optimum dosage for the overdosing remediation in combined hauling time and cold temperatures

Hauling time (min)	Temperature (°C)	Target slump flow (mm)	Actual VMA dosage (ml/100	Calculated VMA dosage (ml/100 kg)	% Error
20	14	651	26.08	23	13.15
20	14	724	32.6	33	-1.33
20	7	651	26.08	23	13.15
20	7	724	32.6	33	-1.33
20	-0.5	651	26.08	23	13.15
20	-0.5	724	32.6	33	-1.33
40	14	651	26.08	25	5.45
40	14	724	32.6	36	-10.32
40	7	651	26.08	25	5.45
40	7	724	32.6	36	-10.32
40	-0.5	651	26.08	25	5.45
40	-0.5	724	32.6	36	-10.32
60	14	651	26.08	27	-2.95
60	14	724	39.22	39	0.16
60	7	651	26.08	27	-2.95
60	7	724	39.22	39	0.16
60	-0.5	651	26.08	27	-2.95
60	-0.5	724	39.22	39	0.16
80	14	651	26.08	29	-12.08
80	14	724	45.75	43	6.81
80	7	651	26.08	29	-12.08
80	7	724	45.75	43	6.81
80	-0.5	651	26.08	29	-12.08
80	-0.5	724	45.75	43	6.81

1 mm = 0.03937 inch; 1 ml/ 100 kg = 0.0153 oz/cwt

placement in order to restore the desired workability. Retempering with admixture instead of water is more suitable, since the use of water can induce side effects on the fresh properties and serviceability of the hardened concrete.

The choice of the initial dosage of admixture preceding the retempering of the fresh matrix at the completion of the mixing and hauling (prior to the placement) is critical for the mixture economy and adequacy. Several scenarios were explored. The most likely ones were:

(a)   Isolation of the effect of hauling time and temperature: In this case the HRWRA and VMA optimum dosages obtained under T21H10 condition were used as initial dosages. This scenario was not suitable since the corresponding concrete sample experienced a very severe slump flow loss to the point that unpractical and uneconomical retempering was observed.

(b)   Isolation of the effect of hauling time: In this case the HRWRA and VMA optimum dosages obtained under T21Hy condition were used as initial dosages; and

(c)   Isolation of the effect of extreme temperatures: In this case the HRWRA and VMA optimum dosages obtained under TxH10 condition were used as initial dosages.

As noted in Figure 6.12, the scenarios (b) and (c) offered similar initial amount of admixtures. The optimum dosages of HRWRA required for the overdosing remediation of slump flow loss induced by the maximum selected elevated temperatures of 43 $^{\circ}$C (109 $^{\circ}$F), i.e. at T43H10 and the corresponding ones at the maximum selected hauling times of 80 minutes, i.e. T21H80 were within a margin of ± 3%. In view of these observations either scenarios (b) or (c) could be used. The scenario (c) was adopted herein for the remediation by way of retempering technique.
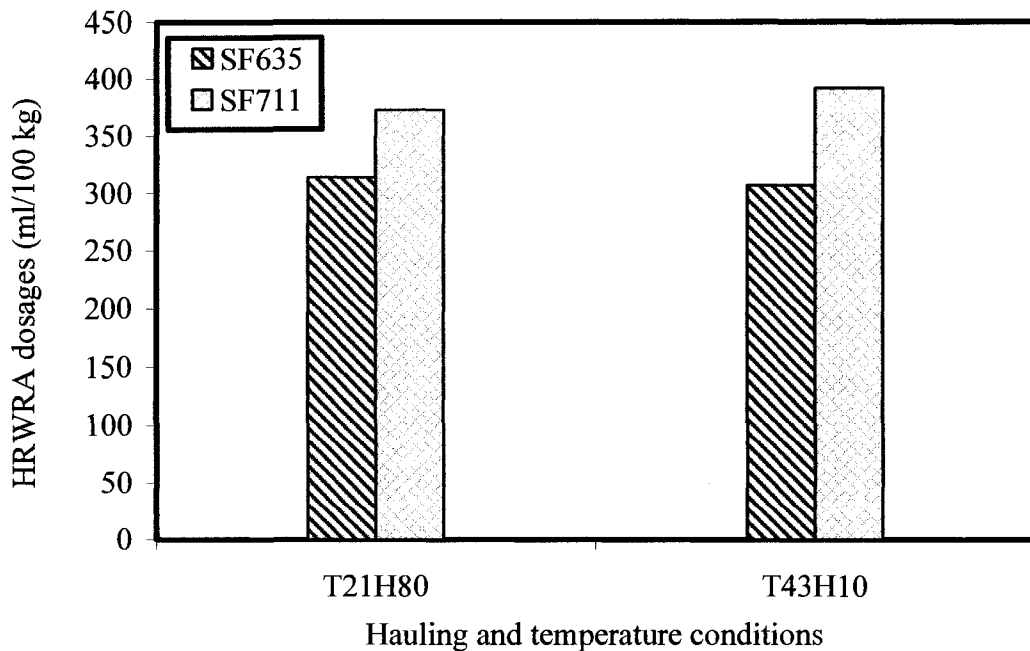
Figure 6.12: Comparison of HRWRA dosages under independent influence of extreme hauling time and temperature conditions

6.3.4.2.1 Optimum HRWRA requirement for retempering remediation

As illustrated in Tables 6.16 through 6.19, and by Figures 6.13 and 6.14, the total HRWRA dosage required for the retempering remediation remained unaffected by the cold and normal room temperatures when compared to the control HRWRA dosage at T21H10 condition. However, it increased when the hauling time increased or when the mixing temperature was elevated from 21 °C to 43 °C (70 to 109 °F).

In cold environment, when the 25 and 28 inches (635 and 711 mm) self-consolidating concretes were hauled for 20 minutes, the increases in HRWRA dosage with respect to the equivalent control dosage were only 3 and 5%, respectively. The same matrices necessitated up to 50 and 60% increases when the mixing environment was changed to the elevated temperature of 43 °C (109 °F). As the hauling time was

294

Table 6.16: Retempering remediation of slump flow loss at 20 minutes hauling time and different temperatures

Temp (°C)	Mix designation	Initial dosage		Retempered dosage		Slump flow (mm)	T_{50} (sec.)	VSI	J ring value (mm)
		HRWRA (ml/100 kg)	VMA (ml/100 kg)	HRWRA (ml/100 kg)	VMA (ml/100 kg)				
43.00	S7.B.SF25	307.19	39.22	6.51	0.00	654	2.16	0	19
	S7.B.SF28	392.16	58.82	13.07	0.00	737	2.00	1	32
21.00	S7.B.SF25	209.15	26.14	6.51	0.00	645	2.42	0	22
	S7.B.SF28	254.90	32.68	13.07	0.00	724	2.16	1	25
-0.50	S7.B.SF25	209.15	26.14	6.51	0.00	638	2.85	0	3
	S7.B.SF28	254.90	32.68	13.07	0.00	715	2.60	1	35

°C = 5/9(°F - 32), 1 ml/100 kg = 0.0153 oz/cwt, 1 mm = 0.03967 inch

Table 6.17: Retempering remediation of slump flow loss at 40 minutes hauling time and different temperatures

Temp (°C)	Mix designation	Initial dosage		Retempered dosage		Slump flow (mm)	T$_{50}$ (sec.)	VSI	J ring value (mm)
		HRWRA (ml/100 kg)	VMA (ml/100 kg)	HRWRA (ml/100 kg)	VMA (ml/100 kg)				
43.00	S7.B.SF25	307.19	39.22	13.07	0.00	648	2.14	0	38
	S7.B.SF28	392.16	58.82	19.60	6.51	724	2.26	1	25
21.00	S7.B.SF25	209.15	26.14	13.07	0.00	648	2.19	0	19
	S7.B.SF28	254.90	32.68	19.60	6.51	727	1.81	1	29
-0.50	S7.B.SF25	209.15	26.14	13.07	0.00	645	2.60	0	6
	S7.B.SF28	254.90	32.68	19.60	6.51	721	2.44	1	32

°C = 5/9(°F - 32), 1 ml/100 kg = 0.0153 oz/cwt, 1 mm = 0.03967 inch

Table 6.18: Retempering remediation of slump flow loss at 60 minutes hauling time and different temperatures

Temp (°C)	Mix designation	Initial dosage		Retempered dosage		Slump flow (mm)	T_{50} (sec.)	VSI	J ring value (mm)
		HRWRA (ml/100 kg)	VMA (ml/100 kg)	HRWRA (ml/100 kg)	VMA (ml/100 kg)				
43.00	S7.B.SF25	307.19	39.22	19.60	0.00	654	1.97	0	44
	S7.B.SF28	392.16	58.82	26.14	13.07	724	2.06	1	32
21.00	S7.B.SF25	209.15	26.14	19.60	0.00	644	2.18	0	25
	S7.B.SF28	254.90	32.68	26.14	13.07	721	1.88	1	25
-0.50	S7.B.SF25	209.15	26.14	19.60	0.00	638	2.81	0	3
	S7.B.SF28	254.90	32.68	26.14	13.07	711	2.27	1	25

°C = 5/9(°F - 32), 1 ml/100 kg = 0.0153 oz/cwt, 1 mm = 0.03967 inch

Table 6.19: Retempering remediation of slump flow loss at 80 minutes hauling time and different temperatures

Temp (°C)	Mix designation	Initial dosage		Retempered dosage		Slump flow (mm)	T_{50} (sec.)	VSI	J ring value (mm)
		HRWRA (ml/100 kg)	VMA (ml/100 kg)	HRWRA (ml/100 kg)	VMA (ml/100 kg)				
43.00	S7.B.SF25	307.19	39.22	26.14	0.00	622	2.07	0	38
	S7.B.SF28	392.16	58.82	32.68	19.60	711	1.88	1	38
21.00	S7.B.SF25	209.15	26.14	26.14	0.00	641	2.25	0	38
	S7.B.SF28	254.90	32.68	32.68	19.60	718	1.97	1	32
-0.50	S7.B.SF25	209.15	26.14	26.14	0.00	648	21.35	0	9
	S7.B.SF28	254.90	32.68	32.68	19.60	721	2.10	1	35

°C = 5/9(°F - 32), 1 ml/100 kg = 0.0153 oz/cwt, 1 mm = 0.03967 inch

Figure 6.13: Optimum dosage of HRWRA for the retempering remediation of slump flow

loss due to the combined hauling time and temperature: Mixture S7.B.SF25

Figure 6.14: Optimum dosage of HRWRA for the retempering remediation of slump flow

loss due to the combined hauling time and temperature: Mixture S7.B.SF28

progressively increased from 20 to up to 80 minutes, an additional 6.51 ml/100 kg (0.1 oz/cwt) per 20 minutes increment in hauling time was sufficient for the effective retempering of fresh matrices at each selected temperature. These results indicated that the yield stress of the fresh concrete at the end of the transportation time was at a level to require only a small amount of additional HRWRA in restoring the fluidity of the matrix back to its target conditions. The relatively small increase in the dosage requirement of the superplasticizer was mainly credited to the use of the initial admixture amount which was sufficient to eliminate the adverse effect of temperature. The additional amount of admixture was primarily useful to mitigate the adverse effects of hauling time.

6.3.4.2.2 Optimum VMA requirement for retempering remediation

The optimum dosage requirements of the viscosity modifying admixture used to remediate the adverse influence of combined hauling time and extreme temperatures on fresh self-consolidating concrete are also shown in Tables 6.16 through 6.19.

Similarly to the case of the HRWRA, the demand in VMA for the 635 mm (25 inches) SCC remained unchanged in cold temperatures and increased in the selected extreme hot temperatures (see Figures 6.15). However, despite the higher demand of HRWRA amount with the increase in transportation time, as discussed in the previous section, the optimum dosage of VMA necessary for the remediation by retempering was unaffected by hauling time. The additional fines brought to the matrix during the hauling enriched the concrete paste. Consequently, the specific surface area of the mortar, SSAm, increased resulting in higher viscosity (T_{50} time between 2 and 5 seconds) and VSI (0 or 1).

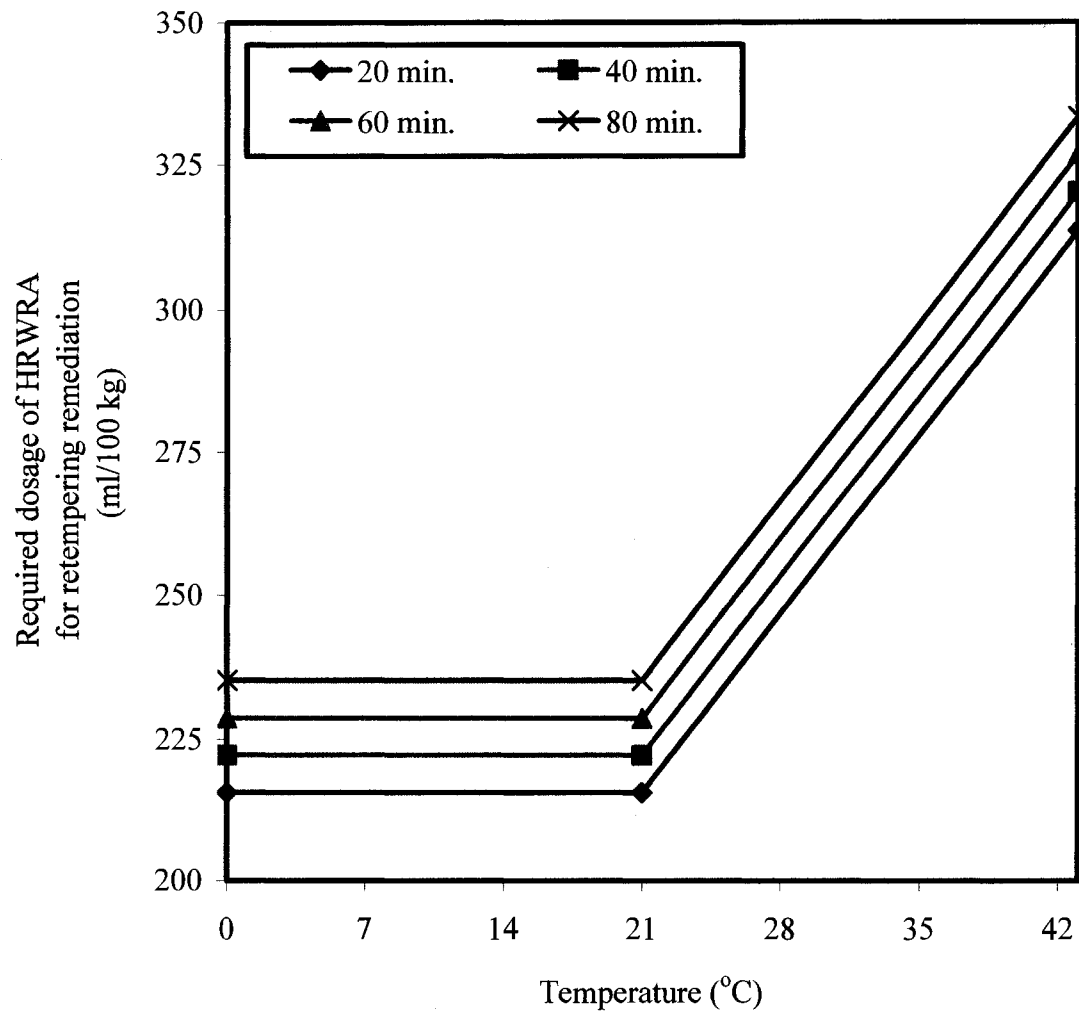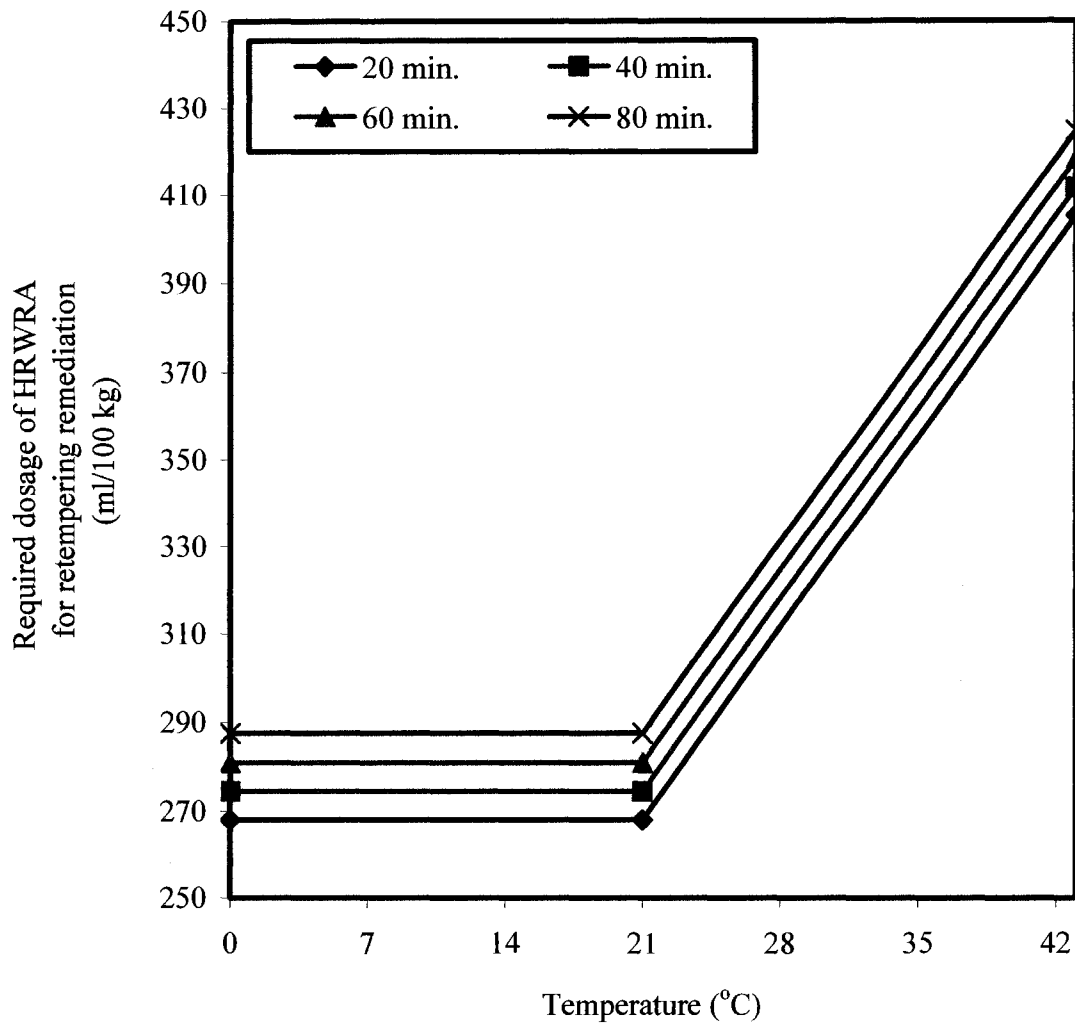On the other hand, the increase in SSAm of the SCCs made with 711 mm (28

Figure 6.15: Optimum dosage of VMA for the retempering remediation of slump flow

loss due to the combined hauling time and temperature: Mixture S7.B.SF25
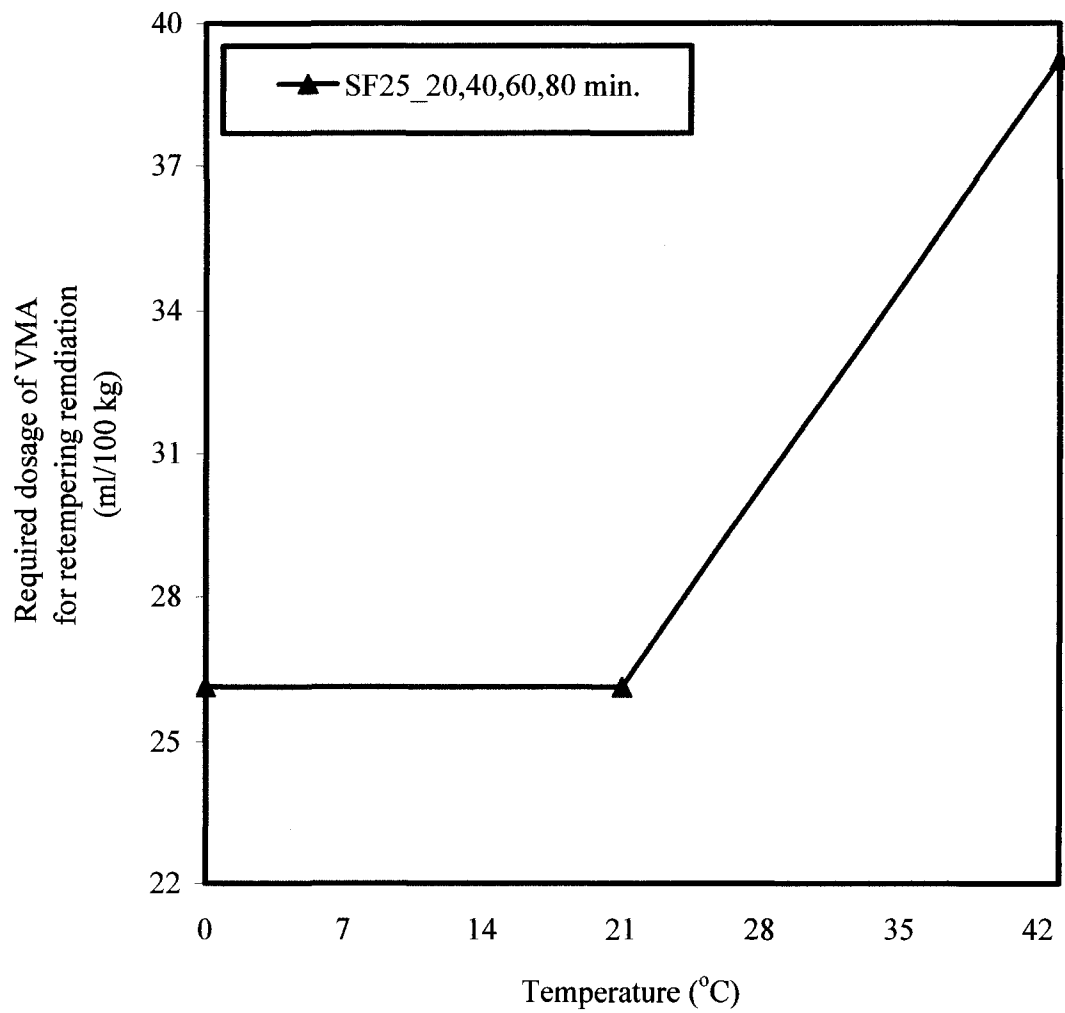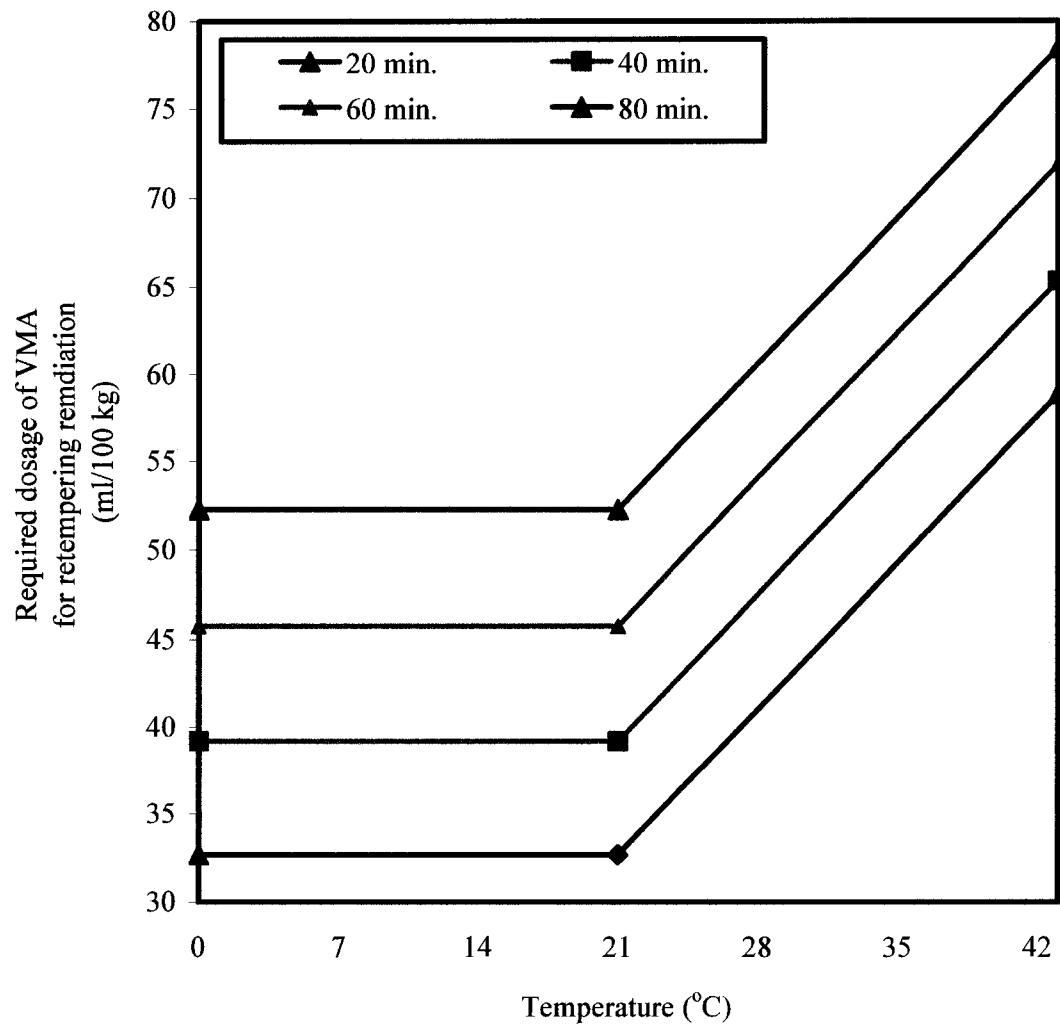
Figure 6.16: Optimum dosage of VMA for the retempering remediation of slump flow

loss due to the combined hauling time and temperature: Mixture S7.B.SF28

inches) slump flow was not enough to mitigate the low plastic viscosity and dynamic stability brought by the increase in hauling time and temperature. For this mixture, as shown in Figure 6.16, the retempering dosage requirement of VMA was impacted by the combination of hauling time and extreme hot temperatures and remained unchanged by the influence of combined hauling time and cold temperatures. The additional VMA helped the viscosity and stability of the plastic concrete to revert to their acceptable levels. In comparing to the control dosage, the total VMA required for the remediation by retempering increased by 80, 100, 120, and 140% when the 711 mm (28 inches) self-consolidating concretes were hauled in 43 °C (109 °F) for 20, 40, 60, and 80 minutes, respectively. The corresponding increases remained at 0, 20, 40, and 60% when the temperatures were varied from -0.5 to 21 °C (31 to 70 °F).

6.3.4.2.3 Prediction of optimized retempering amount of HRWRA and VMA

The most suitable predictive equations of the optimized dosages of HRWRA and VMA as a function of hauling time, extreme hot and cold temperatures, target slump flow, and initial HRWRA and VMA dosages, were determined using a 95% confidence level. The relationships are as follows:

In extreme hot temperature of 109 °F (43 °C):

$$HR_{retemp}hot = 0.32698h_t - 0.06571SF + 0.13577HR_{initial} \tag{6.10}$$

$$\text{Or } HR_{retemp}hot = ah_t + bSF + cHR_{initial}$$

$$VMA_{retemp}hot = 17.148x10^{13} + 0.32652h_t - 291.536x10^{10}VMA_{initial} \tag{6.11}$$

$$\text{Or } VMA_{retemp}hot = a + bh_t + cVMA_{initial}$$

In extreme cold temperature of 31 °F (-0.5 °C):

$$HR_{retemp}cold = 0.32698h_t - 0.10408SF + 0.13590HR_{initial} \tag{6.12}$$

304

Or $HR_{retemp}cold = ah_t + bSF + cHR_{initial}$

$$VMA_{retemp}cold = 60.540x10^{13} + 0.32682h_t - 1852.53x10^{10}VMA_{initial} \qquad (6.13)$$

Or $VMA_{retemp}cold = a + bh_t + cVMA_{initial}$

Where:

HR_{retemp}hot and HR_{retemp}cold = High range water-reducing admixture retempering dosages in hot and cold temperatures, respectively, (ml/100 kg)

$HR_{initial}$ = High range water-reducing admixture initial dosage (ml/100 kg)

VMA_{retemp}hot and VMA_{retemp}cold = Viscosity modifying admixture retempering dosage in hot and cold temperatures, respectively, (ml/100 kg)

$VMA_{initial}$= Viscosity modifying admixture initial dosage (ml/100 kg)

SF = Target slump flow in hot temperature condition (mm),

   with 635 mm ≤ SF ≤ 711 mm ± 25 mm

h_t = Hauling time (min), with 20 min ≤ h_t ≤ 80 min

Equation 6.11 and 6.13 are valid only for slump flow of 711 mm (28 inches), since no VMA was needed for the retempering of slump flow of 635 mm (25 inches).

The predictive equations were tested for accuracy using R^2 (the coefficient of multiple determination) and S (average standard deviation). Correlations between the data predicted from the regression equations and the actual test results were evaluated using F and T tests. The following results were found:

- *For Equation 6.10:*

R^2 = 99 %, S = 0.0074 ml/100 kg

Prob(t) = 0.0000, 0.0000, and 0.0000 for a, b, and c, respectively; Prob(F) = 0.0000.

- *For Equation 6.11:*

R^2 = 99 %, S = 0.0233 ml/100 kg (0.00036 oz/cwt)

Prob(t) = 0.0000, 0.0010, and 0.0000 for a, b, and c, respectively; Prob(F) = 0.0016.

- *For Equation 6.12:*

R^2 = 99 %, S = 0.0074 ml/100 kg (0.00011 oz/cwt)

Prob(t) = 0.0000, 0.0000, and 0.0000 for a, b, and c, respectively; Prob(F) = 0.0000.

- *For Equation 6.13:*

R^2 = 99 %, S = 0.1750 ml/100 kg (0.0027 oz/cwt)

Prob(t) = 0.0000, 0.0076, and 0.0000 for a, b, and c, respectively; Prob(F) = 0.0102.

The regression equations 6.10, 6.11, 6.12, and 6.13 produced R^2 and S values indicative of very strong relationship between the dependent variables (retempered dosages of HRWRA and *VMA*) and the independent variables (hauling time, hot and cold temperatures, target slump flow, and initial dosages of HRWRA and VMA). The F and T tests results indicated that all selected independent variable had similar influence on the predictive retempered dosages of HRWRA and VMA. Tables 6.20 and 6.21 present the actual versus the calculated required optimized admixtures dosages for the retempering remediation of slump flow loss. The predictive equations yielded percentage errors less than 1%, confirming a very strong relationship between the actual and the calculated admixture dosages.

6.3.5 Comparison of overdosing and retempering remediations

The current section presents a comparison of the fresh properties of the remediated self-consolidating concretes. The designed optimum admixture dosages, and the major advantages and disadvantages of the selected two remediation methods are also

Table 6.20: Actual versus calculated HRWRA optimum dosage for the overdosing remediation in combined hauling time and hot temperatures

Hauling time (min)	Target slump flow (mm)	Initial HRWRA dosage (ml/100 kg)	Actual retempered HRWRA dosage (ml/100 kg)	Calculated retempered HRWRA dosage (ml/100 kg)	% Error
Extreme hot temperature of 43 °C					
20	635	307.19	6.51	6.52	-0.17
20	711	392.16	13.07	13.06	0.05
40	635	307.19	13.07	13.06	0.07
40	711	392.16	19.6	19.60	-0.01
60	635	307.19	19.6	19.60	0.00
60	711	392.16	26.14	26.14	-0.01
80	635	307.19	26.14	26.14	0.00
80	711	392.16	32.68	32.68	-0.01
Extreme cold temperature of -0.5 °C					
20	635	209.15	6.51	6.52	-0.17
20	711	254.90	13.07	13.06	0.05
40	635	209.15	13.07	13.06	0.07
40	711	254.90	19.60	19.60	-0.01
60	635	209.15	19.60	19.60	0.00
60	711	254.90	26.14	26.14	-0.01
80	635	209.15	26.14	26.14	0.00
80	711	254.90	32.68	32.68	-0.01

1 mm = 0.03937 inch; 1 ml/ 100 kg = 0.0153 oz/cwt

Table 6.21: Actual versus calculated VMA optimum dosage for the
overdosing remediation in combined hauling time and hot temperatures

Hauling time (min)	Initial VMA dosage (ml/100 kg)	Actual retempered VMA dosage (ml/100 kg)	Calculated retempered VMA dosage (ml/100 kg)	% Error
Extreme hot temperature of 43 $^{\circ}$C				
20	58.82	0.00	0.00	0.00
40	58.82	6.51	6.53	-0.33
60	58.82	13.07	13.06	0.06
80	58.82	19.60	19.59	0.03
Extreme cold temperature of -0.5 $^{\circ}$C				
20	32.68	0.00	-0.13	0.00
40	32.68	6.51	6.50	0.15
60	32.68	13.07	13.00	0.54
80	32.68	19.60	19.50	0.51

1 mm = 0.03937 inch; 1 ml/ 100 kg = 0.0153 oz/cwt

covered.

6.3.5.1 Fresh properties of remediated matrices.

The fresh properties of the remediated freshly-mixed self-consolidating concretes were evaluated using the slump flow, T_{50}, VSI, and J-ring tests. The measured results are tabulated in Table 6.8 through 6.11 for the overdosing method, and Tables 6.16 through 6.19, for the retempering approach. They indicated that all remediated self-consolidating concretes were within the target slump flows ± 25 mm (1 inch), T_{50} time between 2 and 5 seconds, VSI of 0 (highly stable) or 1 (stable), and J-ring value within the allowable limit of 25 to 50 mm (1 to 2 inches). This is particularly encouraging that, under harsh conditions, self-consolidating concrete with suitable unconfined workability, plastic viscosity, dynamic stability, and passing ability can be produced by means of overdosing and retempering techniques of remediation.

6.3.5.2 Admixture dosages

Figures 6.17 and 6.18 compare the overdosed and retempered amount of HRWRA required for the remediations of slump flow losses at various combination of hauling time and extreme temperature. In comparing to the overdosing method, the retempering remediation of the 635 and 711 mm (25 and 28 inches) self-consolidating concretes, hauled for 20 minutes under -0.5 or 21 °C (31 or 70°F) required about 4% less admixture amount. When the hauling time was gradually extended to up to 80 minutes, an additional decrease of 3% per 20 minutes increment in hauling time was needed. Similar trend was observed in hot temperature of 43 °C (109 °F) where the retempering remediation of the selected SCCs necessitated about 3% less amount of superplasticizer than the overdosing method, at the end of 20 minutes hauling time. Beyond that time, an average reduction in HRWRA dosage of about 7% was required per 20 minutes increment in hauling time.

The optimum VMA dosages of the retempered self-consolidating concretes were also lower than their counter parts obtained by the overdosing remediation method. As depicted through Figures 6.19 and 6.20, when the temperature of the raw materials and the mixing environment were set at 21 °C (70 °F) or -0.5 °C (31 °F), the 635 mm (25 inches) slump flow matrices did not require any adjustment under both overdosing and retempering conditions. However, as the temperature increased to 43 °C (109 °F), the same retempered mixture experienced 17% decreases in VMA dosage at 20 and 40 minutes hauling time when compared to that of equivalent overdosed self-consolidating concretes. The reductions were more significant at 60 and 80 minutes hauling time as 33

Figure 6.17: Comparison of total HRWRA dosages of overdosing and retempering
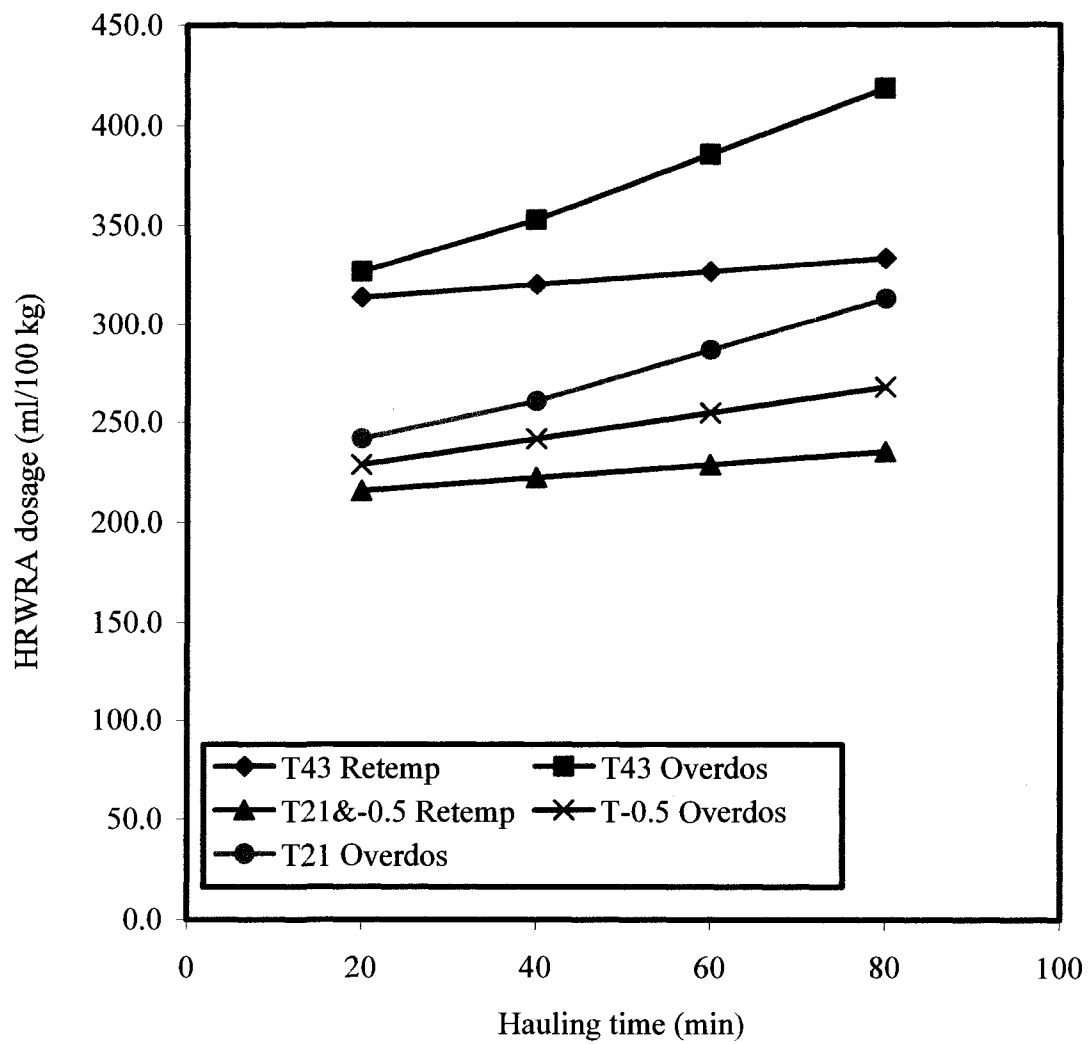
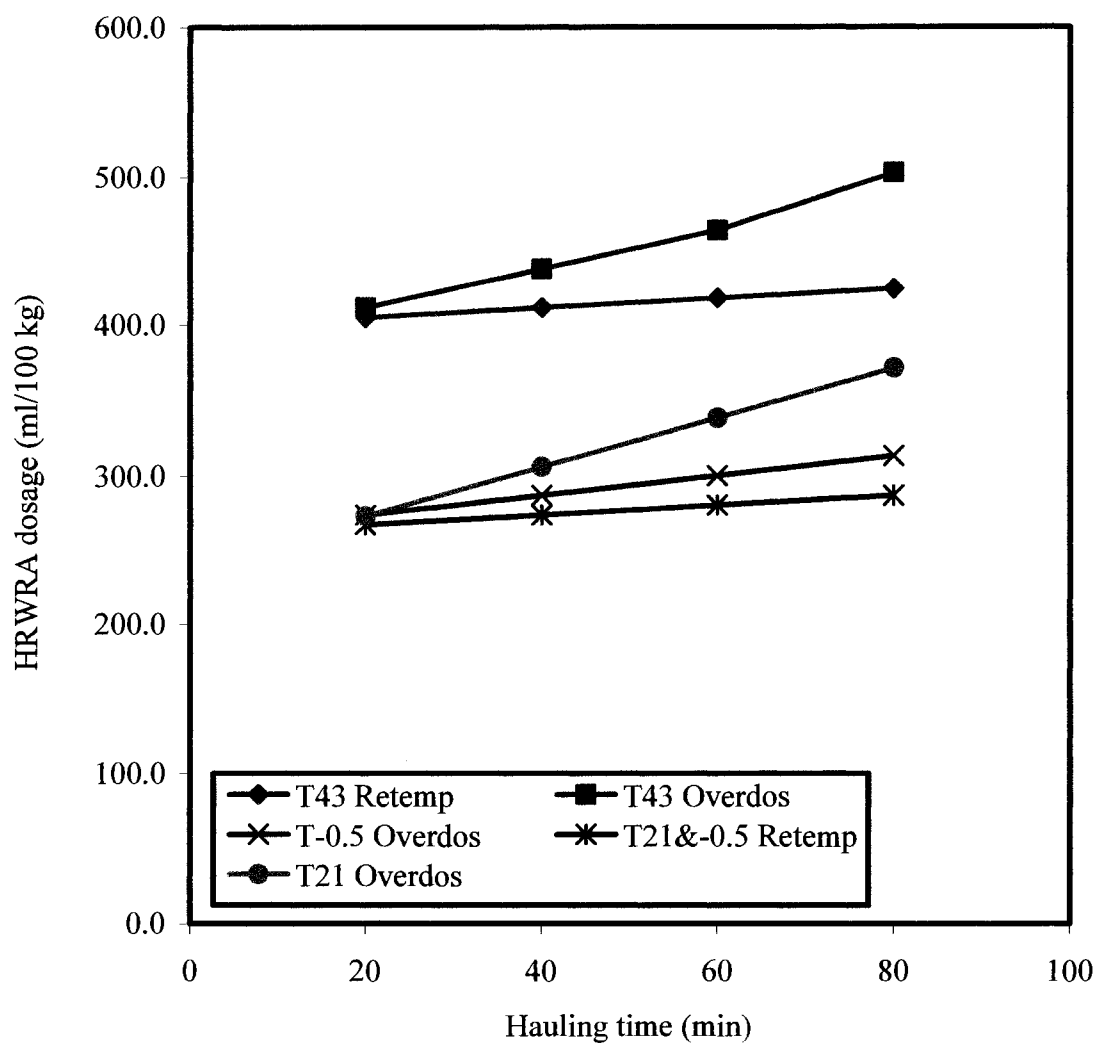remediations of mixture S7.B.SF25

Figure 6.18: Comparison of total HRWRA dosages of overdosing and retempering
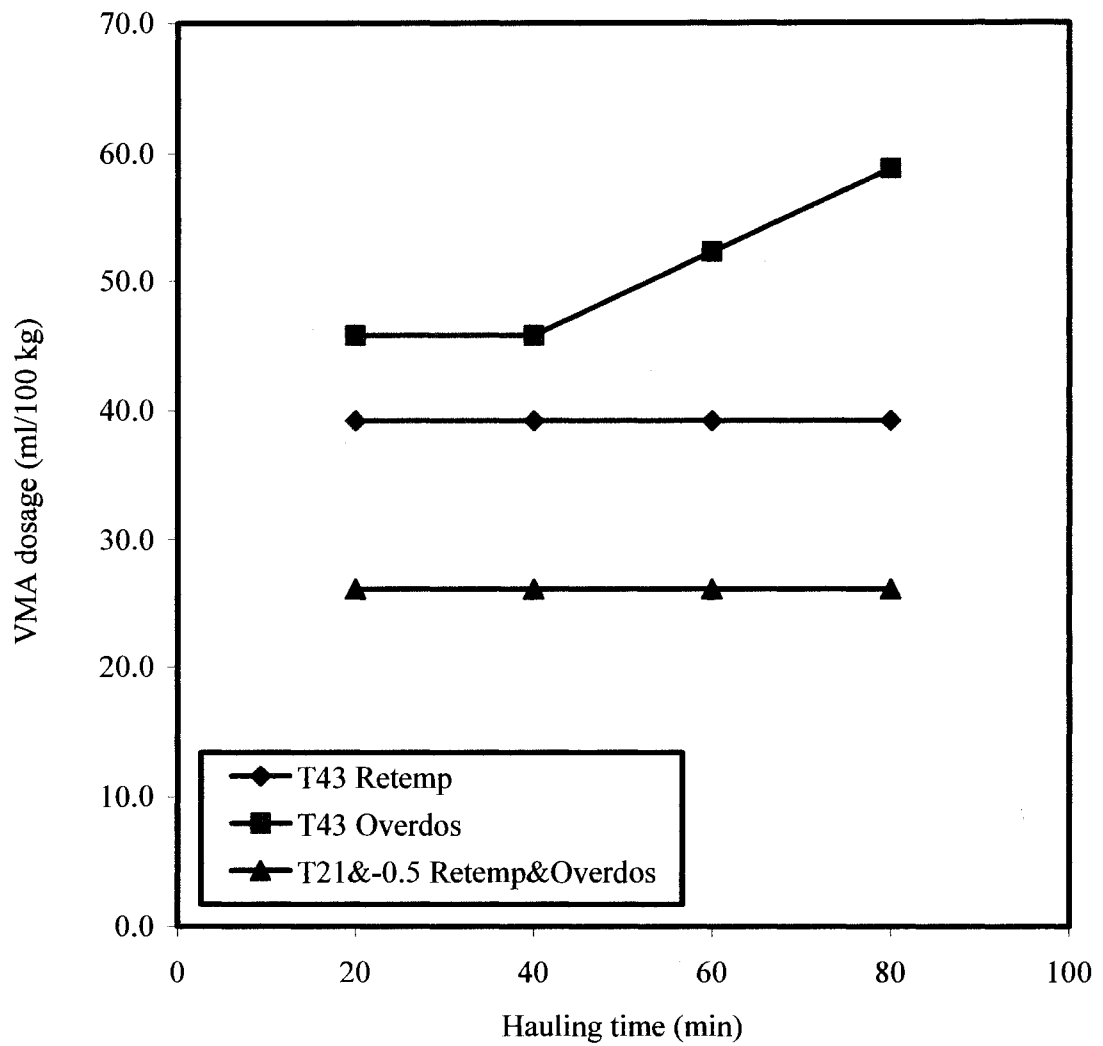
remediations of mixture S7.B.SF28

Figure 6.19: Comparison of total VMA dosages of overdosing and retempering
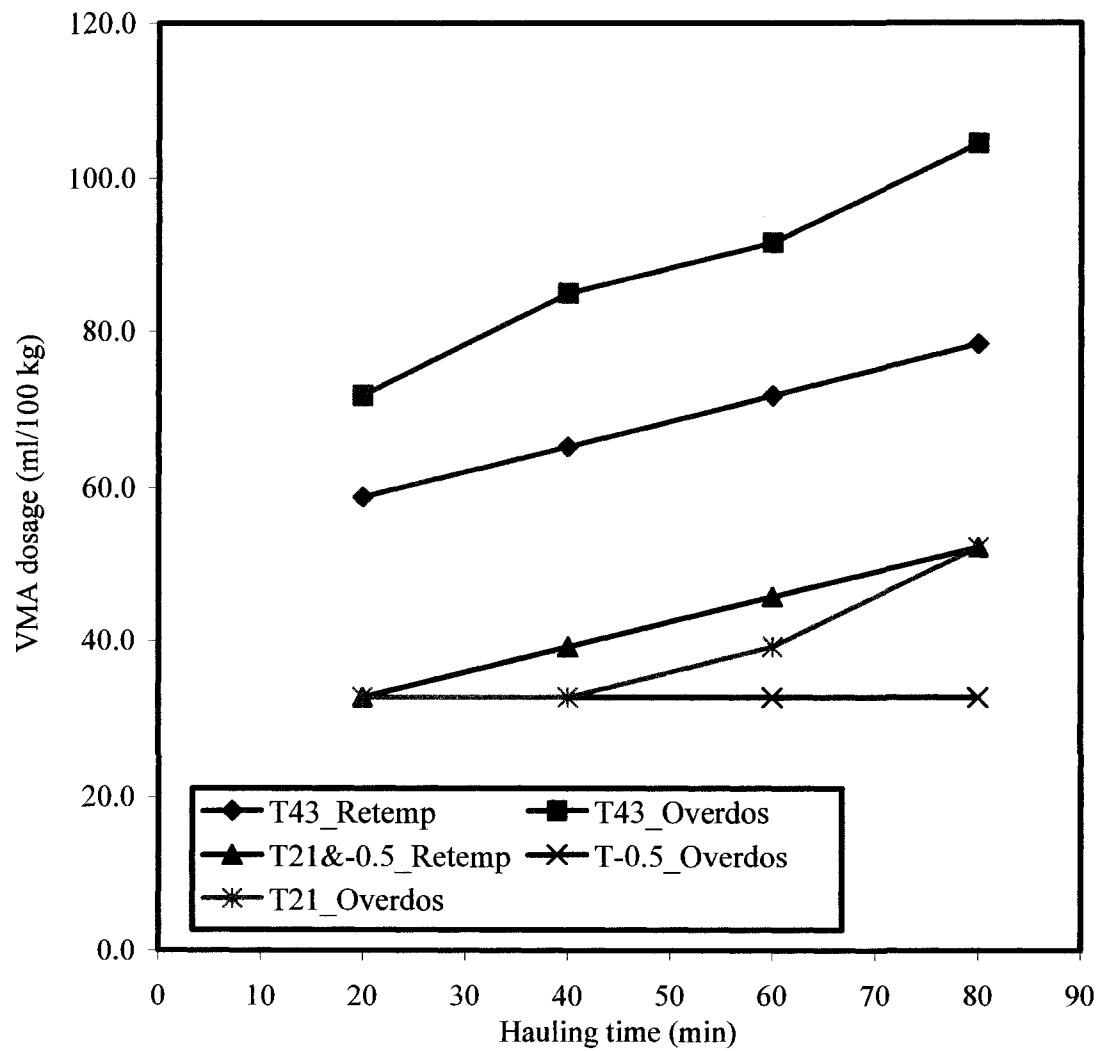
remediations of mixture S7.B.SF25

Figure 6.20: Comparison of total VMA dosages of overdosing and retempering

remediations of mixture S7.B.SF28

and 50% less VMA were needed.

The 711 mm (28 inches) slump flow mixtures generally required VMA to yield suitable flow rate and dynamic segregation resistance under both adopted remediation methods. When the 711 mm (28 inches) slump flow matrix was transported for 20 minutes in cold temperature of -0.5 °C (31 °F) or at normal room temperature of 21 °C (70 °F), the two retempering methods required an identical amount of VMA. As the hauling time increased to 40 minutes, the retempered mixtures had 17% less VMA content than the equivalent overdosed self-consolidating concretes. For the hauling times of 60 and 80 minutes, reduction in VMA dosage of 12 and 9% for the retempering method, versus the overdosing approach, were obtained, respectively. Similar behavior was observed in hot temperatures. After 20 minutes of hauling time in the temperature of 43 °C (109 °C), the retempering remediation of the 711 mm (28 inches) slump flow self-consolidating concrete required 22% less amount of VMA when compared to the overdosing remediation. The reductions became 30, 27, and 33% after 40, 60, and 80 minutes hauling time, respectively.

6.3.5.3   Advantage and disadvantage of the overdosing and retempering remediations

Self-consolidating concrete is a high performance concrete in a fresh state. It is proportioned with high cementitious materials content and adequate chemical admixtures, leading to a relatively high initial material cost. Increases in cost can be compensated when cost savings can be realized given the reduced effort in concrete placement, the reduction in construction time and labor cost, and greater flexibility in placement operation and scheduling. The slump flow loss of fresh concrete is a natural phenomenon mainly when the concrete is mixed and transported for a long period of time in harsh

environmental conditions. As such, remediation becomes an undeniable solution. Both selected remediation methods have unique advantages and disadvantages. The most suitable remediation techniques should be based on the concrete application, and the organization and management of construction. The major factors to be considered for making a decision on the choice of the remediation method should be based on one or the combination of the followings:

- Mixtures economy: In general, the adopted retempering remediation requires less HRWRA and VMA than the overdosing remediation.

- Admixture dosage flexibility: the Mixing and hauling duration can be affected by the traffic or delay in scheduling. The retempering provides flexibility to adjust the admixture dosage just before the placement of the concrete accordingly.

- Qualified personnel: The retempering remediation is usually performed manually. It requires a well trained personnel at the job site to execute the retempering operation. The truck driver can be used for that purpose.

- Quality control: The overdosing remediation provides better quality control than the retempering remediation. The precise measurement of the admixtures is automated at the mixing plant.

6.4 Conclusions

The understanding of the influence of combined hauling time and temperature on the fresh self-consolidating concrete is useful in simulating concrete mixing and hauling by the mean of concrete truck mixer during extreme temperatures. The following conclusions can be drawn from the test results:

a)   In general, the self-consolidating concrete manufactured and hauled in extreme temperatures experienced slump flow losses in hot conditions, and gains in cold environments when compared to the equivalent concretes produced at the control temperature of T21H10 (i.e., 10-minute hauling time under normal room temperature of 21 °C (70 °F)).

The slump flow decreased with the increase in hot temperature and hauling time. The 635 and 711 mm (25 and 28 inches) slump flow SCCs hauled for 20 minutes under 43, 36, and 28 °C (109, 96, and 83 °F) displayed losses in flow ability of 31, 24, and 19%, and 30, 15, and 12%, respectively, when compared to the corresponding slump flow obtained at the control condition of T21H10. Additional decreases in flow ability of 10% per 20 minutes increment in hauling time were observed as the transportation time progressively increased to up to 80 minutes at each of the selected hot temperatures.

When compared to T21H10, the trial self-consolidating concretes also experienced decreases in slump flow in cold temperature, but to a lesser extent. The losses in slump flow after 20 minutes of hauling for the matrices prepared under 14, 7, or -0.5 °C (57, 44, or 31 °F) were about 10 and 2% for the 635 and 711 mm (25 and 28 inches) slump flow SCCs, respectively. For the hauling times of 40 to 80 minutes, an average increase of about 7% per 20 minutes increment was experienced for each selected cold temperature.

b)   The flow rate/plastic viscosity (measured by the T_{50} time) of the selected self-consolidating concretes were also affected by the combination of hauling time and temperature. In comparing to the T_{50} time of the control T21H10 condition, up to 40% increase in flow rate was observed when the 635 mm (25 inches) slump flow self-

consolidating concrete was transported for 20 minutes under 28 °C (83 °F). The corresponding increase was 52% for the 711 mm (28 inches) slump flow concrete. As hauling time increased to 40 minutes for the 635 mm (25 inches) and 60 minutes for the 711 mm (28 inches), the selected self-consolidating concretes displayed severe losses in slump flow at 36 and 43 °C (96 and 109 °F), and their T_{50} times could not be measured since the flow spreads were below the recommended 508 mm (20 inches).

Contrary to what was observed in hot conditions, the self-consolidating concrete made with 635 mm (25 inches) slump flow and hauled for 20 minutes or less under each selected cold temperature displayed an average decrease of 5% in flow rate. Beyond this point, excessive losses in slump flow were observed with increases in hauling time and the T_{50} times could not be evaluated. On the other hand, the T_{50} times of the high slump flow concretes, i.e., the 711 mm (28 inches), could be measured for all selected hauling times. In comparing to the corresponding control (T21H10), the T_{50} times of the 711 mm (28 inches) slump flow self-consolidating concretes decreased by 27, 54, 61, and 89% after 20, 40, 60, and 80 minutes of hauling, respectively.

c)   The combination of hauling time and temperature enhanced the dynamic stability of the 711 mm (28 inches) matrices from stable (VSI = 1) to highly stable (VSI = 0). The 635 mm (25 inches) fresh matrices were unaffected by the combination of temperature and hauling time and remained highly stable under all selected conditions.

d)   The changes in fresh properties of plastic self-consolidating concretes can be explained through the increase or decrease in adsorption amount of admixture per specific surface area of concrete mortar (Ads/SSAm), the contribution of aggregate's moisture content, and partial evaporation of mixing water.

As reported in Chapters 4 and 5, both hauling time and temperature affected the specific surface area of concrete mortar. The Laser diffraction particle size analysis of a concrete paste indicated that the volume of the fine particles (ranging from 1 to 250 μm (39×10^{-6} to 9843×10^{-6} inch) increased as the hauling time increased from 20 to 40, 60, and 80 minutes, leading to an increase in SSAm. The contribution of the hauling time to the increase in SSAm was attributed to the grinding of aggregate and cement particles, and the growth of cement hydrated products. The influence of temperature was explained through the growth of cement hydrated products.

The UV/Vis spectroscopy test revealed that the cement-water-superplasticizer solution concentration in free admixture increased with an increase in hauling time (up to 80 minutes). It also increased with an increase in temperature (up to 36 $^{\circ}$C (96 $^{\circ}$F)). The increases in solution concentration revealed the increase of admixture adsorption (Ads) on cement particles. The contribution of Ads to the fresh performance of the trial matrix under the combined influence of temperature and hauling mainly resulted from the accumulation of Ads_{haul} from hauling time and Ads_{temp} from the temperature. However, despite the augmentation in Ads, the increase in SSAm was sufficient to decrease the Ads/SSAm, resulting in further reduction (in hot temperature) or conservation (in cold temperature) of the unconfined workability for the trial self-consolidating concretes.

e)   The overdosing and retempering methods of remediation were successful in mitigating the adverse effect of combined hauling time and temperature on self-consolidating concrete. Fresh matrices with suitable unconfined workability, plastic viscosity, dynamic stability, and passing ability were achieved once remediated by either of the two methods.

The selection of an appropriate remediation method should be based on one or a combination of the factors, such as mixture economy, admixture dosage flexibility, availability of qualified personnel, and degree of quality control.

f) The statistical equations to predict: (1) the actual slump flow of the self-consolidating concrete prepared and transported for different intended slump flows, hauling times, and hot and cold temperatures; (2) the required optimum overdosed or retempered admixtures (HRWRA and VMA) amount to achieve the desired flow ability and stability under various hauling times and temperatures showed significant relationships between the dependent and independent variables.

CHAPTER 7

CONCLUSIONS AND RECOMMENDATIONS

7.1   Conclusions

As stated earlier, this investigation was intended to evaluate the influence of selected parameters, namely: admixture sources, hauling time, temperature, and combined hauling times and temperatures on the fresh characteristics of self-consolidating concrete (SCC). The admixture sources were ranked based on the optimum dosage required to attain uniform workability (i.e., the flow ability in an unconfined area, the flow rate or plastic viscosity per inference, the dynamic stability, and the passing ability in congested reinforcement areas). The effectiveness of remediation techniques to mitigate the adverse effects of the above-mentioned construction-related variables on the freshly-mixed self-consolidating concretes was also studied. Finally, statistical equations to correlate dependent variables (i.e., HRWRA and VMA dosages, compressive strength, slump flow losses or gains) with independent variables (i.e., concrete paste content, aggregate sizes, hauling time, and hot and cold temperatures) were determined. The main results and conclusions of the study are described below.

7.1.1   Influence of admixture source and slump flow on fresh performance of self-consolidating concrete

Liquid polycarboxylate-based high range water-reducing admixtures (HRWRA) and corresponding viscosity modifying admixtures (VMA), obtained from four different

manufacturers, herein designated as A, B, C, and D, were investigated to find their influence on the optimum dosage and slump flow of self-consolidating concretes. The test results indicated the followings findings:

7.1.1.1   Influence of admixture source on optimum dosage

The optimum dosages requirement of admixtures in obtaining uniform unconfined workability (measured by the slump flow) and dynamic stability (evaluated by the visual stability index (VSI)) varied among the four selected admixture sources. The required optimum dosage of HRWRA was highest for the source A, followed by the sources C, B, and D in descending order. The required optimum amount of VMA was also highest for the source A, but remained uniform for the sources B, C, and D. The self-consolidating concretes prepared with a slump flow of 508 ± 25 mm (20 ± 1 inches) did not require VMA to yield satisfactory unconfined workability and dynamic stability for all selected admixture sources.

The fundamental mechanism of action of a superplasticizer involves adsorption and electrostatic repulsion and steric hindrance forces. As such, the superplasticizer has to be first adsorbed on cement particles before being able to play a dispersing role. Based on this concept, the ultraviolet-visible (UV/Vis) spectroscopy test was used to explain the differences in admixture dosage requirements exhibited by the four admixture manufacturers. Additionally, the chemical type of the admixtures and the calculated VMA-to-HRWRA ratios were also used to explain the variation in the admixtures optimum dosage requirements.

The UV/Vis spectroscopy absorption is not a specific test to quantify or measure the actual amount of adsorption of a polymer. However, it is used to determine the actual

concentration of free admixture in a cement-water-superplasticizer solution. The test results indicated that the increase in admixture concentration led to an increase in adsorption of the carboxylic group (COO⁻) on cement calcium ions (Ca^{2+}) resulting in additional repulsion and dispersion between neighboring cement particles. Additionally, the UV/Vis test results revealed that the concentration of the PC-HRWRA was highest for the source D, followed by the sources B, C, and A in descending order.

The chemical type of the superplasticizers also influenced the dosage requirement in attaining uniform fresh properties. All four superplasticizers were acrylic polymers-based. The behavior of the sources B, C, and D superplasticizers was similar to that of a polycarboxylate-acid type (PCA), while the performance of the source A was comparable to that of polycarboxylate-ester type (PCE). In PCA, the acid portion is predominant when compared to the ester type. The higher acid ratio enhanced the adsorption of PCA polymers on cement grains leading to a higher dispersibility of particles. In the case of polycarboxylate-ester type (PCE), the matrix dispersibility decreased for the similar dosage to that of polycarboxylate-acid. However, the gradual dispersion of ester type admixture increased the slump flow retention of fresh self-consolidating concretes.

The calculated optimum dosages VMA-to-HRWRA ratios also revealed a trend for the four selected admixtures types. The similarity of the VMA-to-HRWRA ratios for the admixture sources B, C, and D is supportive of the hypothesis that these sources have a similar chemical composition. The VMA-to-HRWRA ratio of the source A admixture was higher than the other three admixture manufacturers, mainly due to its thickening mode of functioning which led to the higher required amount of source A VMA in producing highly stable or stable matrices.

7.1.1.2 Influence of slump flow on optimum admixture dosage

Regardless of the admixture sources and the selected self-consolidating concrete groups, the optimum dosages of HRWRA and VMA increased with an increase in slump flow. In the presence of a higher amount of HRWRA, the yield stress of the fresh matrix, i.e., the force needed to disperse its ingredients, gradually reduced as the fresh concrete was allowed to spread further. The increase in HRWRA dosage was usually accompanied by a decrease in plastic viscosity and a viscosity modifying admixture was needed to bring the plastic viscosity of the fresh matrix back to its target level.

7.1.1.3 Influence of admixture source and slump flow on fresh and hardened properties of SCC

The four selected admixture sources were able to produce self-consolidating concretes with suitable flow ability, flow rate/plastic viscosity, dynamic and static stabilities, passing ability, and filling ability. However, the performance of the selected admixtures in attaining a required fresh property varied among the admixture sources. The pair admixture sources A and D displayed higher flow ability or lower plastic viscosity than the sources B and C. The dynamic stability, passing ability, and filling ability of the matrices were similar for all four admixture sources. The admixture sources B and C exhibited better static stability than the sources A and D.

The self-consolidating concrete prepared for 508 ± 25 mm (20 ± 1 inches) slump flow displayed very low plastic viscosity, very high dynamic stability, moderate filling ability, low passing ability, and high static stability. Consequently, it is found unsuitable for congested reinforced structures. All 635 mm (25 inches) and 711 mm (28 inches) slump flow self-consolidating concretes displayed high flow ability, low plastic viscosity

(by inference), high dynamic stability, moderate static stability, moderate passing ability, and moderate to high filling ability, indicating their suitability for most civil engineering applications. The low flow ability (within the acceptable limit) of the 711 ± 25 mm (28 ± 1 inches) slump flow matrix may cause a higher than normal pressure on formwork.

The selected self-consolidating concretes made with different sources of admixtures and various slump flows exhibited insignificant differences in the test results related to the air content, bleeding, time of setting, adiabatic temperature, demolded unit weight, compressive strength, and modulus of elasticity.

7.1.1.4   Statistical analysis

The relationship between the required optimum dosages of HRWRA VMA as dependent variables, and the concrete paste content, aggregate sizes and target slump flow as independent variables was found to be significant. Strong statistical relationships also existed between the compressive strength, target slump flow, and curing age.

7.1.2   Influence of hauling time on fresh performance of self-consolidating concrete

7.1.2.1   Influence of hauling time on freshly-mixed SCC

The selected hauling times affected the freshly-mixed self-consolidating concrete in the form of loss in flow ability (measured by the slump flow), decrease in plastic viscosity (evaluated by the T_{50} time), and gain in dynamic stability (determined through the VSI rating). The loss in flow ability was observed as early as 20 minutes and increased with increasing hauling time. The flow rate also increased with increasing hauling time. However, the T_{50} time of the self-consolidating concretes made with slump flow of 508, 635, and 711 mm (20, 25, and 28 inches) could not be measured after 20, 40, and 60 minutes of hauling time, respectively, due to the severe loss in slump flow.

The change in fresh properties can be characterized by the adsorption amount of admixture per specific surface area of concrete mortar Ads/SSAm. The SSAm of the matrix increased with the increase in hauling time due to the grinding of aggregate and cement particles, and the growth of the cement hydrated products. Laser diffraction particle size analysis was used to support this theory. The analysis performed on representative samples of a freshly-mixed SCC revealed that the volume of fine particles ranging from 1 to 250 μm (39×10^{-6} to 9843×10^{-6} inch) increased as the hauling time increased from 10 to 20, 40, 60, and 80 minutes.

Since an actual measurement of adsorption was beyond the scope of this investigation, an indirect method of evaluation was used. The UV/Vis spectroscopy test was utilized to determine the concentration of free admixture in a cement-water-superplasticizer solution at different hauling times. The test result of the UV/Vis spectroscopy test indicated that the solution concentration of free admixture increased up to 80 minutes. The increase in the admixture concentration led to an increase in the admixture adsorption on cement particles. During the 10 to 80 minutes hauling intervals, the admixture adsorption rate was higher during the first few minutes of the hydration reaction. Beyond the rapid initial adsorption (to saturate the most reactive phases), the admixture uptake by the hydrating cement continued at a reduced rate. The continuation of adsorption occurred mainly due to the growth and abraded product of new hydrated particles. Past 80 minutes of hauling time, the solution concentration of free admixture decreased, and simultaneously the sulfate ion (SO_4^{2-}) concentration increased with elapsed time, as was the case during the induction period of cement hydration. The adsorption of PC-HRWRA on cement may have been prevented by the competitive

adsorption between the sulfate ions and the dissociated carboxylic group on cement particles.

In summary, it was seen that both Ads and SSAm increased with increases in hauling time. However, the contribution of SSAm on the alteration of the workability of the freshly-mixed self-consolidating concrete was greater than that of Ads.

7.1.2.2 Remediation of the adverse influence of hauling time on freshly-mixed SCC

The overdosing method was used to remediate the adverse effects of hauling time on the fresh properties of self-consolidating concretes. The adopted remediation technique was able to produce self-consolidating concretes with a similar flow ability, plastic viscosity, dynamic stability, and passing ability to those obtained at the control hauling time. The admixture dosages increased as the hauling time increased. The rate of HRWRA dosage increment was higher at 20 minutes hauling time (20, 33, and 20 ml/100 kg (0.3, 0.5 and 0.3 oz/cwt) for 508, 635 and 711 mm (20, 25, and 28 inches) slump flows, respectively) and became constant thereafter at about 13 ml/100 kg (0.2 oz/cwt) per 10 minutes hauling time increment, independently of the slump flow. The additional amount of admixture increased its adsorption and generated supplementary repulsive electrostatic and steric hindrance forces between cement particles. These forces further dispersed cement agglomerations provoked by the grinding and hydration of the cement constituents during hauling time.

7.1.2.3 Statistical analysis

The predictive equations to correlate: (1) the actual slump flow loss with the initial slump flow value and hauling time, and (2) the required amount of overdosed admixtures (HRWRA and VMA) with the target slump flow and hauling time showed

326

significant statistical relationships between the dependent and independent variables.

7.1.3 Influence of extreme temperatures on fresh performance of self-consolidating concrete

7.1.3.1 Influence of temperature on freshly-mixed SCC

Both the hot and cold temperatures affected the fresh properties of the selected self-consolidating concrete.

The hot temperatures affected the trial matrices by significantly decreasing their unconfined workability, substantially increasing their flow rate (or decreasing the plastic viscosity per inference), and improving their dynamic stability. The slump flow losses induced by the elevated temperatures were only 5% at 28 °C (83 °F), but increased to about 12 and 25% at 36 and 43 °C (96 and 109 °F), respectively, when compared to that obtained at the control temperature of 21 °C (70 °F).

The flow rate of the selected self-consolidating concretes increased as the temperature increased. The T_{50} time of the mixture made for 508 mm (20 inches) slump flow could not be measured in any of the selected hot temperatures since its flow spread was below the established limit of 508 mm (20 inches). At the temperatures of 36 and 28 °C (96 and 83 °F), the mixtures made for 635 and 711 mm (25 and 28 inches) slump flow displayed increases in T_{50} time of about 9 and 5%, and 54 and 40%, respectively, when compared to that of the control temperature. The 635-mm (25-inches) slump flow concrete ceased to be self-consolidating at 43 °C (109 °F) and its T_{50} could not be measured. However, the 711-mm (28-inches) matrix displayed 68% increases in flow rate at 43 °C (109 °F). In hot temperatures, the visual stability index (VSI) of the mixtures made with 28 inches (711 mm) slump flow improved from 1 (stable matrix) to 0

327

(highly stable matrix). The others two SCC types (slump flows of 20 and 25 inches (508 and 635 mm)) remained highly stable at the selected elevated temperatures.

The effect of cold temperature on the fresh performance of the selected self-consolidating concretes was manifested in the form of a marginal gain in flow ability (averaging 3%) and small variations in flow rate (averaging 6%) when compared to those obtained under the control temperature. In cold temperatures, the matrice made with slump flow of 711mm (28 inches) exhibited an increase in resistance to segregation from VSI of 1 (stable) to VSI of 0 (highly stable). On the other hand, the VSI of the trial SCCs prepared with slump flows of 508 and 635 mm (20 and 25 inches) were unaffected by the selected cold temperatures.

The alteration of the fresh properties induced by the selected hot and cold temperatures were explained through the adsorption amount of admixture per specific surface area of concrete paste (Ads/SSAp), the change in the aggregate's moisture content, and the partial evaporation of mixing water in the case of elevated temperatures. A summarized explanation of the test results is given below.

• The ultraviolet-visible spectroscopy test indicated that the free concentration of HRWRA-cement-water solution changed with material temperatures. The free admixture concentration remained uniform at temperatures ranging from 14 to 36 °C (57 to 96 °F) and decreased gradually as the temperatures was elevated to 43 °C (109 °F) or decrease towards the water freezing point. While the calculated concentrations do not represent the actual amounts of adsorbed HRWRA on cement particles, their increases in the solution lead to an augmentation of the adsorbed amount of the PC-HRWRA carboxylic group (COO^-) on cement grains, favoring further increase or decrease in electrostatic

328

repulsion and steric hindrance forces.

- In general, the relative humidity around the raw material was increased in cold temperatures, leading to an increase in the moisture content of the aggregates. The same aggregates experienced the opposite phenomenon in hot temperatures. The test results revealed that an increase in aggregate's temperature from -0.5 to 43 °C (31 to 109 °F) required about 5 kg/m^3 (8 lb/yd^3) of additional mixing water to maintain the same slump flow. Additionally, the mixing water was partially evaporated and/or absorbed by the elevated temperatures and low relative humidity, causing further decline in the slump flow of freshly-mixed concrete.

- The hot temperatures affected self-consolidating concrete by increasing the specific surface area of concrete paste, SSAp, through the increase rate of hydration. Despite the augmentation in adsorption as discussed above, the increase in SSAp was able to reduce the overall workability of the fresh concrete. On the other hand, the selected cold temperatures did not significantly impact the specific surface area of the cement hydrated products since continued hydration in cold temperature was at a lower rate. In this case, Ads nearly gained on SSAp, as little to no change in the workability of the fresh matrix was observed.

7.1.3.2   Remediation of the adverse effect of extreme temperature on freshly-mixed SCC

The increase in slump flow of the trial matrices in cold temperatures were less than 25 mm (1.0 inch), and both the flow rate and dynamic segregation resistance were unaffected by the selected cold temperatures. As a result, the selected self-consolidating concretes did not require any remediation in cold temperatures of 14, 7 and -0.5 °C (57, 44 and 31 °F).

A remediation method by way of admixture overdosing was successful to reverse the change in fresh properties of the selected self-consolidating concretes in elevated temperatures. The additional amount of admixtures increased workability (up to 36 $^{\circ}$C (96 $^{\circ}$F)) through generation of supplementary repulsive electrostatic and steric hindrance forces between cement particles and was able to offset the loss of workability caused by the growth of the cement hydrated products engendered during hot temperatures. The selected remediation method was able to produce SCCs with a similar unconfined workability, flow rate or plastic viscosity per inference, dynamic stability, and passing ability to those obtained for the equivalent matrices at the control temperature.

7.1.3.3 Statistical analysis

Predictive equations to correlate slump flow loss or gain with the target temperature and slump flow revealed a significant statistical relationship between the dependant and independent variables. For the remediation purpose in hot temperature, the required optimum admixture dosages (HRWRA and VMA) were also predicted for the selected target slump flows and elevated temperatures. A strong statistical relationship between the dependent and independent variables of the remediated concrete was also obtained.

7.1.4 Influence of combined hauling time and temperature on fresh performance of self-consolidating concrete

The understanding of the influence of combined hauling time and temperature on the fresh self-consolidating concrete is useful in simulating concrete mixing and hauling by the mean of concrete truck mixer during extreme temperatures. The following conclusions can be drawn from the test results:

7.1.4.1   Influence of hauling time and temperature on freshly-mixed SCC

7.1.4.1.1   Slump flow

In general, the self-consolidating concrete manufactured and hauled in extreme temperatures experienced slump flow losses in hot conditions, and gains in cold environments when compared to the equivalent concretes produced at the control temperature of T21H10 (i.e., 10-minute hauling time under normal room temperature of 21 °C (70 °F)).

The slump flow decreased with the increase in hot temperature and hauling time. The 635 and 711 mm (25 and 28 inches) slump flow SCCs hauled for 20 minutes under 43, 36, and 28 °C (109, 96, and 83 °F) displayed losses in flow ability of 31, 24, and 19%, and 30, 15, and 12%, respectively, when compared to the corresponding slump flow obtained at the control condition of T21H10. Additional decreases in flow ability of 10% per 20 minutes increment in hauling time were observed as the transportation time progressively increased to up to 80 minutes at each of the selected hot temperatures.

When compared to T21H10, the trial self-consolidating concretes also experienced decreases in slump flow in cold temperature, but to a lesser extent. The losses in slump flow after 20 minutes of hauling for the matrices prepared under 14, 7, or -0.5 °C (57, 44, or 31 °F) were about 10 and 2% for the 635 and 711 mm (25 and 28 inches) slump flow SCCs, respectively. For the hauling times of 40 to 80 minutes, an average increase of about 7% per 20 minutes increment was experienced for each selected cold temperature.

7.1.4.1.2   Flow rate

The flow rate/plastic viscosity (measured by the T_{50} time) of the selected self-

consolidating concretes were also affected by the combination of hauling time and temperature. In comparing to the T_{50} time of the control T21H10 condition, up to 40% increase in flow rate was observed when the 635 mm (25 inches) slump flow self-consolidating concrete was transported for 20 minutes under 28 $^{\circ}$C (83 $^{\circ}$F). The corresponding increase was 52% for the 711 mm (28 inches) slump flow concrete. As hauling time increased to 40 minutes for the 635 mm (25 inches) and 60 minutes for the 711 mm (28 inches), the selected self-consolidating concretes displayed severe losses in slump flow at 36 and 43 $^{\circ}$C (96 and 109 $^{\circ}$F), and their T_{50} times could not be measured since the flow spreads were below the recommended 508 mm (20 inches).

Contrary to what was observed in hot conditions, the self-consolidating concrete made with 635 mm (25 inches) slump flow and hauled for 20 minutes or less under each selected cold temperature displayed an average decrease of 5% in flow rate. Beyond this point, excessive losses in slump flow were observed with increases in hauling time and the T_{50} times could not be evaluated. On the other hand, the T_{50} times of the high slump flow concretes, i.e., the 711 mm (28 inches), could be measured for all selected hauling times. In comparing to the corresponding control (T21H10), the T_{50} times of the 711 mm (28 inches) slump flow self-consolidating concretes decreased by 27, 54, 61, and 89% after 20, 40, 60, and 80 minutes of hauling, respectively.

7.1.4.1.3 Dynamic stability

The combination of hauling time and temperature enhanced the dynamic stability of the 711 mm (28 inches) matrices from stable (VSI = 1) to highly stable (VSI = 0). The 635 mm (25 inches) fresh matrices were unaffected by the combination of temperature and hauling time and remained highly stable under all selected conditions.

The changes in fresh properties of plastic self-consolidating concretes can be explained through the increase or decrease in adsorption amount of admixture per specific surface area of concrete mortar (Ads/SSAm), the contribution of aggregate's moisture content, and partial evaporation of mixing water.

As reported in Chapters 4 and 5, both hauling time and temperature affected the specific surface area of concrete mortar. The Laser diffraction particle size analysis of a concrete paste indicated that the volume of the fine particles (ranging from 1 to 250 μm (39×10^{-6} to 9843×10^{-6} inch) increased as the hauling time increased from 20 to 40, 60, and 80 minutes, leading to an increase in SSAm. The contribution of the hauling time to the increase in SSAm was attributed to the grinding of aggregate and cement particles, and the growth of cement hydrated products. The influence of temperature was explained through the growth of cement hydrated products.

The UV/Vis spectroscopy test revealed that the cement-water-superplasticizer solution concentration in free admixture increased with an increase in hauling time (up to 80 minutes). It also increased with an increase in temperature (up to 36 $^{\circ}$C (96 $^{\circ}$F)). The increases in solution concentration revealed the increase of admixture adsorption (Ads) on cement particles. The contribution of Ads to the fresh performance of the trial matrix under the combined influence of temperature and hauling mainly resulted from the accumulation of Ads_{haul} from hauling time and Ads_{temp} from the temperature. However, despite the augmentation in Ads, the increase in SSAm was sufficient to decrease the Ads/SSAm, resulting in further reduction (in hot temperature) or conservation (in cold temperature) of the unconfined workability for the trial self-consolidating concretes.

7.1.4.2 Remediation of the adverse effect of combined hauling time and temperature on freshly-mixed SCC

The overdosing and retempering methods of remediation were successful in mitigating the adverse effect of combined hauling time and temperature on self-consolidating concrete. Fresh matrices with suitable unconfined workability, plastic viscosity, dynamic stability, and passing ability were achieved once remediated by either of the two methods.

The selection of an appropriate remediation method should be based on one or a combination of the factors, such as mixture economy, admixture dosage flexibility, availability of qualified personnel, and degree of quality control.

7.1.4.3 Statistical analysis

The statistical equations to predict: (1) the actual slump flow of the self-consolidating concrete prepared and transported for different intended slump flows, hauling times, and hot and cold temperatures; (2) the required optimum overdosed or retempered admixtures (HRWRA and VMA) amount to achieve the desired flow ability and stability under various hauling times and temperatures showed significant relationships between the dependent and independent variables.

7.2 Recommendations

Future studies on the fresh performance of self-consolidating may include:

(1) Rheological study of self-consolidating concrete

The rheological properties of concrete, i.e., yield stress and plastic viscosity are of great importance. Self-consolidating concrete is considered high performance in fresh state. As such, the evaluation by mean of a standard rheometer, rather than using T_{50}

334

time, may be helpful in understanding and controlling the fresh behavior of self-consolidating concrete.

(2)   Laboratory study of self-consolidating concrete to simulate field pumping

The test results of a companion investigation conducted in a concrete mixing plant by Ghafoori, N., Diawara, H., and Barfield M., indicated that pumping adversely affected the fresh performance of the self-consolidating concrete by decreasing the unconfined workability, flow rate, and passing ability; and by increasing the dynamic segregation resistance. Pumping also impacted the rheological properties of self-consolidating concrete by a moderate increase in relative yield stress and a significant decrease in relative plastic viscosity. The air void characteristics were affected by the pumping, but did not exceed the recommend limits. The pumping generated larger sizes of air bubbles (or lower specific area) and increased voids spacing factors.

To further support and explain these findings, a laboratory study may be used by subjecting fresh matrices to shear actions in simulating the field pumping. The shear action can be created by mixing action and energy.

(3)   Influence of cement type on hauled self-consolidating concrete under extreme hot temperatures

The slump flow losses observed during the present study was partly due to the rapid growth of the cement hydrated products caused by the high amount of tricalcium aluminate (C_3A) of Type V Portland cement. The use of Portland cement Types I and III, which contain a lower amount of C_3A than Type V, may produce lower slump flow losses, thus requiring a smaller amount of admixture in producing the same slump flow.

(4)   The influence of supplementary cementitious material type and content on self-consolidating concrete

Since strength and durability are not of great concern due to the high cementitious materials content used in self-consolidating concrete, replacing a portion of Portland cement by fly ash can be considered. The study on the content and type of fly ash, particularly large volume fly ash, on the fresh properties of self-consolidating concrete can make a significant contribution to the state of the knowledge on this subject.

(5)   Drying shrinkage and creep of self-consolidating concrete

The increase use of self-consolidating concrete in prestressed concrete applications requires mixture design and proportioning suitable for permissible drying shrinkage and creep. The high fluidity of fresh self-consolidating concrete necessitates a control of its hardened deformations.

APPENDIX I

CONVERSION FACTORS

1 mm = 0.0394 inch

1 nm = 10^{-9} m =

1 kg = 2.20 lb

$^{\circ}C = (5/9)\,(^{\circ}F - 32)$

1 MPa = 145 psi

1 kg/m^3 = 1.684 lb/yd^3 = 0.0624 lb/ft^3

1 kg/m^3 = 0.0624 lb/ft^3

1 ml/100 kg = 0.0153 oz/cwt

APPENDIX II

GLOSSARY

The intent of this glossary is to define terminologies used in this report. The following definitions apply:

Admixture: Material added during the mixing process of concrete in small quantities related to the mass of cementitious binder to modify the properties of fresh or hardened concrete

Binder: The combined Portland cement and fly ash

Bingham fluid: A fluid characterized by a non-null yield stress and a constant viscosity regardless of flow rate

Confined flowability: The ability of a fresh concrete to flow in a form characterized by a low ratio of horizontal form surface to total form surface

Dynamic stability: The characteristic of a fresh SCC mixture that ensures uniform distribution of all solid particles and air voids as the SCC is being transported and placed

Filling ability: The confined workability or the ability of fresh concrete to flow into and fill all spaces within the formwork under its own weight

Flow ability: The ease of flow of fresh concrete when unconfined by formwork and/or reinforcement

High range water reducing admixture: Admixture added to fresh concrete to increase its fluidity

Mortar: The fraction of the concrete comprising paste plus those aggregates passing #4 sieve (0.187 in. (4.75 mm))

Mortar Halo: A concentration of mortar that can form at the perimeter of the slump flow patty

Paste: The fraction of the concrete comprising powder, water and air, plus admixture, if applicable

Passing ability: The ability of fresh concrete to flow through tight openings such as spaces between steel reinforcing bars without segregation or blocking

Powder: Material of particle size passing the No. 100 sieve (0.006 in. (0.15 mm))

Self-consolidating concrete (SCC): Concrete that is able to flow and consolidate under its own weight, completely fill the formwork even in the presence of dense reinforcement, whilst maintaining homogeneity and without the need for any additional compaction

Segregation resistance: The ability of concrete to remain homogeneous in composition while in its fresh state

Slump flow: The mean diameter of the spread of fresh concrete using a conventional slump cone

Rheological properties: Properties dealing with the deformation and flow of the fluid fresh SCC mixture.

Thixotropy: The tendency of a material (e.g. SCC) to progressively lose fluidity when allowed to rest undisturbed but to regain its fluidity when energy is applied

Unconfined workability: The ability of a fresh concrete to flow in a form characterized by a high ratio of horizontal form surface to total form surface

Viscosity: The resistance to flow of a material (e.g. SCC) once flow has started.

Viscosity Modifying Admixture (VMA): Admixture added to fresh concrete to increase cohesion and segregation resistance.

Yield point of concrete: The force needed to start the concrete moving.

APPENDIX III

INFLUENCE OF ADMIXTURE SOURCE ON OPTIMUM ADMIXTURE DOSAGE

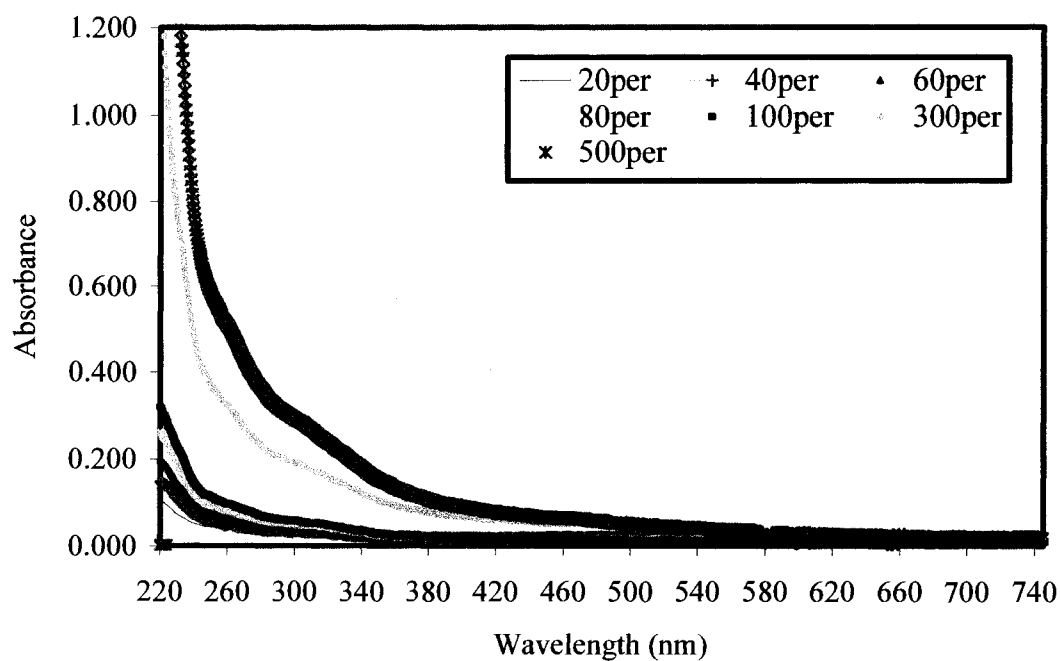Ultraviolet-visible absorbance spectra for the calibrations curves
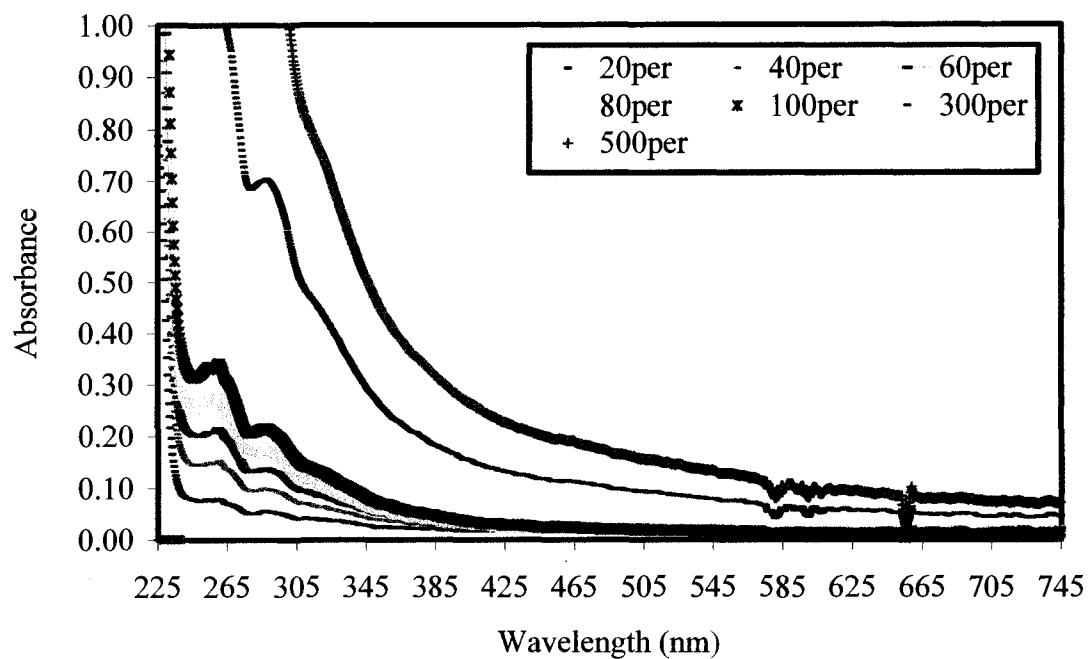

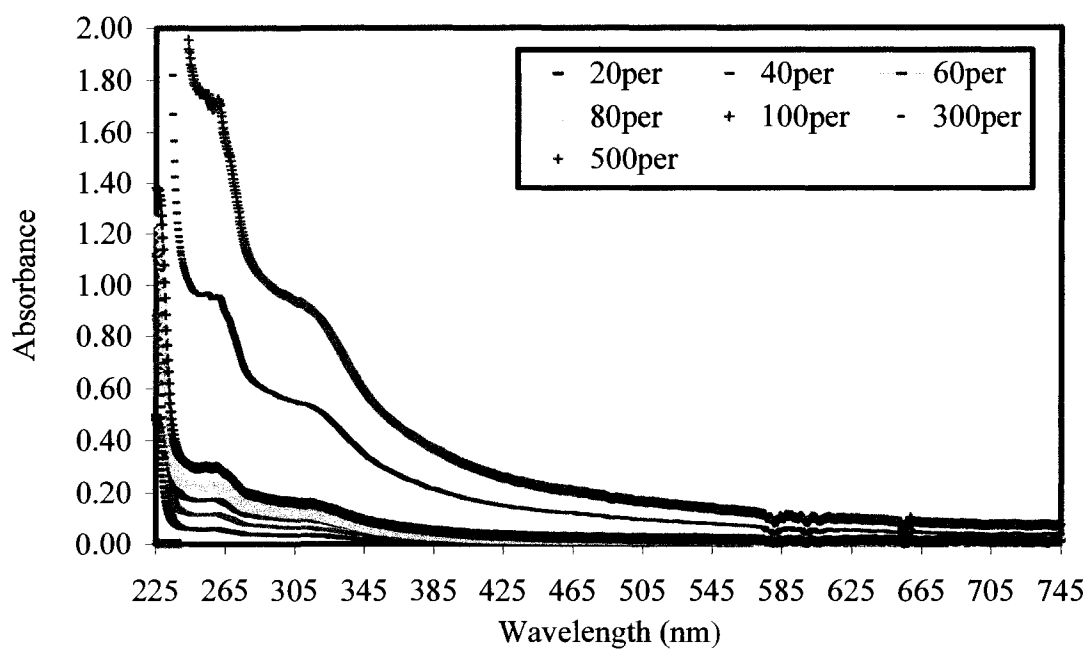Figure III.1: Admixture source A

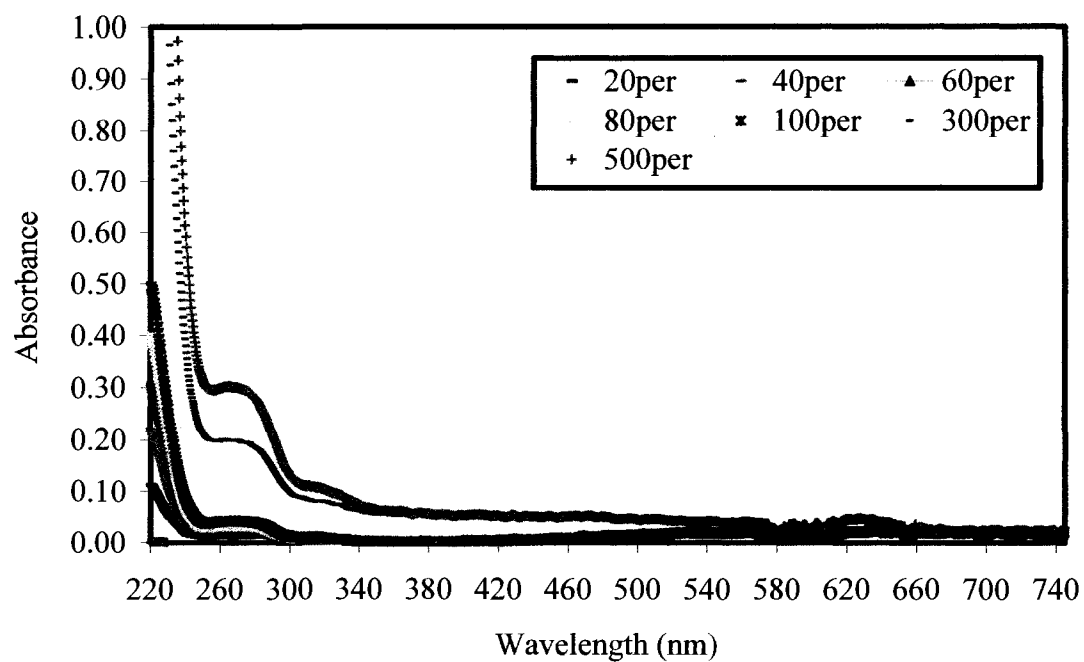Figure III.2: Admixture source B

Figure III.3: Admixture source C

341

Figure III.4: Admixture source D

APPENDIX IV

INFLUENCE OF HAULING TIME ON FRESH PERFORMANCE OF SCC

Laser diffraction particle size distribution
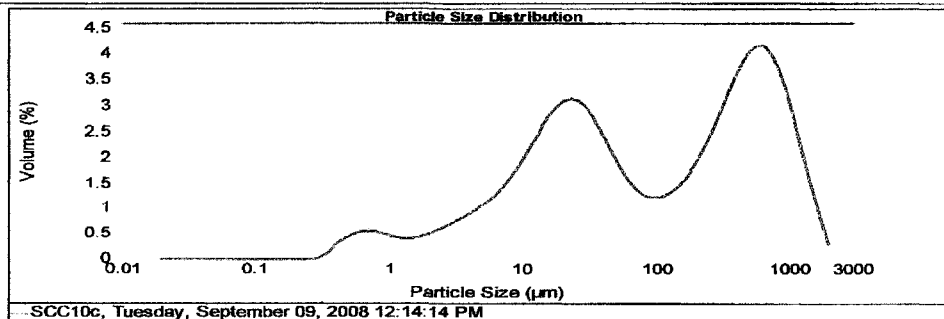
MASTERSIZER 2000

Result Analysis Report

Sample Name: 10 minutes hauling time

Sample Source & type:
BSNE = Nellis

Sample bulk lot ref:

SOP Name:
dust project Nellis Dunes

Measured by:
Administrator

Result Source:
Measurement

Measured:
Tuesday, September 09, 2008 12:14:14 PM

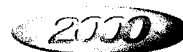**Analysed:**
Tuesday, September 09, 2008 12:14:16 PM

Particle Name:
Silica 0.0

Particle RI:
1.544

Dispersant Name:
Water

Accessory Name:
Hydro 2000S (A)

Absorption:
0.1

Dispersant RI:
1.330

Analysis model:
General purpose

Size range:
0.020   to   2000.000   um

Weighted Residual:
0.951   %

Sensitivity:
Enhanced

Obscuration:
21.65   %

Result Emulation:
Off

Concentration:
0.0388   %Vol

Specific Surface Area:
0.625   m²/g

Span :
9.840

Surface Weighted Mean D[3,2]:
9.607   um

Uniformity:
3.14

Vol. Weighted Mean D[4,3]:
301.431   um

Result units:
Volume

---

d(0.1):   5.385   um   d(0.5):   88.660   um   d(0.9):   877.759   um

Particle Size Distribution

SCC10c, Tuesday, September 09, 2008 12:14:14 PM

Size (μm)	Volume In %	Size (μm)	Volume In %	Size (μm)	Volume In %	Size (μm)	Volume In %	Size (μm)	Volume In %	Size (μm)	Volume In %
0.020	0.00	0.142	0.00	1.002	0.34	7.096	1.13	50.298	1.40	355.656	2.67
0.022	0.00	0.159	0.00	1.125	0.31	7.962	1.26	56.368	1.23	399.052	2.79
0.025	0.00	0.178	0.00	1.262	0.30	8.934	1.40	63.246	1.10	447.744	2.97
0.028	0.00	0.200	0.00	1.416	0.31	10.024	1.55	70.963	1.00	502.377	3.09
0.032	0.00	0.224	0.00	1.589	0.32	11.247	1.72	79.621	0.94	563.677	3.14
0.036	0.00	0.252	0.00	1.783	0.35	12.619	1.88	89.337	0.91	632.456	3.10
0.040	0.00	0.283	0.01	2.000	0.39	14.159	2.03	100.237	0.92	709.627	2.97
0.045	0.00	0.317	0.06	2.244	0.43	15.887	2.17	112.468	0.96	796.214	2.76
0.050	0.00	0.356	0.16	2.518	0.48	17.825	2.28	126.191	1.02	893.367	2.46
0.056	0.00	0.399	0.24	2.825	0.53	20.000	2.34	141.589	1.10	1002.374	2.11
0.063	0.00	0.448	0.30	3.170	0.59	22.440	2.36	158.866	1.21	1124.683	1.73
0.071	0.00	0.502	0.35	3.557	0.64	25.179	2.33	178.250	1.34	1261.915	1.34
0.080	0.00	0.564	0.39	3.991	0.69	28.251	2.25	200.000	1.50	1415.892	0.96
0.089	0.00	0.632	0.41	4.477	0.76	31.698	2.12	224.404	1.68	1588.656	0.62
0.100	0.00	0.710	0.41	5.024	0.83	35.566	1.99	251.785	1.88	1782.502	0.34
0.112	0.00	0.796	0.39	5.637	0.92	39.905	1.77	282.508	1.88	2000.000	
0.126	0.00	0.893	0.38	6.325	1.01	44.774	1.58	316.979	2.10		
0.142		1.002		7.096		60.238		355.656	2.34		

MASTERSIZER 2000

Result Analysis Report

**Sample Name:** *20 minutes hauling time*

Sample Source & type: BSNE = Nellis

Sample bulk lot ref:

SOP Name: dust project Nellis Dunes

Measured by: Administrator

Result Source: Measurement

Measured: Tuesday, September 09, 2008 12:19:34 PM

Analysed: Tuesday, September 09, 2008 12:19:35 PM

Particle Name: Silica 0.0

Particle RI: 1.544

Dispersant Name: Water

Accessory Name: Hydro 2000S (A)

Absorption: 0.1

Dispersant RI: 1.330

Analysis model: General purpose

Size range: 0.020 to 2000.000 um

Weighted Residual: 0.804 %

Sensitivity: Enhanced

Obscuration: 30.54 %

Result Emulation: Off

Concentration: 0.0450 %Vol

Span: 15.893

Uniformity: 4.79

Result units: Volume

Specific Surface Area: 0.816 m²/g

Surface Weighted Mean D[3,2]: 7.354 um

Vol. Weighted Mean D[4,3]: 213.669 um

d(0.1): 3.542 um   d(0.5): 41.493 um   d(0.9): 663.074 um

Particle Size Distribution
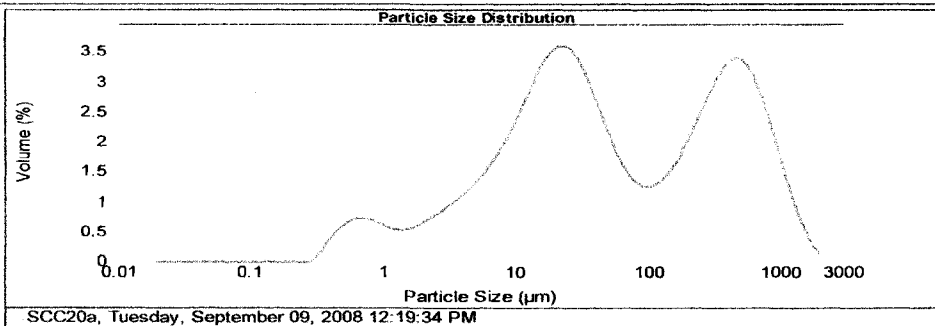
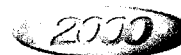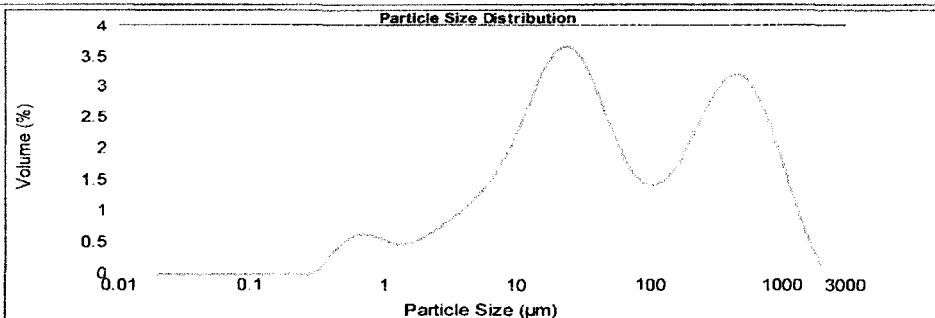SCC20a, Tuesday, September 09, 2008 12:19:34 PM

Size (µm)	Volume In %	Size (µm)	Volume In %	Size (µm)	Volume In %	Size (µm)	Volume In %	Size (µm)	Volume In %	Size (µm)	Volume In %
0.020	0.00	0.142	0.00	1.002	0.45	7.096	1.37	50.238	1.54	355.656	2.43
0.022	0.00	0.159	0.00	1.125	0.42	7.962	1.52	56.368	1.34	399.052	2.52
0.025	0.00	0.178	0.00	1.262	0.40	8.934	1.69	63.246	1.18	447.744	2.55
0.028	0.00	0.200	0.00	1.416	0.40	10.024	1.86	70.963	1.06	502.377	2.51
0.032	0.00	0.224	0.00	1.589	0.42	11.247	2.04	79.621	0.96	563.677	2.40
0.035	0.00	0.252	0.00	1.783	0.46	12.619	2.21	89.337	0.95	632.455	2.23
0.040	0.00	0.283	0.02	2.000	0.51	14.159	2.38	100.237	0.95	709.627	2.01
0.045	0.00	0.317	0.11	2.244	0.56	15.887	2.52	112.468	0.99	796.214	1.74
0.050	0.00	0.356	0.22	2.518	0.62	17.825	2.63	126.191	1.05	893.367	1.45
0.056	0.00	0.399	0.33	2.825	0.68	20.000	2.70	141.589	1.15	1002.374	1.16
0.063	0.00	0.448	0.41	3.170	0.74	22.440	2.71	158.866	1.27	1124.683	0.88
0.071	0.00	0.502	0.48	3.557	0.80	25.179	2.68	178.250	1.42	1261.915	0.64
0.080	0.00	0.564	0.52	3.991	0.87	28.251	2.55	200.000	1.58	1415.892	0.44
0.089	0.00	0.632	0.54	4.477	0.95	31.698	2.39	224.404	1.76	1588.656	0.24
0.100	0.00	0.710	0.54	5.024	1.04	35.566	2.20	251.785	1.95	1782.502	0.14
0.112	0.00	0.796	0.52	5.637	1.13	39.905	1.98	282.508	2.13	2000.000	
0.126	0.00	0.893	0.49	6.325	1.13	44.774	1.98	316.979	2.13		
0.142		1.002		7.096	1.25	50.238	1.75	355.656	2.30		

MASTERSIZER 2000

Result Analysis Report

Sample Name: *40 minutes hauling time*

SOP Name:
dust project Nellis Dunes

Measured:
Tuesday, September 09, 2008 1:06:58 PM

Sample Source & type:
BSNE = Nellis

Measured by:
Administrator

Analysed:
Tuesday, September 09, 2008 1:06:59 PM

Sample bulk lot ref:

Result Source:
Measurement

Particle Name:
Silica 0.0

Accessory Name:
Hydro 2000S (A)

Analysis model:
General purpose

Sensitivity:
Enhanced

Particle RI:
1.544

Absorption:
0.1

Size range:
0.020 to 2000.000 um

Obscuration:
17.68 %

Dispersant Name:
Water

Dispersant RI:
1.330

Weighted Residual:
0.804 %

Result Emulation:
Off

Concentration:
0.0264 %Vol

Span :
14.975

Uniformity:
4.48

Result units:
Volume

Specific Surface Area:
0.728 m²/g

Surface Weighted Mean D[3,2]:
8.244 um

Vol. Weighted Mean D[4,3]:
216.652 um

d(0.1): 4.300 um   d(0.5): 44.689 um   d(0.9): 673.513 um

Particle Size Distribution
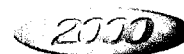
SCC40b, Tuesday, September 09, 2008 1:06:58 PM

Size (µm)	Volume In %	Size (µm)	Volume In %	Size (µm)	Volume In %	Size (µm)	Volume In %	Size (µm)	Volume In %	Size (µm)	Volume In %
0.020	0.00	0.142	0.00	1.002	0.40	7.096	1.30	50.238	1.71	356.656	2.34
0.022	0.00	0.159	0.00	1.125	0.37	7.962	1.45	56.368	1.52	399.052	2.40
0.025	0.00	0.178	0.00	1.262	0.36	8.934	1.61	63.246	1.35	447.744	2.41
0.028	0.00	0.200	0.00	1.416	0.36	10.024	1.79	70.963	1.22	502.377	2.37
0.032	0.00	0.224	0.00	1.589	0.38	11.247	1.97	79.621	1.13	563.677	2.27
0.036	0.00	0.252	0.00	1.783	0.42	12.619	2.16	89.337	1.09	632.456	2.13
0.040	0.00	0.283	0.01	2.000	0.46	14.159	2.35	100.237	1.06	709.627	1.94
0.045	0.00	0.317	0.06	2.244	0.51	15.887	2.51	112.468	1.08	796.214	1.72
0.050	0.00	0.356	0.17	2.518	0.57	17.825	2.64	126.191	1.14	893.367	1.49
0.056	0.00	0.399	0.28	2.825	0.62	20.000	2.72	141.589	1.23	1002.374	1.22
0.063	0.00	0.448	0.35	3.170	0.68	22.440	2.76	158.866	1.34	1124.683	0.96
0.071	0.00	0.502	0.42	3.557	0.75	25.179	2.74	178.250	1.48	1261.915	0.72
0.080	0.00	0.564	0.45	3.991	0.81	28.251	2.65	200.000	1.63	1415.892	0.51
0.089	0.00	0.632	0.48	4.477	0.89	31.698	2.52	224.404	1.79	1588.656	0.32
0.100	0.00	0.710	0.48	5.024	0.97	35.566	2.34	251.785	1.95	1782.502	0.17
0.112	0.00	0.796	0.46	5.637	1.06	39.905	2.14	282.508	2.11	2000.000	
0.126	0.00	0.893	0.43	6.325	1.17	44.774	1.92	316.979	2.24		
0.142		1.002		7.096		50.238		356.656			

Operator notes:

345

MASTERSIZER 2000

Result Analysis Report

Sample Name: 60 minutes tumbling time

Sample Source & type: BSNE = Nellis

Sample bulk lot ref:

SOP Name: dust project Nellis Dunes

Measured by: Administrator

Result Source: Measurement

Measured: Tuesday, September 09, 2008 12:49:28 PM

Analysed: Tuesday, September 09, 2008 12:49:29 PM

Particle Name: Silica 0.0

Particle RI: 1.544

Dispersant Name: Water

Accessory Name: Hydro 2000S (A)

Absorption: 0.1

Dispersant RI: 1.330

Analysis model: General purpose

Size range: 0.020 to 2000.000 um

Weighted Residual: 0.742 %

Sensitivity: Enhanced

Obscuration: 23.49 %

Result Emulation: Off

Concentration: 0.0335 %Vol

Span : 14.941

Uniformity: 4.41

Result units: Volume

Specific Surface Area: 0.795 m²/g

Surface Weighted Mean D[3,2]: 7.550 um

Vol. Weighted Mean D[4,3]: 186.605 um

d(0.1): 3.790 um   d(0.5): 38.987 um   d(0.9): 586.313 um

Particle Size Distribution
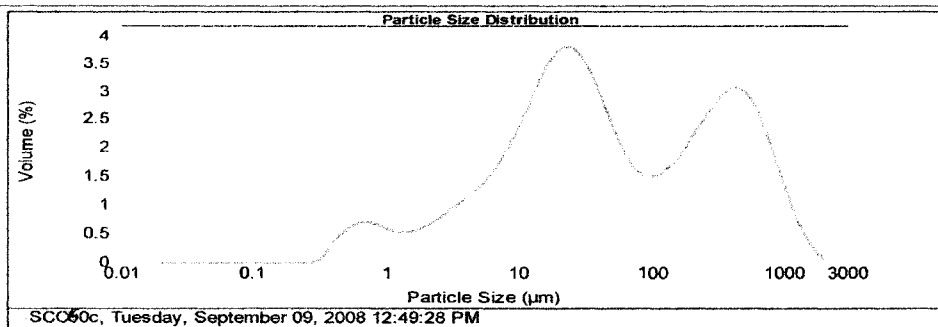
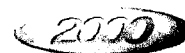SCO60c, Tuesday, September 09, 2008 12:49:28 PM

Size (μm)	Volume In %	Size (μm)	Volume In %	Size (μm)	Volume In %	Size (μm)	Volume In %	Size (μm)	Volume In %	Size (μm)	Volume In %
0.020	0.00	0.142	0.00	1.002	0.44	7.096	1.38	50.238	1.72	355.656	2.26
0.022	0.00	0.159	0.00	1.125	0.41	7.962	1.53	56.368	1.52	399.052	2.30
0.025	0.00	0.179	0.00	1.262	0.39	8.934	1.70	63.246	1.35	447.744	2.28
0.028	0.00	0.200	0.00	1.416	0.40	10.024	1.88	70.960	1.23	502.377	2.21
0.032	0.00	0.224	0.00	1.589	0.42	11.247	2.08	79.621	1.16	563.677	2.08
0.036	0.00	0.252	0.00	1.783	0.45	12.619	2.27	89.337	1.13	632.456	1.89
0.040	0.00	0.283	0.01	2.000	0.50	14.159	2.46	100.237	1.13	709.627	1.65
0.045	0.00	0.317	0.08	2.244	0.55	15.887	2.62	112.468	1.16	796.214	1.41
0.050	0.00	0.356	0.19	2.518	0.61	17.825	2.75	126.191	1.24	893.367	1.14
0.056	0.00	0.399	0.31	2.825	0.67	20.000	2.83	141.589	1.33	1002.374	0.89
0.063	0.00	0.448	0.39	3.170	0.73	22.440	2.86	158.866	1.43	1124.683	0.65
0.071	0.00	0.502	0.46	3.557	0.80	25.179	2.83	178.250	1.55	1261.915	0.45
0.080	0.00	0.564	0.51	3.991	0.87	28.251	2.73	200.000	1.68	1415.892	0.30
0.089	0.00	0.632	0.53	4.477	0.94	31.698	2.58	224.404	1.81	1589.656	0.16
0.100	0.00	0.710	0.53	5.024	1.03	35.566	2.39	251.785	1.94	1782.502	0.09
0.112	0.00	0.796	0.53	5.637	1.13	39.905	2.17	282.508	2.07	2000.000	
0.125	0.00	0.893	0.51	6.325	1.24	44.774	2.17	316.979	2.18		
0.142	0.00	1.002	0.47	7.096		50.238	1.94	355.650			

MASTERSIZER 2000

Result Analysis Report

Sample Name: 80 minutes having time

Sample Source & type:
BSNE = Nellis

Sample bulk lot ref:
.

SOP Name:
dust project Nellis Dunes

Measured by:
Administrator

Result Source:
Measurement

Measured:
Tuesday, September 09, 2008 1:40:31 PM

Analysed:
Tuesday, September 09, 2008 1:40:32 PM

Particle Name:
Silica 0.0

Particle RI:
1.544

Dispersant Name:
Water

Accessory Name:
Hydro 2000S (A)

Absorption:
0.1

Dispersant RI:
1.330

Analysis model:
General purpose

Size range:
0.020 to 2000.000 um

Weighted Residual:
0.798 %

Sensitivity:
Enhanced

Obscuration:
14.78 %

Result Emulation:
Off

Concentration:
0.0243 %Vol

Specific Surface Area:
0.639 m²/g

Span :
11.935

Surface Weighted Mean D[3,2]:
9.386 um

Uniformity:
3.71

Vol. Weighted Mean D[4,3]:
263.980 um

Result units:
Volume

d(0.1): 5.053 um   d(0.5): 65.750 um   d(0.9): 739.783 um

Particle Size Distribution
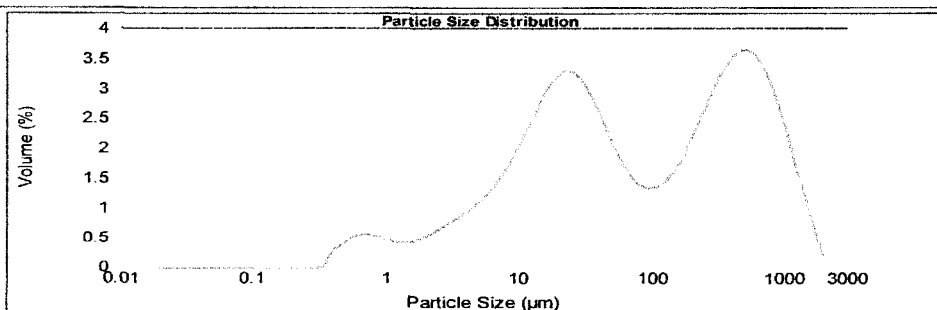
SCC80c, Tuesday, September 09, 2008 1:40:31 PM

Size (µm)	Volume In %	Size (µm)	Volume In %	Size (µm)	Volume In %	Size (µm)	Volume In %	Size (µm)	Volume In %	Size (µm)	Volume In %
0.020	0.00	0.142	0.00	1.002	0.36	7.096	1.18	50.238	1.53	355.656	2.57
0.022	0.00	0.159	0.00	1.125	0.34	7.962	1.31	56.368	1.36	399.052	2.68
0.025	0.00	0.178	0.00	1.262	0.32	8.934	1.46	63.246	1.22	447.744	2.73
0.028	0.00	0.200	0.00	1.416	0.32	10.024	1.62	70.963	1.11	502.377	2.74
0.032	0.00	0.224	0.00	1.589	0.33	11.247	1.79	79.621	1.05	563.677	2.74
0.036	0.00	0.252	0.00	1.783	0.35	12.619	1.96	89.337	1.02	632.456	2.69
0.040	0.00	0.283	0.00	2.000	0.38	14.159	2.12	100.237	1.03	709.627	2.59
0.045	0.00	0.317	0.00	2.244	0.42	15.887	2.27	112.468	1.07	796.214	2.43
0.050	0.00	0.356	0.13	2.518	0.46	17.825	2.38	126.191	1.14	893.367	2.21
0.056	0.00	0.399	0.25	2.825	0.51	20.000	2.45	141.589	1.25	1002.374	1.96
0.063	0.00	0.448	0.30	3.170	0.56	22.440	2.48	158.865	1.38	1124.683	1.67
0.071	0.00	0.502	0.37	3.557	0.62	25.179	2.45	178.250	1.53	1261.915	1.37
0.080	0.00	0.564	0.41	3.991	0.68	28.251	2.38	200.000	1.71	1415.892	1.06
0.089	0.00	0.632	0.42	4.477	0.74	31.698	2.25	224.404	1.89	1588.656	0.79
0.100	0.00	0.710	0.42	5.024	0.80	35.566	2.09	251.785	2.08	1782.502	0.50
0.112	0.00	0.796	0.41	5.637	0.88	39.905	1.91	282.508	2.25	2000.000	0.28
0.126	0.00	0.893	0.38	6.325	0.98	44.774	1.71	316.979	2.43		
0.142		1.002		7.096	1.07	50.238		355.656			

Ultraviolet-visible absorbance spectra at various hauling time
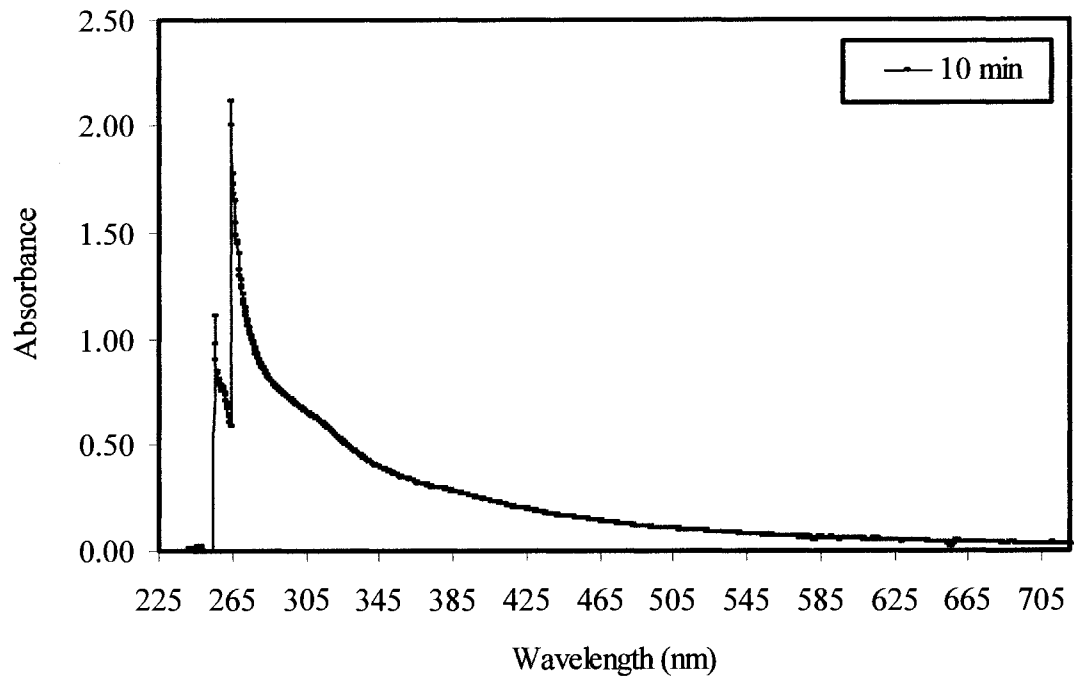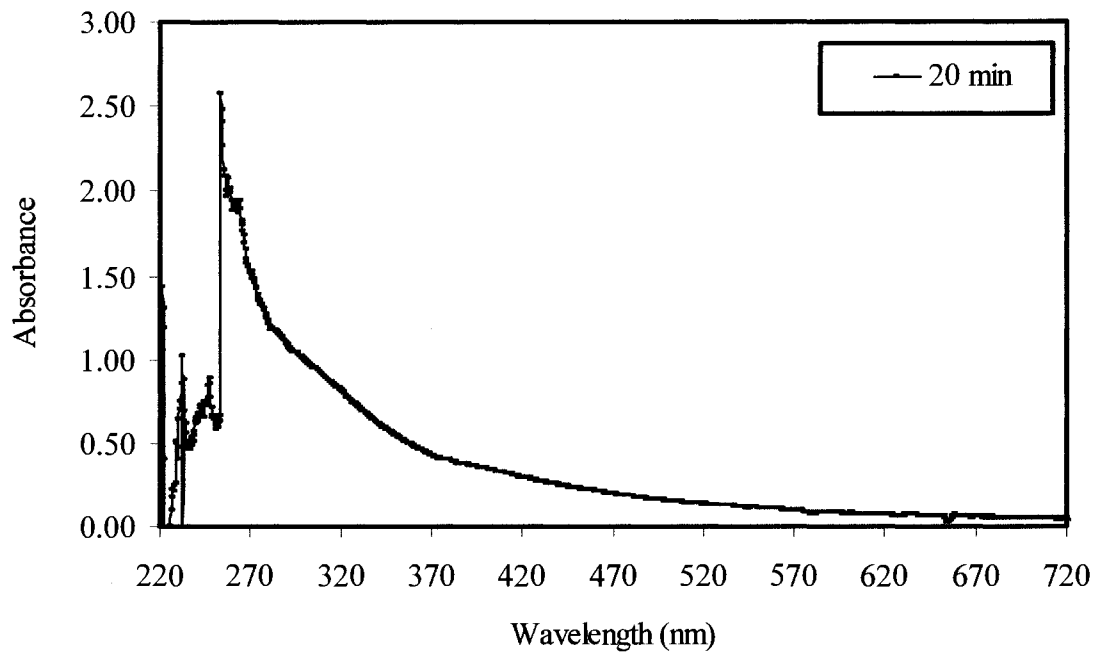

Figure IV.1: 10-minute hauling time
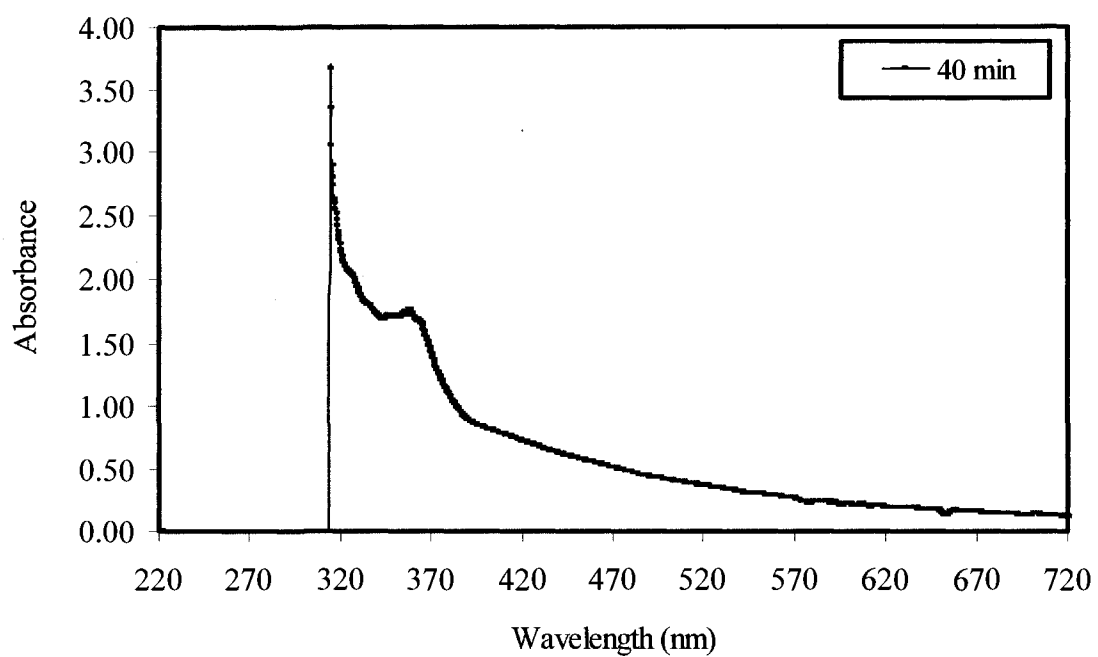

Figure IV.2: 20-minute hauling time

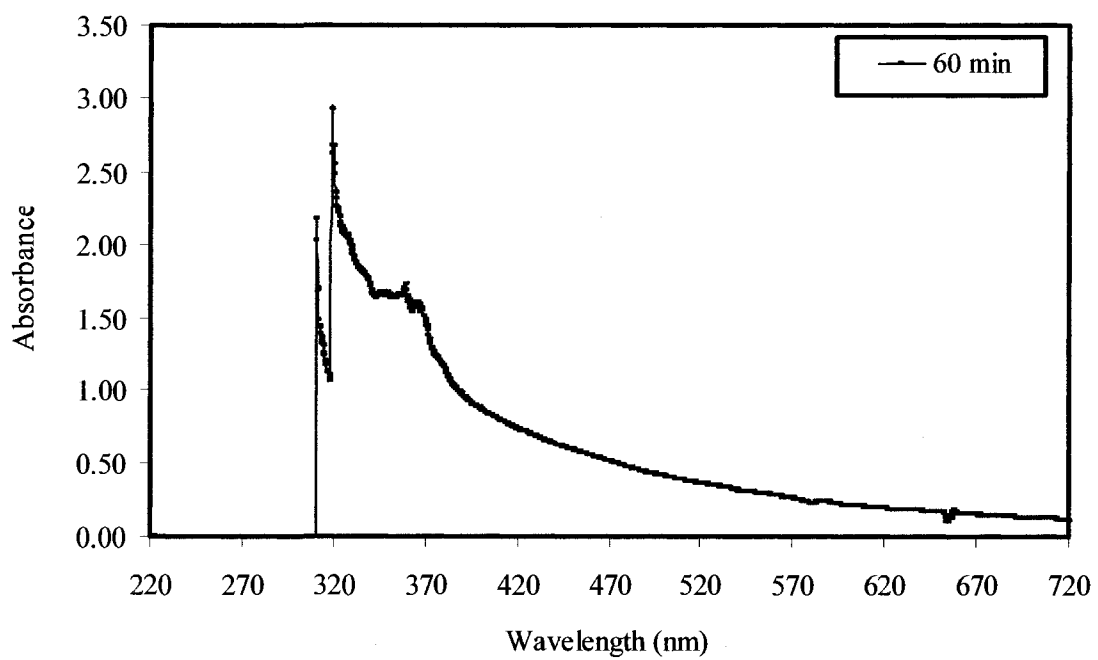Figure IV.3: 40-minute hauling time

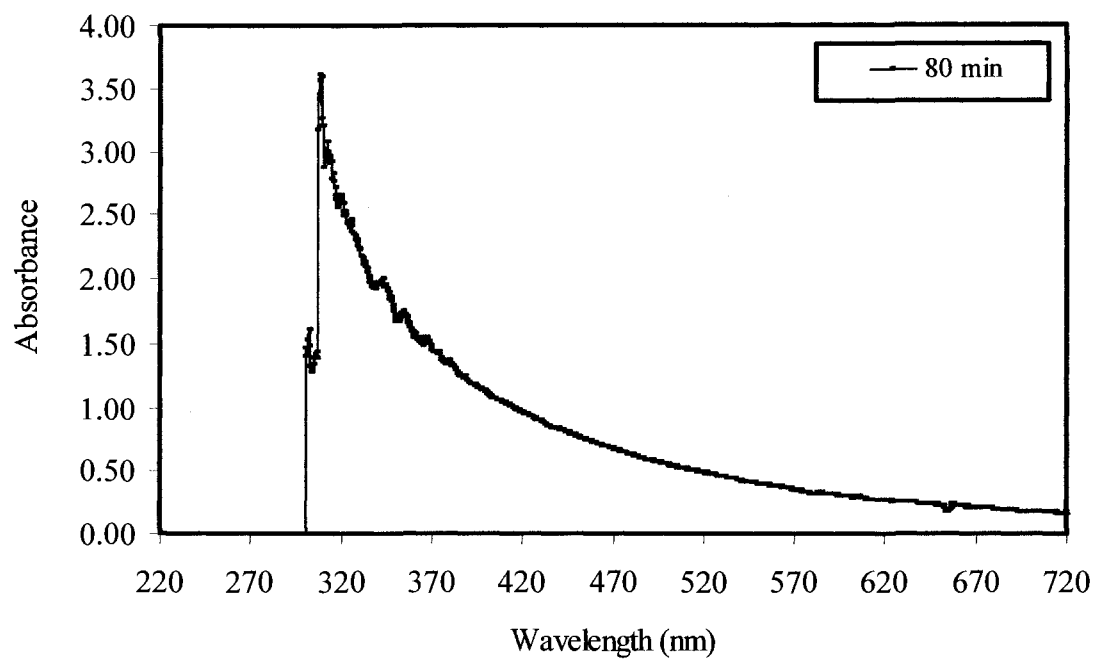Figure IV.4: 60-minute hauling time
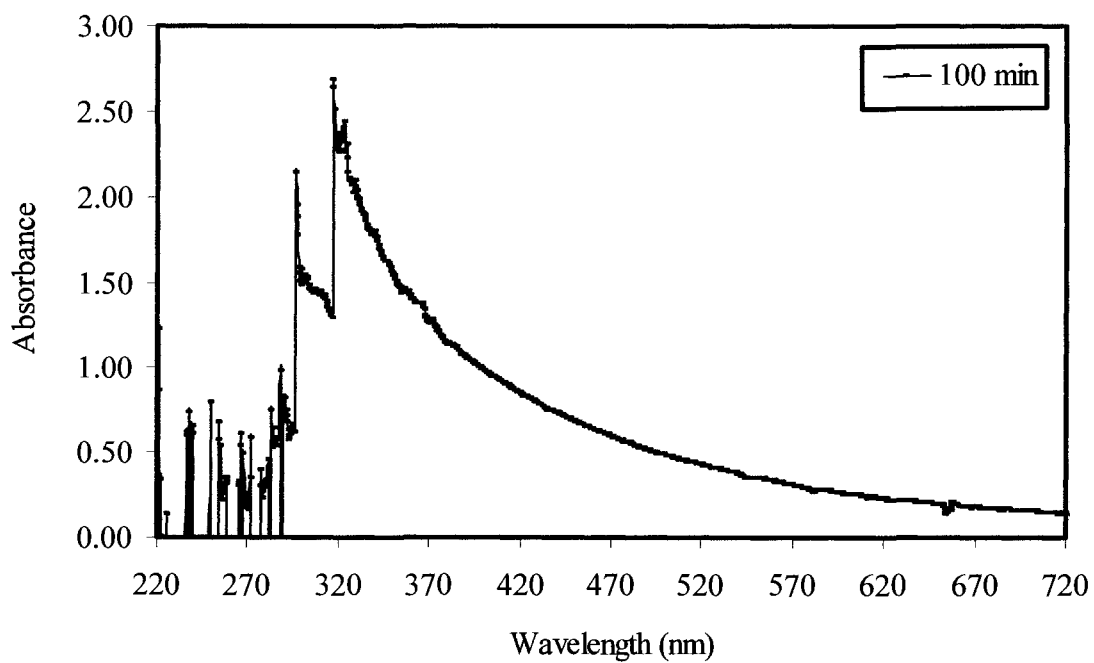
Figure IV.5: 80-minute hauling time
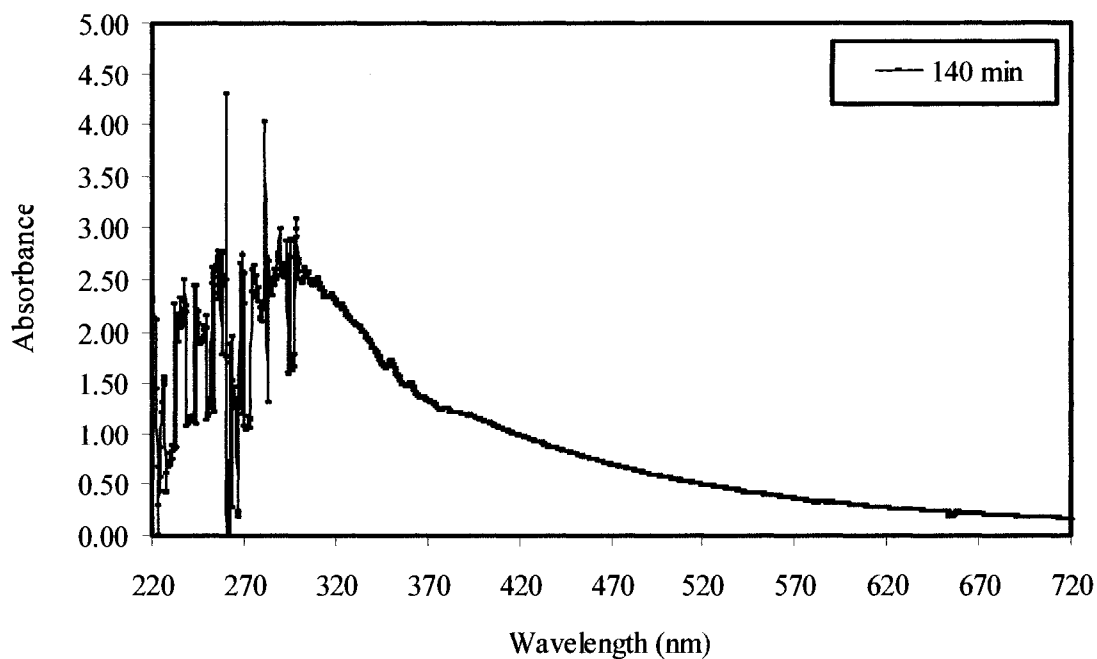

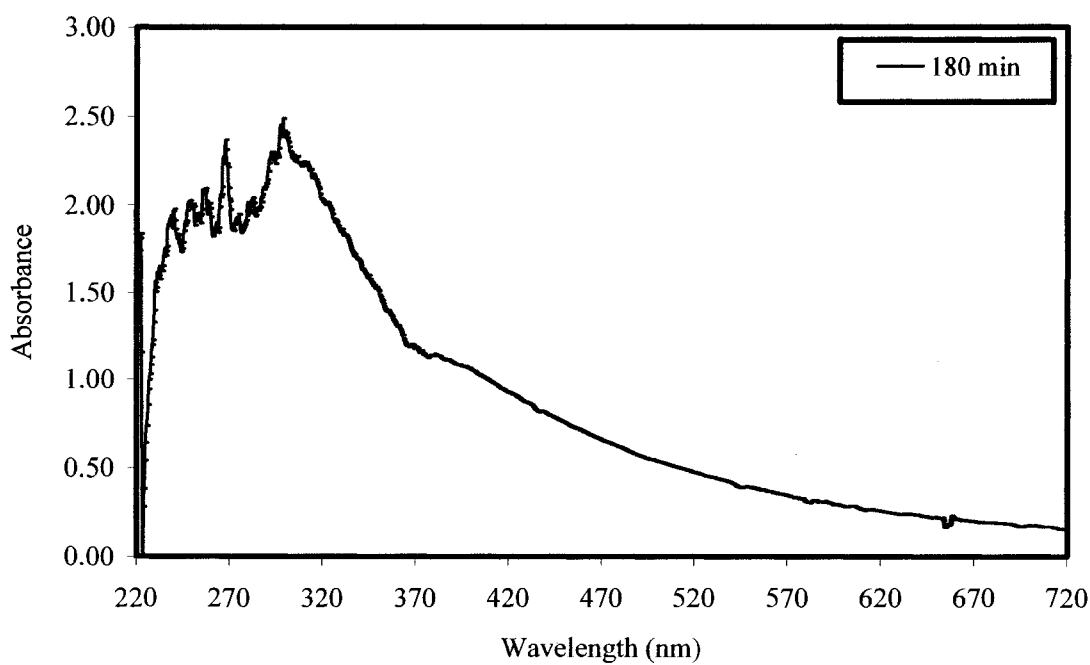Figure IV.6: 100-minute hauling time

350

Figure IV.7: 140-minute hauling time

Figure IV.8: 180-minute hauling time

351

APPENDIX V

INFLUENCE OF EXTREME TEMPERATURE ON FRESH PERFORMANCE OF SCC

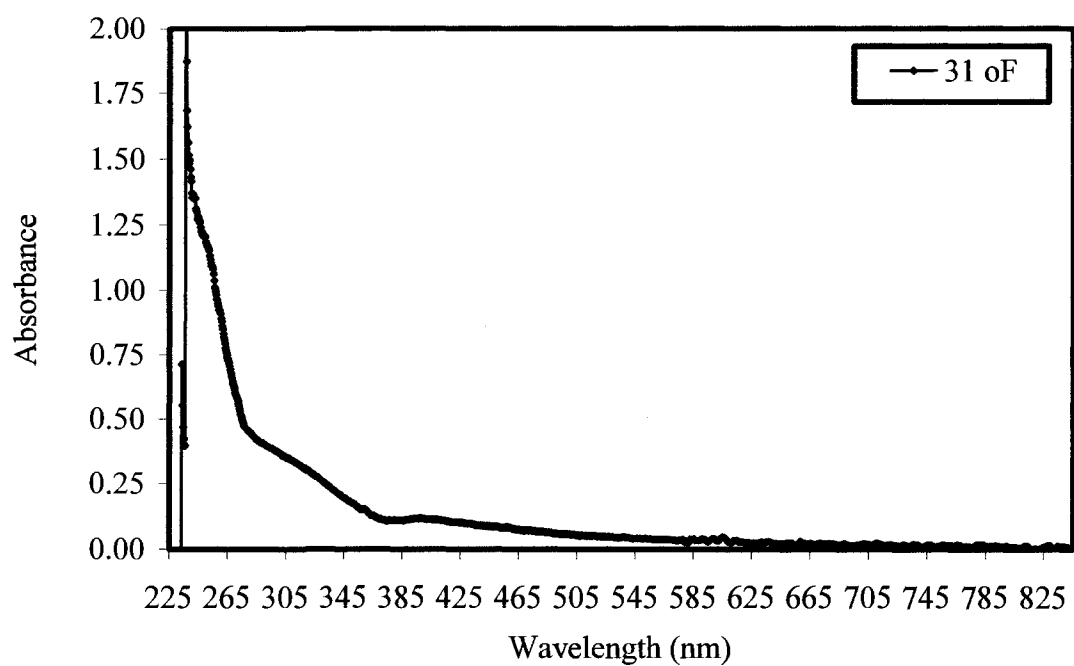Ultraviolet-visible absorbance spectra at various temperatures

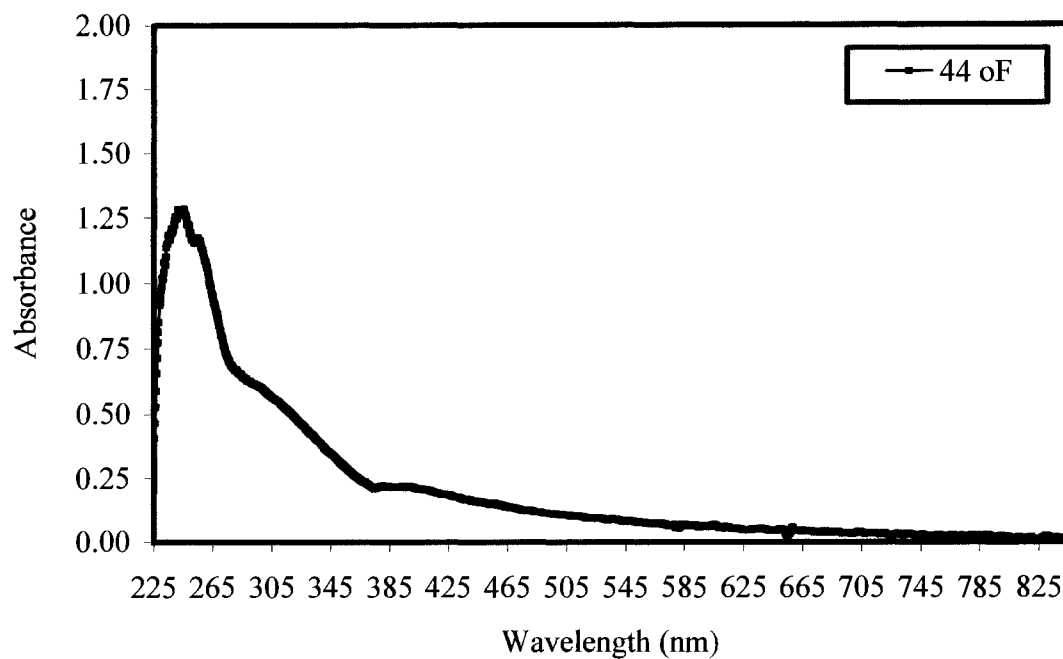Figure V.1: Temperature of -0.5 °C (31 °F)
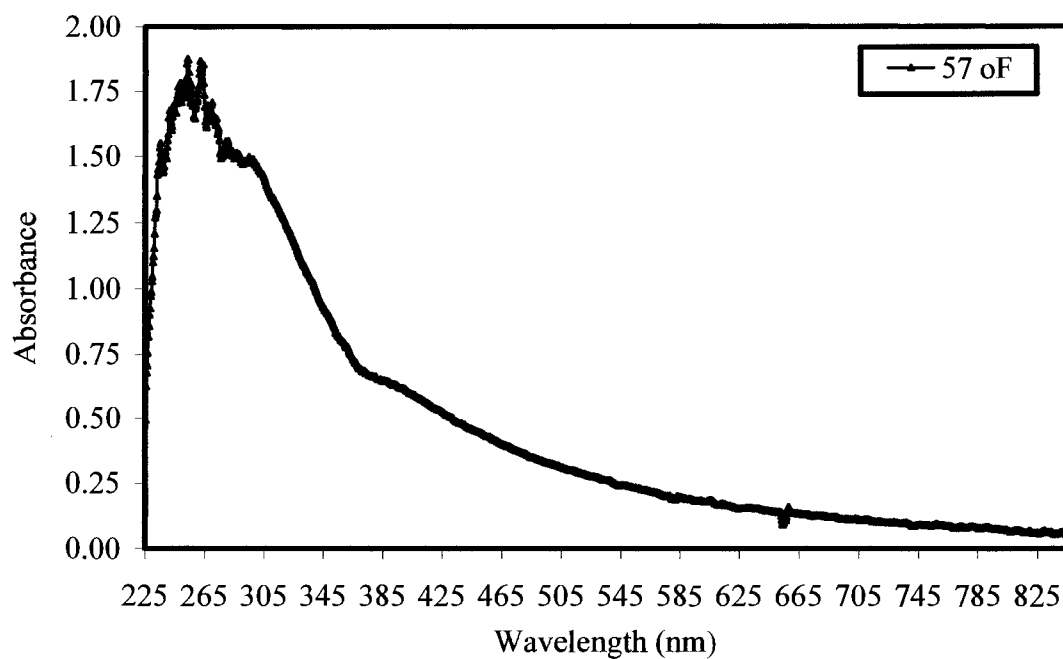
Figure V.2: Temperature of 7 °C (44 °F)

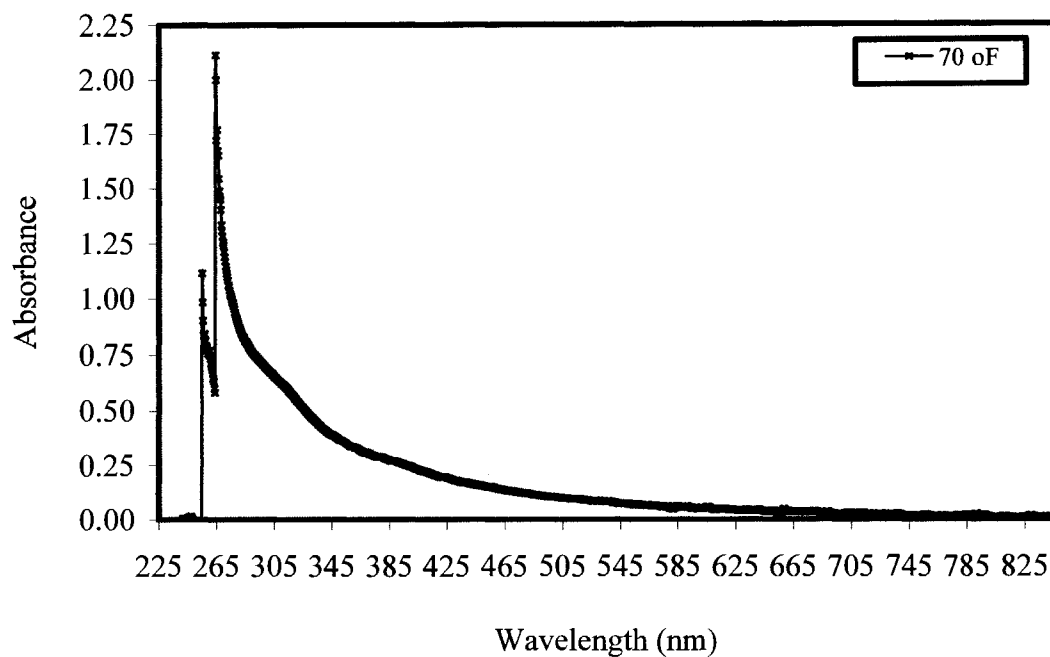Figure V.3: Temperature of 14 °C (57 °F)

353

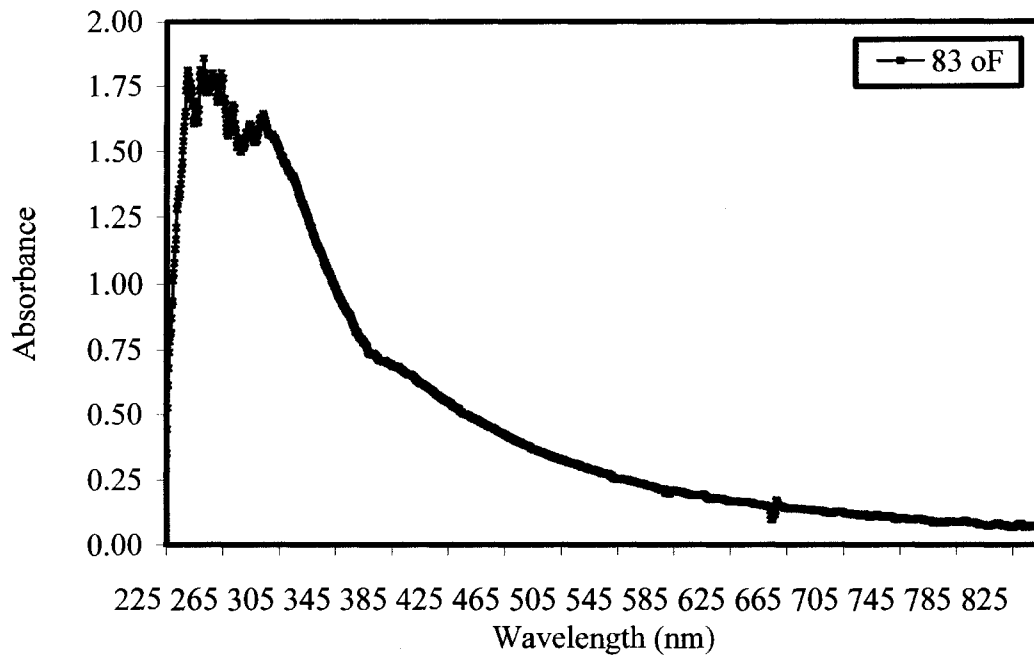Figure V.4: Temperature of 21 °C (70 °F)
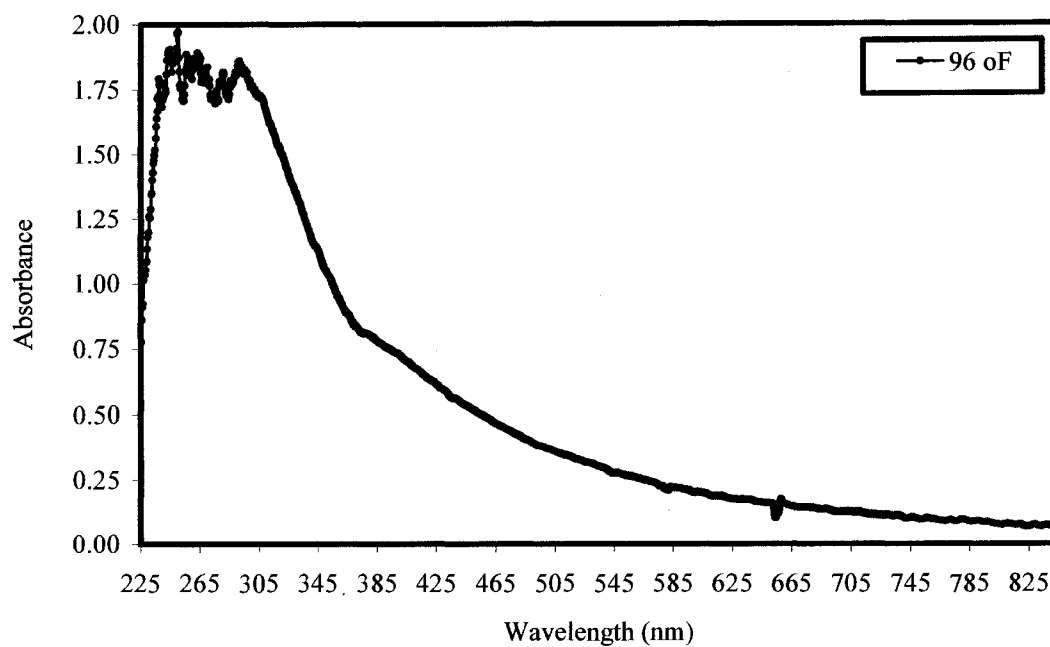

Figure V.5: Temperature of 28 °C (83 °F)

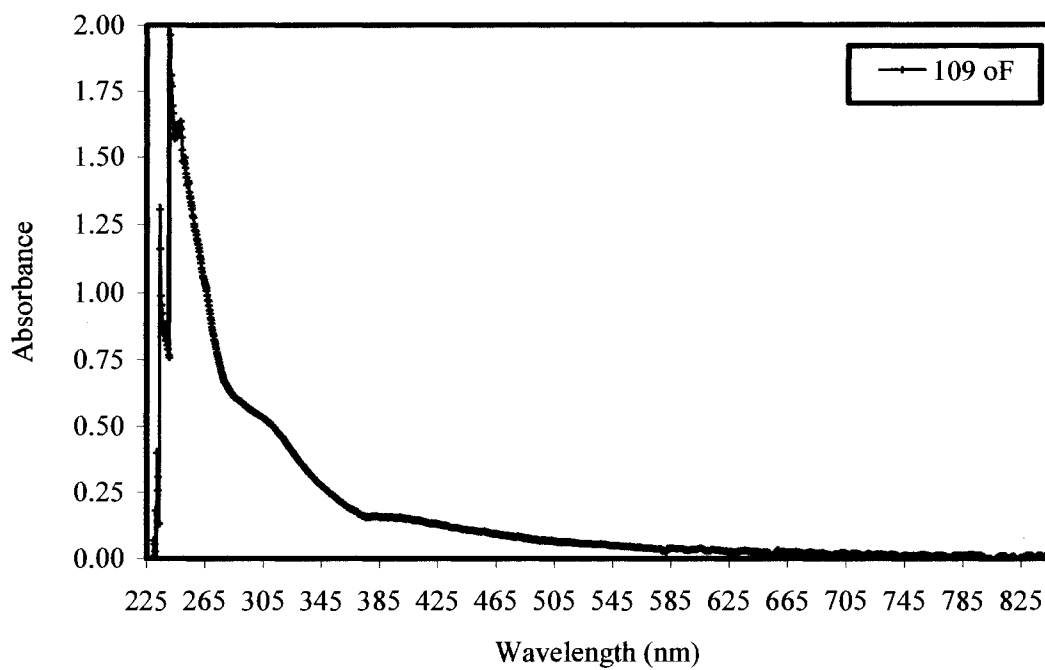Figure V.6: Temperature of 36 °C (96 °F)

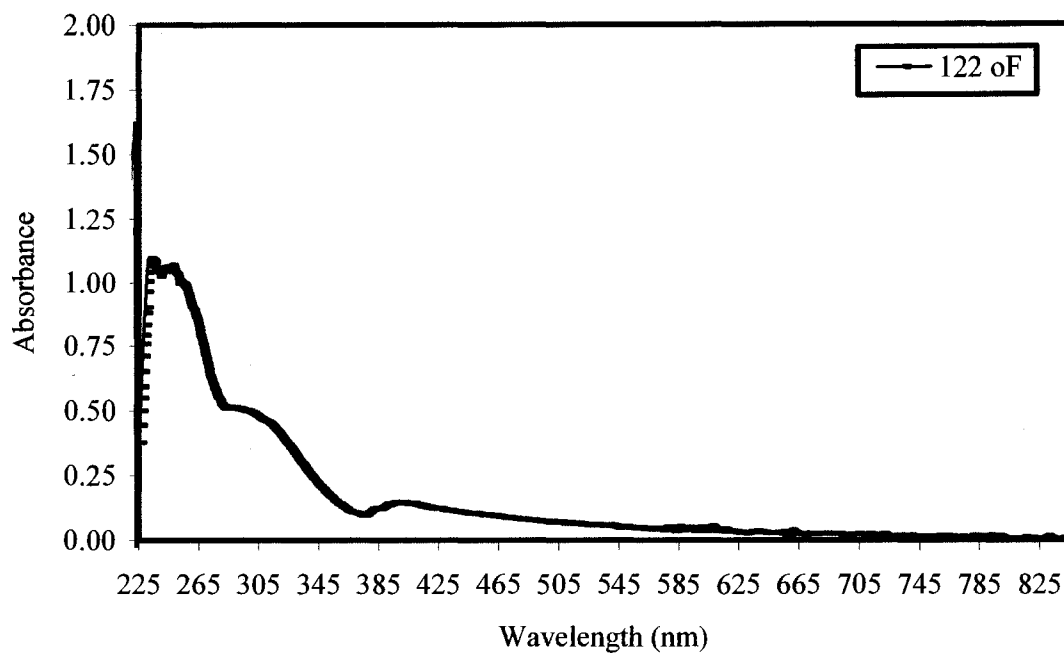Figure V.7: Temperature of 43 °C (109 °F)

355

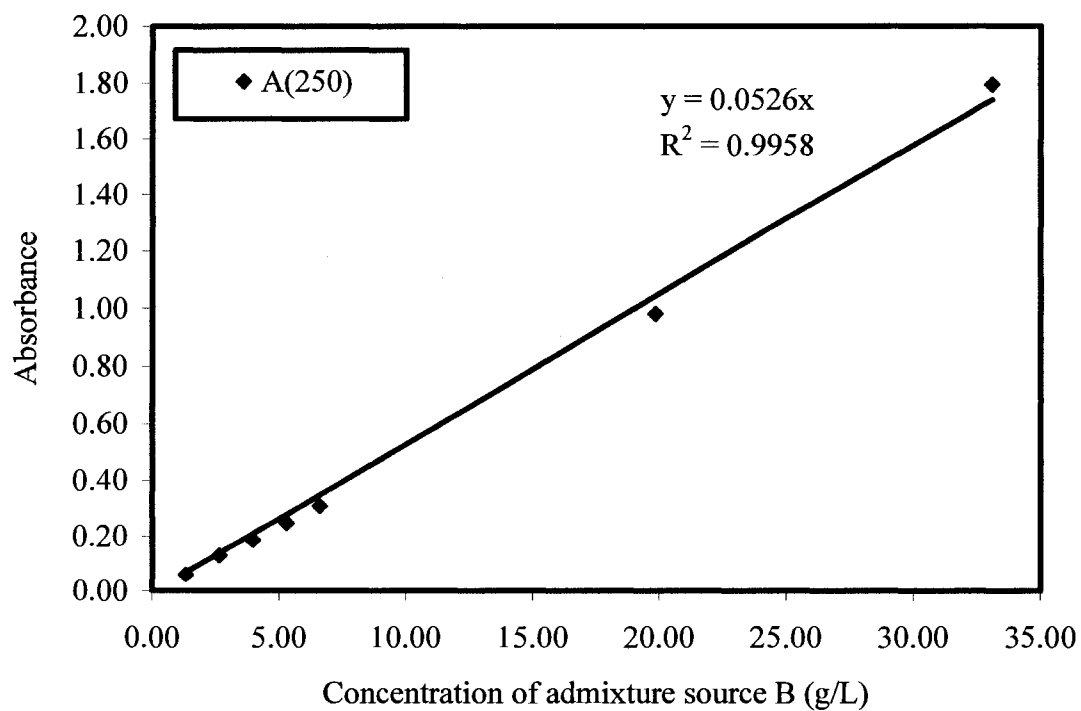Figure V.8: Temperature of 50 °C (122 °F)

Figure E8: Calibration curve for absorption at 250 nm (for NaOH)

REFERENCES

1. American Concrete Institute, "Self-Consolidating Concrete", Reported by the Committee 237, 2007, pp. 30.

2. Bonen, D., and Shah, S. P., "Fresh and hardened properties of self-consolidating concrete," Prog. Struct. Engineering Materials, 2005, Vol. 7, pp. 14-26.

3. Japan Society of Civil Engineering, 1998, "Recommendations for Self-Compacting Concrete," Concrete Engineering Series, JSCE Vol. 31 (1999) 77 pp.

4. Khayat, K., "Workability, Testing and Performance of Self-Consolidating Concrete," ACI Material Journal, 1999, Vol. 96, No. 3, May-June.

5. Europeans Guidelines for Self-Consolidating Concrete, May 2005; 68 pp.

6. Ouchi, M., "Self-Compacting Concrete-Development, Application and Investigation," Nordic Concrete Research, 1999, p. 29-34.

7. Kwan, A., "Use of Condensed Silica Fume for Making High-Strength, Self-Consolidating Concrete," 2000, NRC Canada, pp 620-627.

8. Ghafoori, N., and Aqel, M., "Performance of Self Consolidating Concrete in Sulfate Rich Environment," Proceedings of the combined 4th International RILEM Symposium and 2nd North American Conference on Self-Consolidating Concrete, October 30 – November 2, 2005, Chicago, USA.

9. European Federation of Concrete Admixture Associations-EFNARC, "Guidelines for Viscosity Modifying Admixtures For Concrete," ENC 180VMA r13, 2006, pp. 1-11.

10. Kosmatka, S. H., Kerkhoff, B., and Panarese, W. C., "Design and Control of Concrete Mixtures," 14th Edition, Portland Cement Association, Skokie, Illinois, 2002, 358 pp.

11. Neville, A. M., and Brooks, J. J., "Concrete Technology," Longman Scientific and Technical Publisher, 1987, 438 pp.

12. Mehta, P. K., and Monteiro Paulo, J. M., "Concrete-Structure, Properties, and Materials, Prentice-Hall, Inc., Englewood Cliffs, NJ, 2002, pp. 450 548 pp.

13. American Society for Testing and Materials, "Standard Specification for Portland Cement," (ASTM C 150), Annual Book of ASTM Standards, Vol. 4.01, 2004, pp. 150-157.

14. Griesser, A., "Cement-Superplasticizer Interactions at Ambient Temperatures," Dissertation for the degree of Doctor of Technical Science, Swiss, 2002, 146 pp.

15. Beaulieu J., "Etude de Caractérisation de Bétons Contenant du Ciment Type 20 avec et sans Fumée de Silice," Master Thesis, Sherbrooke (Quebec), Canada, January 1995, 179 pp. (in French)

16. Jolicoeur, C., and Simard, M. A., "Chemical Admixture-Cement Interactions: Phenomenology and Physico-chemical Concepts," Cement and Concrete Composites, Vol.20, 1998, pp. 87-101.

17. Bedard C., "The use of Chemical Admixtures in Concrete. Part I: Admixture-Cement Compatibility," Journal of Performance of Constructed Facilities, ASCE, November 2005, PP. 263-266.

18. American Concrete Educational Bulletin E4-03, "Chemical Admixtures for Concrete," Prepared under the direction and supervision of ACI Committee E-701 Materials for Concrete for Construction, 2003, pp. E4-1 to E4-12.

19. American Concrete Institute (ACI 212.03), "Guide for the Use of High Range Water Reducing Admixtures (Superplasticizers) in Concretes," Reported by ACI Committee 212, 2003, pp. 212.3R1-212.3R13

20. Rixom, M. R., and Mailvagaman, N. P., "Chemical Admixtures for Concrete," E. & F.N. Spon, New York, 1986, 306 pp.

21. American Society for Testing and Materials, "Standard Specification for Chemical Admixture for Concrete," (ASTM C 494), Annual Book of ASTM Standards, Vol. 4.02, 2004, pp. 271-279.

22. Lea, F. M., "The Chemistry of Cement and Concrete," Chemical Publishing Company. Inc., New York, 1971, pp. 302-310, 414-489.

23. Collepardi, M., "Admixtures Used to Enhance Placing Characteristics of Concrete," Cement and Concrete Composites, Vol. 20, 1998, pp. 103-112.

24. Cement Admixture Association, EFCA, "Normal Plasticizing/water reducing," Dec. 2006, 4 pp.

25. Plank, J., and Hirsch, C., "Impact of Zeta Potential of Early Cement Hydration Phases on Superplasticizer Adsorption," Cement and Concrete Research, 2007, Vol. 37, pp. 537–542.

26. Houst, Y. F., Boween, and P., Perche, F., "Towards Tailored Superplasticizers," 6th International Congress, Global Construction: Ultimate Concrete Opportunities, Dundee, Scotland, 5-7 July, 2005.pp. 1-10.

27. Kauppi, A., Andersson, K. M., and Bergstrom, L., "Probing the Effect of Superplasticizer Adsorption on the Surface Forces Using the Colloidal Probe AFM Technique," Cement and Concrete Research, Vol. 35, Issue 1, 2005, pp. 133-140.

28. http://www.cem.msu.edu/~reusch/VirtualText/Spectrpy/UV-Vis/spectrum.htm, 6 pp.

29. Skoog, D. A., Holler, F. J., and Nieman, T. A., "Principles of Instrumental Analysis," 5th Edition, Harcourt Brace College Publishers, 1998, 849 pp.

30. http://www.nbtc.cornell.edu/facilities/downloads/Zetasizer.htm , 12 pp.

31. Flatt, R. J., Houst, Y. F., Bowen, P., Hofmann, H., Widmer, J., Sulser, U., Maeder, U., and Burge, T. A., "Interaction of Superplasticizers with Model Powders in a Highly Alkaline Medium," Proceedings of the 5th Canmet/ACI International Conference on Superplasticizers and Other Chemical Admixtures in concrete, 1997, SP-173, pp. 743-762.

32. Puertas, F., Santos, H., Palacios, M., and Martinez-Raminez, S., "Polycarboxylate Superplasticizer Admixtures: Effect on Hydration, Microstructure and Rheological Behavior in Cement pastes," Advances in Cement Research, 2005, Vol. 17, No. 2, pp. 77-89.

33. American Concrete Institute (ACI 212.04-04), "Guide for the Use of High Range Water Reducing Admixtures (Superplasticizers) in Concretes," Reported by ACI Committee 212, 2004, pp. 212.4R1-212.4R13.

34. Sugamata, T., Ohno, A., and Ouchi, M., "Trends in Research into Polycarboxylate-based Superplasticizers in Japan," pp. 6.

35. Uchikawa, H., Hanehara, S., and Sawaki, D., " The Role of Steric Repulsive Force in the Dispersion of Cement Particles in Fresh Paste Prepared with Organic Admixture," Cement and Concrete Research, 1997, Vol. 27, No. 1, pp. 37-50.

36. Khayat, K. H., "Viscosity-Enhancing Admixtures for Cement-Based Materials – An Overview," Cement and Concrete Composites 20, 1998, pp. 171-188.

37. Kawai, T., and Okada, T., "Effect of superplasticizer and viscosity-increasing admixture on properties of light-weight aggregate concrete," ACI, SP-19, 1989, pp. 583-604.

38. BASF Chemical Company, "Rheomac, Family of Viscosity–Modifying," 2 pp.

39. Headwaters Resources, "Fly ash for concrete," 11 pp.

40. American Society for Testing and Materials, "Standard Test Method for Coal Fly Ash and Raw or Calcined Natural Pozzolan for Use as a Mineral Admixture in Concrete," (ASTM C 618), Annual Book of ASTM Standards, Vol. 4.02, 2004, pp. 319-312.

41. American Society for Testing and Materials "Standard Terminology Relating to Concrete and Concrete Aggregates," (ASTM C 125), Annual Book of ASTM Standards, Vol. 4.02, 2004, pp. 64-67.

42. American Society for Testing and Materials, "Standard Specification for Silica Fume Use in Hydraulic-Cement Concrete and Mortar," (ASTM C 1240), Annual Book of ASTM Standards, Vol. 4.02, 2004, pp. 662-668.

43. American Society for Testing and Materials, "Standard Specification for Ground Granulated Blast-Furnace Slag for Use in Concrete and Mortars," (ASTM C 989), Annual Book of ASTM Standards, Vol. 4.02, 2004, pp. 528-532.

44. American Society for Testing and Materials, "Standard Specification for Concrete Aggregates," (ASTM C 33), Annual Book of ASTM Standards, Vol. 4.02, 2004, pp. 10-16.

45. American Society for Testing and Materials, "Standard Specification for Blended Hydraulic Cements," (ASTM C 595), Annual Book of ASTM Standards, Vol. 4.01, 2004, pp. 340-346.

46. American Society for Testing and Materials, "Standard Performance Specification for Hydraulic Cement," (ASTM C 1157), Annual Book of ASTM Standards, Vol. 4.01, 2004, pp. 550-555.

47. Ghafoori, G., and Diawara, H., "Prescriptive mixture design of self-consolidating concrete," NDOT research agreement No. P077-06-803, 2008, 295pp.

48. American Association of State Highway and Transportation Officials, "Standard Specification for Ready-Mixed Concrete," (AASHTO M 157).

49. ACI 310, "Building Code Requirements for Reinforced Concrete," 2005.

50. American Association of State Highway and Transportation Officials, "Standard Specification for Chemical Admixtures For Concrete," (AASHTO M 194).

51. American Society for Testing and Materials, "Standard Specification for Chemical Admixtures for Use in Producing Flowing Concrete," (ASTM C 1017), Annual Book of ASTM Standards, Vol. 4.02, 2004, pp. 535-543.

52. American Society for Testing and Materials, "Standard Specification for Air-Entraining Admixture for Concrete," (ASTM C 260), Annual Book of ASTM Standards, Vol. 4.02, 2004, 165-167.

53. American Society for Testing and Materials, "Standard Specification for Pigments for Integrally Colored Concrete," (ASTM C 979), Annual Book of ASTM Standards, Vol. 4.02, 2004, pp. 523-527.

54. American Society for Testing and Materials, "Standard Practice for Making and Curing Concrete Test Specimen in Laboratory," (ASTM C 192) Annual Book of ASTM Standards, Vol. 4.02, 2005, 126-133.

55. American Society for Testing and Materials, "Standard Test Method for Slump Flow of Self-Consolidating Concrete," (ASTM C 1611) Annual Book of ASTM Standards, Vol. 4.02, 2005, 36-41.

56. American Association of State Highway and Transportation Officials, "Standard Specification for Slump of Hydraulic Cement Concrete," (AASHTO T 119).

57. American Society for Testing and Materials Subcommittee C09.47 on Self-Consolidating Concrete, part of ASTM International Committee C09 on Concrete and Concrete Aggregates.

58. American Society for Testing and Materials, "Standard Test Method for Passing Ability of Self-Consolidating Concrete by J-Ring," (ASTM C 1621) Annual Book of ASTM Standards, Vol. 4.02, 2005, 42-45.

59. American Society for Testing and Materials, "Standard Test Method for Static Segregation of Self-Consolidating Concrete Using Column Technique," (ASTM C 1610) Annual Book of ASTM Standards, Vol. 4.02, 2005, 46-49.

60. American Society for Testing and Materials, "Standard Specification for Poly(Vinyl Chloride) (PVC) Plastic Pipe, Schedules 40, 80, and 120," (ASTM D 1785) Annual Book of ASTM Standards, Vol. 08.04, 2004, 36-46.

61. American Association of State Highway and Transportation Officials, "Standard Specification for Wire-Cloth Sieves for Testing Purposes," (AASHTO M 92).

62. American Society for Testing and Materials, "Standard Test Method for Time of Setting of Concrete Mixture by Penetration Method," (ASTM C 403), Annual Book of ASTM Standards, Vol. 4.02, 2004, pp. 230-235.

63. American Society for Testing and Materials, "Standard Test Method for Bleeding of Concrete," (ASTM C 232), Annual Book of ASTM Standards, Vol. 4.02, 2004, pp. 155-159.

64. American Society for Testing and Materials, "Standard Test Method for Air Content of Freshly Mixed Concrete by the Pressure Method," (ASTM C 231), Annual Book of ASTM Standards, Vol. 4.02, 2004, pp. 146-154.

65. American Society for Testing and Materials, "Standard Test Method for Density (Unit Weight), Yield, and Air Content (Gravimetric) of Concrete," (ASTM C 138), Annual Book of ASTM Standards, Vol. 4.02, 2004, pp. 89-92.

66. American Society for Testing and Materials, "Standard Test Method for Air Content of Freshly Mixed Concrete by Volumetric Method," (ASTM C 173), Annual Book of ASTM Standards, Vol. 4.02, 2007, pp. 116-123.

67. American Society for Testing and Materials, "Standard Test Method for Temperature of Freshly Mixed Portland Cement Concrete," (ASTM C 1064), Annual Book of ASTM Standards, Vol. 4.02, 2004, pp. 562-563.

68. DataQ Instruments, DI 1100 TC, Instrumentation Modules for Temperature Measurements.

69. DataQ Instruments, WinDaq Acquisition, Waveform Recording Software.

70. American Society for Testing and Materials, "Standard Test Method for Compressive Strength of Cylindrical Concrete Specimens," (ASTM C 39), Annual Book of ASTM Standards, Vol. 4.02, 2004, pp. 21-25.

71. American Concrete Institute (ACI 363), "Guide to Quality Control and Testing of High-Strength Concrete," 2006.

72. American Society for Testing and Materials, "Standard Practice for Use of Unbonded Caps in Determination of Compressive Strength of Hardened Concrete Cylinders," (ASTM C 1231), Annual Book of ASTM Standards, Vol. 4.02, 2004, pp. 658-661.

73. American Society for Testing and Materials, "Standard Test Method for Static Modulus of Elasticity and Poisson's Ratio of Concrete in Compressive," (ASTM C 469), Annual Book of ASTM Standards, Vol. 4.02, 2004, pp. 256-260.

74. http://www.malvern.co.uk/processeng/systems/laser_diffraction/technology/technology.htm

75. Rodden, R. A., et al., "Guiding Principles for the Optimization of the OMP PCC Mix Design," Technical Note, Center for Excellence for Airport Technology, 2005, pp. 1-6.

76. American Society for Testing and Materials, "Standard Test Method for Bulk Density ("Unit Weight") and Voids in Aggregate," (ASTM C 29) Vol. 4.02, 2004, pp. 1-4.

77. Barfield, M. E., "Air Void Characteristics of Air-Entrained Self-Consolidating Concrete," Thesis for the degree of Master of Science, University of Nevada, Las Vegas (UNLV), USA, 2008, 199 pp.

78. Murdock, L. J., Brook, K. M., and Dewar, J. D., "Concrete Material and Practice," Sixth Edition, England, 470 pp.

79. DataFit 8.1, Linear and Nonlinear regression (curve fitting), statistical analysis and data plotting software.

80. Nawy, E. G., "Reinforced Concrete, a Fundamental Approach," Fifth, 2003, Prentice Hall, 821 pp.

81. Building Code Requirements for Structural Concrete and Commentary ACI Committee 318.

82. Carrasquillo, P. M., and Carrasquillo R. L., "Evaluation of the Use of Current Concrete Practice in the Production of High-Strength Concrete," ACI Materials Journal, 1998, 85(1), pp. 49-54.

83. Carrasquillo, R., Nilson, A., and Slate, F., "Properties of High Strength Concrete Subject to Short-Term Loads," ACI Journal, 1981 78(3), pp. 171-178.

84. Ferraris, C. F., "Concrete Mixing Methods and Concrete Mixers: State of Art," Journal of Research of the National Institute of standards and Technology, Vol. 106, No. 2, 2001, pp. 391-399.

85. American Society for Testing and Materials, "Standard Specification for Ready-Mixed Concrete," (ASTM C 94), Annual Book of ASTM Standards, Vol. 4.02, 2004, pp. 47-56.

86. American Society for Testing and Materials, "Standard Specification for Concrete Made by Volumetric Batching and Continuous Mixing," (ASTM C 685), Annual Book of ASTM Standards, Vol. 4.02, 2004, pp. 367-375.

87. American Association of State Highway and Transportation Officials, "Standard Specification for Concrete Made by Volumetric Batching and Continuous Mixing," (AASHTO M 241).

88. The International Union of Laboratories and Experts in Construction Materials, Systems and Structures (RILEM, from the name in French - Réunion Internationale des Laboratoires et Experts des Matériaux, systèmes de construction et ouvrages)

89. Connecticut Department of Transportation, (Conndot), Concrete Pavement, Section 4.01, pp. 1-12.

90. Stieβ, M., "Mechanische Verfahrenstechnik 1," Second issue, Springer Berlin 1995.

91. Lowke, D., and Schiessl, P., "Effect of Mixing Energy on Fresh Properties of SCC," pp. 6.

92. Yamada, K., and Hanehara, S., "Working Mechanism of Polycarboxylate Superplasticizer Considering the Chemical Structure and Cement Characteristics," Proceedings of the 11th International Congress on the Chemistry of Cement (ICCC)

'Cement's Contribution to the Development in the 21st Century,' 2003, pp. 538-549.

93. Brite Euram, " Self-Compacting Concrete: Mixing and Transport," 2000, 65 pp.

94. Sakai, E., Yamada, K., and Ohta, A., "Molecular Structure and Dispersion-Adsorption Mechanisms of Comb-Type Superplasticizers used in Japan," Journal of Advanced Concrete Technology, Vol. 1, No. 1, 2003, pp. 16-25.

95. Uchikawa, H., Uchida, S., Ogawa, K., and Okamura, T., "Influence of $CaSO_4 \cdot 2H_2O$, $CaSO_4 \cdot 1/2H_2O$, and $CaSO_4$ on the Initial Hydration of Clinker Having Different Burning Degree," Onoda Research Report, 1984, Vol. 36(112), pp. 56-67.

96. ACI Committee 305, ACI 305.R-88, Hot Weather Concreting, American Concrete Institute, Detroit, Michigan, 1988.

97. ACI Committee 306, ACI 306.R-88, Cold Weather Concreting, American Concrete Institute, Detroit, Michigan, 1988.

98. Jolicoeur, C., Sharman J., Otis N., Lebel A., Simard M. A., and Page M., "The Influence of Temperature on the Rheological Properties of Superplasticized Cement Paste," 5th CANMET/ACI International Conference on Superplasticizers and Other Chemical Admixtures in concrete, 1997, Rome, pp. 379-405.

99. Nawa, T., Ichiboji, H. Kinoshita, M., "Influence of Temperature on the Fluidity of Cement Paste Containing Superplasticizer with Polyethylene Oxide Graft Chains," 6th CANMET/ACI International Conference on Superplasticizers and Other Chemical Admixtures in concrete, 2000, Nice, pp. 195-210.

100. Burg, R., G., "The Influence of Casting and Curing Temperature on the Properties of Fresh and Hardened Concrete," Portland Cement Association and Development Bulletin RD113, 1996, pp. 1-13.

101. Klieger, P., "Effect of Mixing and Curing Temperature on Concrete on Concrete Strength," Research Bulletin RX103, Portland Cement Association, Skokie, Illinois, 1958.

102. Baes, C. F.; Mesmer, R. E., "The Hydrolysis of Cations," (1976), Wiley, New York, 489 pp.

103. Berhane, Z., "The Behaviour of Concrete in Hot Climates," Materials and Structures, 1992, 25, pp. 157-162.

104. Ludwig, N. C., and Pence S. A., "Properties of Portland Cement Pastes Cured at Elevated Temperature-Pressure," ACI Journal 52(6), 1956, pp. 673-764.

VITA

Graduate College
University of Nevada, Las Vegas

Hamidou Diawara

Local Address:
    4235 Cottage Circle, #3
    Las Vegas, N.V., 89119

Home Address:
    C/O Fousseyni SIDIBE Banque de l'Habitat du Mali
    B.P. 2614, Agence Halles de Bamako
    Bamako Mali, République du Mali, West Africa

Degrees:
    Bachelor of Science, Civil Engineering, 1987
    National School of Engineering (E.N.I.), Mali

    Master of Science, Southern Illinois University at Carbondale (SIUC), 1998
    Southern Illinois University at Carbondale (SIUC), USA

Special honors:
    Full scholarship of $89,000 for the Master degree program from the
    United States Agency for International Development (US-AID), 1995 – 1998

    Full Scholarship from for Bachelor degree program from the
    Minister of Education of Mali, 1983-1987

Publications:

Published refereed journal articles:
    1   Ghafoori, N., and **Diawara, H.**, "Abrasion Resistance of Fine Aggregate-Replaced Silica Fume Concrete," ACI Material Journal, V. 96, No.5, Sept-Oct 1999, pp. 559-567.
    2   Ghafoori, N., and **Diawara, H.**, "Strength and Wear Resistance of Sand-Replaced Silica Fume Concrete," ACI Material Journal, V. 104, No.2, March-April 2007, pp. 206-214.
    3   Ghafoori, N., **Diawara, H.**, and Beasley, S., "Resistance to External Sodium Sulfate Attack For Early-Opening-To-Traffic Portland Cement Concrete," Cement and Concrete Composite, June 2007

4 Ghafoori, N., **Diawara, H.**, and Beasley, S., "Sodium Sulfate Resistance of Fast-Track Portland Cement Concretes," ACI Material Journal, V. 104, No.6, Nov-Dec 2007, pp. 303-311.

5 Ghafoori, N., and **Diawara, H.**, "Influence of Admixture Source and Slump Flow on Fresh Properties of Self- Consolidating Concrete," under preparation for publication in the Journal of Journal of Materials (ACI).

Refereed journal articles under preparation:

1 Ghafoori, N., and **Diawara, H.**, "Influence of Hauling Time on Fresh Performance of Self Consolidating Concrete," under preparation for publication in the ACI Material Journal.

2 Ghafoori, N., and **Diawara, H.**, "Influence of Extreme Temperature on Fresh Properties of Self-Consolidating Concrete," under preparation for publication in the ACI Material Journal.

3 Ghafoori, N., and **Diawara, H.**, "Influence of Combined Hauling Time and Extreme Temperature on Fresh Properties of Self-Consolidating Concrete," under preparation for publication in the Journal of Cement & Concrete Composite.

4 Ghafoori, N., and **Diawara, H.**, "Influence of Pumping on Fresh Properties of Self-Consolidating Concrete," under preparation for publication in the Journal of Materials in Civil Engineering (ASCE).

5 Ghafoori, N., and **Diawara, H.**, "Remediation of Freshly-Mixed Hauled Self - Consolidating Concrete," under preparation for publication in the ACI Material Journal (ACI).

6 Ghafoori, N., and **Diawara, H.**, "Remediation of Fresh Self-Consolidating Concrete Due to Extreme Temperature," under preparation for publication in the Journal of Materials in Civil Engineering (ASCE).

7 Ghafoori, N., and **Diawara, H.**, "Remediation of Fresh Self Consolidating Concrete Due Combined Hauling Time and Extreme Temperature," under preparation for publication in the Journal of Cement & Concrete Composite.

8 Ghafoori, N., Wang. L., and **Diawara, H.**, "Use of Pulverized and Fluidized Combustion Coal Ash in Secondary Road Constructions," under preparation for publication in the Journal of Cement and Concrete Research.

9 Ghafoori, N., Wang, L., Kassel, S., and **Diawara, H.**, "Field Demonstration Project of Using Conventional and Clean Coal Technology By-Products for Paving Materials," under preparation for publication in the Journal of Transportation Engineering (ASCE).

10 Ghafoori, N., Wang, W., and **Diawara, H.**, "Performance of Concrete Containing Secondary Cementing Materials, "under preparation for publication in the Journal of Materials in Civil Engineering (ASCE).

11 Ghafoori, N., and **Diawara, H.**, "Structural Concrete Utilizing Low-Calcium Dry Bottom Ash," under preparation for publication in the Journal of Materials in Civil Engineering (ASCE).

12 Ghafoori, N., Wang W., and **Diawara, H.**, "Laboratory Evaluations of Non-Cement Concrete Containing Coal-Based Industrial By- Products," under preparation for publication in the ACI Material Journal.

13 Ghafoori, N., Aqel, M., **and Diawara, H.**, "Chloride Iron Penetration of Self-Consolidating Concrete," under preparation for publication in the ACI Material Journal.

14 Ghafoori, N., Aqel, **M., and Diawara, H.**, "Abrasion Resistance of Self-Consolidating Concrete," under preparation for publication in the Journal of Materials in Civil Engineering (ASCE).

15 Ghafoori, N., Aqel, M., and **Diawara, H.**, "Abrasion Resistance of Self-Consolidating Concrete," under preparation for publication in the Journal of Cement and Concrete Composite.

16 Ghafoori, N., and **Diawara, H.**, "Influence of Exposure Types on Sodium Sulfate Resistance of Fly Ash Concretes," under preparation for publication in the ACI Material Journal.

Published refereed conference proceedings

1 Ghafoori, N., and **Diawara, H.,** "Curing of Fine Aggregate-Replaced Silica Fume Concrete: Strength and Wear Resistance," Fifth International Conference on Concrete under Severe Conditions: Environment and Loading (CONSEC'07) Tour France, 2007, pp. 1153-1162.

2 Ghafoori, N., and **Diawara, H.**, "Sulfate Resistance of Fly Ash Concrete in Wet-Dry Conditions," The Fourth International Conference on Innovations in Structural Engineering & Construction (ISEC-4) Conference, Australia, 2007, pp. 583-587.

3 Ghafoori, N., and **Diawara, H.**, "Influence of Source-Based High Range Water Reducing Admixture on Properties of Self-Consolidating Concrete," Conference proceedings: Advances in Cement Based Materials and Applications to Civil Infrastructure (ACBM-ACI), Lahore, December 12-14, 2007, Pakistan.

4 Ghafoori, N., and **Diawara, H.**, "Resistance to wear of Silica Fume Concrete by way of Fine Aggregate Replacement," Proceedings of the International Symposium on Cement and Concrete Technology in the 2000s, September 6-10, 2000, Istanbul, Turkey, pp. 331-344.

Accepted refereed conference proceedings

1 Ghafoori, N., and **Diawara, H.**, "Influence of Hauling Time on Fresh Performance of Self Consolidating Concretes," Third North American Conference on Design and Use of Self-Consolidating Concrete - SCC 2008.

2 Ghafoori, N., and **Diawara, H.**, "Influence of Hot Temperature on Freshly-Mixed Self-Consolidating Concrete," 5th International Engineering & Construction Conference August 27-29, 2008, Irvine, CA, USA.

3 Ghafoori, N., and **Diawara, H.**, "Remediation of Slump Flow Loss of Fresh Self-Consolidating Concrete Induced By Hauling Time," Third International Conference on Concrete Repair, Venice/Padua, Italy.29 the June to 2nd July 2009.

4 Ghafoori, N., Kassel, K., and **Diawara, H.**, "Use of PCC/FBC Coal By-Products in Secondary Roads," The Sixth International Conference on Maintenance and Rehabilitation of Pavement and Technological Control, Politecnico Di Torino – Torino, Italy – July 8 – 10, 2009.

Dissertation Title: Parametric Studies of Self-Consolidating concrete

Dissertation Examination Committee:
    Chairperson, Dr. Nader Ghafoori, Ph.D.
    Committee Member, Dr. Samaan Ladkany, Ph.D.
    Committee Member, Dr. Moses Karakouzian, Ph.D.
    Committee Member, Dr. Aly Said, Ph.D.
    Committee Member, Dr. Spencer M. Steinberg, Ph.D.
    Graduate College Faculty Representative, Dr. Samir Moujaes, Ph.D.

370